

**GABRIEL VASCO**

**MODELING CLIMATE AND LAND-USE CHANGE IMPACTS ON  
WATER RESOURCES IN THE SÃO FRANCISCO RIVER BASIN, BRAZIL**

Recife/PE – Brazil  
2023

**GABRIEL VASCO**

**Modeling climate and land-use change impacts on water resources in the São Francisco River Basin, Brazil**

Doctoral Thesis submitted to the Examining Board from the Graduate Programme in Agricultural Engineering at Federal Rural University of Pernambuco (UFRPE), in partial fulfillment of the requirements for attaining the Doctor in Engineering, majoring in WATER AND SOIL ENGINEERING.

Advisors: Prof. Suzana Maria Gico Lima Montenegro (UFPE – Brazil), and Dr. Rodrigo de Queiroga Miranda (University of Guelph – Canada)

Recife/PE – Brazil  
2023

Dados Internacionais de Catalogação na Publicação  
Universidade Federal Rural de Pernambuco  
Sistema Integrado de Bibliotecas  
Gerada automaticamente, mediante os dados fornecidos pelo(a) autor(a)

---

V331m Vasco, Gabriel  
Modeling climate and land-use change impacts on water resources in the São Francisco River Basin, Brazil / Gabriel Vasco. - 2023.  
189 f. : il.

Orientadora: Suzana Maria Gico Lima Montenegro.  
Coorientador: Rodrigo de Queiroga Miranda.  
Inclui referências, apêndice(s) e anexo(s).

Tese (Doutorado) - Universidade Federal Rural de Pernambuco, Programa de Pós-Graduação em Engenharia Agrícola, Recife, 2023.

1. water balance. 2. hydrology. 3. water resources management. 4. climate data ensemble. 5. trend analysis. I. Montenegro, Suzana Maria Gico Lima, orient. II. Miranda, Rodrigo de Queiroga, coorient. III. Título

**GABRIEL VASCO**

**MODELING CLIMATE AND LAND-USE CHANGE IMPACTS ON WATER  
RESOURCES IN THE SÃO FRANCISCO RIVER BASIN, BRAZIL**

This Ph.D. thesis was defended and approved by the following examining board committee:

**Prof. Suzana Maria Gico Lima Montenegro**  
Advisor / Federal University of Pernambuco – UFPE

**Dr. Rodrigo de Queiroga Miranda**  
Co-Advisor / University of Guelph – U of Guelph

**Prof. Danielle Bressiani**  
Examiner / Federal University of Pelotas – UFPel

**Prof. Eduardo Mario Menciondo**  
Examiner / University of São Paulo – EESC/USP

**Prof. Richarde Marques**  
Examiner / Federal University of Paraíba – UFPB

**Prof. Josiclêda Domiciano Galvício**  
Examiner / Federal University of Pernambuco – UFPE

The Certificate of Defense Approval for the Doctoral Thesis is on the academic records of the  
Ph.D. Candidate.

Recife/PE – Brazil  
2023

To my beloved parents, Júlia Vasco, and Vasco Inoque (*in memoriam*),  
for their unconditional and dimensionless love.

**I OFFER**

To my brothers: Neto, Nádio, Gilda, Tércio and Arlete.

**I DEDICATE**

## Acknowledgments

As stated by Nelson Rolihlahla MANDELA, [...] *it always seems impossible until it's done*. As we come to this stage, I vividly believe there is no better quote to describe this phase of my life. This thesis appears as the result of a long academic hard-working journey over the last five years, involving a lot of activities regarding data retrieval and processing – exposure to a challenging research atmosphere, full of stressful moments, plenty of heartbreaks, and a lot of crying, as well as many joys, achievements, and self-growth. Truly, there were instances I thought of quitting due to high pressure, but (a) God (all the way) whose grace and power strengthened me to work forward, (b) the real-time unconditional assistance, guidance, suggestions, and encouragement that I received from many institutions, and people were crucial to concluding this thesis and doctoral degree, as well. Therefore, as I draw this chapter of my life to an end (*leading to a series of reflections regarding what it means to develop a doctoral thesis successfully*), and looking forward to beginning a new one, this section (even short), lends itself to my deepest gratitude to the institutions and exceptional individuals who supported and guided me throughout this transformative journey, enabling me to successfully obtain my doctorate despite the many unforeseen obstacles that arose. **These include:**

My advisor, Prof. Suzana Maria Gico Lima Montenegro of the Department of Civil Engineering at the Federal University of Pernambuco, and my co-advisor, Dr. Rodrigo de Queiroga Miranda (the University of Guelph-based Postdoctoral Fellow, Canada) for their blind acceptance as their doctoral student to oversee this thesis, working actively throughout the doctoral activities since 2018, as well as for entrusting and allowing me to prepare and write this doctoral thesis within an extraordinary international research environment, as well as for the open doors whenever I ran into a trouble spot or had a question about my research or writing.

The Coordination and the Collegiate of Didactic Coordination (CCD), represented by its coordinator and secretary, for receiving me so amazingly and supporting me so quickly during my advanced 3<sup>rd</sup> cycle studies abroad. Extended thanks to classmates, staff, and the whole professors for their kind support.

My research colleagues, the members of the Water Resources Group (GRH) led by Prof. Suzana Maria Gico Lima Montenegro; Remote Sensing, and Geoprocessing Laboratory (SERGEO), and the Graduate Programme in Development and Environment (PRODEMA) led by Prof. Josiclêda Domiciano Galvêncio, both from Federal University of Pernambuco (UFPE). They made these years more enjoyable and provided me with a lot of technical discussions and support in the fields of hydrology and water resources research. I am deeply grateful to Dr. Jussara Freire de Souza (UFPE//CAPES Postdoctoral Fellow) for her support during the SWAT model calibration

and validation steps; in addition to her kind effort to bias correction (trendline) of multi-model ensemble climate data; and for proofreading each chapter of this doctoral thesis.

The examination board members for their kind acceptance to evaluate my doctoral research proposal (a), pre-doctoral exams (b), and final doctoral thesis defense (c), whose suggestions and support contributed undoubtedly to improving the quality of the final version of this thesis.

The awarded full Ph.D. scholarship from the Brazilian Federal Agency for Support and Evaluation of Graduate Education (CAPES) – Finance Code 001 (GCUBProf. nr. 001/2018). Research grants received from other funding sources to support this research, are also acknowledged. Furthermore, I could not fail to thank the Brazilian Federal Government for the emergency aid due to the SARS-CoV-2 pandemic.

My gurus in the hydrology and distributed hydrological modeling worlds, Dr. João Antônio dos Santos Pereira and Dr. Gabriela Chiquito Gesualdo; thanks for our hottest technical discussions on statistical hydrology, besides all the extensive help in GIS programs for converting data and all kind of support in MATLAB, Python and R programming languages.

The SWAT model developers, represented by Prof. Raghavan Srinivasan and his team from Texas A&M University – US, for their valuable contributions, quickly responding to all inquiries, and the three lectured workshops about the model.

The calibration/validation SWAT-CUP model developers, represented by Dr. Karim Abbaspour and his 2w2e Consulting GmbH team at the Swiss Federal Institute of Aquatic Science and Technology – Switzerland, for all kinds of support on model calibrations and validations procedures. Extended thanks to the SWAT+ Toolbox model developer, Dr. Celray James Chawanda, and his team at Vrije Universiteit Brussel - Belgium, for all kinds of support on hydrological model calibration/validation.

All partner universities, Professors, technical-administrative members, and colleague researchers of the BIS research project entitled *SWAT-based Integrated Water Management Model for BIS Countries Under Climate Change Scenarios* (CNPq/MCTIC/BRICS-STI 29/2017), fully funded by CNPq – Brazil, NRF – South Africa, and DST – India, for your collaboration, shared data and scripts, and technical discussions on hydrological modeling and climate analysis.

All Lecturers of the Land Change Modeling Course (CST-401/Fall 2020), Prof. Ana Paula Dutra Aguiar, Dr. Gilney Bezerra, and Dr. Talita Assis, for accepting me into this joint Course between the National Institute for Space Research (INPE), Brazil and the Stockholm Resilience Centre of Stockholm University, Sweden. I also thank my classmate, Dr. Gisele Milaré, for her valuable contributions during our deepest technical discussions on TerraME (a programming

environment for spatial dynamical modeling) and LuccME applications for building scenarios to support land use/cover changes policymakers.

The Institute of Hydraulic Research of the Federal University of Rio Grande do Sul, for giving me the first opportunity (during my master's degree), to dive into the water resources area, especially to Prof. Alexandre Beluco, for all kinds of encouragement to begin with 3<sup>rd</sup> cycle of superior studies, as well as, for the issued recommendation letters for the selection process, 2018/2 intake.

The Shuttle Radar Topography Mission (SRTM) of the National Aeronautics and Space Administration (NASA), Ministry of the Environment (MMA), National Supply Company (CONAB), Brazilian Institute of Geography and Statistics (IBGE), Brazilian Agricultural Research Corporation (EMBRAPA), MAPBIOMAS initiative, National Water Agency (ANA), Pernambuco State Agency for Water and Climate (APAC), National Institute of Meteorology (INMET), for the given data that enabled this study, and to the Supercomputing CPTEC/INPE staff, represented by Prof. Chou Sin Chan (Senior Research Scientist at the National Institute for Space Research – INPE), for their efforts in providing the ETA model regional data (CMIP5), and technical discussion on climate change projections.

The Rector of Zambeze University, for allowing completion of my doctoral academic training, and to the human resources staff, for their kind effort and efficient support concerning my leaving formalities.

All Scholars2Scholars executive board members and brothers from different parents – Hercílio Zimila, Agnaldo Neves, and Jéssica Alface, for the joint effort and brainstorming we made together during this period to successfully founder this humanitarian not-for-profit NGO, to foster job and scholarship opportunities and provide expert advice to improve access to high-quality education for youth from disadvantaged communities.

My friends, Dr. João Filipe Papel, and Ms. Cecília Rafael Tivir for their kind support during my graduate studies abroad.

My sweetheart, Anisa Nhassengo (aka *Grude*), for all her love and emotional support, for being so understanding, and for being such a great friend – especially during my stay in Brazil and South Africa, always upholding my decisions. Thanks for always being a part of my world and being with me through the ups and downs of this difficult journey. Her support and unwavering belief in me have been a source of strength, inspiration, and motivation. *I LOVE YOU!*

My family, for being extremely supportive throughout five years of hardworking Ph.D. research period away from them, made me always feel their presence. Their endless

encouragement, understanding, and sacrifices played an integral role in reaching this significant and monumental accomplishment in my academic career.

All other people not mentioned here (*sorry if I have forgotten anyone*), but who were important in my doctoral training and the development of this thesis. Warm thanks!

Myself, for never having abandoned me throughout this journey (a), for the moments when everything went dark and in stormy days (b), for the days that I deprived myself of many things and I didn't sleep (others that I slept sadly heartbroken) (c), and for so many thousand reasons to give up (d) — but I never gave up and needed to believe in myself first, to keep focused and coping with various difficulties.

I will be forever grateful!

Yours ever: VASCO

## RESUME

GABRIEL VASCO, well-known as VASCO, son of Vasco Inoque and Júlia Vasco, was born on November 23<sup>rd</sup>, 1990, in the Manica district of central Mozambique. In December 2007, attained his high-school diploma at Jécua Secondary School, in Manica district.

In February 2009, started his undergraduate studies at the Pedagogical University of Mozambique – UPM (Department of Chemistry), where he became a Bachelor of Science in Chemical Sciences (majoring in ENVIRONMENTAL CHEMISTRY) on June 1<sup>st</sup>, 2013.

In August 2015 he outbound abroad to pursue a Post-graduate Program in WATER RESOURCES AND ENVIRONMENTAL SANITATION at the Institute of Hydraulic Research of the Federal University of Rio Grande do Sul – UFRGS, in Brazil, and successfully awarded the Master of Science degree on July 26<sup>th</sup>, 2017.

Aiming to advance expertise in conducting research that can be translated into sound water and environmental policy recommendations, in August 2018, he decided to start his doctoral studies at the Federal Rural University of Pernambuco (UFRPE) of Brazil, under the guidance of Prof. Suzana Maria Gico Lima Montenegro and Dr. Rodrigo de Queiroga Miranda, having successfully defended his thesis in partial fulfillment of the requirements for attaining the Doctor in Engineering (majoring in WATER AND SOIL ENGINEERING) on July 26<sup>th</sup>, 2023.

His main research interests include groundwater and surface water hydrology; water resources management; watershed modeling and management using numerical, soft computing, and geospatial methods; and climate change impact studies. The main focuses of his work are the impacts of global change (climate, land use, socio-economy) on the regional scale and the analysis of effects on different sectors, e.g., water supply (households, industry, agriculture), wind power generation, thermal power generation and hydropower generation. Integrated water management and development of adaptation strategies, based on mathematical simulations, for these connected sectors are an important part of his work.

Professionally, since July 2015, he has been working as an ASSISTANT LECTURER at Zambeze University – Mozambique, lecturing subjects on Water Resources Management and Environmental Modeling, and from June 2022 was appointed as a CHARTERED ENVIRONMENTAL CONSULTANT by the Mozambican Ministry of Land and Environment.

If everything seems under control, you're just not going fast enough – M.

ANDRETTI

## Table of contents

Copyright statement.....	3
Acknowledgments .....	6
RESUME .....	10
List of figures .....	15
List of tables .....	17
List of acronyms .....	18
Abstract.....	20
Resumo .....	21
1. Background and general introduction.....	24
1.1 Research hypothesis .....	27
1.2 Objectives.....	27
1.2.1 General objective.....	27
1.2.2 Specific objectives.....	27
1.3 LITERATURE REVIEW.....	30
1.3.1 Integrated water resources management and water security concepts.....	30
1.3.2 Spatially explicit land-use changes.....	32
1.3.3 Climate change impacts.....	34
1.3.3.1 Bias correction methods.....	37
1.3.4 Mathematical and hydrological modeling .....	39
1.3.4.1 The Watershed Model – Soil and Water Assessment Tool (SWAT) .....	41
1.3.4.2. Hydrologic Soil Groups.....	44
1.3.4.3 Curve Number Values and Antecedent Runoff Conditions.....	46
1.3.4.4 SWAT model advances and limitations.....	49
1.3.4.5 Sensitivity analysis, calibration, and model validation.....	50
1.4 STUDY AREA .....	53
1.4.1 The São Francisco River Transposition Project .....	57
References .....	58
Spatially explicit land use scenarios for the São Francisco River Basin, Brazil.....	83
Abstract.....	83
2.1 Introduction .....	84
2.2 Material and Methods.....	85
2.2.1 Study area brief description .....	85

2.2.2 Modeling Approach .....	86
2.2.2.2 Model description .....	87
2.2.2.3 Model parameterization/calibration .....	90
2.2.2.4 Model validation .....	92
2.2.3 Scenario assumptions.....	92
2.3 Results and Discussion .....	93
2.3.1 Model performance.....	93
2.3.2 Scenarios of land-use Change .....	96
2.4 Conclusion.....	99
References .....	100
Multi-model ensemble for long-term statistical trend analysis of observed gridded precipitation and temperature data in the São Francisco River Basin, Brazil .....	104
Abstract.....	104
3.1 Introduction .....	105
3.2 Materials and Methods .....	106
3.2.1 Study area brief description .....	106
3.2.2 Data description .....	107
3.2.3 The Multi-Model Ensemble Approach .....	107
3.2.4 Non-parametric trend tests.....	110
3.2.4.1 Teste de Mann-Kendall (MK).....	110
3.2.4.2 Mann–Kendall test of pre-whitened time series data having a serial correlation. ....	111
3.2.4.3 Bias corrected pre-whitening MK test. ....	112
3.2.4.4 Spearman’s rank correlation (SRC) test .....	113
3.2.5 Future climate change and land-use scenarios.....	113
3.2.6 Statistical Bias Correction Method .....	113
3.2.7. Bilinear interpolation and IDW .....	115
3.3 Results and Discussion.....	116
3.3.1 Analysis of observed trends in precipitation.....	118
3.3.2 Analysis observed trends in minimum temperature .....	126
3.3.3 Observed trends in maximum temperature .....	128
3.4 Conclusions .....	131
References .....	132
Appendix C: Spatial variation of Z-value and trend showing grid points in four trend tests for three sub-regions for the entire São Francisco River basin.....	143

Climate and land-use change impact assessment on water resources in the São Francisco River Basin .....	152
Abstract.....	152
4.1 Introduction .....	153
4.2 Materials and Methods .....	155
4.2.1 Study area description.....	155
4.2.2 Brief description of the used SWAT hydrological model .....	155
4.2.2.1. Input data and SWAT model setup.....	155
4.2.2.2 SWAT model calibration procedures .....	161
4.2.2.3 Model parameterization and simulations in SWAT-CUP .....	162
4.2.3 Linear scaling technique for bias correction.....	163
4.2.4 Assessment of climate and land-use change impacts on water resources .....	164
4.3 Results and Discussions .....	164
4.3.1. Performance analysis of the simulated hydrographs by the SWAT model with the observed data .....	164
4.3.2 Hydrological Processes under future climate change and land-use scenarios.....	167
4.3.3 Variations in streamflow under climate and land-use change .....	168
4.4. Conclusions .....	171
References .....	172
APPENDIX D .....	184
Technical Note on SWAT+ hydrological model: A brief description and limitations.....	184
CHAPTER V .....	188
Key findings and concluding remarks.....	188

## List of figures

Figure 1: Overview and relationship of the main topics covered in this Ph.D. thesis.....	29
Figure 2: Scheme of the conceptual model of water balance in the SWAT hydrological model .	42
Figure 3: Components associated with the SWAT model standard Curve Number method – SCS .....	43
Figure 4: Geographic location map of the São Francisco River basin, Brazil .....	55
Figure 5: A conceptual structure for projecting the scenarios of land use changes through the LuccME framework.....	86
Figure 6: Percentage of agriculture, natural forest, and pasture observed versus simulated in 10 x 10 km <sup>2</sup> cells in 2019, and the spatial distribution of omission and commission errors.....	94
Figure 7: Percentage of the mosaic of agriculture and pasture, forest plantation observed versus simulated in 10 x 10 km <sup>2</sup> cells in 2019, and the spatial distribution of errors of omission and commission.....	95
Figure 8: Spatial distribution (%) of areas and land use according to the scenarios from 2010 to 2050 .....	96
Figure 9: Spatial distribution of selected stations along the São Francisco River basin.....	116
Figure 10: Performance analysis of RMSD and NRMSD metrics of precipitation (a), and minimum (b) and maximum temperature (c) for 9 RCMs in 10 points.....	117
Figure 11: Models weights (Va) for precipitation (a), and minimum (b) and maximum temperature (c) based on their individual performance to create the multi-model.....	118
Figure 12: Mean annual precipitation (mm) for the entire São Francisco River basin .....	119
Figure 13: Spatial variation of Z-value and trend showing grid points in four trend tests of precipitation data annual period over the São Francisco River Basin.....	120
Figure 14: Station-wise means monthly precipitation (mm) in the dry (a), rainy (b), and pre-season (c) periods over Lower São Francisco.....	121
Figure 15: Station-wise mean monthly precipitation (mm) in the dry (a), rainy (b), and pre-season (c) periods over Middle and Sub-Middle São Francisco.....	123
Figure 16: Station-wise mean monthly precipitation (mm) in the dry (a), rainy (b), and pre-season (c) periods over Upper São Francisco .....	124
Figure 17: Mean annual minimum (a) and maximum (b) temperature (°C) for the entire São Francisco River basin .....	124
Figure 18: Spatial variation of Z-value and trend showing grid points in four trend tests of minimum temperature data annual period over the São Francisco River Basin.....	125

Figure 19: Spatial variation of Z-value and trend showing grid points in four trend tests of maximum temperature data annual period over the São Francisco River Basin.....	126
Figure 20: Station-wise mean monthly minimum temperature (°C) in the dry (a), rainy (b), and pre-season (c) periods over Lower São Francisco .....	127
Figure 21: Station-wise mean monthly minimum temperature (°C) in the dry (a), rainy (b), and pre-season (c) periods over Middle and Sub-Middle São Francisco .....	127
Figure 22: Station-wise mean monthly minimum temperature (°C) in the dry (a), rainy (b), and pre-season (c) periods over Upper São Francisco.....	128
Figure 23: Station-wise mean monthly maximum temperature (°C) in the dry (a), rainy (b), and pre-season (c) periods over Lower São Francisco .....	129
Figure 24: Station-wise mean monthly maximum temperature (°C) in the dry (a), rainy (b), and pre-season (c) periods over Middle and Sub-Middle São Francisco .....	129
Figure 25: Station-wise mean monthly maximum temperature (°C) in the dry (a), rainy (b), and pre-season (c) periods over Upper São Francisco.....	130
Figure 26: Flow chart of data processing, SWAT model setup, and bias correction methodology .....	156
Figure 27: Slope (a), land-use (b), and soil type (c) maps of the São Francisco River Basin.....	159
Figure 28: Monthly hydrogram with data observed and simulated by the SWAT model in the calibration period (1966 – 2016) in the São Francisco Basin, considering stations 127 (A), 187 (B), and 268 (C).....	166
Figure 29: Mean monthly simulated streamflows for the future periods under RCPs scenarios	170

## List of tables

Table 1: Hydrologic soil groups (HSG) based on infiltration characteristics of the soils.....	44
Table 2: Classification of Hydrologic Soil Groups (HSG) for Brazilian soils.....	45
Table 3: Runoff curve numbers for agricultural lands. CN: Curve Number; HSG: Hydrologic Soil Group; HSC: Hydrologic Surface Condition.....	47
Table 4: Model Performance Ratings for monthly time-step.....	53
Table 5: Predominant climate characteristics for the São Francisco River basin (SFRB) according to Köppen’s classification .....	56
Table 6: The physical structure of the PISF. ....	57
Table 7: Land demand parameters.....	89
Table 8: Description of model components, temporal, and spatial resolution, selected determinant variables, and scenario assumptions regarding land use projections .....	91
Table 9: Percentage of spatial adjustment and errors .....	93
Table 10: The direction of change in land use change, according to classes and scenarios between 2010 and 2050 .....	97
Table 11: The mathematical equations and ideal values of performance metrics.....	108
Table 12: Methodology of entropy technique .....	109
Table 13: Sub-regions and stations for trend analysis in the dry, rainy, and pre-season periods	115
Table 14: SWAT input data used for the São Francisco River basin model setup.....	158
Table 15: The main characteristics of the main reservoirs considered in this study .....	160
Table 16: Most used Pedo-transfer Functions (PTF).....	160
Table 17: Used parameters in the calibration of the São Francisco River basin (sub-medium region) .....	162
Table 18: Average annual hydrological processes for the SFRB simulated by the SWAT model .....	168

## **List of acronyms**

ANA – National Water and Sanitation Agency

APAC – Pernambuco State Agency for Water and Climate

ARQ. – Architect

BESM – Brazilian Earth System Model

CanESM2 – The second-generation Canadian Earth System Model

CAPES – Brazilian Federal Agency for Support and Evaluation of Graduate Education

CHESF – Hydro Electric Company of São Francisco River basin.

Cmhyd model – *Climate Model Data for Hydrologic Modeling*

CNES – National Center for Space Study

CNPq – Brazilian National Council for Scientific and Technological Development

CONAB – National Supply Company

CPTEC – Center for Weather Forecasting and Climate Studies

Dr. – Doctor

DST – Department of Science & Technology

EMBRAPA – Brazilian Agricultural Research Corporation

Eta-MIROC5 – Model for Interdisciplinary Research on Climate, version 5

GCUB – Coimbra Group of Brazilian Universities

GIS – Geographic Information System

GRH – Water Resources Group

HadGEM2 – the Hadley Centre Global Environment Model version 2

IBGE – Brazilian Institute of Geography and Statistics

INMET – National Institute of Meteorology

INPE – National Institute for Space Research

IWRM – Integrated Water Resources Management

LuccME – Land Use and Cover Change (LUCC) Modeling Framework

LULC – Land-use and land-cover changes

MMA – Ministry of the Environment

MME – Multi-model Ensemble

MW – Megawatt

NASA – National Aeronautics and Space Administration

NRF – National Research Foundation

NSE – Nash-Sutcliffe Efficiency Coefficient

PBIAS – Percent Bias Statistic

PE – Pernambuco

PGEA – Graduate Programme in Agricultural Engineering

Ph.D. – Doctor of Philosophy

Prof. – Professor

$r^2$  – coefficient of determination

RCP – Representative Concentration Pathways

REA – Reliable Ensemble Averaging approach

SERGEO – Remote Sensing and Geoprocessing Laboratory

SFRB – São Francisco River Basin

sq km – square kilometers

SRTM – Shuttle Radar Topography Mission

SUFI-2 – Sequential Uncertainty Fitting Algorithm

SWAT – Soil and Water Assessment Tool

SWAT+ – Soil and Water Assessment Tool Plus

SWAT-CUP – Calibration Uncertainty Program for SWAT model

SWATplusCUP – Calibration Uncertainty Program for SWAT+ model

U.S. – United States

UFPE – Federal University of Pernambuco

UFRPE – Federal Rural University of Pernambuco

## Abstract

VASCO, Gabriel, 2023. **Modeling climate and land-use change impacts on water resources in the São Francisco River Basin, Brazil**. Thesis (Doctorate), Federal Rural University of Pernambuco, Recife – PE, Brazil.

Socio-global changes strongly affect water resources, impairing both water quantity and water quality worldwide. As demand hits the limits of supply, inter-sectoral competition increases, water quality declines and climate change represent an additional challenge for water resources management. Assessments of the hydrologic impacts of climate change and land-use change are, therefore, carried out around the world, including in Brazil. However, simultaneously effects of these two stressors on water resources are not often comprehensively investigated and need to be studied to evaluate the potential adaptability strategies of water resources management for coping with climate uncertainties. Therefore, in this thesis, the impacts of climate and land-use change on water resources were modeled to support water security policy in the São Francisco River Basin. **Chapter 1** addresses the general introduction of this thesis (containing the hypothesis, main and specific goals), and a literature review to better understand the state of the art, highlighting the importance of addressing water security concerns in the context of climate change and land use and land cover changes. **Chapter 2** describes how the developed land-use spatially explicit model through the LuccME modeling framework, was applied to forecast land-use scenarios for future pathways up to 2050. **Chapter 3** details how a total of nine Global Circulation Models (GCMs) were combined and termed as Multi-Model Ensemble (MME) using the Reliable Ensemble Averaging (REA) approach, which in turn was submitted for bias-correction using the CMhyd model, to address the underlying uncertainties in climate modeling. After that, the developed MME was applied for a statistical long-term trends analysis of observed gridded precipitation and temperature data using four no-parametric trend tests in annual, dry, rainy, and pre-season periods, being spatially interpolated using Inverse Distance Weighting (IDW) geostatistical technique. **Chapter 4** describes the evaluation of the impacts of climate change on water resources in the SFRB, considering two scenarios of greenhouse gas emissions: RCP 4.5 and RCP 8.5, and three time periods: short-, medium-, and long-term by the end of the 21<sup>st</sup>-century. Finally, **Chapter 5** contains the summary of the main findings, drawing comprehensive conclusions from this thesis. The results obtained in this thesis showed the feasibility of coupled land-use changes, hydrological, and climatic studies using spatially explicit, mathematical, and computational modeling, being promising for the water resources management of the São Francisco River basin. All the findings will serve as a basis for the development of more effective climatic adaptation strategies to ensure more coordinated management between different aspects of water issues which will be useful for the Integrated Water Resources Management Model (IWRM) for the selected watersheds of India, Brazil, and South Africa, under development within the ongoing multilateral BRICS project. Overall, the results achieved, and the lessons learned in this thesis can help researchers around the world to better understand how to couple different approaches to assess the combined impacts of land-use change and climate change on hydrological behavior and how to draw up the strategies for coping with its risks in different climatic conditions.

**Keywords:** water balance, hydrology, water resources management, climate data ensemble, trend analysis, temperature, precipitation, climate uncertainties, water security, SWAT model, land-use scenarios, São Francisco river basin.

## Resumo

VASCO, Gabriel, 2023. **Modelagem dos impactos das mudanças climáticas e do uso da terra sobre os recursos hídricos na Bacia do Rio São Francisco, Brasil**. Tese (Doutorado), Universidade Federal Rural de Pernambuco, Recife – PE, Brasil.

As mudanças socioglobais afetam fortemente os recursos hídricos, prejudicando tanto a quantidade quanto a qualidade da água em todo o mundo. À medida que a demanda atinge os limites da oferta, a concorrência intersetorial aumenta, a qualidade da água diminui e as mudanças climáticas representam um desafio adicional para a gestão dos recursos hídricos. Avaliações dos impactos hidrológicos das mudanças climáticas e do uso da terra são, portanto, realizadas em todo o mundo, inclusive no Brasil. No entanto, os efeitos simultâneos dos dois estressores sobre os recursos hídricos não são frequentemente investigados de forma abrangente e precisam ser estudados para avaliar as potenciais estratégias de adaptabilidade da gestão de recursos hídricos para lidar com as incertezas climáticas. Assim, nesta tese modelou-se os impactos das mudanças climáticas e do uso da terra nos recursos hídricos para subsidiar a política de segurança hídrica na bacia do rio São Francisco. O **capítulo 1** aborda a introdução geral desta tese (contendo a hipótese, objetivos principais e específicos), e uma revisão da literatura para melhor compreender o estado da arte, destacando a importância de abordar as preocupações de segurança hídrica no contexto das alterações climáticas, e mudanças do uso e ocupação da terra. O **Capítulo 2** descreve como o modelo desenvolvido de mudanças no uso da terra, usando a abordagem espacialmente explícita por meio da estrutura de modelagem LuccME, foi aplicado para prever cenários de uso da terra para caminhos futuros até 2050. O **Capítulo 3** detalha como nove Modelos Climáticos Globais e Regionais (GCM/RCMs) foram agrupados em um único modelo climático usando a abordagem *Reliable Ensemble Averaging* (REA), bem como, posteriormente, a correção de viés do multimodelo (MME) desenvolvido usando o modelo CMhyd. Além disso, uma análise estatística de tendências de longo prazo dos dados de precipitação e temperatura em grade observados usando quatro métodos diferentes em períodos anuais, secos, chuvosos e pré-estação foi feita e interpolada espacialmente usando a técnica geoestatística de Ponderação de Distância Inversa (IDW). O **Capítulo 4** descreve a avaliação dos impactos das mudanças climáticas nos recursos hídricos na bacia do rio São Francisco, considerando dois cenários de emissões de gases de efeito estufa: RCP 4.5 e RCP 8.5, e três períodos de tempo: curto, médio prazo e longo prazo até o final do século 21. Finalmente, o **Capítulo 5** contém o resumo dos principais achados, e conclusões abrangentes desta tese. Os resultados obtidos nesta tese mostraram a viabilidade de acoplar de estudos hidrológicos, climáticos e de mudanças de uso da terra, utilizando modelagem espacialmente explícita, matemática e computacional, sendo promissores para a gestão dos recursos hídricos da bacia do rio São Francisco. Todas as descobertas servirão de base para o desenvolvimento de estratégias de adaptação climática mais eficazes para garantir uma gestão mais coordenada entre os diferentes aspectos das questões hídricas, o que será útil para o Modelo Integrado de Gestão de Recursos Hídricos (GIRH) para as bacias hidrográficas selecionadas da Índia, Brasil e África do Sul, em desenvolvimento dentro do projeto multilateral BRICS em andamento. No geral, os resultados alcançados e as lições aprendidas nesta tese podem ajudar pesquisadores de todo o mundo a entender melhor como combinar diferentes abordagens para avaliar os impactos combinados das mudanças no uso da terra e das mudanças climáticas no comportamento hidrológico e como elaborar as estratégias para lidar com seus riscos em diferentes condições climáticas.

**Palavras-chave:** balanço hídrico, hidrologia, gestão de recursos hídricos, multimodelo, análise de tendências, temperatura, precipitação, incertezas climáticas, segurança hídrica, modelo SWAT, cenários de uso da terra, bacia do rio São Francisco.

–This page intentionally LEFT BLANK–

# **CHAPTER I**

---

**Background, general introduction,  
research hypotheses, objectives, and  
literature review**

## 1. Background and general introduction

Population growth and urbanization<sup>1</sup> are two of the main modulators of Water, Energy, and Food (WEF) nexus demands (FAO, 2011; FAO, 2015; UN, 2015a; YAN *et al.*, 2017), as the growing demand for human needs, raises pressure on resources.

It is predicted that by 2050 agricultural production may increase by up to 70% compared to the year 2000 so that it becomes possible to produce food for over 9 billion people worldwide (ALEXANDRATOS; BRUINSMA, 2012).

Because agriculture relies heavily on water, which is a scarce and finite resource, sustainable management is essential to reduce green water footprint (fraction of green water that is consumed by agricultural soils, for example, evapotranspiration from cultivation areas and permanent pastures), as well as the blue water footprint that represents the consumptive use of blue water sources (surface waters and groundwater bodies) (HOEKSTRA, 2003; HOEKSTRA *et al.*, 2011; ALDAYA *et al.*, 2012).

The global water footprint at the end of the 20<sup>th</sup> century was estimated at approximately 9000 km<sup>3</sup>/per year, where agriculture consumed 92%, and the remaining 8% was for industrial, domestic, and other sectors (HOEKSTRA and MEKKONEN, 2012). By 2050, demand for food production in developing countries is expected to increase by 100% (ROSEMARIN *et al.*, 2011), and global energy demand will increase by 36% by 2035 (IEA, 2014), while Brazil plans to triple electricity consumption by 2030 (MENDES; BELUCO; CANALES, 2017).

This will increase water demand (BIEMANS *et al.*, 2011), not only to supply energy production but also to several sectors that are heavily dependent on the water including economic activities, which will reach a demand of about 2,600 m<sup>3</sup>/s in 2030 (ANA, 2019).

Land use/cover changes are important due to their direct effects on the hydrological and ecological characteristics of the watershed (VIOLA *et al.*, 2014). These alter the soil water balance, with reflections in both superficial and sub-superficial layers (Kundu *et al.*, 2017), which may reduce the availability of water sources by silting (APARECIDO *et al.*, 2016), in addition to contributing to changes (increased temperature due to anthropogenic activities, the poor spatiotemporal distribution of precipitation, the occurrence of extreme climatic events, such as floods and droughts) (TUCCI, 2009; SOARES *et al.*, 2012; NAZEMI and MADANI, 2018).

These are not only the main modulators of water security, but also affect the average and variability of hydroclimatic systems, causing a series of socioeconomic and environmental impacts (HUSSEN; MEKONNEN; PINGALE, 2018; TAN and FOO, 2018).

---

<sup>1</sup>As stated by IBGE (2022), based on the 2012 demographic census, 61% of the Brazilian population were urban.

The above-mentioned modulators of water security have a considerable influence on land use/cover dynamics, mainly in the reservoir flow, with an increase or decrease in the volume of water (MARQUES, GUNKEL, and SOBRAL, 2019), an increase in changes in the socio-natural scenarios (ZHUANG *et al.*, 2017).

Increased temperatures, droughts, and floods affect global hydrology and have the potential to alter water availability for the water-food-energy nexus (GESUALDO *et al.*, 2019; SOLAUN and CERDÁ, 2019), in addition to contributing to the occurrence of multiple stressors that compromise the integrity of water resources and aquatic ecosystems (Molina-Navarro *et al.*, 2018), which places water security among the main socioeconomic and environmental challenges nowadays (BAJRACHARYA *et al.*, 2019).

Both climate change and land use can affect several demographic parameters and there may be interactive effects (OLIVER; MORECROFT, 2014), in complex ways through multiple hydrological, biophysical, and biochemical feedback (JIA *et al.*, 2022). Extensive studies have been devoted to climate and land use/cover changes impacts on water resources management in different regions around the world (ABDO *et al.*, 2009; NÓBREGA *et al.*, 2011; BRAVO *et al.*, 2014; KUNDU, KHARE, and MONDAL, 2017; GASHAW *et al.*, 2018; ZHUANG *et al.*, 2018; OLIVEIRA *et al.*, 2019).

The simultaneous effects of these two major global problems, in a multi-model ensemble approach, have not yet been extensively investigated, and proper research highly demands finding their relationships and impacts on the future (THAPA, 2021).

Therefore, even being challenging, it's imperative to assess the sensitivity and vulnerability of their impacts on water resources, as they are key factors in the dynamics of hydrological processes (MARHAENTO; BOOIJ; HOEKSTRA, 2018), to support the environmental and water resources policy decision-making (ABERA *et al.*, 2019).

In addition to the lack of knowledge on how to address the future challenges on ecosystem services listed by Francesconi *et al.* (2016), it is challenging to couple spatially explicit, hydrologic, and climatic modeling approaches (which converge to great potential) to assess the independent and/or combined impact of these two stressors on water resources (JONES and ELLIOTT, 2007; ZHANG *et al.*, 2014; ABBASPOUR *et al.*, 2015; FARJAD *et al.*, 2017; FU *et al.*, 2019).

This aims to support water resources decision-makers (MONTENEGRO *et al.*, 2014; EDUARDO *et al.*, 2016), since the prediction of climate change impacts, can generate previously mitigating measures to mainly avoid the desertification of risk areas in Brazil (LINS, 2022).

Therefore, it's in this context, that this research was directed, developing hydrological, climate, and land use change assessments on water resources through coupling different modeling approaches and multi-model ensemble.

This doctoral thesis aims to present information regarding the space-time dynamics of climate and land-use change, which can be fundamental for the development of flood warning systems for governmental agencies (e.g., the Integrated Disaster Information System – S2ID, a platform of the National System of Protection and Civil Defense). Through such systems, it will be possible to automatically inform (via SMS, emails, and phone calls) the estimated occurrence of possible floods in risk areas.

By proposing the development of warning systems to anticipate floods and flooding, this research seeks to contribute to addressing the challenge of the increasing occurrence of almost 39 thousand natural disasters in Brazil between 1991 and 2012 (84% of these disasters are associated with excess and lack of water), affecting approximately 127 million people and causing losses of R\$ 182.7 billion (SOUZA & OLIVEIRA, 2019).

It is expected that the design of these alert systems will contribute to anticipating the occurrence of natural disasters (such as floods), thus allowing mitigation actions to be anticipated by the competent sectors (e.g., National Center for Risk and Disaster Management – CENAD) and informing the population so that they can safeguard their property and lives. This will reduce the vulnerability of communities, the economy, and infrastructures to climate risks and natural and anthropogenic disasters.

Furthermore, this doctoral thesis aligns with the United Nations' Sustainable Development Goals (SDGs), particularly SDG 6: Clean Water and Sanitation, which aims to ensure water and sanitation availability and sustainable management for all.

Moreover, this research is conducted as part of the ongoing multilateral BRICS research project, titled “*Integrated Water Management Model for Brazil, India, and South Africa under climate change scenarios*” (BURI *et al.*, 2022). This project aims to develop a WebGIS environment, an Integrated Water Resource Management (IWRM) Modeling Framework, as stated by Ortiz-Partida *et al.* (2020), as an excellent approach to cope with future climate uncertainties.

## 1.1 Research hypothesis

- This research assumes the intensification of climate and land-use changes will directly impact water availability in the São Francisco River basin.

## 1.2 Objectives

### 1.2.1 General objective

- The main goal was to investigate/analyze the space-time dynamic of hydrological processes and trend impacts of future climate and land use changes on water resources for the São Francisco River basin, in Brazil.

### 1.2.2 Specific objectives

- a) Identify, on a regional scale, which environmental and socioeconomic factors are related to the dynamics of land use change, and analyze the location, intensity, and direction of change, using the LuccME spatially explicit land change modeling framework, considering the factors previously selected.
- b) Project land-use scenarios through a land-use spatially explicit model for the São Francisco River basin.
- c) Analyze the long-term trend of gridded precipitation and temperature data available using a bias-corrected multi-model and four different trend tests in annual, dry, wet, and pre-season periods.
- d) Assessment of climate and land-use change scenarios impacts on water resources under two RCPs.

## 1.3. Thesis structure

To answer the aforementioned established objectives, a series of studies were developed that are presented in chapters **II-IV** in the form of articles, written based on the following proposed manuscripts to be submitted for publication, as described below, and overviewed in Figure 1<sup>2</sup>:

**Chapter II:** Spatially explicit land-use scenarios for the São Francisco River Basin, Brazil. In this chapter, the LuccME modeling framework was applied to set up a LULC model used to project future pathways considering three scenarios, namely: the sustainable development scenario (SSP1 RCP 1.9), the middle of the road scenario (SSP2 RCP 4.5), and the strong inequality scenario

---

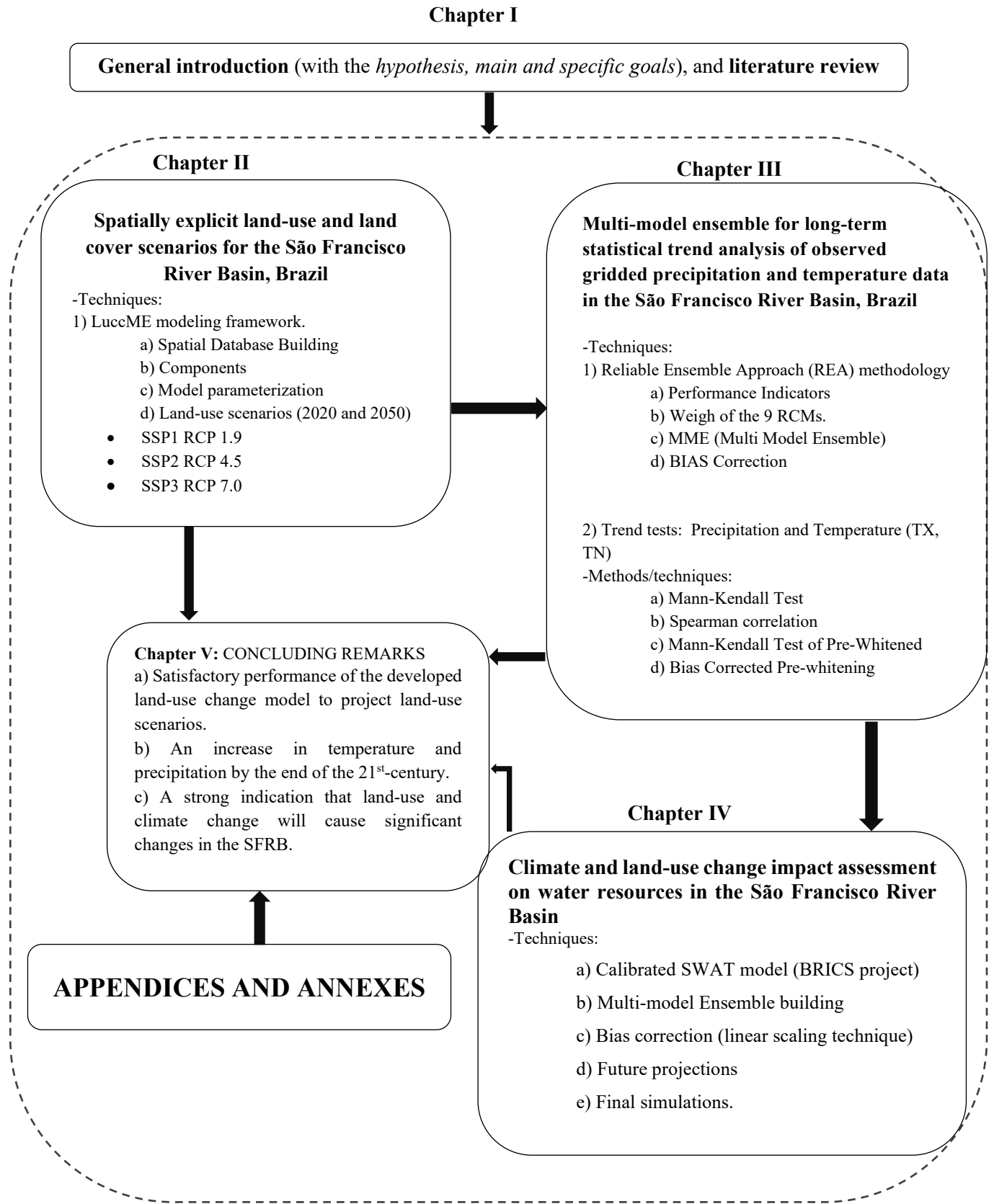
<sup>2</sup>Figure 1 presents a global overview of the topics covered in each chapter, focused on different proposed specific goals using different methodologies and correspondent databases. A summary of their respective contributions and the relationship between them is provided below at the end of this introductory chapter.

(SSP3 RCP 7.0). The projected scenarios represent a diverse range of biophysical, environmental, and socioeconomic assumptions about the future and capture a broad range of regional and gridded-level uncertainties typical in the current model, in line with the SSPs and RCPs described by Bezerra *et al.* (2022).

**Chapter III:** Multi-model ensemble for long-term statistical trend analysis of observed gridded precipitation and temperature data in the São Francisco River Basin, Brazil. This chapter analyzed the various uncertainties in the precipitation and temperature datasets of NASA Earth Exchange Global Daily Downscaled Projections (NEX-GDDP) under two Representative Concentrative Pathways (RCPs) 4.5 and 8.5 over the São Francisco River Basin, in Brazil. A total of nine Regional Climate Models (RCMs), namely, CAnESM2, CM5A-MR, CSIRO, EC-EARTH, GFDL-ESM2M, HadGEM2-ES, MIROC5, NORESM1, and SHMI-ESM, were ensembled using Reliable Ensemble Averaging (REA) approach. After that, the data were revised using the CMhyd model adopting the Linear Scaling bias correction technique of the ensemble climate model, followed by a trend analysis of precipitation, and the maximum and minimum temperature in the São Francisco River Basin. For this, were used four different no-parametric trend tests (Mann-Kendall, Mann-Kendall Test of Pre-Whitened, Bias Corrected Pre-whitening, Spearman correlation) in annual, dry, rainy, and pre-season periods (each one of) ten selected grids through Principal Component Analysis (PCA) methodology to detect trends in extreme climatic indices in the São Francisco River basin. To generate spatial plots, the inverse distance weighting (IDW) geostatistical interpolation technique was used by considering the Z-value of respective trend tests.

**Chapter IV:** Climate and land-use change impact assessment on water resources in the São Francisco River basin. The SWAT hydrological model used in this chapter was calibrated as part of the ongoing multilateral BRICS research project. In this chapter a computer-based, geospatial SWAT2009\_LUC tool, was used to integrate into a new and single shapefile of all developed three scenarios for dynamically updating land use changes being coupled to the ensembled climate data, aiming to evaluate the combined impacts of land-use change and climate change on water resources in the São Francisco River basin, considering two scenarios of greenhouse gas emissions: RCP 4.5 and RCP 8.5, and three-time periods: short-term (2011 to 2040), medium-term (2041 to 2070), and long-term (2071 to 2100).

Finally, **Chapter V:** the thesis concludes by providing a summary of the key findings, drawing overarching conclusions, and presenting recommendations as a way forward for future works.



**Chapter IV**

**Climate and land-use change impact assessment on water resources in the São Francisco River Basin**

-Techniques:

- a) Calibrated SWAT model (BRICS project)
- b) Multi-model Ensemble building
- c) Bias correction (linear scaling technique)
- d) Future projections
- e) Final simulations.

Figure 1: Overview and relationship of the main topics covered in this Ph.D. thesis

## 1.3 LITERATURE REVIEW

### 1.3.1 Integrated water resources management and water security concepts

The global surface freshwater availability is estimated between 9,000 and 14,000 km<sup>3</sup>, but only 4,200 km<sup>3</sup> is available for consumption and other related domestic activities (CANTÚ-MARTÍNEZ, 2012). Even so, worldwide societies face increasingly complex water-related problems that are characterized by high uncertainty about their sources and effects at diverse levels, scales, and temporalities (INGOLD and TOSUN, 2020).

About a billion people in developing countries do not have access to clean and safe drinking water (SILVA *et al.*, 2016), and a worldwide synthesis of water security considering human and biodiversity perspectives carried out by Vörösmarty *et al.* (2010), found that nearly 80% (4.8 billion) of the world's population lives in areas where either incident human water security or biodiversity threat exceeds the 75<sup>th</sup> percentile.

These problems range from water scarcity, floods, droughts, or water pollution, being heavily interrelated with issues of biodiversity, climate change, land use/cover changes, and socio-economic issues (VOGEL *et al.*, 2015). Thus, water depletion and pollution are the serious challenges of the 20<sup>th</sup> century due to anthropogenic, and climate change (TIWARI *et al.*, 2021).

Nonetheless, the rapid development of land use and climate change is expected to impact water insecurity to 1.8 million people by 2025 (WWDR, 2015), and affect aquatic ecosystems, landscape patterns and functioning of ecosystems, the ability of hydrological processes regulations in arid and semi-arid regions due to their fragile climatic conditions (GEBREMICAEL *et al.*, 2013; GWATE *et al.*, 2015; SHIRMOHAMMADI *et al.*, 2020).

Aiming to minimize the problem of water resources management, the World Summit on Sustainable Development in 2002, proposed an answer having appealed for the development of an integrated water resources management approach (HERING and INGOLD, 2012).

The IWRM approach is currently implemented as the dominant paradigm in developing countries (FULAZZAKY, 2014), for better coordination in an integrative manner during water resources management together with other natural resources (INGOLD *et al.*, 2016).

This process promotes the coordinated development and management of water, and related resources, to maximize the resultant economic and social welfare equitably without compromising the sustainability of the vital ecosystem. In the past decade, the most traditional dominant discourse

of the IWRM approach has been challenged by water security which has emerged as a new narrative on water governance (GERLAK and MUKHTAROV, 2015).

The concept of water security is a multi-faceted one and is interrelated with the broader frameworks and concepts related to water, characterizing the interactions between hydro-climatic conditions, ecosystem functioning, and societal needs (SCOTT *et al.*, 2013).

Among several proposed definitions (FALKENMARK and LUNDQVIST, 1998; LAUTZE and MANTHRITHILAKE, 2012; COOK and BAKKER, 2012), the concept of water security goes beyond the mere balance between water availability and water demand, having availability as the common denominator, access to an adequate quantity and quality of water for the population and industry, in addition to an acceptable level of risk due to extreme hydrometeorological impacts and environmental deterioration (ARREGUIN-CORTES *et al.*, 2019).

As a common denominator among all proposed definitions and their related methodologies, consider the availability and access to an adequate quantity and quality of water for the population and industry, along with an acceptable level of risk from the impacts of hydro-meteorological extremes and environmental deterioration (ARREGUIN-CORTES *et al.*, 2019).

The concept of water security can be seen as an extension of sustainable development thinking to water resources with a focus on the quantity and quality of water supply for societal and ecological needs (GERLAK and MUKHTAROV, 2015).

This brings together concepts related to water characterizing the interactions between water conditions, ecosystem functioning, and societal needs (SCOTT *et al.*, 2013). Thus, water security consists of having access to water in acceptable quantity and quality for health, livelihoods, ecosystems, and production, along with an acceptable level of water-related environmental and economic risks to people (GREY and SADOFF, 2007), besides water vulnerability in the face of threats from extreme weather events (GUNDA; BENNEYWORTH; BURCHFIELD, 2014).

This is an acceptable level of water-related risks for humans and ecosystems, together with water availability in sufficient quantity and quality to support livelihoods and ecosystem services, which makes water security one of the greatest socio-environmental and economic challenges of the 21st century (XIA *et al.*, 2007; BAKKER, 2012; BOGARDI *et al.*, 2012; SRINIVASAN; KONAR; SIVAPALAN, 2017).

However, applications of this type of study on a regional scale are also necessary, since achieving water security requires coordinating actors within the context of overarching water-

related standards and targets which may be optimally designed and set by higher orders of government (BAKKER and MORINVILLE, 2013).

Thus, in Brazil, the IWRM approach is based on river basin-scale management, and due to the multiple dominance of water bodies in a single Brazilian river basin, provided in Federal Law no. 9 433/1997, the harmonization of federal and state laws is required.

In addition, are also required the formulation of norms and procedures of the different water resources management agencies, aiming to meet the water security index for all the Brazilian micro basins, recently established by the National Water and Sanitation Agency from Brazil (ANA, 2019).

This will help to guide the investments of the Brazilian Water Security National Plan recently introduced in 2014 (RODRIGUES *et al.*, 2014), to prioritize the investment pathways in different sectors closely dependent on water (TEIXEIRA *et al.*, 2021).

### **1.3.2 Spatially explicit land-use changes**

The land use/land cover (LULC) changes have been identified as the main driving forces of local, regional, and global environmental changes (VERBURG *et al.*, 2015), and can be considered the primary force drive of the transformations of rural systems, bringing direct socioeconomic and environmental effects on rural sustainability (LONG and QU, 2018). For example, the need to meet the growing energy and food demand has created adverse impacts on the environment (VAN ASSELEN and VERBURG, 2013), especially in developing countries (including Brazil), that are striving for economic growth to sustain an ever-growing human population.

The land use/cover changes for the development of industrial activities, urbanization, intensification of agricultural practices, pasture, and mining, without any planning implies aggression to the environment (AREENDRAN *et al.*, 2013 and KARAKUS; CERIT; KAVAK, 2015), reduction of agricultural areas through the depletion of the productive capacity of the soil (RAWAT and KUMAR, 2015).

Vegetation cover is strongly associated with water quality in two main ways (FERREIRA *et al.*, 2019): i) reduction of soil erosion and sediment load and ii) filtering of contaminants by riparian vegetation. Water plays a crucial role in maintaining water availability, nutrient cycling, soil protection, temperature regulation, and maintenance of the water cycle, restoring water to the atmosphere through evapotranspiration (PONTES *et al.*, 2019).

However, knowledge of land use/cover is of strategic importance for any country as it provides spatial information for a better understanding of the spatio-temporal dynamics of the landscape, changes, and interactions between anthropogenic/industrial activities and natural phenomena (KARAKUS; CERIT; KAVAK, 2015).

The knowledge referred to above, assists in the definition of natural resource management policies (MARENCO *et al.*, 2018; ARMENTERAS *et al.*, 2019), management of agricultural practices and urbanization processes, monitoring of habitats and ecosystem services (MACEDO *et al.*, 2018), assistance in the management of water salinity (SINGH, 2018).

This includes the understanding of the soil water balance (VIOLA *et al.*, 2014), which is directly affected by land use/cover changes, through runoff, discharge, low flow occurrences, and other hydrological important processes (GUZHA *et al.*, 2018).

The increase of the computational capacity for spatial data acquisition and GIS advances, for high spatial-temporal resolution processing of satellite images, has allowed the development of functional models for more routine and consistent studies, including the simulation and modeling of dynamic land use/cover processes at different spatial and temporal scales (YANG *et al.*, 2003; ALMEIDA *et al.*, 2005; DEZHAKAM *et al.*, 2017).

For example, the application of remote sensing techniques (use of geospatial images to detect changes using multispectral satellite images) allows to support research (identify, map, and monitor), socio-environmental planning (e.g., the Spatio-temporal dynamics of land use/cover changes) in less time, low cost and with better precision (RAWAT and KUMAR, 2015).

And when coupled with GIS (SILVA, 2007) they have shown great potential to assist in the discrimination of elements of the landscape, in the planning and regulation of environmental changes, studies of land use and occupation, mapping of natural resources, spatialization of preservation areas (ZEILHOFER and TOPANOTTI, 2008), details on the selection of agricultural, urban and/or industrial areas (WONDRADE; DICK; TVEITE, 2014).

Land use/land cover (LULC) change models are powerful tools used to understand and explain the causes and effects of LULC dynamics, and scenario-based analyses with these models can support land management and decision-making better (REN *et al.* 2019).

Due to their vital role as computational laboratories for experiments to explore land system behavior (ROUNSEVELL *et al.*, 2012), these can provide a framework to address and separate the complex suite of biophysical and socioeconomic factors (VERBURG *et al.* 2004).

These facts make them useful research tools in land management, forecasting multiple land-use change conversions' effects (the rate, quantity, extent, and location) on climate change, landscape changes, carbon cycling, biodiversity, water budgets, and the provision of other critical ecosystem services (ALEXANDER *et al.*, 2017). They also can support the analyses of potential land-use changes under multiple scenarios and provide insights into land-use policymakers.

A wide array of land-use change models is currently available and under development worldwide; and even ranging from inductive or deductive, pattern- or agent-based, dynamic, or static, spatial, or non-spatial, and regional or global (REN *et al.*, 2019). These modeling approaches usually are implemented jointly and iteratively in practice.

Accordingly, among the five principal approaches reviewed by Ren et al. (2019), cellular-based models (combined with other modeling approaches to improve their availability and performance) have been widely used because of their simplicity, flexibility, and intuitiveness in reflecting spatiotemporal changes in land use patterns.

Besides Markov chains and logistic regression employed to quantify future land changes, and the spatial patterns determined by cellular models (ARSANJANI et al., 2013), neural networks and support vector machines are some novel techniques merged with cellular models to parameterize the various variables and define the transition rules (CHARIF *et al.*, 2017).

Furthermore, novel modeling frameworks, e.g., LANDSCAPE (LAND System Cellular Automata model for Potential Effects) and LLUC-CA (Local Land Use Competition Cellular Automata model) were developed to address issues such as allocation sequences and local effects within the neighborhoods (KE *et al.*, 2017; YANG *et al.*, 2016), to focus research on cellular-based models.

### **1.3.3 Climate change impacts**

The Intergovernmental Panel on Climate Change (IPCC, 2001), the main and worldwide scientific reference on the subject, defines the term “climate change” as a *statistically significant variation in the average conditions of the climate or in its variability, which persists for a long period. It may arise from natural processes or persistent anthropogenic changes in the composition of the atmosphere or land use.*

This dynamic force that transforms many aspects of the environment has the potential to impose additional pressures on almost all regions, can influence the configuration of regions of the

Earth, the structure of the soil, and consequently the occurrence of natural processes, such as extreme climatic, changes in solar radiation, and the Earth's orbital movements.

In recent decades, climate change has been one of the most and world widely topics debated by the scientific community, public decision-makers, and society in general. The concern with the issue is linked to the possible impacts that this phenomenon can cause on natural and socioeconomic systems (FERREIRA *et al.*, 2018).

The central concern with the issue is linked to the possible impacts that this phenomenon can have on natural and socioeconomic systems (FERREIRA *et al.*, 2018). According to Liu *et al.* (2017), climate change has been recognized as one of the main 21st-century environmental problems throughout the world, as it causes major impacts on water resources and agricultural productivity, especially in arid and semi-arid environments.

For what is high on the agendas of many international and national organizations, ranging from non-governmental organizations to the United Nations, international scientific research institutions, universities, and society in general.

The climate changes already observed and projected (increase in the average temperature of the planet, higher frequency of tropical storms, floods, heatwaves, droughts, snowstorms, hurricanes, tornadoes, and tsunamis) (WOOLWAY and MERCHANT, 2019), are making the hydrological cycle less predictable global impact and affected spatial-temporal variability, the intensity of rain events, and the associated risk of floods or droughts (FONTOLAN *et al.*, 2019). This may directly impact sectors that are heavily dependent on water, like domestic and industrial supply, generation hydropower, and agricultural practices (ABERA *et al.*, 2019; LUO *et al.*, 2019).

The expansion of energy consumption activities in the industry, places Brazil as the 9th largest consumer of electricity, with around 68% of installed capacity based on hydroelectricity (BODUNRIN *et al.*, 2018; KUWAJIMA *et al.*, 2019), and the São Francisco River basin has 94% of the installed hydroelectric capacity in Northeast Brazil, which represents 70% of the total electricity generation in this region (MARQUES; GUNKEL; SOBRAL, 2019).

However, this generation capacity is threatened due to climate change (JONG *et al.*, 2019), which requires greater investment to insert renewable sources of energy generation for electricity supply (MENDES; BELUCO; CANALES, 2017).

The global average surface temperature (continent and ocean), which increased by 0.85 °C between 1880-2012 (BERLATO and CORDEIRO, 2018), will affect evapotranspiration and

concomitantly the water demand for crops (GONDIM *et al.*, 2018), the poor spatial and temporal distribution of extreme weather events (FONTOLAN *et al.*, 2019), reduction in the number of precipitation days (CARVALHO *et al.*, 2020), significant change in the global hydrological cycle (ARNELL *et al.*, 1999; CHRISTENSEN *et al.*, 2004; ABDO *et al.*, 2009) and threats to biodiversity (NASCIMENTO *et al.*, 2019).

Summed the above-mentioned impacts, will increase inevitable consequences for the availability of freshwater for people and ecosystems in most regions that already suffer from water shortage (UKKOLA and PRENTICE, 2013), and more severe droughts in southwestern Australia, the southwestern United States, the Mediterranean (JENKINS and WARREN, 2015).

This will be also impactful in northeastern Brazil, where the estimate of economic losses caused by water-related disasters, between 1994 to 2015, was around R\$ 182.7 billion (KUWAJIMA *et al.*, 2019).

According to Lacerda *et al.* (2016), evidence of climate change was found in the State of Pernambuco showing increases in air temperature of up to 4 °C in the maximum daily temperature between 1961 and 2009; period in which there was an average reduction of 275 mm in precipitation (corresponding to 57% of the total) with the increase in the maximum periods of drought, from 20 to 35 days (NOBRE, 2011).

However, due to global warming in Brazil (which can increase from 3°C to 6°C by 2100, especially in North and Northeast regions), a situation that would be even more critical with a possible bad distribution of rainfall that can reach 45% (JONG *et al.*, 2018), and if combined with deforestation, burning in the biome, intensive land use/cover changes and deforestation (responsible for most greenhouse gas emissions in Brazil), can make northeast Brazil one of the most vulnerable in the world to climate change (MARENGO; TORRES; ALVES, 2017).

Its impacts on the economic performance of the agricultural sector and migration in the Brazilian semiarid can create situations of socioeconomic vulnerability (BARBIERI *et al.*, 2010; TORRES *et al.*, 2012; GONDIM *et al.*, 2018), and the flow of currents in semiarid regions (such as the São Francisco river basin) is particularly vulnerable to more frequent and intense prolonged droughts due to changes climate (JONG *et al.*, 2019), elements that require appropriate and consistent adaptation policy design, in response to the effects of climate change (as opposed to mitigation, which is what we do to prevent further climate change).

Founded in 1988 by the World Meteorological Organization (WMO) and the United Nations Environment Program (UNEP), the Intergovernmental Panel on Climate Change (IPCC), developed through data from the *Coupled Model Intercomparison Project Phase 5 (CMIP 5)* inter-comparison project, four climate change scenarios, representing four target levels of radiative forces - which take into account the conditions of air temperature, radiation, rain, and air humidity, the so-called *Representative Concentration Pathways (RCPs)*, namely: RCP 2.6 (very low priority level), RCP 4.5, RCP 6.0 (medium stabilization scenarios) and RCP 8.5 (scenario very high emission) corresponding to approximately 490, 650, 850, and 1,370 ppm, respectively, between 1961 and 2100 (TAN *et al.*, 2014; VAN VUUREN *et al.*, 2011).

- RCP 2.6 is a "very stringent" pathway. This was developed by the IMAGE (Integrated Model to Assess the Global Environment) modeling team at PBL Netherlands Environmental Assessment Agency, is the most optimistic, which will increase linearly until 2060, and will decrease and stabilize at the end of the century (CHOU *et al.*, 2014).
- RCP 4.5, developed by the modeling team at the JGCRI (Pacific Northwest National Laboratory's Joint Global Change Research Institute) in the USA, is considered an "intermediate" scenario, based on obtaining global forcing radiation of  $4.5 \text{ Wm}^{-2}$  and a stabilized  $\text{CO}_2$  concentration of 650 ppm by the end of the century.
- RCP 6.0, developed by the AIM modeling team at NIES (National Institute for Environmental Studies) in Japan, is a stabilization scenario in which the total radiative force is stabilized shortly after 2100, through the application of a series of technologies and strategies. to reduce greenhouse gas emissions.
- Finally, the radiative forcing RCP 8.5, developed using the MESSAGE model and the IIASA (International Institute for Applied Systems Analysis) integrated assessment framework in Austria, is a "pessimistic" scenario, characterized by an increase in solar radiation to  $8.5 \text{ Wm}^{-2}$ , with a probability of  $\text{CO}_2$  concentration reaching 1370 ppm and warming of approximately  $4^\circ\text{C}$  until the end of the 21<sup>st</sup> century (GESUALDO *et al.*, 2019).

#### **1.3.3.1 Bias correction methods**

The well-known four climate change scenarios, the so-called *Representative Concentration Pathways (RCPs)*, were developed based on the driving force, such as population growth, socio-economic development, and greenhouse gas emissions (MCGUIRE *et al.*, 2001 and WILLEMS *et*

*al.*, 2011) to examine their effects on either, hydrology and water resources in the global-, regional-, and local-scale (FEREIDOOON *et al.*, 2018).

Global Climate Models – GCMs or General Circulation Models, Atmosphere-Ocean Coupled Global Circulation Models – AOGCM, or even Earth System Models – ESM, are highly complex global-scale physic-mathematical representations of the terrestrial climate system, and their resolutions are generally too coarse to be useful for assessment of the future climate changes at local scales, for example, impacts on the watersheds (ANDRADE *et al.*, 2021).

To obtain this information, the IPCC uses coupled global models (ocean-atmosphere) aiming at a better scientific understanding of climate changes around the globe, still needing relevant projections on a regional scale (ALVES and MARENGO, 2010) as the outputs from GCMs and RCMs – such as precipitation and temperatures data – generally contain systematic errors and cannot be used directly in hydrological modeling, since they can generate significant deviations between simulated and observed data (CHEN *et al.*, 2016 and DE OLIVEIRA *et al.*, 2017).

The general procedure for assessing the impact of climate change on water resources is to first obtain climate change data through Global Circulation Models – GCM<sup>3</sup>; small-scale climate projections (from global to regional scale – e.g., Eta Regional Climate Model<sup>4</sup>) (MARENGO *et al.*, 2012 and FONTOLAN *et al.* 2019), followed by the insertion of the corrected data in the calibrated and validated hydrological model.

All three of these processes involve, for example, the uncertainties of the climate projection (GIORGI; MEARNS, 2002 and TEBALDI *et al.* 2005), the uncertainties in spatial resolutions that are excessively coarse (ranging from 100 to 300 km), and seasonal variations incorrect due to conceptual errors and discretization, which can generate significant deviations between observed and simulated data (underestimation or overestimation, respectively) (CROSBIE *et al.*, 2010 and SORRIBAS *et al.*, 2016), limiting their ability to assess the impacts of climate change on a regional scale (WOOD *et al.*, 2004; COOLEY and SAIN, 2010; CHOU *et al.*, 2014).

---

<sup>3</sup>Also known as Global Climate Models – GCM or General Circulation Models, Atmosphere-Ocean Coupled Global Circulation Models – AOGCM, or even Earth System Models – ESM, are physic-mathematical representations of the terrestrial climate system based on laws of conservation of mass, energy and momentum, and laws of thermodynamics and radiation (LIMA and AGHAKOUCHAK, 2017).

<sup>4</sup>Originally developed by INPE to provide projections of climate change (and its's impacts) in South America in high resolution. The model is configured with 20 km horizontal resolution and 38 layers in the vertical direction. Scale reductions are driven by global climate models MIROC5 and HadGEM2-ES, in the RCP 4.5 and RCP 8.5 greenhouse gas emission scenarios for the period between 1961 and 2100 (WANDERLEY, 2020).

However, this means that the outputs of the Global Circulation Models are not recommended for direct use in the study of regional hydrology, due to the uncertainties of the hydrological model parameters that arise from the equifinality of the model's parameter sets (BEVEN and FREER, 2001), quality and quantity of the available observation data used and the choice of the calibration period of the adopted hydrological model (SORRIBAS *et al.*, 2016).

Within this context, Regional Climate Models (RCMs: e.g., Eta) nested to Global Climate Models (GCMs: e.g., HadGEM2-ES and MIROC5) must be used to assess the potential impacts of climate change at regional scales (FONTOLAN *et al.*, 2019).

Among several methods to minimize the uncertainties of significant deviations between the observed and simulated data, nesting of the Regional Climate Models to the General Circulation Models (COOLEY *et al.*, 2010; CHOU *et al.*, 2014; GESUALDO *et al.*, 2019), distribution mapping ("quantile-quantile") (SORRIBAS *et al.*, 2016), spatial *downscaling* (dynamic or statistical) (CHEN *et al.*, 2011), and bias correction (trendline) from Global Circulation Models data (MARCHANE *et al.*, 2017), are some examples of techniques that can be useful to provide adequate spatial resolution and more detailed regional information for studies of climate change impacts on hydrological processes at a regional scale.

#### **1.3.4 Mathematical and hydrological modeling**

Despite the availability of more complex and sophisticated tools, due to the great interest in understanding global hydrology coupled with the analytical difficulties due to the complexity of representing the dynamics of the different processes that occur at the watershed level, several researchers and government agents have resorted to modeling tools (MCINTYRE *et al.*, 2014). They allow simplifying reality to isolate the most relevant variables and try to predict the phenomenon that interests us for decision-making.

Specifically, physical-based hydrological modeling tools provide information that is normally unavailable, given the technical difficulties and high costs of in situ data measurement, especially in the case of continuous monitoring on a large scale.

The models (i) assist in the understanding of hydrological processes and their relationship with other geophysical processes, and (ii) serve as a basis for Hydrological Forecast Systems aimed at reducing the vulnerability of the local population to extreme events.

The development of hydrological models has advanced a lot since the 1960s when a digital revolution took place worldwide that enabled the integration of different components of the hydrological cycle and simulation of almost the entire hydrographic basin scale (SINGH and WOOLHISER, 2002).

These are in constant development due to the increase in computational capacity, the new availability of remote sensing data (to feed these tools), and their integration with geographic information systems (ROUHOLAHNEJAD *et al.*, 2012; LOPES *et al.*, 2018), to quantify water availability under current and future conditions, to subsidize policies for integrated natural resources management.

There are currently hundreds of models available, which makes the choice a difficult process, that requires parsimony between the complexity of the model, its capacity, and its robustness (EISENBIES *et al.*, 2007).

Undoubtedly, the effectiveness of hydrological modeling largely depends on the choice of the appropriate hydrological model, whose selection depends on the research objectives, the availability of input data for its running, and the uncertainties in interpreting the output results obtained. Hence, hydrological models can be classified according to the types of variables used (stochastic or deterministic), the form of data representation (continuous or discrete), the existence or not of spatial relationships (lumped or distributed), and the type of relationships between the variables (empirical or conceptual/physical-based models) (BERTONI and TUCCI, 2007; FAN *et al.*, 2021).

Given the physical processes' representation and computational efficiency recently improved, these models have offered simulation capabilities on a local-, regional-, continental-, or even global-scale distributed information for water resource management (GAO *et al.*, 2010; YAMAZAKI; ALMEIDA; BATES, 2013; SOOD and SMAKHTIN, 2015; SIQUEIRA *et al.*, 2018), a fact that has reached some local relevance, as described in the "hyper-resolution" initiative by Wood *et al.* (2011) and Bierkens *et al.* (2015).

Worldwide, to date, there are numerous hydrological models developed to assess climate change (SORRIBAS *et al.*, 2016), land use/cover changes (CHU *et al.*, 2010; KUNDU *et al.*, 2017), including the impacts (of these stressors) on water resources (WIJESEKARA *et al.*, 2014; DOTTORI *et al.*, 2016; FALTER *et al.*, 2016; KOMI *et al.*, 2017; FLEISCHMANN, PAIVA, and COLLISCHONN, 2019), space-time connectivity of hydrological processes (KAUFFELDT *et al.*,

2016), biogeochemical cycles - natural processes in which chemical elements circulate between living beings and the environment (ZHANG *et al.*, 2002), water quality, to assess the effects of diffuse or even punctual pollution, through the simulation of nutrient cycles, effects of agricultural pesticides, discharge of sewers and self-cleaning in water bodies (HESSION and STORM, 2000; FAN *et al.*, 2015).

Among several hydrological models that have been developed to be used to aid water resources management (BONUMÁ *et al.*, 2015; DEVIA, GANASRI, and DWARAKISH, 2015); the SWAT (*Soil and Water Assessment Tool*) (ARNOLD *et al.*, 1996; ARNOLD *et al.*, 1998) has been highlighted by several studies (DOUGLAS- MANKIN *et al.*, 2010; BRESSIANI *et al.*, 2015; QIN *et al.*, 2018; ANDRADE *et al.*, 2018), as being computationally efficient to simulate medium and large hydrographic basins (>1 000 sq km) and continuous in time (ARNOLD *et al.*, 1996).

#### **1.3.4.1 The Watershed Model – Soil and Water Assessment Tool (SWAT)**

The Soil and Water Assessment Tool (SWAT), is a public domain, physical-based model (its equations are based on physical laws), semi-conceptual, distributed (its parameters depend on space or time), continuous over time (by simulating hydrological processes for periods greater than 50 years) originally developed by the United States Department of Agriculture, Agricultural Research Service (USDA-ARS) and Texas A&M AgriLife Research (ARNOLD *et al.*, 1998), and freely available at: <http://swat.tamu.edu/>.

History of its first version emerged in the early 1990s, as a result of SWRRB (Simulator for Water Resources in Rural Basins) model improvement (ARNOLD and WILLIAMS, 1987), which is the fusion of models such as Chemicals, Runoff, and Erosion from Agriculture Management Systems (CREAMS), Groundwater Loading Effects on Agricultural Management Systems (GLEAMS), and Environmental Impact Policy Climate (EPIC).

The SWAT hydrological model integrates water quality and quantity modules to study the environmental impacts at a high level of discretization of the hydrographic basin, based on the water balance equation (Equation 3) (ARNOLD *et al.*, 1998), comprising studies of evapotranspiration, infiltration, surface, and subsurface runoff (BRIGHENTI *et al.*, 2016), transport of pollutants, which include inorganic and organic forms of nitrogen (N) and phosphorus (P) (ARNOLD *et al.*, 2012).

Also, the SWAT hydrological model allows for quantifying the impacts of climate change on water resources, the interaction between the aquifer and runoff, evaluation of model parameters

with changes in land use and occupation, simulation of the space-time dynamics of hydrological and sedimentological processes for entire river basin (MOLINERO, 2013; ANDRADE; MELLO; BESKOW, 2013; ZHOU *et al.*, 2013; ZENG and CAI, 2014; RAPOSO; DAFONTE; BRESSIANI *et al.*, 2015).

$$SW_t = SW_0 + \sum_{i=1}^t (P - Q_s - ET - W_s - Q_{gw}) \quad \text{Eq. 3}$$

where,  $SW_0$  and  $SW_t$ , correspond to the initial and final soil water content in time  $t$  (mm);  $t$  is time (days),  $P$  is precipitation in time  $t$  (mm);  $Q_s$  is a surface runoff in time  $t$  (mm),  $ET$  is actual evapotranspiration in time  $t$  (mm),  $W_s$  is percolation in time  $t$  (mm);  $Q_{gw}$  is the baseflow in time  $t$  (mm) (ARNOLD *et al.*, 1998; NEITSCH *et al.*, 2011).

The hydrological component of the model includes runoff subroutines, percolation, infiltration, subsurface lateral flow, shallow aquifer flow, and evapotranspiration, as briefly schematized in Figure 2 (ABBASPOUR *et al.*, 2015). For the calculation of runoff, the model uses the modified SCS formula of Curve Number (USDA Soil Conservation Service, 1972) or the Green & Ampt infiltration method (GREEN and AMPT, 1911).

To calculate the runoff, the equation requires data precipitation daily and calculates infiltration as a function of the matric potential of the moisture front and effective hydraulic conductivity, assuming the profile of the soil is homogeneous and moisture foregoing is uniformly distributed in space (ARNOLD *et al.*, 1995).

Further, in this study was used the model standard method is the Penman-Monteith-FAO, which requires meteorological variables such as solar radiation, temperature, relative humidity, and wind speed (NEITSCH *et al.*, 2005).

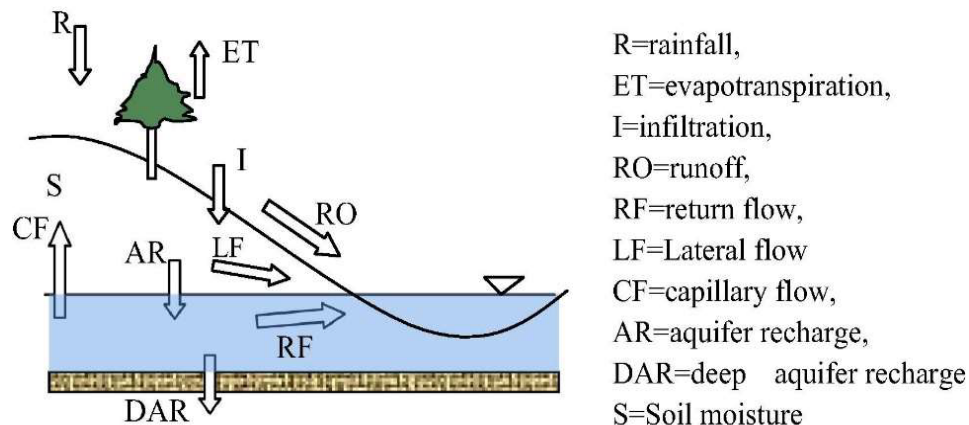


Figure 2: Scheme of the conceptual model of water balance in the SWAT hydrological model

Source: modified from Abbaspour *et al.* (2015)

The SWAT hydrological model uses the Curve Number method as the standard one, linked to the United States Department of Agriculture (SCS – USDA). From this method it is possible to perform an estimation of the surface runoff blade, considering precipitation data and parameters that characterize the basin (PRUSKI *et al.*, 2008).

According to the standardized Curve Number method, the accumulated precipitation varies linearly with time, that is, the precipitation intensity is considered constant for a given duration of rainfall, as presented in Figure 3. Then, until the time  $t_{Ia}$ , all the precipitation incident is converted into initial abstractions (including surface storage, interception, and infiltration before runoff), and after it ends, surface runoff begins (PRUSKI *et al.*, 2008).

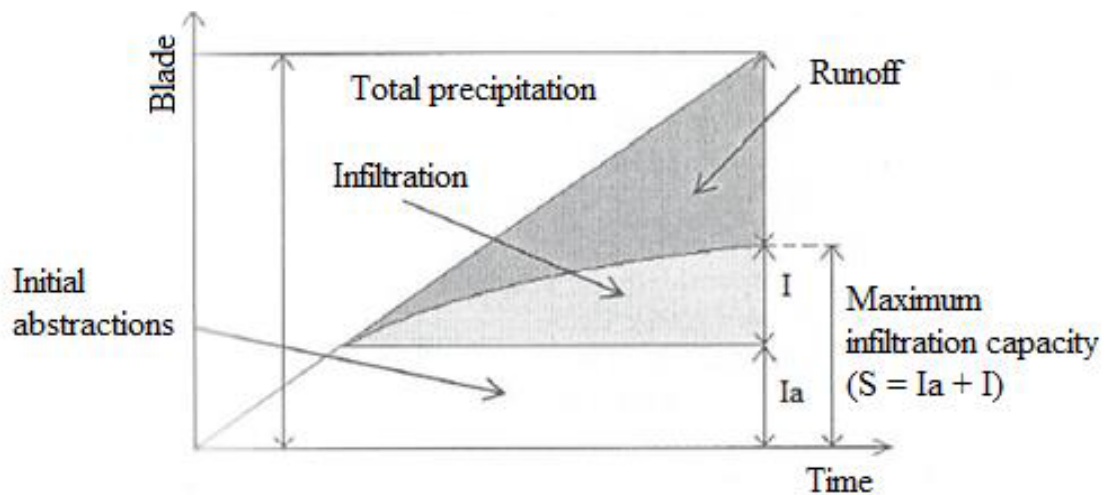


Figure 3: Components associated with the SWAT model standard Curve Number method – SCS

Source: modified from Pruski *et al.* (2008) apud Andrade (2018)

And based on The assessment, review, and hydrological reclassification of soils proposed by Lombardi Neto *et al.* (1989), provides a consistent basis for quantifying runoff under various types and uses of the soil, which according to Magalhaes *et al.* (2018), takes into account, in addition to hydraulic conductivity, characteristics such as depth, texture, the textural ratio between the surface and subsurface horizon and soil permeability influenced by its porosity and clay activity, including agricultural management practices (RALLISON and MILLER, 1982), where the number of curves varies non-linearly with the soil moisture content.

$$Q_{sup} = \frac{(R_d - I_a)^2}{(R_d - I_a + S)} \quad \text{Eq. 4}$$

where:  $Q_{sup}$  is the accumulated runoff or excess precipitation (mm H<sub>2</sub>O),  $R_d$  corresponds to the precipitated blade for the day (mm H<sub>2</sub>O),  $I_a$  includes surface storage, interception, and infiltration before discharge (mm H<sub>2</sub>O), commonly approximated to 20% of the soil water retention

parameter (S), which may vary spatially due to soil change, soil use, management, slope, and time due to changes in the content of soil water, which can be determined from equation 5.

$$S = 25.4 * \left( \frac{1000}{CN} - 10 \right) \quad \text{Eq. 5}$$

where: *S* is the parameter of water retention in the soil; CN is a soil permeability function, land use, and background water conditions on the ground, taking the moisture condition II with tabulated values by the Soil Conservation Service Engineering Division (CRONSHEY, 1986).

### 1.3.4.2. Hydrologic Soil Groups

Due to the extremely variable aspect of soil types, a new classification reflecting the influence of soil properties over the surface runoff was required by the NCRS method. Thereby, SCS (1972) and NRCS (1986) assumed that soil profiles with similar characteristics respond similarly to long-term rainfall and high intensity.

On the other hand, the Curve Number (CN) parameter varies as a function of soil permeability, land use, and soil antecedent moisture conditions, whose values are provided through tables by the SCS-USDA (placing soils in one of four hydrologic soil groups based on infiltration characteristics of the soils: A, B, C, and D, or three dual classes<sup>5</sup>, A/D, B/D, and C/D for certain wet soils that can be adequately drained), whose presented soil types are summarized in Table 1.

Table 1: Hydrologic soil groups (HSG) based on infiltration characteristics of the soils

HSG	Soil type description (characteristics)	Infiltration rate
A	Soils that have low runoff potential and high infiltration rate even when thoroughly wetted. Soils are well-drained to excessively drained sand or gravels, deep, with low levels of silt and clay.	> 7.62 mm.h <sup>-1</sup>
B	These types of soils are less permeable than type A, have a moderate infiltration rate when thoroughly wetted but with above-average permeability, and are moderately well-drained to well-drained soils.	3.81 to 7.62 mm.h <sup>-1</sup>
C	These are soils capable of generating above-average flow and low infiltration rates. They have a considerable amount of clay and are shallow.	1.27 to 3.81 mm.h <sup>-1</sup>
D	Soils with very low infiltration capacity when thoroughly wetted, resulting in a high runoff potential. Shallow soils contain expansive clays.	< 1.27 mm.h <sup>-1</sup>

Source: adapted from Neitsch *et al.* (2005) and Andrade (2018).

<sup>5</sup>The first letter applies to the drained condition, the second to the undrained. Only soils that are rated D in their natural condition are assigned to dual classes.

The SWAT model can determine the CN factor daily, with a numerical variation from 1 to 100, the lower limit being representative of fully permeable soil, and the upper limit (which can be considered fully impermeable), of soil that will convert all precipitation in flow throughout the entire watershed (NEITSCH *et al.*, 2011). According to Britto *et al.* (2014), the results of simulation with SWAT, which combines climatic, topographic, edaphic, and land use/cover change factors, are essential to assess the variation of hydrological conditions and can be applied efficiently in the development of basin management plans hydrographic.

As the flow equation proposed by SCS is an empirical method developed in the 1950s, the Curve Number (CN) method (Equation 4), was adapted by Sartori, Lombardi Neto, and Genovez (2005) to the Brazilian soil conditions and proposed 19 criteria for HSG soil classification based on a survey of 58 soil profile and hydrodynamic data in Brazil (Sartori, 2010), as described in Table 2.

Table 2: Classification of Hydrologic Soil Groups (HSG) for Brazilian soils.

Depth to the water table	Restrictive layer		Further soil characteristics	HSG
	Hard	Moderate		
> 100 cm			Sandy texture throughout the well-drained hydromorphic soil profile.	A
			Sandy or medium texture (< 20% clay) down to a restrictive layer.	
			Medium to very clayey texture, with low colloidal activity and high FeO content and/or acidic properties.	
> 100 cm	–	50 and 100 cm	Sandy or medium texture down to moderate restrictive layer and clay with low colloidal activity.	B
			Medium to very clayey texture, with low colloidal activity and high FeO content and/or acidic properties	
> 100 cm	–	≤ 50 cm	Sandy or medium texture down to moderate restrictive layer and clay with high colloidal activity.	C
			Sandy to very sandy texture with abrupt clayey change and low colloidal clay activity.	
> 100 cm	–	≤ 50 cm	Medium, clayey, or very clayey texture down to moderate restrictive layer and low clay colloidal activity.	C

				Sandy to very clayey texture with abrupt change and high clay colloidal activity.	D
				Clayey/clayey or clayey/very clayey texture, with low colloidal activity and a textural ratio of less than 1.5.	
				Medium/medium, medium/clayey, or clayey/very clayey texture, with low colloidal clay activity.	
				Clayey/very clayey texture, with low colloidal activity, low/medium FeO content, and non-acric.	B
> 100 cm	–	Absent		Incipient B horizon, with morphological characteristics similar to the subsurface ferralsol horizon.	
				Medium/medium, medium/clayey, or clayey/very clayey texture, with high colloidal clay activity.	C
				Medium/clayey, clayey/clayey, or clayey/very clayey texture and vertical horizon.	D
> 100 cm	50 and 100 cm	–		Sandy to very clayey texture, with low clay colloidal activity; or medium with high clay activity.	C
				Medium texture ( $\geq 20\%$ clay), clayey or very clayey, with high colloidal clay activity.	D
> 100 cm					
$\leq 100$ cm	–	–			D

Source: Sartori (2010).

### 1.3.4.3 Curve Number Values and Antecedent Runoff Conditions

When HSG is combined with land use/cover, soil treatment, and hydrological surface conditions, a hydrological soil-cover complex is formed (SCS, 1972; NRCS, 2002). Vegetation, crop residues, exposed soil, water, and impermeable surfaces are all included in land use classes. Land treatment is mainly focused on agricultural land and includes both mechanical practices such as contouring and terracing, as well as management practices like grazing control and crop rotation. Hydrological surface condition is typically labeled as poor, fair, or good. Arranged in three tables by the NRCS (2004), the various hydrological complexes are divided based on their characteristics in agricultural lands, urban areas, and arid/semiarid rangelands. Interpolated or calculated from

rainfall-runoff observances in American watersheds, each complex holds a unique mean CN value that mirrors its potential surface runoff.

Therefore, the CN (Curve Number) is a dimensionless index ranging from 0 (no runoff,  $S = \infty$ ) to 100 (all precipitation becomes runoff,  $S = 0$ ). In this study, all possible CN values were selected from NRCS (2004) tables, and then spatially assigned to hydrological soil-cover complexes in a GIS platform. A look-up table was built and used for geoprocessing the combination of HSG (assigned by soil type characteristics in Table 3) and land use/cover by MapBiomas collection 5.1 (NRCS, 1986).

Table 3: Runoff curve numbers for agricultural lands. CN: Curve Number; HSG: Hydrologic Soil Group; HSC: Hydrologic Surface Condition.

Cover description			CN for HSG			
Cover type	Treatment	HSC	A	B	C	D
Fallow	Bare soil	–	77	86	91	94
Forest*	–	Good	30	55	70	77
Pasture**	–	Good	39	61	74	80
Urban area***	–	–	77	85	90	92
Mosaic****	SR + CR	Good	67	78	85	89

\*Woods are protected from grazing, and litter and brush adequately cover the soil.

\*\*Pasture/grassland having the ground covered higher than 75%, and lightly or only occasionally grazed.

\*\*\*Townhouses by average lot size lower than 1/8 acres (506 m<sup>2</sup>) with 65% average impervious area.

\*\*\*\*Mosaic of agriculture cultivated in straight rows (SR) with pasture/crop residue (CR) cover.

Source: NRCS (2004).

The runoff potentiality before the surface runoff event is also considered in the SCS–CN method by the Antecedent Runoff Condition (ARC) index. Three ARCS are then considered, namely: ARC-I, which denotes the dry soils able to be plowed and cultivated; ARC-II, which denotes the moderately wet soils, mostly due to flood occurrence; ARC-III, which denotes the practically saturated soils, due to antecedent rainy events.

As stated by Hawkins et al. (2010), the ARC-II is the benchmark condition for obtaining the listed CN values (Table 3), whereas the dry (ARC-I) and wet (ARC-III) conditions are obtained by empirical equations for defined application ranges.

Plenty of empirical equation for ARC-I and ARC-III calculation are available in literature (Ajmal et al., 2015; Ajmal and Kim, 2015; Arnold et al., 1990; Chow, Maidment and Mays, 1988;

Hawkins, Hjelmfelt and Zevenbergen, 1985; Lal et al., 2016; Lal, Mishra, and Kumar, 2019; Mishra et al., 2008; Sobhani, 1975; Woodward et al., 2003).

Most of these equations may be obtained by fitting the parameters of Equation (6) – minimizing the sum of squared residuals – using rainfall-runoff datasets monitored or published in the literature. Lal, Mishra, and Kumar (2019) performed comparative analyses of different, well-known methods and three proposed methods, using data from 63 watersheds spread over almost all continents worldwide. The better performance was found by fitting Equations (4) and (5), from which CNI and CNIII ( $\lambda=0.03$ ) with Probability Of Exceedance (POE) equal to 12% and 88%.

$$CN = \frac{CN_{II}}{a - bCN_{II}}, \text{ where } b = \frac{(1-a)}{100} \quad \text{Eq. 6}$$

In this study, the CNI and CNIII values were determined under ARC-I and ARC-III conditions, respectively, by Equations (47) and (48) (Lal, Mishra, and Kumar, 2019). For selecting the proper condition, the 5-day-antecedent cumulative precipitations ( $P_{5d}$ , mm) were spatially calculated from ground-based and IMERG products. To this end, similarly to Ajmal et al. (2015), Ajmal and Kim (2015), and Lal, Mishra, and Kumar (2019), intervals were considered for distinguishing the ARC, and the  $P_{5d}$  values were calculated to determine them. For the Growing Season (GS, from March to July) and Dormant Season (DS, from August to February), the ARC intervals were the following: for ARC-I, if  $P_{5d} < 35.56$  mm (GS) or  $P_{5d} < 12.7$  mm (DS); for ARC-II, if  $35.56 \leq P_{5d} \leq 53.34$  mm (GS) or  $12.70 \leq P_{5d} \leq 27.94$  mm (DS); and, for ARC-III, if  $P_{5d} > 53.34$  mm (GS) or  $P_{5d} > 27.94$  mm (DS) (Chow, Maidment, and Mays, 1988; SCS, 1972). While the urban area and bare soil were considered only in DS condition, the forest was considered only in GS condition.

$$CN_{I,\lambda=0.03} = \frac{CN_{II,\lambda=0.03}}{2.42081 - 0.01421CN_{II,\lambda=0.03}} \quad \text{Eq. 7}$$

$$CN_{III,\lambda=0.03} = \frac{CN_{II,\lambda=0.03}}{0.42405 + 0.00576CN_{II,\lambda=0.03}} \quad \text{Eq. 8}$$

As shown in Equations (7) and (8), the CNII values must be obtained for  $\lambda$  equal to 0.03 instead of the conventional  $\lambda$  equal to 0.20 before estimating the surface runoff. Lal, Mishra, and Kumar (2019) found that in 61 out of 63 watersheds throughout the world, the  $\lambda$  was lower than 0.20, among which roughly 50% featured  $\lambda$  lower than 0.05. In Southern Brazil, da Costa et al. (2019) found that 67% of the rainfall events held  $\lambda$  lower than 0.06, whereas only 12% held  $\lambda$  higher than 0.20.

#### 1.3.4.4 SWAT model advances and limitations

Although this model has been expanding its boundaries in the scientific environment, as it has a modeling profile that encompasses several hydrological and agronomic components, assisting public agencies in decision-making in situations of conflict in land use and improvement (CHU *et al.*, 2005), some studies have identified several limitations (ARNOLD and FOHRER, 2005) and need to develop the model (KRYSANOVA and ARNOLD, 2008).

The limitations ranged from the incorrect explanation of the transport and deposition processes in the landscape, which are added to the level of the sub-basin and added directly to the entire basin of interest, making it difficult to accurately identify critical source areas and to place conservation practices and techniques within the sub-basin (BIEGER *et al.*, 2017).

To face present and future challenges in water resource modeling and management and motivated by the *U.S. Clean Water Act* and the *European Water Framework Directive* (which require the quantification of polluting loads in water bodies), the need to modify the SWAT code arose to streamline the development of the model, resulting in SWAT+ (BIEGER *et al.*, 2017), a completely revised version of SWAT, for improved simulation of landscape position, overland routing, and floodplain processes within the watershed.

Although it uses the SWAT model similar equations in estimating runoff and/or infiltration, evapotranspiration, plant growth, and routing, SWAT+ is considerably more flexible concerning the discretization and spatial configuration/representation of interactions and processes in the watershed, as summarized by Bieger *et al.* (2017), with the most important model modifications and their advantages.

The Hydrological Response Units (HRUs), channels, reservoirs, aquifers, lagoons, point sources, and inlets are spatially separate objects, whose hydrological interaction can be defined by the user so that it represents the physical characteristics of a hydrographic basin in the most realistic way possible. The decision tables introduced in the modified code allow the user to specify conditions for various management activities within the SWAT+ (ARNOLD *et al.*, 2018).

The SWAT+ model is considerably more flexible concerning the discretization and configuration of the basin, scenic drives, HRUs, aquifers, canals, reservoirs, ponds, and point sources of pollution are separate space objects that allow the separation of processes high ground of humid areas (BIEGER *et al.*, 2017), unlike the SWAT which divides into multiple sub-basins,

considering a single watercourse per sub-basin, which in turn is subdivided into an unlimited number of hydrological response units (HRU).

The HRU consists of an area, within the sub-basin, characterized by the same type of soil and land use, agricultural management, and slope classes (ARNOLD *et al.*, 2012).

As stated by Farias (2021), another important point of introducing the SWAT+ version is the possibility of adding space objects, such as channels, bombs, herds, and water rights, facilitating the integration with other sciences and modules into the SWAT+ algorithm to improve the detailed simulation of climate change and LULCC impacts on water resources.

#### **1.3.4.5 Sensitivity analysis, calibration, and model validation**

Like several predictive models, the ability of SWAT to simulate the hydrology of a watershed is assessed through calibration and validation processes (WHITE and CHAUBEY, 2005), which are quite critical, as the models present a series of uncertainties involved in a phenomenon as complex as the hydrological cycle processes.

However, it is necessary to carry out a sensitivity analysis to define which parameters most affect the model's responses, which according to Feyereisen *et al.* (2007), makes it possible to identify the input parameters that have the greatest effect (quantitative and qualitative) on the model output, allowing the establishment of the most sensitive set of parameters, which should be used in the calibration process (KANNAN *et al.*, 2007), disregarding the parameters identified as having less sensitivity (ABBASPOUR *et al.*, 2004), since they have less influence on the processes under analyzing.

The determination of the most sensitive parameters is the first step in the calibration and validation process of the model, which can be performed based on sensitivity analysis and/or expert opinion (ARNOLD *et al.*, 2012a). The sensitivity of hundreds of input variables in the SWAT model can be assessed using the IPEAT+ (YEN *et al.*, 2014; YEN *et al.*, 2019), SWAT-CUP (ABBASPOUR *et al.*, 2007; ARNOLD *et al.*, 2012).

The SWATplusCUP model is an independent *software* developed for sensitivity analysis, and model calibration and validation processes, which comprises five calibration procedures, as follows: *Generalized Likelihood Uncertainty Estimation* - GLUE, *Parameter Solution* - ParaSol, *Sequential Uncertainty Fitting Algorithm* - SUFI-2), Monte Carlo methods via Chains Markov (Markov chain Monte Carlo - MCMC) and Particle Swarm method (*Particle Swarm Optimization*

- PSO), and eleven objective functions, such as, mult, sum, NS, ssqr, PBIAS, KGE, RSR, MNS (ABBASPOUR *et al.*, 2015).

Among the calibration procedures previously mentioned, the SUFI-2 algorithm (ABBASPOUR; JOHNSON; VAN GENUCHTEN, 2004), which can be consulted in full in Abbaspour (2014), stands out for its speed and precision in processing, which consists of three major steps: modifying the values of the SWAT inputs, running the SWAT model, and extracting the desired output values, in addition to combining in the optimization of the objective function and analysis of uncertainties (ABBASPOUR *et al.*, 2007; MEHAN *et al.*, 2017) and deal with the smallest possible number of uncertainty, and with a large number of parameters in the calibration of a numerical forecasting model (VOUDOURI *et al.*, 2017).

For uncertainty analysis, the SUFI-2 algorithm considers the uncertainty in the input variables, the conceptual model, and the uncertainties in the parameters and measured data (MIRANDA *et al.*, 2017), verifying if the data of flow and/or index of the leaf area are inserted in 95% of uncertainty compared to the initial values (BRESSIANI *et al.*, 2015).

The degree to which all uncertainties are accounted for is quantified by a measure referred to as P-factor and R-factor, where the P-factor which is the percentage of measured data bounded by the 95% prediction uncertainty (95PPU), varies between 0 and 100%, while the R-factor is characterized by representing the average thickness of the 95PPU band divided by the standard deviation of the measured data, varying between 0 and infinite (ABBASPOUR, 2014), with the P-factor being 1 and the R-factor of 0 indicating a simulation that has a perfect fit (ABBASPOUR *et al.*, 2015).

The two measures that quantify the efficiency of a calibration and uncertainty analysis, evaluate the reliability of the adjustment and the degree of efficiency of the model calibrated for the uncertainties, which according to Abbaspour (2014), often a balance between the two values (factor -R and P-factor) must be achieved.

According to Abbaspour *et al.* (2015) among the eleven objective functions of SWAT-CUP, the most used to verify the performance of the model are clearly described as follows:

- i. Coefficient of determination ( $r^2$ ) (equation 9), which measures the linear association between two variables, with the value, obtained being dimensionless, ranging between 0 and 1 (MELO NETO *et al.*, 2014), where the forecast model will be more efficient if the coefficient of determination is closer to 1 (TUPPAD *et al.*, 2011).

$$\bullet \quad r^2 = \frac{[\sum_{i=1}^n (Q_{obs,i} - \bar{Q}_{obs})(Q_{sim,i} - \bar{Q}_{sim})]^2}{\sum_i (Q_{obs,i} - \bar{Q}_{obs})^2 \sum_i (Q_{sim,i} - \bar{Q}_{sim})^2} \quad \text{Eq. 9}$$

- ii. Nash- Sutcliffe Simulation Efficiency Coefficient (NSE) (equation 10), correlates two linear variables (making it possible to point out overestimated magnitudes) to indicate how much the model's predictions are better than those of a model that simply predicts the averages of the observed data (NASH and SUTCLIFFE, 1970), ranging from  $-\infty$  to 1, in which 1 represents a perfect fit between the observed and simulated data, while negative values indicate that the average of the observed data is a better predictor than the results of the model (LIN, CHEN, and YAO, 2017). On the other hand, Moriasi *et al.* (2007) report that values of  $0.75 < \text{NSE} \leq 1.00$  are considered an optimal fit and  $0.5 < \text{NSE} \leq 0.65$  as satisfactory.

$$\bullet \quad \text{NSE} = 1 - \frac{\sum_{i=1}^n (Q_{obs} - Q_{sim})^2 i}{[\sum_{i=1}^n (Q_{obs,i} - \bar{Q}_{obs})^2]} \quad \text{Eq. 10}$$

- iii. The Percent bias (PBIAS) (equation 11), on the other hand, indicates the average trend between the simulated values compared to those observed ones, and when a result is a positive number, it indicates an overestimation of the calculated variable and negative otherwise. The optimal fit value of PBIAS is 0.0, with low-magnitude values indicating accurate model simulation (MORIASI *et al.*, 2007), with the positive values of this objective function indicating a tendency to underestimate the simulated data, while the negative values indicate overestimation (VENZON; PINHEIRO; KAUFMANN, 2018).

$$\bullet \quad \text{PBIAS} = 100 \frac{\sum_{i=1}^n (Q_{obs} - Q_{sim}) i}{\sum_{i=1}^n (Q_{obs,i})} \quad \text{Eq. 11}$$

where:  $Q_{obs}$  is the observed discharge;  $Q_{sim}$  is the simulated discharge;  $\bar{Q}_{obs}$  is the mean observed discharge and  $\bar{Q}_{sim}$  is the mean simulated discharge.

In this thesis, the three (3) performance rating indices described above were adopted, to assess the performance of the SWAT model, within the range of variation summarized in Table 2 (MORIASI *et al.*, 2007), which considers the evaluation of the modeling at a time-step.

Table 4: Model Performance Ratings for monthly time-step

<b>Performance</b>	<b><math>r^2</math></b>	<b>NSE</b>	<b>PBIAS</b>
Very good	$0,80 < r^2 \leq 1,00$	$0,75 < NSE \leq 1,00$	$PBIAS < \pm 10$
Good	$0,70 < r^2 \leq 0,80$	$0,65 < NSE \leq 0,75$	$\pm 10 < PBIAS \leq \pm 15$
Satisfactory	$0,60 < r^2 \leq 0,70$	$0,50 < NSE \leq 0,65$	$\pm 15 < PBIAS \leq \pm 25$
Unsatisfactory	$r^2 \leq 0,60$	$NSE \leq 0,50$	$PBIAS \geq \pm 25$

Source: Moriasi *et al.* (2007)

## 1.4 STUDY AREA

With an area of around 640,000 km<sup>2</sup> (7.5% of Brazil), the São Francisco River basin was the site of the investigation, occupying the region between 7.2° – 21.1° S and 36.3° – 47.6° W, as shown in Figure 4. The region's variable precipitation patterns and biomes led to its classification into four physiographic regions: Upper (100,076 km<sup>2</sup> – 16%), Middle (402,351 km<sup>2</sup> – 63%), Sub-Middle (110,446 km<sup>2</sup> – 17%), and Lower São Francisco (25,523 km<sup>2</sup> – 4%).

The São Francisco River Basin has approximately 14,3 million inhabitants (71.74 inhabitants per square kilometer and about half located in the Upper São Francisco region) with a predominantly urban population, represented by 77% of the total population (ANA, 2018), distributed (in 503 municipalities) among seven Brazilian states, namely: Bahia (contains 48.2% of the SFB), Minas Gerais (36.8%), Pernambuco (10.9%), Alagoas (2.2%), Sergipe (1.2%), Goiás (0.5%), and part of the Federal District (0.2%) (TORRES *et al.* 2011).

Along the river, there are several large dams listed, and among eight reservoirs constructed up to the time of submission of this thesis (mid-June 2023): only, the five largest and main reservoirs are situated in the middle course of the São Francisco River.

In this thesis were considered the main reservoirs mentioned by Farias *et al.* (2023), are as follows: Luiz Gonzaga/Itaparica (3,549 hm<sup>3</sup>) and Sobradinho (28,669 hm<sup>3</sup>) located in the Sub-Middle São Francisco, Paulo Afonso I–IV (26,0 hm<sup>3</sup>) located in Upper São Francisco, Xingó (0,4028 hm<sup>3</sup>) located in the Lower São Francisco, clearly detailed by Vasco *et al.* (2022).

All of the aforementioned reservoirs are managed by Hydro Electric Company of São Francisco River basin (CHESF), and Três Marias (15,278 hm<sup>3</sup>), located in the Upper São Francisco and managed by CEMIG, a Belo Horizonte-headquartered power company, the capital city of Minas Gerais state.

A study developed by Fernandes (2015) highlighted the existence of 68 billion m<sup>3</sup> of water accumulated in reservoirs for electricity generation, human and industrial supply, flow regulation, improvement in river navigability, flood control, irrigation, tourism, recreation, and fishing enterprise. The important role of the São Francisco River is in generating electricity, with an installed potential of 10,708 MW by 2013 (to supply ~12% of the country's total) (BARRETO *et al.* 2020), where Luiz Gonzaga/Itaparica (1,479 MW), Sobradinho (1,050 MW), Paulo Afonso I–IV (2,462 MW) and Xingó (3,162 MW) are the largest hydroelectric plants (CBHSF, 2015).

This covers 94% of the installed capacity for hydroelectric power generation in Northeast Brazil, which represents approximately 70% of the total electric power generation capacity in this region (MARQUES; GUNKEL; SOBRAL, 2019). The vegetation cover within the São Francisco River basin is diverse: it includes the Atlantic Forest (headwaters), the Cerrado (Upper and Middle São Francisco), the Caatinga (Middle and Sub-Middle São Francisco), and the Atlantic Forest and native formations (mangrove and coastal vegetation) (Lower São Francisco) (BARRETO *et al.*, 2020; LUCAS *et al.*, 2021).

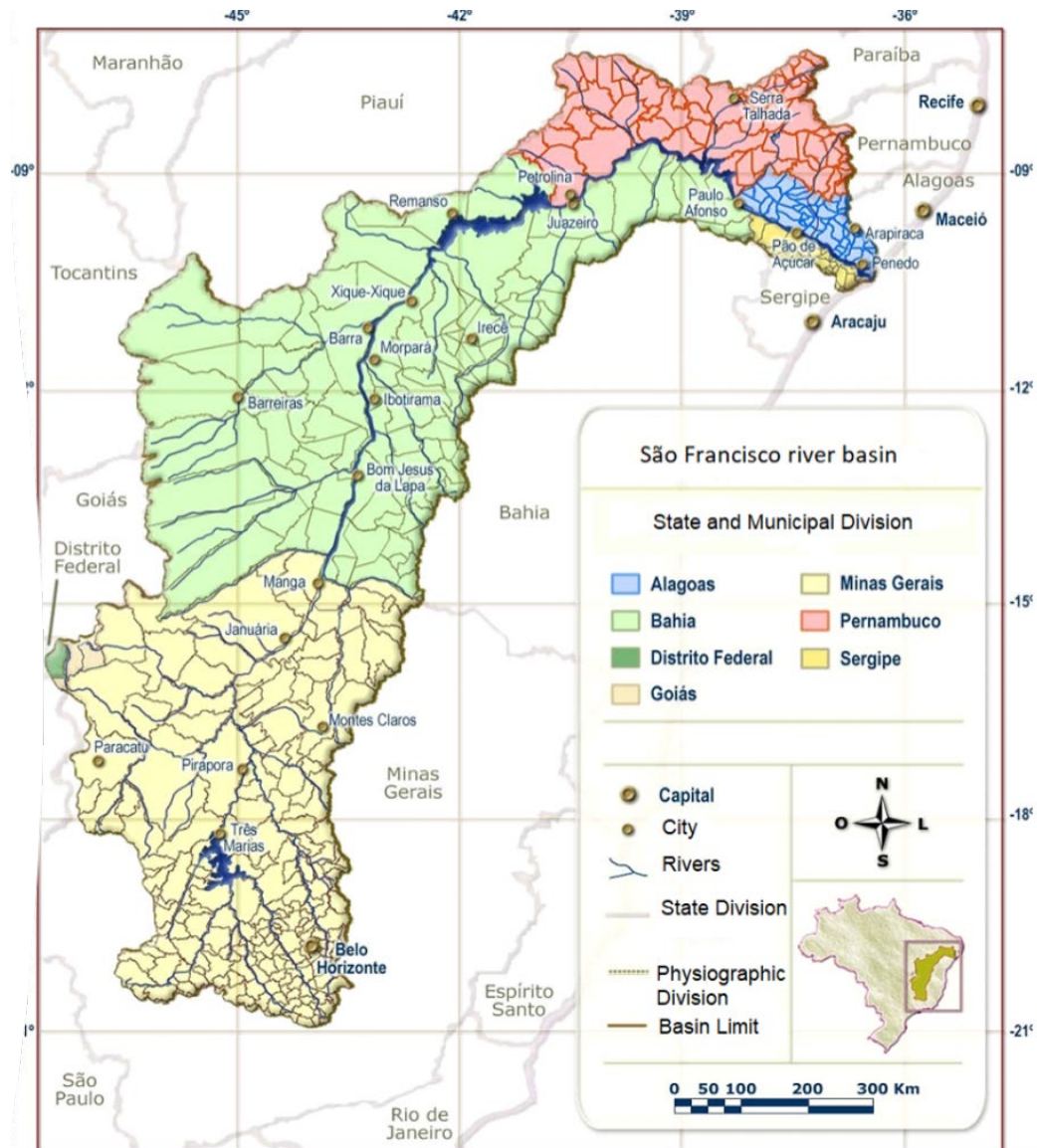


Figure 4: Geographic location map of the São Francisco River basin, Brazil

Source: modified from Matos and Zoby (2004).

The study area has soils suitable for the practice of irrigated agriculture in the Upper, Middle, and Lower São Francisco (MARQUES; GUNKEL; SOBRAL, 2019). The basin has 64 million hectares, of which 35.5 million hectares are arable, with greater concentration in the vicinity of valleys and urban areas, with 300 thousand hectares of irrigated crops, which represents only 10% of the potential of suitable areas for irrigation (FERNANDES, 2015), corresponding to 50.5% of water use (MARQUES; GUNKEL; SOBRAL, 2019).

The São Francisco River Basin presents the smallest rainfall indices relative to other semi-arid basins in Brazil, with annual precipitations around 938 mm, average annual temperatures of

23 to 27° C, an evaporation average of 2000 mm/year, and annual evapotranspiration of 896 mm (MARQUES; GUNKEL; SOBRAL, 2019), in addition to irregularity in onset as well as overall shortening of the rainy season, delay of the arrival of potentially useful rains, poor distribution of rainfall over the year, high temperatures, drought spells, and floods (CARVALHO *et al.*, 2020); as about 58% of the basin’s territory is within the semiarid region, mostly in northeastern Brazil (BARRETO *et al.* 2020).

Although the average precipitation is 938 mm year<sup>-1</sup> over the entire basin, there is a large variation in precipitation within the São Francisco River basin (LUCAS *et al.*, 2021), with November to January being the wettest quarter, contributing 55 to 60% of annual precipitation, while the driest quarter is from June to August. As summarized in Table 5, the São Francisco River basin presents different climate conditions according to Köppen’s classification.

Table 5: Predominant climate characteristics for the São Francisco River basin (SFRB) according to Köppen’s classification

<b>Region</b>	<b>Predominant climate characteristic</b>
Higher SFRB	Aw, type – hot and humid with summer rains.
Middle SFRB	Aw and BShw (semiarid).
Sub-Middle SFRB	BShw (semiarid) – with seven to eight dry months and an autumn rainfall regime with an annual total of about 550 mm, mainly concentrated between November and March.
Lower SFRB	As – hot and humid with winter rains, and BSh (semiarid with a short-wet season).

Source: CBHSF (2015), MARQUES; GUNKEL; SOBRAL (2019), and LUCAS *et al.* (2021)

The SFRB is the fourth-longest in Latin America and is popularly called “*the river of national integration*” not only because of the volume of transported water, linking southeast and northeast Brazil, but also because it crosses a variety of biomes, climates, landscapes, and socioeconomic statuses throughout its extension (LUCAS *et al.*, 2021), and national strategic importance due to its potential for agriculture, agribusiness, fishing, hydropower electricity, urban and industrial water supply, and tourism (TUCCI, 2005). This diversification in the use of its water resources recognizes the knowledge of hydrological and climatic characteristics for these uses to be optimized without degrading the environment (NASCIMENTO *et al.*, 2019) since the SFRB has faced serious water-related problems due to water conflicts for multiple uses and particularly its importance for food production by irrigation (LUCAS *et al.*, 2021).

### 1.4.1 The São Francisco River Transposition Project

The transposition project of the Sao Francisco River into the semi-arid watersheds of the Northeast region has been seen as a solution to the scarcity of water in the semi-arid for more than a century (MINISTÉRIO INTEGRAÇÃO NACIONAL, 2004), after a severe drought in the Northeast. The transposition project, termed PISF, is structured throughout 477 km comprising channels, tunnels, and aqueducts, and classified into two axes, North and East, as clearly detailed in table 6.

With an investment estimated at USD 2.85 billion (MDR, 2019), the PISF project aims to transport water from the São Francisco River at a flow of up to 127 m<sup>3</sup>/s, at 99 m<sup>3</sup>/s in the North Axis and 28 m<sup>3</sup>/s in the East Axis (GALDINO *et al.*, 2020), to branches that will supply to about 12 million people settled in 390 municipalities throughout the four Northeastern Brazilian states.

According to the Brazilian Ministry of Integration, the São Francisco River integration project will assure the supply needs of municipalities in the semi-arid region, Agreste Pernambucano, and Fortaleza Metropolitan region and would be the solution to the problems brought about by the scarcity of water and severe droughts.

Table 6: The physical structure of the PISF.

	North Axis	East Axis	Total
Distance	260 km	217 km	477 km
Pumping stations (EB)	3	6	9
Installed pumps (Stage 1)	6	12	18
Predicted pumps (Stage 2)	24	24	48
Flow rate	99 m <sup>3</sup> /s	28 m <sup>3</sup> /s	127 m <sup>3</sup> /s
Substations	230 kV/6.9 kV	69 kV/6.9 kV	-
	8	1	9
Transmission lines (230 kV)		250 km	
Distribution lines		6.9 kV, 13.8 kV and 69 kV	
Aqueducts		13	
Tunnels		4	
Reservoirs		27	
Recovered weirs		23	

Source: GALDINO *et al.* (2020).

The PISF project was not the focus of this study, although its significance cannot be overlooked as it has the potential to spur development in Northeastern Brazil and provide access to electricity and water. It is suggested that future research incorporate the PISF project to better

understand the impact of climate and land-use changes in the SFRB, ultimately ensuring water security stated by Galdino *et al.* (2020).

## References

- ABBASPOUR, K. C. SWAT-CUP 2012: SWAT Calibration and Uncertainty Programs—A User Manual: Swiss Federal Institute of Aquatic Science and Technology. 2014.
- ABBASPOUR, K. C., ROUHOLAHNEJAD, E., VAGHEFI, S., SRINIVASAN, R., YANG, H., KLØVE, B. A continental-scale hydrology and water quality model for Europe: Calibration and uncertainty of a high-resolution large-scale SWAT model. **Journal of Hydrology**, v. 524, p. 733-752, 2015.
- ABBASPOUR, K.C.; YANG, J.; MXIMOV, I.; SIBER, R.; BOGNER, K.; MIELEITNER, J.; ZOBRIST, J.; SRINIVASAN, R. Modelling hydrology and water quality in the pre-alpine/alpine Thur watershed using SWAT. **Journal of Hydrology**, v. 333, n. 2-4, p. 413-430, 2007.
- ABBASPOUR, Karim C.; JOHNSON, C. A.; VAN GENUCHTEN, M. Th. Estimating uncertain flow and transport parameters using a sequential uncertainty fitting procedure. **Vadose Zone Journal**, v. 3, n. 4, p. 1340-1352, 2004.
- ABDO, K. S., FISEHA, B. M., RIENTJES, T. H. M., GIESKE, A. S. M., HAILE, A. T. Assessment of climate change impacts on the hydrology of Gilgel Abay catchment in Lake Tana basin, Ethiopia. **Hydrological Processes: An International Journal**, v. 23, n. 26, p. 3661-3669, 2009.
- ABERA, W., TAMENE, L., ABEGAZ, A., SOLOMON, D. Understanding climate, and land surface changes impact on water resources using Budyko framework and remote sensing data in Ethiopia. **Journal of Arid Environments**, v. 167, p. 56-64, 2019.
- AJMAL, M. et al. Investigation of SCS-CN and its inspired modified models for runoff estimation in South Korean watersheds. **Journal of Hydro-Environment Research**, v. 9, n. 4, p. 592–603, 2015.
- AJMAL, M.; KIM, T.-W. Quantifying excess stormwater using SCS-CN–based rainfall runoff models and different Curve Number determination methods. **Journal of Irrigation and Drainage Engineering**, v. 141, n. 3, p. 1–12, 2015.

- ALDAYA, M. M., CHAPAGAIN, A. K., HOEKSTRA, A. Y., MEKONNEN, M. M. **The water footprint assessment manual: Setting the global standard**. Routledge, 2012.
- ALEXANDER, Peter et al. Assessing uncertainties in land cover projections. **Global change biology**, v. 23, n. 2, p. 767-781, 2017.
- ALEXANDRATOS, Nikos; BRUINSMA, Jelle. World agriculture towards 2030/2050: the 2012 revision. 2012.
- ALMEIDA, C. M. D., MONTEIRO, A. M. V., CÂMARA, G., SOARES-FILHO, B. S., CERQUEIRA, G. C., PENNACHIN, C. L., BATTY, M. GIS and remote sensing as tools for the simulation of urban land-use change. **International Journal of Remote Sensing**, v. 26, n. 4, p. 759-774, 2005.
- ALVES, Lincoln M.; MARENGO, José. Assessment of regional seasonal predictability using the PRECIS regional climate modeling system over South America. **Theoretical and Applied Climatology**, v. 100, n. 3, p. 337-350, 2010.
- ANA – Agência Nacional de Águas. 2018. Accessed on June 4<sup>th</sup>, 2021. Available: <http://www.snirh.gov.br/hidroweb/serieshistoricas>.
- ANA – Agência Nacional de Águas. Conjuntura dos Recursos Hídricos no Brasil 2019: Informe Anual; Agência Nacional de Águas: Brasília, Brazil, 2019.
- ANA – Agência Nacional de Águas. **Plano Nacional de Segurança Hídrica**. Agência Nacional de Águas. Brasília, ISBN: 978-85-8210-059-2, 2019. 112p.
- ANDRADE, C. W. L. **Hydrological modeling and scenarios of land use and climate changes in a representative basin, northeastern Brazil**. 2018. Doctoral Thesis (Universidade Federal Rural de Pernambuco). 161p.
- ANDRADE, C. W., MONTENEGRO, S. M., MONTENEGRO, A. A., LIMA, J. R. D. S., SRINIVASAN, R., JONES, C. A. Soil moisture and discharge modeling in a representative watershed in northeastern Brazil using SWAT. **Ecohydrology & Hydrobiology**, v. 19, n. 2, p. 238-251, 2018.
- ANDRADE, Carolyne WL, et al. Climate change impact assessment on water resources under RCP scenarios: A case study in Mundaú River Basin, Northeastern Brazil. **International Journal of Climatology**, 2021, 41: E1045-E1061.

- ANDRADE, Márcio A.; MELLO, Carlos R. de; BESKOW, Samuel. Simulação hidrológica em uma bacia hidrográfica representativa dos Latossolos na região Alto Rio Grande, MG. **Revista brasileira de engenharia agrícola e ambiental**, v. 17, n. 1, p. 69-76, 2013.
- APARECIDO, C. F. F.; VANZELA, L. S.; VAZQUEZ, G. H.; LIMA, R. C. Manejo de bacias hidrográficas e sua influência sobre os recursos hídricos. **Irriga**, v. 21, n. 2, p. 239, 2018.
- AREENDRAN, G., RAO, P., RAJ, K., MAZUMDAR, S., PURI, K. Land use/land cover change dynamics analysis in mining areas of Singrauli district in Madhya Pradesh, India. **Tropical Ecology**, v. 54, n. 2, p. 239-250, 2013.
- ARMENTERAS, D., MURCIA, U., GONZÁLEZ, T. M., BARÓN, O. J., ARIAS, J. E. Scenarios of land use and land cover change for NW Amazonia: Impact on forest intactness. **Global Ecology and Conservation**, v. 17, p. e00567, 2019.
- ARNELL, Nigel W. Climate change, and global water resources. **Global environmental change**, v. 9, p. S31-S49, 1999.
- ARNOLD, J. G. et al. **SWRRB: a basin scale simulation model for soil and water resources management**. Colege Station: Texas A&M University Press, 1990.
- ARNOLD, J. G., KINIRY, J. R., SRINIVASAN, R., WILLIAMS, J. R., HANEY, E. B., NEITSCH, S. L. Soil, and water assessment tool input/output documentation version 2012. **Texas Water Resources Institute**, v. 7, 2012.
- ARNOLD, J. G., SRINIVASAN, R., MUTTIAH, R. S., WILLIAMS, J. R. Large area hydrologic modeling and assessment part I: model development 1. **JAWRA Journal of the American Water Resources Association**, v. 34, n. 1, p. 73-89, 1998.
- ARNOLD, J. G.; ALLEN, P. M.; MUTTIAH, R. S.; BERNHARDT, G. Automated baseflow separation, and recession analysis techniques. **Groundwater**, v. 33, n. 6, p. 1010-1018, 1995.
- ARNOLD, J. G.; WILLIAMS, J. R.; SRINIVASAN, R.; KING, K. W. The soil and water assessment tool (SWAT) user's manual. **Temple, TX**, 1996.
- ARNOLD, J.G.; BIEGER, K.; WHITE, M.J.; SRINIVASAN, R.; DUNBAR, J.A.; ALLEN, P.M. Use of decision tables to simulate management in SWAT+. **Water**, v. 10, n. 6, p. 713, 2018.
- ARNOLD, J.G.; MORIASI, D.N.; GASSMAN, P.W.; ABBASPOUR, K.C.; WHITE, M.J.; SRINIVASAN, R.; SANTHI, C.; HARMEL, R.D.; VAN GRIENSVEN, A.; VAN LIEW,

- M.W.; KANNAN, N.; JHA, M.K. SWAT: Model use, calibration, and validation. **Transactions of the ASABE**, v. 55, n. 4, p. 1491-1508, 2012.
- ARNOLD, Jeffrey G.; FOHRER, Nicola. SWAT2000: Current capabilities and research opportunities in applied watershed modeling. **Hydrological Processes: An International Journal**, v. 19, n. 3, p. 563-572, 2005.
- ARREGUIN-CORTES, F. I., SAAVEDRA-HORITA, J. R., RODRIGUEZ-VARELA, J. M., TZATCHKOV, V. G., CORTEZ-MEJIA, P. E., LLAGUNO-GUILBERTO, O. J., SAINOS-CANDELARIO, A., SANDOVAL-YOVAL, L., ORTEGA-GAUCIN, D., MENDOZA-CAZARES, E. Y., NAVARRO-BARRAZA, S. Municipal level water security indices in Mexico. **SN Applied Sciences**, v. 1, n. 10, p. 1194, 2019.
- ARSANJANI, Jamal Jokar et al. Integration of logistic regression, Markov chain, and cellular automata models to simulate urban expansion. **International Journal of Applied Earth Observation and Geoinformation**, v. 21, p. 265-275, 2013.
- BAJRACHARYA, R. M., DAHAL, N., NEUPANE, K. R., SINGH, V., HABEEB, R. Urban water security challenges in the Nepal and Indian Himalaya in the context of climate change. **Resources and Environment**, v. 9, n. 1, p. 9-18, 2019.
- BAKKER, Karen. Water security: research challenges and opportunities. **Science**, v. 337, n. 6097, p. 914-915, 2012.
- BARBIERI, A. F., DOMINGUES, E., QUEIROZ, B. L., RUIZ, R. M., RIGOTTI, J. I., CARVALHO, J. A., RESENDE, M. F. Climate change and population migration in Brazil's Northeast: scenarios for 2025–2050. **Population and Environment**, v. 31, n. 5, p. 344-370, 2010.
- BARRETO, I. D. de C. et al. Complexity analyses of Sao Francisco River streamflow: influence of dams and reservoirs. **Journal of Hydrologic Engineering**, v. 25, n. 10, p.1–8, 2020.
- BERLATO, Moacir Antonio; CORDEIRO, Ana Paula Assumpção. Sinais de mudanças climáticas globais e regionais, projeções para o século XXI e as tendências observadas no Rio Grande do Sul: uma revisão. **Agrometeoros**, v. 25, n. 2, 2018.
- BERTONI, J. C.; TUCCI, C. E. M. Hidrologia: ciência e aplicação. **Porto Alegre: UFRGS**, p. 177-241, 2007.

- BEVEN, Keith; FREER, Jim. Equifinality, data assimilation, and uncertainty estimation in mechanistic modelling of complex environmental systems using the GLUE methodology. **Journal of Hydrology**, v. 249, n. 1-4, p. 11-29, 2001.
- BIEGER, K., Arnold, Jeffrey G., RATHJENS, H., WHITE, Michael J., BOSCH, David D., ALLEN, Peter M., VOLK, M., SRINIVASAN, Raghavan. Introduction to SWAT+, a completely restructured version of the soil and water assessment tool. **JAWRA Journal of the American Water Resources Association**, v. 53, n. 1, p. 115-130, 2017.
- BIEMANS, H., HADDELAND, I., KABAT, P., LUDWIG, F., HUTJES, R., HEINKE, J., VON BLOH, W., and Gerten, D. Impact of reservoirs on river discharge and irrigation water supply during the 20th century. **Water Resources Research**, v. 47, n. 3, 2011.
- BIERKENS, Marc FP et al. Hyper-resolution global hydrological modeling: What is next? “Everywhere and locally relevant”. **Hydrological processes**, v. 29, n. 2, p. 310-320, 2015.
- BODUNRIN, Michael O. et al. The availability of life-cycle assessment, water footprinting, and carbon footprinting studies in Brazil. **The International Journal of Life Cycle Assessment**, v. 23, n. 8, p. 1701-1707, 2018.
- BOGARDI, J. J., DUDGEON, D., LAWFORD, R., FLINKERBUSCH, E., MEYN, A., PAHL-WOSTL, C., VIELHAUER, K., VÖRÖSMARTY, C. Water security for a planet under pressure: interconnected challenges of a changing world call for sustainable solutions. **Current Opinion in Environmental Sustainability**, v. 4, n. 1, p. 35-43, 2012.
- BONUMÁ, N. B., REICHERT, J. M., RODRIGUES, M. F., MONTEIRO, J. A. F., ARNOLD, J. G., SRINIVASAN, R. Modeling surface hydrology, soil erosion, nutrient transport, and future scenarios with the ecohydrological SWAT model in Brazilian watersheds and river basins. **Tópicos Ci. Solo**, v. 9, p. 241-290, 2015.
- BRAVO, J. M., COLLISCHONN, W., DA PAZ, A. R., ALLASIA, D., DOMEQ, F. Impact of projected climate change on the hydrologic regime of the Upper Paraguay River basin. **Climatic change**, v. 127, n. 1, p. 27-41, 2014.
- BRESSIANI, D., GASSMAN, P. W., FERNANDES, J. G., GARBOSSA, L. H. P., SRINIVASAN, R., BONUMÁ, N. B., MENDIONDO, E. M. Review of soil and water assessment tool (SWAT) applications in Brazil: Challenges and prospects. **International Journal of Agricultural and Biological Engineering**, v. 8, n. 3, p. 9-35, 2015.

- BRIGHENTI, Tássia Mattos; BONUMÁ, Nadia Bernardi; CHAFFE, Pedro Luiz Borges. Calibração hierárquica do modelo swat em uma bacia hidrográfica Catarinense. **Revista Brasileira de Recursos Hídricos**, v. 21, n. 1, p. 53-64, 2016.
- BRITTO, F. B., MENEZES NETO, E. L., NETTO, A., REGO, N. Sustentabilidade hídrica da Sub-bacia do Rio Sangradouro, Sergipe. **Revista Brasileira de Geografia Física**, v. 7, n. 1, p. 155-164, 2014.
- BURI, Eswar Sai et al. Spatio-Temporal Analysis of Climatic Variables in the Munneru River Basin, India, Using NEX-GDDP Data and the REA Approach. **Sustainability**, v. 14, n. 3, p. 1715, 2022.
- CANTÚ-MARTÍNEZ, Pedro César. Sustentabilidad Ecológica; El conflicto ambiental del agua en los albores del siglo XXI. **Ciencia UANL**, v. 15, n. 59, p. 20-29, 2012.
- CARVALHO, A. A., MONTENEGRO, A. A. A., SILVA, H. P., LOPES, I., MORAIS, J. E. F., SILVA, T. G. F. Trends of rainfall and temperature in Northeast Brazil. **Revista Brasileira de Engenharia Agrícola e Ambiental**, v. 24, n. 1, p. 15-23, 2020.
- CBHSF—São Francisco River Basin Committee. Water Resources Plan for the São Francisco River Basin 2016-2025. RP1A—Diagnosis of the Technical and Institutional Dimension. Volume 7—Uses, water balance, and synthesis of the diagnosis, Rev.1—August; Nemos: Lisboa, Portugal, 2015.
- CHARIF, Omar, et al. A multi-label cellular automata model for land change simulation. **Transactions in GIS**, v. 21, n. 6, p. 1298-1320, 2017.
- CHEN, Jie; BRISSETTE, François P.; LÉCONTE, Robert. Uncertainty of downscaling method in quantifying the impact of climate change on hydrology. **Journal of Hydrology**, v. 401, n. 3-4, p. 190-202, 2011.
- CHEN, Jie; BRISSETTE, François P.; LUCAS-PICHER, Philippe. Transferability of optimally selected climate models in the quantification of climate change impacts on hydrology. **Climate Dynamics**, v. 47, n. 9, p. 3359-3372, 2016.
- CHOU, Sin Chan, et al. Evaluation of the Eta simulations nested in three global climate models. **American Journal of Climate Change**, v. 3, n. 05, p. 438, 2014.
- CHOW, V.; MAIDMENT, D.; MAYS, L. **Applied hydrology**. New York/NY: McGraw-Hill, 1988.

- CHRISTENSEN, N. S., WOOD, A. W., VOISIN, N., LETTENMAIER, D. P., PALMER, R. N. The effects of climate change on the hydrology and water resources of the Colorado River basin. **Climatic change**, v. 62, n. 1-3, p. 337-363, 2004.
- CHU, H. J., LIN, Y. P., HUANG, C. W., HSU, C. Y., CHEN, H. Y. Modelling the hydrologic effects of dynamic land-use change using a distributed hydrologic model and a spatial land-use allocation model. **Hydrological Processes**, v. 24, n. 18, p. 2538-2554, 2010.
- CHU, T. W., SHIRMOHAMMADI, A., MONTAS, H., ABBOTT, L., SADEGHI, A. Watershed level BMP evaluation with SWAT model. In: **2005 ASAE Annual Meeting**. American Society of Agricultural and Biological Engineers, 2005. p. 1.
- COOK, Christina e BAKKER, Karen. Water security: Debating an emerging paradigm. **Global environmental change**, v. 22, n. 1, p. 94-102, 2012.
- COOLEY, Daniel; SAIN, Stephan R. Spatial hierarchical modeling of precipitation extremes from a regional climate model. **Journal of Agricultural, Biological, and Environmental Statistics**, v. 15, n. 3, p. 381-402, 2010.
- COSTA, A. M. et al. Groundwater recharge potential for sustainable water use in urban areas of the Jequitiba river. **Sustainability**, v. 11, n. 2955, p. 1–20, 2019.
- CRONSHEY, Roger. **Urban hydrology for small watersheds**. US Dept. of Agriculture, Soil Conservation Service, Engineering Division, 1986.
- CROSBIE, Russell S. et al. Modeling climate-change impacts on groundwater recharge in the Murray-Darling Basin, Australia. **Hydrogeology Journal**, v. 18, n. 7, p. 1639-1656, 2010.
- DE OLIVEIRA, Vinícius A. et al. Assessment of climate change impacts on streamflow and hydropower potential in the headwater region of the Grande River basin, Southeastern Brazil. **International Journal of Climatology**, v. 37, n. 15, p. 5005-5023, 2017.
- DEVIA, Gayathri K.; GANASRI, B. P.; DWARAKISH, G. S. A review on hydrological models. **Aquatic Procedia**, v. 4, n. 1, p. 1001-1007, 2015.
- DEZHKAM, S., JABBARIAN AMIRI, B., DARVISHSEFAT, A. A., SAKIEH, Y. Performance evaluation of land change simulation models using landscape metrics. **Geocarto international**, v. 32, n. 6, p. 655-677, 2017.
- DOTTORI, F., SALAMON, P., BIANCHI, A., ALFIERI, L., HIRPA, F. A., FEYEN, L. Development and evaluation of a framework for global flood hazard mapping. **Advances in water resources**, v. 94, p. 87-102, 2016.

- DOUGLAS-MANKIN, K. R.; SRINIVASAN, R.; ARNOLD, J. G. Soil, and Water Assessment Tool (SWAT) model: Current developments and applications. **Transactions of the ASABE**, v. 53, n. 5, p. 1423-1431, 2010.
- EDUARDO, E. N., MELLO, C. R. D., VIOLA, M. R., OWENS, P. R., CURI, N. Hydrological simulation as subsidence for management of surface water resources at the Mortes River Basin. **Ciência e Agrotecnologia**, v. 40, n. 4, p. 390-404, 2016.
- EISENBIES, M. H.; AUST, W. M., BURGER, J. A.; ADAMS, M., B. Forest operations, extreme flooding events, and considerations for hydrologic modeling in the Appalachians - a review. **Forest Ecology and Management**, 242, p. 77–98, 2007.
- FALKENMARK, Malin; LUNDQVIST, Jan. Towards water security: political determination and human adaptation crucial. In: **Natural Resources Forum**. Oxford, UK: Blackwell Publishing Ltd, 1998. p.37-51.
- FALTER, D., DUNG, N. V., VOROGUSHYN, S., SCHRÖTER, K., HUNDECHA, Y., KREIBICH, H., ...MERZ, B. Continuous, large-scale simulation model for flood risk assessments: proof-of-concept. **Journal of Flood Risk Management**, v. 9, n. 1, p. 3-21, 2016.
- FAN, F. M., FLEISCHMANN, A. S., COLLISCHONN, W., AMES, D. P., RIGO, D. Large-scale analytical water quality model coupled with GIS for simulation of point sourced pollutant discharges. **Environmental Modelling & Software**, v. 64, p. 58-71, 2015.
- FAN, Jihui et al. Assessment of land cover resolution impact on flood modeling uncertainty. **Hydrology Research**, v. 52, n. 1, p. 78-90, 2021.
- FAO–Food and Agriculture Organization. Energy Smart Food for People and Agriculture. Rome, Italy., 2011.
- FAO–Food and Agriculture Organization. The State of Food Insecurity in the World 2015. Intl. Food for Agric. Dev. World Food Program, Rome, Italy., 2015.
- FARIAS, Carolyne Wanessa Lins, et al. Técnica de calibração para modelagem da bacia hidrográfica do Rio São Francisco, Brasil, utilizando o SWAT. **Revista Brasileira de Geografia Física**, v. 16, n. 03, p. 1621-1628, 2023.
- FARIAS, Vanine Elane Menezes de. **Avaliação da influência das resoluções espaciais de MDE na estimativa do escoamento superficial de uma bacia hidrográfica usando o modelo**

- SWAT+. 2021. Dissertação (Mestrado em Engenharia Civil e Ambiental), Universidade Federal da Paraíba. 67p.
- FARJAD, B., GUPTA, A., RAZAVI, S., FARAMARZI, M., MARCEAU, D. An integrated modeling system to predict hydrological processes under climate and land-use/cover change scenarios. **Water**, v. 9, n. 10, p. 767, 2017.
- FEREIDOON, Majid; KOCH, Manfred. SWAT-MODSIM-PSO optimization of multi-crop planning in the Karkheh River Basin, Iran, under the impacts of climate change. **Science of the Total Environment**, v. 630, p. 502-516, 2018.
- FERNANDES, Josimar Gurgel. **Estimativa de vazão e produção de sedimentos na bacia hidrográfica do rio São Francisco, utilizando o modelo SWAT**. 2015. Tese (Doutorado em Geografia), Universidade Federal de Pernambuco). 186p.
- FERREIRA, P., VAN SOESBERGEN, A., MULLIGAN, M., FREITAS, M., VALE, M. M. Can forest buffer negative impacts of land-use and climate changes on water ecosystem services? The case of a Brazilian megalopolis. **Science of The Total Environment**, v. 685, p. 248-258, 2019.
- FEYEREISEN, G. W., STRICKLAND, T. C., BOSCH, D. D., SULLIVAN, D. G. Evaluation of SWAT manual calibration and input parameter sensitivity in the Little River watershed. **Transactions of the ASABE**, v. 50, n. 3, p. 843-855, 2007.
- FLEISCHMANN, Ayan; PAIVA, Rodrigo; COLLISCHONN, Walter. Can regional to continental river hydrodynamic models be locally relevant? A cross-scale comparison. **Journal of Hydrology X**, v. 3, p. 100027, 2019.
- FONTOLAN, M., XAVIER, A. C. F., PEREIRA, H. R., BLAIN, G. C. Using climate change models to assess the probability of weather extremes events: a local-scale study based on the generalized extreme value distribution. **Bragantia**, v. 78, n. 1, p. 146-157, 2019.
- FONTOLAN, Mariana et al. Using climate change models to assess the probability of weather extremes events: a local scale study based on the generalized extreme value distribution. **Bragantia**, v. 78, p. 146-157, 2019.
- FRANCESCONI, W., SRINIVASAN, R., PÉREZ-MIÑANA, E., WILLCOCK, S. P., QUINTERO, M. Using the Soil and Water Assessment Tool (SWAT) to model ecosystem services: A systematic review. **Journal of Hydrology**, v. 535, p. 625-636, 2016.

- FU, Q., SHI, R., LI, T., SUN, Y., LIU, D., CUI, S., HOU, R. Effects of land-use change and climate variability on streamflow in the Woken River basin in Northeast China. **River research and applications**, v. 35, n. 2, p. 121-132, 2019.
- FULAZZAKY, Mohamad Ali. Challenges of integrated water resources management in Indonesia. **Water**, v. 6, n. 7, p. 2000-2020, 2014.
- GALDINO, Jean Carlos da Silva et al. Creating the Path for Sustainability: Inserting Solar PV in São Francisco Transposition Project. **Sustainability**, v. 12, n. 21, p. 8982, 2020.
- GAO, H., TANG, Q., SHI, X., ZHU, C., BOHN, T.J., SU, F., SHEFFIELD, J., PAN, M., LETTENMAIER, D.P., WOOD, E.F. Water budget record from Variable Infiltration Capacity (VIC) model. Algorithm Theoretical Basis Document for Terrestrial Water Cycle Data Records. 2010.
- GASHAW, T., TULU, T., ARGAW, M., WORQLUL, A. W. Modeling the hydrological impacts of land use/land cover changes in the Andassa watershed, Blue Nile Basin, Ethiopia. **Science of the Total Environment**, v. 619, p. 1394-1408, 2018.
- GEBREMICAEL, T. G. et al. Trend analysis of runoff and sediment fluxes in the Upper Blue Nile basin: A combined analysis of statistical tests, physically based models, and land use maps. **Journal of Hydrology**, v. 482, p. 57-68, 2013.
- GERLAK, Andrea K.; MUKHTAROV, Farhad. ‘Ways of knowing water: integrated water resources management and water security as complementary discourses. **International environmental agreements: politics, law, and economics**, v. 15, n. 3, p. 257-272, 2015.
- GESUALDO, G. C., OLIVEIRA, P. T., RODRIGUES, D. B. B., GUPTA, H. V. Assessing water security in the São Paulo metropolitan region under projected climate change. **Hydrology and Earth System Sciences**, v. 23, n. 12, p. 4955-4968, 2019.
- GIORGI, Filippo; MEARNNS, Linda O. Calculation of average, uncertainty range, and reliability of regional climate changes from AOGCM simulations via the “reliability ensemble averaging” (REA) method. **Journal of Climate**, v. 15, n. 10, p. 1141-1158, 2002.
- GONDIM, R., SILVEIRA, C., DE SOUZA FILHO, F., VASCONCELOS, F., CID, D. Climate change impacts on water demand and availability using CMIP5 models in the Jaguaribe basin, semi-arid Brazil. **Environmental Earth Sciences**, v. 77, n. 15, p. 550, 2018.
- GREEN, W. Heber; AMPT, G. A. Studies on Soil Physics. **The Journal of Agricultural Science**, v. 4, n. 1, p. 1-24, 1911.

- GUNDA, Thushara; BENNEYWORTH, Laura; BURCHFIELD, Emily. Exploring water indices and associated parameters: a case study approach. **Water Policy**, v. 17, n. 1, p. 98-111, 2014.
- GUZHA, A. C., RUFINO, M. C., OKOTH, S., JACOBS, S., NÓBREGA, R. L. B. Impacts of land use and land cover change on surface runoff, discharge, and low flows: Evidence from East Africa. **Journal of Hydrology: Regional Studies**, v. 15, p. 49-67, 2018.
- GWATE, Onalenna; WOYESSA, Yali E.; WIBERG, David. Dynamics of land cover and impact on streamflow in the Modder River Basin of South Africa: a case study of a Quaternary Catchment. **Int. J. Environ. Prot. Policy**, v. 3, p. 31-38, 2015.
- HAWKINS, R. H. et al. **Continuing evolution of rainfall-runoff and the curve number precedent**. 2nd Joint Federal Interagency Conference. **Annals...** Las Vegas/NV: 2010.
- HAWKINS, R. H.; HJELMFELT, A. T.; ZEVENBERGEN, A. W. Runoff probability, storm depth, and curve numbers. **Journal of Irrigation and Drainage Engineering**, v. 111, n. 4, p. 330–340, 1985.
- HERING, Janet G.; INGOLD, Karin M. Water resources management: What should be integrated? **Science**, v. 336, n. 6086, p. 1234-1235, 2012.
- HESSION, W. C.; STORM, D. E. Watershed-level uncertainties: Implications for phosphorus management and eutrophication. **Journal of Environmental Quality**, v. 29, n. 4, p. 1172-1179, 2000.
- HOEKSTRA, A. Y., CHAPAGAIN, A. K., MEKONNEN, M. M., ALDAYA, M. M. **The water footprint assessment manual: Setting the global standard**. Routledge, 2011.
- HOEKSTRA, A. Y.; MEKONNEN, M. M. The water footprint of humanity, *P. Natl. Acad. Sci.*, 109, 3232–3237. 2012.
- HOEKSTRA, Arjen Y. Virtual water trade: A quantification of virtual water flows between nations to international crop trade. In: **Proceedings of the International Expert Meeting on Virtual Water Trade 12, Delft, 2003**. 2003. p. 25-47.
- HUSSEN, Behailu; MEKONNEN, Ayalkebet; PINGALE, Santosh Murlidhar. Integrated water resources management under climate change scenarios in the sub-basin of Abaya-Chamo, Ethiopia. **Modeling Earth Systems and Environment**, v. 4, n. 1, p. 221-240, 2018.
- IBGE – Instituto Brasileiro de Geografia e Estatística. **Censo Demográfico 2010**. 2010. Available at: <https://www.ibge.gov.br/>. Access on February 24<sup>th</sup>, 2022.

- IEA – International Energy Agency. **Key world energy statistics**. Paris: International Energy Agency, 2014.
- INGOLD, Karin et al. Water Management Across Borders, Scales, and Sectors: Recent developments and future challenges in water policy analysis. **Environmental Policy and Governance**, v. 26, n. 4, p. 223-228, 2016.
- INGOLD, Karin; TOSUN, Jale. Special Issue “Public Policy Analysis of Integrated Water Resource Management”. 2020.
- JENKINS, Katie; WARREN, Rachel. Quantifying the impact of climate change on drought regimes using the Standardized Precipitation Index. **Theoretical and Applied Climatology**, v. 120, n. 1-2, p. 41-54, 2015.
- JIA, Shuaishuai et al. Heterogeneous Impact of Land-Use on Climate Change: Study From a Spatial Perspective. **Frontiers in Environmental Science**, p. 510, 2022.
- JONES, I. D.; ELLIOTT, J. A. Modelling the effects of changing retention time on abundance and composition of phytoplankton species in a small lake. **Freshwater Biology**, v. 52, n. 6, p. 988-997, 2007.
- JONG, P., BARRETO, T. B., TANAJURA, C. A., KOULOUKOU, D., OLIVEIRA-ESQUERRE, K. P., KIPERSTOK, A., TORRES, E. A. Estimating the impact of climate change on wind and solar energy in Brazil using a South American regional climate model. **Renewable energy**, v. 141, p. 390-401, 2019.
- JONG, P., TANAJURA, C. A. S., SÁNCHEZ, A. S., DARGAVILLE, R., KIPERSTOK, A., TORRES, E. A. Hydroelectric production from Brazil's São Francisco River could cease due to climate change and inter-annual variability. **Science of the Total Environment**, v. 634, p. 1540-1553, 2018.
- KANNAN, N., WHITE, S. M., WORRALL, F., WHELAN, M. J. Sensitivity analysis, and identification of the best evapotranspiration and runoff options for hydrological modeling in SWAT-2000. **Journal of Hydrology**, v. 332, n. 3-4, p. 456-466, 2007.
- KARAKUS, Can Bülent; CERIT, Orhan; KAVAK, Kaan Sevki. Determination of land use/cover changes and land use potentials of Sivas city and its surroundings using Geographical Information Systems (GIS) and Remote Sensing (RS). **Procedia Earth and Planetary Science**, v. 15, p. 454-461, 2015.

- KAUFFELDT, A., WETTERHALL, F., PAPPENBERGER, F., SALAMON, P., THIELEN, J. Technical review of large-scale hydrological models for implementation in operational flood forecasting schemes on a continental level. **Environmental Modelling & Software**, v. 75, p. 68-76, 2016.
- KE, Xinli, et al. A CA-based land system change model: LANDSCAPE. **International Journal of Geographical Information Science**, v. 31, n. 9, p. 1798-1817, 2017.
- KOMI, K., NEAL, J., TRIGG, M. A., DIEKKRÜGER, B. Modelling of flood hazard extent in data-sparse areas: a case study of the Oti River basin, West Africa. **Journal of Hydrology: Regional Studies**, v. 10, p. 122-132, 2017.
- KRYSANOVA, Valentina; ARNOLD, Jeffrey G. Advances in ecohydrological modeling with SWAT—a review. **Hydrological Sciences Journal**, v. 53, n. 5, p. 939-947, 2008.
- KUNDU, Sananda; KHARE, Deepak; MONDAL, Arun. Past, present, and future land-use changes and their impact on water balance. **Journal of Environmental Management**, v. 197, p. 582-596, 2017.
- KUWAJIMA, J. I., FAN, F. M., SCHWANENBERG, D., DOS REIS, A. A., NIEMANN, A., MAUAD, F. F. Climate change, water-related disasters, flood control, and rainfall forecasting: a case study of the São Francisco River, Brazil. **Geological Society, London, Special Publications**, v. 488, p. SP488-2018-128, 2019.
- LACERDA, F. F. et al. Tendência do clima do semiárido frente as perspectivas das mudanças climáticas globais; o caso de Araripina, Pernambuco. **Revista do Departamento de Geografia**, v. 31, p. 132–141, 2016.
- LAL, M. et al. Evaluation of the Soil Conservation Service curve number methodology using data from agricultural plots. **Hydrogeology Journal**, v. 25, n. 1, p. 151–167, 2016.
- LAL, M.; MISHRA, S. K.; KUMAR, M. Reverification of antecedent moisture condition dependent runoff curve number formulae using experimental data of Indian watersheds. **Catena**, v. 173, p. 48–58, 2019.
- LAUTZE, Jonathan; MANTHRITHILAKE, Herath. Water security: old concepts, new package, what value? In: **Natural Resources Forum**. Oxford, UK: Blackwell Publishing Ltd, 2012. p. 76-87.

- LIMA, Carlos HR; AGHAKOUCHAK, Amir. Droughts in Amazonia: spatiotemporal variability, teleconnections, and seasonal predictions. **Water Resources Research**, v. 53, n. 12, p. 10824-10840, 2017.
- LIN, F., CHEN, X., YAO, H. Evaluating the use of Nash-Sutcliffe efficiency coefficient in goodness-of-fit measures for daily runoff simulation with SWAT. **Journal of Hydrologic Engineering**, v. 22, n. 11, 2017.
- LOMBARDI NETO, F., BELLINAZZI Jr, R., GALETI, P. A., LEPSCH, I., OLIVEIRA, J. D. Nova abordagem para cálculo de espaçamento entre terraços. **Simpósio Sobre Soloceamento Agrícola**, p. 99-124, 1989.
- LONG, Hualou; QU, Yi. Land use transitions and land management: A mutual feedback perspective. **Land Use Policy**, v. 74, p. 111-120, 2018.
- LOPES, V. A. R., FAN, F. M., PONTES, P. R. M., SIQUEIRA, V. A., COLLISCHONN, W., DA MOTTA MARQUES, D. A first integrated modeling of a river-lagoon large-scale hydrological system for forecasting purposes. **Journal of Hydrology**, v. 565, p. 177-196, 2018.
- LUCAS, Murilo Cesar et al. Significant Baseflow Reduction in the Sao Francisco River Basin. **Water**, v. 13, n. 1, p. 2, 2021.
- LUO, M., LIU, T., MENG, F., DUAN, Y., BAO, A., XING, W., ...FRANKL, A. Identifying climate change impacts on water resources in Xinjiang, China. **Science of the Total Environment**, v. 676, p. 613-626, 2019.
- MACEDO, R. D. C., SCHMITT FILHO, A. L. S., FARLEY, J. C., FANTINI, A. C., CAZELLA, A. A., SINISGALLI, P. A. D. A. Land use and land cover mapping in detailed scale: a case study in Santa Rosa de Lima-SC. **Boletim de Ciências Geodésicas**, v. 24, n. 2, p. 217-234, 2018.
- MAGALHÃES, Adriana Guedes et al. Hydrological modeling of an experimental basin in the semiarid region of the Brazilian State of Pernambuco. **Revista Ambiente & Água**, v. 13, n. 6, 2018.
- MARCHANE, Ahmed et al. Climate change impacts surface water resources in the Rheraya catchment (High Atlas, Morocco). **Hydrological Sciences Journal**, v. 62, n. 6, p. 979-995, 2017.

- MARENGO, J. A., SOUZA, C. A., THONICKE, K., BURTON, C., HALLADAY, K., BETTS, R. A., SOARES, W. R. Changes in climate and land use over the Amazon Region: Current and future variability and trends. **Frontiers in Earth Science**, v. 6, p. 228, 2018.
- MARENGO, Jose A. et al. Development of regional future climate change scenarios in South America using the Eta CPTEC/HadCM3 climate change projections: climatology and regional analyses for the Amazon, São Francisco, and the Paraná River basins. **Climate dynamics**, v. 38, n. 9, p. 1829-1848, 2012.
- MARENGO, José A.; TORRES, Roger Rodrigues; ALVES, Lincoln Muniz. Drought in Northeast Brazil—past, present, and future. **Theoretical and Applied Climatology**, v. 129, n. 3-4, p. 1189-1200, 2017.
- MARHAENTO, Hero; BOOIJ, Martijn J.; HOEKSTRA, Arjen Y. Hydrological response to future land-use change and climate change in a tropical catchment. **Hydrological Sciences Journal**, v. 63, n. 9, p. 1368-1385, 2018.
- MARQUES, Érika Tavares; GUNKEL, Günter; SOBRAL, Maria Carmo. Management of Tropical River Basins and Reservoirs under Water Stress: Experiences from Northeast Brazil. **Environments**, v. 6, n. 6, p. 62, 2019.
- MCGUIRE, A. D. et al. Carbon balance of the terrestrial biosphere in the twentieth century: Analyses of CO<sub>2</sub>, climate, and land use effects with four process-based ecosystem models. **Global biogeochemical cycles**, v. 15, n. 1, p. 183-206, 2001.
- McIntyre, N., BALLARD, C., BRUEN, M., BULYGINA, N., BUYTAERT, W., CLUCKIE, I., ...HESS, T. Modelling the hydrological impacts of rural land-use change. **Hydrology Research**, v. 45, n. 6, p. 737-754, 2014.
- MEHAN, Sushant; NEUPANE, Ram P.; KUMAR, Sandeep. Coupling of SUFI 2 and SWAT for improving the simulation of streamflow in an agricultural watershed of South Dakota. **Hydrol. Curr. Res**, v. 8, n. 3, 2017.
- MELO NETO, J. D. O., SILVA, A. D., MELLO, C. D., MELLO JÚNIOR, A. V. Simulação hidrológica escalar com o modelo SWAT. **Revista Brasileira de Recursos Hídricos**, v. 19, n. 1, p. 177-188, 2014.
- MENDES, Carlos André B.; BELUCO, Alexandre; CANALES, Fausto Alfredo. Some important uncertainties related to climate change in projections for the Brazilian hydropower expansion in the Amazon. **Energy**, v. 141, p. 123-138, 2017.

- MIRANDA, R. D. Q., GALVÍNCIO, J., de MOURA, M. S. B., SRINIVASAN, R. Parallelization of the SUFI2 algorithm: a Windows HPC approach. **Revista Brasileira de Geografia Física**. v.10, p. 1535-1544, 2017.
- MISHRA, S. K. et al. Comparison of AMC-dependent CN-conversion Formulae. **Water Resources Management**, v. 22, p. 1409–1420, 2008.
- MOLINA-NAVARRO, E., ANDERSEN, H. E., NIELSEN, A., THODSEN, H., TROLLE, D. Quantifying the combined effects of land use and climate changes on streamflow and nutrient loads: A modeling approach in the Odense Fjord catchment (Denmark). **Science of the total environment**, v. 621, p. 253-264, 2018.
- MONTENEGRO, S. M. G. L., SILVA, B. B., ANTONINO, A. C. D., LIMA, J. R. S., SOUZA, E. S., OLIVEIRA, L. M. M., MOURA, A. E. S. S., SOUZA, R. M. S. Hydrological studies in experimental and representative basins in Pernambuco State, Brazil. **Proceedings of the International Association of Hydrological Sciences**, v. 364, p. 422-428, 2014.
- MORIASI, D. N., ARNOLD, J. G., VAN LIEW, M. W., BINGNER, R. L., HARMEL, R. D., VEITH, T. L. Model evaluation guidelines for systematic quantification of accuracy in watershed simulations. **Transactions of the ASABE**, v. 50, n. 3, p. 885-900, 2007.
- MORIASI, D. N., GITAU, M. W., PAI, N., DAGGUPATI, P. Hydrologic, and water quality models: Performance measures and evaluation criteria. **Transactions of the ASABE**, v. 58, n. 6, p. 1763-1785, 2015.
- NASCIMENTO, M. N., MARTINS, G. S., CORDEIRO, R. C., TURCQ, B., MOREIRA, L. S., BUSH, M. B. Vegetation response to climatic changes in western Amazonia over the last 7,600 years. **Journal of Biogeography**, 2019.
- NASH, J. Eamonn; SUTCLIFFE, Jonh V. River flow forecasting through conceptual models, part I—A discussion of principles. **Journal of Hydrology**, v. 10, n. 3, p. 282-290, 1970.
- NAZEMI, Ali; MADANI, Kaveh. Urban water security: Emerging discussion and remaining challenges. **Sustainable Cities and Society**, v. 41, p. 925-928, 2018.
- NEITSCH, S. L. et al. Section 2 Chapter 1-Equations: surface runoff. **Soil and Water Assessment Tool Theoretical Documentation**, 2005.
- NEITSCH, S. L., ARNOLD, J. G., KINIRY, J. R., WILLIAMS, J. R. **Soil, and water assessment tool theoretical documentation version 2009**. Texas Water Resources Institute, 2011.

- NOBRE, P. **Mudanças climáticas e desertificação: os desafios para o Estado Brasileiro**. Instituto ed. Campina Grande, PB: [s.n.]. v. 4
- NÓBREGA, M. T., COLLISCHONN, W., TUCCI, C. E. M., PAZ, A. R. Uncertainty in climate change impacts on water resources in the Rio Grande Basin, Brazil. **Hydrology and Earth System Sciences**, v. 15, n. 2, p. 585-595, 2011.
- NRCS. Hydrologic soil-cover complexes. In: MOCKUS, V.; MOODY, H. F.; NRCS (Eds.). **Part 630 Hydrology, National Engineering Handbook**. Washington/DC: Natural Resources Conservation Service (NRCS), United States Department of Agriculture (USDA), p. 1–20, 2004.
- NRCS. Land use and treatment. In: VICTOR MOCKUS; NRCS (Eds.). **Part 630 Hydrology, National Engineering Handbook**. Washington/DC: Natural Resources Conservation Service (NRCS), United States Department of Agriculture (USDA). p. 1–11, 2002.
- NRCS. **Urban hydrology for small watersheds**. Natural Resources Conservation Service (NRCS), United States Department of Agriculture (USDA), 1986.
- NRCS. **Urban hydrology for small watersheds**. Natural Resources Conservation Service (NRCS), United States Department of Agriculture (USDA), 1986.
- OLIVEIRA, V. A., DE MELLO, C. R., BESKOW, S., VIOLA, M. R., SRINIVASAN, R. Modeling the effects of climate change on hydrology and sediment load in a headwater basin in the Brazilian Cerrado biome. **Ecological Engineering**, v. 133, p. 20-31, 2019.
- OLIVER, Tom H.; MORECROFT, Mike D. Interactions between climate change and land use change on biodiversity: attribution problems, risks, and opportunities. **Wiley Interdisciplinary Reviews: Climate Change**, v. 5, n. 3, p. 317-335, 2014.
- ORTIZ-PARTIDA, J. P., SANDOVAL-SOLIS, S., ARELLANO-GONZALEZ, J., MEDELLÍN-AZUARA, J., TAYLOR, J. E. Managing water differently: Integrated Water Resources Management as a framework for adaptation to climate change in Mexico. In: **Integrated Water Resource Management**. Springer, Cham, 2020. p. 59-72.
- PONTES, P. R., CAVALCANTE, R. B., SAHOO, P. K., DA SILVA JÚNIOR, R. O., DA SILVA, M. S., DALL'AGNOL, R., SIQUEIRA, J. O. The role of protected and deforested areas in the hydrological processes of Itacaiúnas River Basin, eastern Amazonia. **Journal of Environmental Management**, v. 235, p. 489-499, 2019.

- PRUSKI, F. F., BRANDÃO, V. S., SILVA, D. D. Escoamento superficial. 2ed. Editora UFV. Universidade Federal de Viçosa – Viçosa: UFV. 87p. 2008
- QIN, G., LIU, J., WANG, T., XU, S., SU, G. An Integrated Methodology to Analyze the Total Nitrogen Accumulation in a Drinking Water Reservoir Based on the SWAT Model Driven by CMADS: A Case Study of the Biliuhe Reservoir in Northeast China. **Water**, v. 10, n. 11, p. 1535, 2018.
- RALLISON, Robert E.; MILLER, Norman. Past, present, and future SCS runoff procedure. In: **Rainfall-runoff relationship/proceedings, International Symposium on Rainfall-Runoff Modeling held May 18-21, 1981, at Mississippi State University, Mississippi State, Mississippi, USA/edited by VP Singh**. Littleton, Colo.: Water Resources Publications, c1982., 1982.
- RAPOSO, Juan Ramón; DAFONTE, Jorge; MOLINERO, Jorge. Assessing the impact of future climate change on groundwater recharge in Galicia-Costa, Spain. **Hydrogeology Journal**, v. 21, n. 2, p. 459-479, 2013.
- RAWAT, J. S.; KUMAR, Manish. Monitoring land use/cover change using remote sensing and GIS techniques: A case study of Hawalbagh block, district Almora, Uttarakhand, India. **The Egyptian Journal of Remote Sensing and Space Science**, v. 18, n. 1, p. 77-84, 2015.
- Regional Development Ministry—MDR: What Is the Project? Available online: <http://www.mdr.gov.br/projeto-rio-sao-francisco/o-que-e-o-projeto/> (accessed on 27 August 2019).
- REN, Yanjiao et al. Spatially explicit simulation of land use/land cover changes: Current coverage and prospects. **Earth-Science Reviews**, v. 190, p. 398-415, 2019.
- RODRIGUES, Dulce BB; GUPTA, Hoshin V.; MENDIONDO, Eduardo M. A blue/green water-based accounting framework for assessment of water security. **Water Resources Research**, v. 50, n. 9, p. 7187-7205, 2014.
- ROSEMARIN, A., SCHRODER, J. J., DAGERSKOG, L., CORDELL, D., SMIT, A. L. Future supply of phosphorus in agriculture and the need to maximize the efficiency of use and reuse. **International Fertilizer Society. Proceedings**, v. 685, p. 1-28, 2011.
- ROUHOLAHNEJAD, E., ABBASPOUR, K. C., VEJDANI, M., SRINIVASAN, R., SCHULIN, R., LEHMANN, A.A parallelization framework for calibration of hydrological models. **Environmental Modelling & Software**, v. 31, p. 28-36, 2012.

- ROUNSEVELL, Mark DA; ROBINSON, Derek T.; MURRAY-RUST, Dave. From actors to agents in socio-ecological systems models. **Philosophical Transactions of the Royal Society B: Biological Sciences**, v. 367, n. 1586, p. 259-269, 2012.
- SARTORI, A. **Desenvolvimento de critérios para classificação hidrológica dos solos e determinação de valores de referência para o parâmetro CN**. PhD thesis. Campina State University, 2010.
- SARTORI, Aderson; LOMBARDI NETO, F.; GENOVEZ, Abel Maia. Classificação hidrológica de solos brasileiros para a estimativa da chuva excedente com o método do Serviço de Conservação do Solo dos Estados Unidos Parte 1: Classificação. **Revista Brasileira de Recursos Hídricos**, v. 10, n. 4, p. 05-18, 2005.
- SCS. Section 4: Hydrology. In: **National engineering handbook**. Washington/DC: Soil Conservation Service (SCS), United States Department of Agriculture (USDA), 1972.
- SHIRMOHAMMADI, Bagher, et al. Scenario analysis for integrated water resources management under future land-use change in the Urmia Lake region, Iran. **Land Use Policy**, 2020, 90: 104299.
- SILVA, R.M da. Introdução ao Geoprocessamento: conceitos, técnicas e aplicações. **Novo Hamburgo: Feevale**, 2007.
- SILVA, V., DE OLIVEIRA, S., HOEKSTRA, A., DANTAS NETO, J., CAMPOS, J., BRAGA, C., DE ARAÚJO, Lincoln Eloi, ALEIXO, Danilo de Oliveira, DE BRITO, José Ivaldo B., DE SOUZA, Márcio Dionísio, DE HOLANDA, R. Water footprint and virtual water trade of Brazil. **Water**, v. 8, n. 11, p. 517, 2016.
- SINGH V.P, WOOLHISER D.A. Mathematical modeling of watershed hydrology.” **Journal of Hydrology Engineering**, Jul/Ago, p.270–292, 2002.
- SINGH, Ajay. Managing the salinization and drainage problems of irrigated areas through remote sensing and GIS techniques. **Ecological indicators**, v. 89, p. 584-589, 2018.
- SIQUEIRA, V.A., PAIVA, R.C.D., FLEISCHMANN, A.S., FAN, F.M., RUHOFF, A.L., PONTES, P.R.M., PARIS, A., CALMANT, S., COLLISCHONN, W. Toward continental hydrologic–hydrodynamic modeling in South America. **Hydrology and Earth System Sciences. Göttingen: Copernicus. Vol. 22, n. 9 (set. 2018), p. 4815-4842**, 2018.

- SOARES, M. C. S., MARINHO, M. M., AZEVEDO, S. M., BRANCO, C. W.; HUSZAR, V. L. Eutrophication and retention time affecting spatial heterogeneity in a tropical reservoir. **Limnologica-Ecology and Management of Inland Waters**, v. 42, n. 3, p. 197-203, 2012.
- SOBHANI, G. **A review of selected small watershed design methods for possible adoption to Iranian conditions**. Master thesis. Logan/UT: Utah State University, 1975.
- SOLAUN, Kepa; CERDÁ, Emilio. Climate change impacts renewable energy generation. A review of quantitative projections. **Renewable and Sustainable Energy Reviews**, v. 116, p. 109415, 2019.
- SOOD, Aditya; SMAKHTIN, Vladimir. Global hydrological models: a review. **Hydrological Sciences Journal**, v. 60, n. 4, p. 549-565, 2015.
- SORRIBAS, M. V., PAIVA, R. C., MELACK, J. M., BRAVO, J. M., JONES, C., CARVALHO, L., Beighley, E., Bruce Forsberg, B. Costa, M. H. Projections of climate change effects on discharge and inundation in the Amazon basin. **Climatic Change**, v. 136, n. 3-4, p. 555-570, 2016.
- SORRIBAS, Mino Viana et al. Projections of climate change effects on discharge and inundation in the Amazon basin. **Climatic change**, v. 136, n. 3, p. 555-570, 2016.
- SOUZA, Fernanda Abreu Oliveira; OLIVEIRA, Mauro Márcio. Panorama dos danos humanos provocados por secas e cheias no Brasil e uma proposta de regionalização de investimentos na gestão de riscos. **Desenvolvimento e Meio Ambiente**, v. 51, 2019.
- SRINIVASAN, Veena; KONAR, Megan; SIVAPALAN, Murugesu. A dynamic framework for water security. **Water Security**, v. 1, p. 12-20, 2017.
- TAN, M. L., FICKLIN, D. L., IBRAHIM, A. L., YUSOP, Z. Impacts and uncertainties of climate change on streamflow of the Johor River Basin, Malaysia using a CMIP5 General Circulation Model ensemble. **Journal of Water and Climate Change**, v. 5, n. 4, p. 676-695, 2014.
- TEBALDI, Claudia et al. Quantifying uncertainty in projections of regional climate change: A Bayesian approach to the analysis of multimodel ensembles. **Journal of Climate**, v. 18, n. 10, p. 1524-1540, 2005.
- TEIXEIRA, Alexandre Lima de F. et al. Operationalizing Water Security Concept in Water Investment Planning: Case Study of São Francisco River Basin. **Water**, v. 13, n. 24, p. 3658, 2021.

- THAPA, Pawan. The Relationship between Land Use and Climate Change: A Case Study of Nepal. In: **The Nature, Causes, Effects and Mitigation of Climate Change on the Environment**. IntechOpen, 2021.
- TIWARI, Ashwani Kumar, et al. Role of Integrated Approaches in Water Resources Management: Antofagasta Region, Chile. *Sustainability*, 2021, 13.3: 1297.
- TORRES, M. D. O., MANETA, M., HOWITT, R., VOSTI, S. A., WALLENDER, W. W., BASSOI, L. H., RODRIGUES, L. N. Economic impacts of regional water scarcity in the São Francisco River Basin, Brazil: an application of a linked hydro-economic model. **Environment and Development Economics**, v. 17, n. 2, p. 227-248, 2012.
- TORRES, Marcelo de O. et al. Spatial patterns of rural poverty: an exploratory analysis in the São Francisco River Basin, Brazil. **Nova Economia**, v. 21, p. 45-66, 2011.
- TUCCI, C. E. M. Hidrologia: ciência e aplicação. Porto Alegre: Ed. da Universidade: ABRH: EDUSP. **Tucci, CEM (org.)**, 2009.
- TUCCI, C. Integrated management of land-based activities in the São Francisco River basin. **Terminal evaluation report of GEF project no GF/1100-99-14, sl**, 2005.
- TUPPAD, P., DOUGLAS-MANKIN, K. R., LEE, T., SRINIVASAN, R., ARNOLD, J. G. Soil and Water Assessment Tool (SWAT) hydrologic/water quality model: Extended capability and wider adoption. **Transactions of the ASABE**, v. 54, n. 5, p. 1677-1684, 2011.
- UKKOLA, A. M.; PRENTICE, I. C. A worldwide analysis of trends in water-balance evapotranspiration. **Hydrology and Earth System Sciences**, v. 17, n. 10, p. 4177-4187, 2013.
- UN–United Nations. World Population Prospects: The 2015 Revision, Key Findings and Advance Tables, Working Pap. ESA/P/WP.241, 59p., United Nations Dept. of Econ. and Soc. Affairs (UNDESA), New York., 2015a.
- VAN ASSELEN, Sanneke; VERBURG, Peter H. Land cover change or land-use intensification: simulating land system change with a global-scale land change model. **Global change biology**, v. 19, n. 12, p. 3648-3667, 2013.
- VAN VUUREN, D. P., EDMONDS, J., KAINUMA, M., RIAHI, K., THOMSON, A., HIBBARD, K., HURTT, G. C., KRAM, T., KREY, V., LAMARQUE, J., MASUI, T., MEINSHAUSEN, M., NAKICENOVIC, N., SMITH, S. J., ROSE, S. K. The

- representative concentration pathways: an overview. **Climatic change**, v. 109, n. 1-2, p. 5, 2011.
- VASCO, G.; SILVA, F. S.; CARVALHO, V. S. de.; DUTRA, M. T. D.; BARBOSA, I. M. B. R. A reading of the Water Resources Plan of the São Francisco River Basin in light of the Sustainable Development Goals of the 2030 Agenda. *Research, Society, and Development*, [S. l.], v. 11, n. 13, p. e473111334354, 2022. DOI: 10.33448/rsd-v11i13.34354.
- VENZON, Pedro Thiago; PINHEIRO, Adilson; KAUFMANN, Vander. Hydrological simulation uncertainties in small basins through the SWAT model. **RBRH**, v. 23, 2018.
- VERBURG, Peter H. et al. Land system science and sustainable development of the earth system: A global land project perspective. **Anthropocene**, v. 12, p. 29-41, 2015.
- VERBURG, Peter H. et al. Land use change modeling: current practice and research priorities. **GeoJournal**, v. 61, n. 4, p. 309-324, 2004.
- VIOLA, M. R., MELLO, C. R., BESKOW, S., NORTON, L. D. Impacts of land-use changes on the hydrology of the Grande River basin headwaters, Southeastern Brazil. **Water resources management**, v. 28, n. 13, p. 4537-4550, 2014.
- VOGEL, Richard M. et al. Hydrology: The interdisciplinary science of water. **Water Resources Research**, v. 51, n. 6, p. 4409-4430, 2015.
- VÖRÖSMARTY, Charles J. et al. Global threats to human water security and river biodiversity. **nature**, v. 467, n. 7315, p. 555-561, 2010.
- VOUDOURI, A. et al. Objective calibration of numerical weather prediction models. **Atmospheric research**, v. 190, p. 128-140, 2017.
- WANDERLEY, Silva. Precipitação e temperatura do ar simuladas pelo modelo ETA/CPTEC-HADCM3 para o estado do Rio de Janeiro. **Revista Brasileira de Geografia Física**, v. 13, n. 05, p. 2037-2052, 2020.
- WATANABE, M., SUZUKI, T., O'Ishi, R., KOMURO, Y., WATANABE, S., EMORI, S., TAKEMURA, T., CHIKIRA, M., OGURA, T., SEKIGUCHI, M., TAKATA, K., YAMAZAKI, D., YOKOHATA, T., NOZAWA, T., HASUMI, H., TATEBE, H., KIMOTO, M. Improved climate simulation by MIROC5: mean states, variability, and climate sensitivity. **Journal of Climate**, v. 23, n. 23, p. 6312-6335, 2010.

- WHITE, Kati L.; CHAUBEY, Indrajeet. Sensitivity analysis, calibration, and validations for a multisite and multivariable SWAT model 1. **JAWRA Journal of the American Water Resources Association**, v. 41, n. 5, p. 1077-1089, 2005.
- WIJESEKARA, G. N., FARJAD, B., GUPTA, A., QIAO, Y., DELANEY, P., MARCEAU, D. J. A comprehensive land-use/hydrological modeling system for scenario simulations in the Elbow River watershed, Alberta, Canada. **Environmental management**, v. 53, n. 2, p. 357-381, 2014.
- WILLEMS, Patrick; VRAC, M. Statistical precipitation downscaling for small-scale hydrological impact investigations of climate change. **Journal of Hydrology**, v. 402, n. 3-4, p. 193-205, 2011.
- WONDRADE, Nigatu; DICK, Øystein B.; TVEITE, Havard. GIS-based mapping of land cover changes utilizing multi-temporal remotely sensed image data in Lake Hawassa Watershed, Ethiopia. **Environmental monitoring and assessment**, v. 186, n. 3, p. 1765-1780, 2014.
- WOOD, Andrew W. et al. Hydrologic implications of dynamical and statistical approaches to downscaling climate model outputs. **Climatic change**, v. 62, n. 1, p. 189-216, 2004.
- WOOD, Eric F. et al. Hyperresolution global land surface modeling: Meeting a grand challenge for monitoring Earth's terrestrial water. **Water Resources Research**, v. 47, n. 5, 2011.
- WOODWARD, D. E. et al. **Runoff curve number method: Examination of the initial abstraction ratio**. World Water and Environmental Resources Congress. **Annals...** 2003.
- WOOLWAY, R. Iestyn; MERCHANT, Christopher J. Worldwide alteration of lake mixing regimes in response to climate change. **Nature Geoscience**, v. 12, n. 4, p. 271-276, 2019.
- WWDR – World Water Development Report. The United Nations World Water Development Report 2015, United Nations Educational, Scientific and Cultural Organization. Paris, France., 2015.
- XIA, J., ZHANG, L., LIU, C., YU, J. Towards better water security in North China. **Water Resources Management**, v. 21, n. 1, p. 233-247, 2007.
- YAMAZAKI, Dai; DE ALMEIDA, Gustavo AM; BATES, Paul D. Improving computational efficiency in global river models by implementing the local inertial flow equation and a vector-based river network map. **Water Resources Research**, v. 49, n. 11, p. 7221-7235, 2013.

- YAN, H., WU, D., HUANG, Y., WANG, G., SHANG, M., XU, J., SHI, X., SHAN, K., ZHOU, B., ZHAO, Y. Water eutrophication assessment based on rough set and multidimensional cloud model. **Chemometrics and Intelligent Laboratory Systems**, v. 164, p. 103-112, 2017.
- YANG, Jun, et al. A local land use competition cellular automata model and its application. **ISPRS International Journal of Geo-Information**, v. 5, n. 7, p. 106, 2016.
- YANG, L., XIAN, G., KLAVER, J. M., DEAL, B. Urban land-cover change detection through sub-pixel imperviousness mapping using remotely sensed data. **Photogrammetric Engineering & Remote Sensing**, v. 69, n. 9, p. 1003-1010, 2003.
- YEN, H., PARK, S., ARNOLD, J. G., SRINIVASAN, R., CHAWANDA, C. J., WANG, R., FENG, Q., WU, J., MIAO, C., BIEGER, K., DAGGUPATI, P., GRIENSVEN, A. V., KALIN, L., Lee, S., SHESHUKOV, A. Y., WHITE, M. J., YUAN, Y., YEO, In-Young, ZHANG, M., ZHANG, X. IPEAT+: A Built-In Optimization and Automatic Calibration Tool of SWAT+. **Water**, v. 11, n. 8, p. 1681, 2019.
- YEN, H., WANG, X., FONTANE, D. G., HARMEL, R. D., ARABI, M. A framework for the propagation of uncertainty contributed by parameterization, input data, model structure, and calibration/validation data in watershed modeling. **Environmental Modelling & Software**, v. 54, p. 211-221, 2014.
- ZEILHOFER, Peter; TOPANOTTI, Valdinir Piazza. GIS and ordination techniques for evaluation of environmental impacts in informal settlements: A case study from Cuiaba, central Brazil. **Applied Geography**, v. 28, n. 1, p. 1-15, 2008.
- ZENG, R.; CAI, Ximing. Analyzing streamflow changes: Irrigation-enhanced interaction between aquifer and streamflow in the Republican River Basin. **Hydrology and Earth System Sciences**, v. 18, n. 2, p. 493-502, 2014.
- ZHANG, Y. Y., SHAO, Q. X., YE, A. Z., XING, H. T. An integrated water system model considering hydrological and biogeochemical processes at basin scale: model construction and application. **Hydrology and Earth System Sciences Discussions**, v. 11, n. 8, p. 9219-9279, 2014.
- ZHANG, Y., LI, C., TRETTIN, C. C., LI, H., SUN, G. An integrated model of soil, hydrology, and vegetation for carbon dynamics in wetland ecosystems. **Global Biogeochemical Cycles**, v. 16, n. 4, p. 9-1-9-17, 2002.

- ZHOU, F., XU, Y., CHEN, Y., XU, C. Y., GAO, Y., DU, J. Hydrological response to urbanization at different Spatio-temporal scales simulated by coupling of CLUE-S and the SWAT model in the Yangtze River Delta region. **Journal of Hydrology**, v. 485, p. 113-125, 2013.
- ZHUANG, X. W., LI, Y. P., NIE, S., FAN, Y. R., HUANG, G. H. Analyzing climate change impacts on water resources under uncertainty using an integrated simulation-optimization approach. **Journal of Hydrology**, v. 556, p. 523-538, 2018.

## CHAPTER II

---

# Spatially explicit land use scenarios for the São Francisco River Basin, Brazil<sup>6</sup>

### Abstract

Future land use change in the São Francisco River Basin (SFRB) is critical to the future of regional climate and biodiversity, given the large heterogeneity among the four climate types within the basin. These changes in SFRB depend on the link between global and national factors due to its role as one of the world's major exporters of raw materials and national to local institutional, socioeconomic, and biophysical contexts. In this work, LuccME's spatially explicit land change distribution modeling framework is used, aiming to develop three models that balance global (e.g., GDP growth, population growth, per capita agricultural consumption, international trade policies, and climate conditions) and regional/ scene. Local factors (such as land use, agricultural structure, agricultural suitability, protected areas, distance from roads and other infrastructure projects), are consistent with the global structure Shared Socio-Economic Pathways (SSP) and Representative Concentration Pathways (RCP), namely: SSP1/RCP 1.9 (sustainable development scenario), SSP2/RCP 4.5 (moderate scenario) and SSP3/RCP 7.0 (high inequality scenario). Based on detailed biophysical, socioeconomic, and institutional factors for each region of the São Francisco River Basin, spatially explicit land use scenarios to 2050 were created, considering the following categories: agriculture, natural forest, rangeland, agriculture, rangeland, and forest. Mosaic Plantation. The results show that the performance of the developed model is satisfactory. The average spatial fitting index between observed data and simulated data in 2019 is 89.48%, the average fitting error percentage corresponding to omissions is 2.59%, and the commission error is approximately 2.16%. Regarding the projected scenarios, the results show that three classes, agriculture, pasture, and mosaic of agriculture and pasture will continue in the same direction (increasing), regardless of the scenario considered, differently to the class of natural forest and forest plantation, which will decrease in scenarios of the middle road and strong inequality, and sustainable development, respectively.

**Keywords:** LuccME modeling framework, model validation, Shared Socioeconomic Pathways.

---

<sup>6</sup>A modified version of this chapter will be shortly submitted to a peer-review international journal.

## 2.1 Introduction

Land-use and land-cover (LULC) changes have been identified as one of the greatest global and regional socio-environmental challenges of the 21<sup>st</sup> century (PRESTELE et al., 2016), due to the important impacts on the environment (VAN ASSELEN; VERBURG, 2013), such as variation of various natural support systems, which range from WEF nexus security, agricultural frontier (BEZERRA et al., 2022), biodiversity and ecosystem services (FRANCESCONI et al., 2016).

However, understanding spatial patterns of LULC changes is essential because these affect important biogeochemical, social, economic, biophysical, and ecological variables such as soil fertility, local climate, and biodiversity (PRESTELE et al., 2016).

For example, the urbanization process and the implementation of governmental policies for agricultural practices can intensify the spatial-temporal land-use and land-cover (LULC) changes as well as, people that will face large changes in their environment (FONSECA et al., 2019).

The interactions between these systems are commonly modeled using globally integrated assessment models (VAN BEEK et al., 2020), e.g. LuccME modeling framework (AGUIAR et al., 2012), which represent complex interactions and feedback on a long-term scale between the socioeconomic and natural systems.

Thus, a spatially explicit assessment of uncertainties is required to identify not only the amount but also the geographic extent and location of uncertainty (PRESTELE et al., 2016), aiming to provide important contributions to support LULC and environmental policymakers.

The environmental assessments heavily rely on the provision of historical reconstructions and future projections of LULC change trajectories generated by models, to assess the direction and strength of anthropogenic LULC change effects on ecosystems and the climate.

Onward to the development of several activities that are strategically important for socioeconomic development, the São Francisco River Basin Region stands out for the intensification of changes in use and coverage over the last few years, based on Mapbiomas<sup>7</sup> (SOUZA et al., 2020; TEIXEIRA et al., 2021) – an open-source raster database that presents the evolution of land use and land cover in Brazil, from 1985 to present days.

In this context, the main goal of this chapter was to project land-use scenarios through a spatially explicit model for the São Francisco River Basin.

---

<sup>7</sup>The MapBiomas project is an initiative of the Greenhouse Gas Emission and Removal System/Climate Observatory (SEEG/OC), composed of a collaborative network and launched in 2015, which that provides annual national-level land use and land cover transitions in all biomes of the Brazilian territory with a 30-m spatial resolution on annual basis. The MapBiomas classification comprises 33 classes, grouped in the following themes: native vegetation, non-forest natural formation, tillage, non-vegetated area, and water.

Specifically, was identified, on a regional scale, which environmental and socioeconomic factors are related to the dynamics of land use change in the period 2000 and 2010 (1), and analyzed the location, intensity, and direction of change in areas of land use change, using the LuccME spatially explicit land change modeling framework, considering the factors previously selected (2).

The projected scenarios represent a diverse range of biophysical, environmental, and socioeconomic assumptions about the future and capture a broad range of regional- and gridded-level uncertainties typical in current models based on the framework developed in the AMAZALERT project for the Brazilian Amazon (ZIMM; SPERLING; BUSCH, 2018), in line with the SSPs and RCPs to be useful to environmental policymakers on land use changes (BEZERRA et al., 2022).

This chapter is divided into four sections. The first section, i.e., an introduction provides a brief background of other related studies while the second section deals with the materials and methods, which includes a description of the study area, socioeconomic status, database building containing variables, and algorithm structure of LuccME, model calibration and validation. The third section, results, and discussion provide outcomes followed by the concluding remarks of this study and some suggestions and recommendations that can be utilized for the protection and conservation of land resources.

## **2.2 Material and Methods**

### **2.2.1 Study area brief description**

This work was carried out in the São Francisco River Basin, one of the largest in Brazil, extending approximately 2,700 km, annual discharge of 94,000,000 m<sup>3</sup> and a flow rate between 2,100 and 2,800 m<sup>3</sup>/s (FERNANDES, 2015; TEIXEIRA et al., 2021).

The river has its source in the Serra da Canastra National Park (Minas Gerais, the southern region of Brazil) and its mouth is in the Atlantic Ocean, between the states of Alagoas and Sergipe (the northeast coast of Brazil). Therefore, the São Francisco River encompasses four different climate types: a dry subhumid climate in the southern hemisphere with a dry season coinciding with winter (Upper São Francisco), a semi-arid climate (Central São Francisco), a semi-arid and arid climate (Lower São Francisco) (BEZERRA et al., 2019).

The climatology of the São Francisco River Basin is characterized by high spatial-temporal variability due to the action of different large-scale, meso, and local meteorological systems (OLIVEIRA; SANTOS E SILVA; LIMA, 2017). The average annual rainfall ranges from 1,500 mm

(Hight São Francisco in Minas Gerais) to 350 mm (Lower São Francisco) (MARQUES; GUNKEL; SOBRAL, 2019), and soils with an aptitude for irrigated agriculture predominate in this basin.

### 2.2.2 Modeling Approach

In this work, we adopted a top-down modeling approach/protocol (VERBURG et al., 2015), whose conceptual structure for the projection of the scenarios of land-use change for the SFRB region through the LuccME framework, is presented in Figure 5.

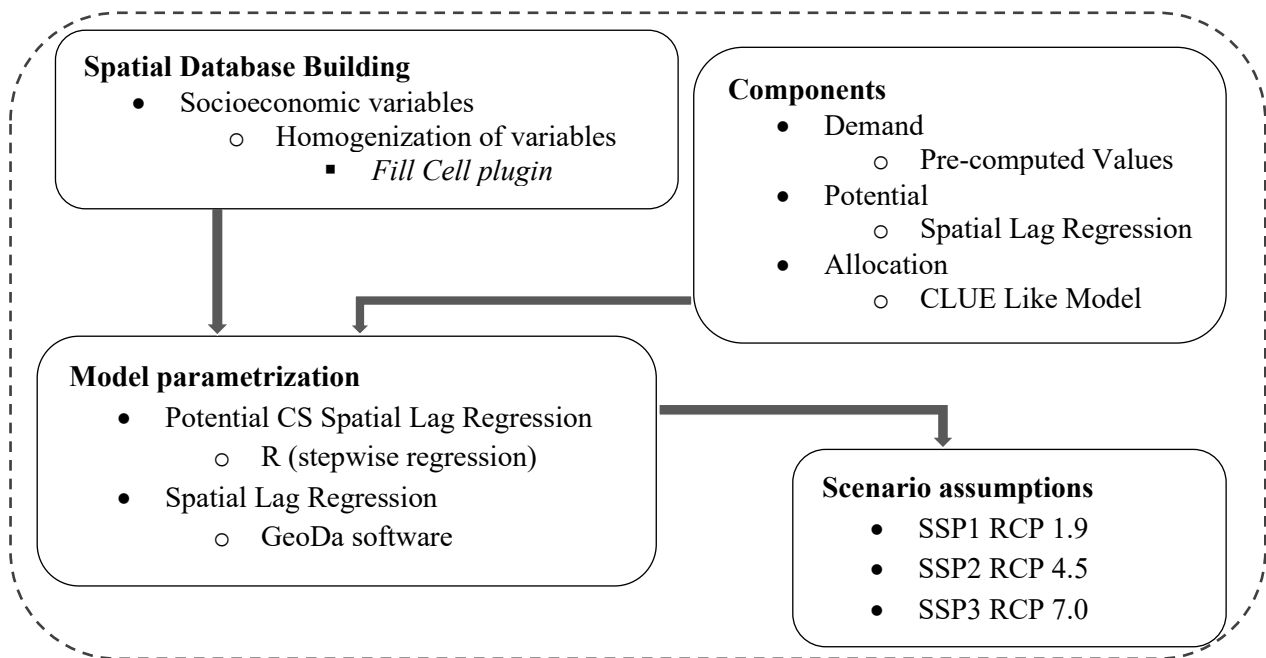


Figure 5: A conceptual structure for projecting the scenarios of land use changes through the LuccME framework.

Source: adapted by the author (2023).

#### 2.2.2.1 Spatial Database Building

One of the relevant steps for the development of the model presented in this work was the construction of the database, containing biophysical and anthropic factors as potentially important factors in the process of land-use change for the entire São Francisco River basin.

From the Water Resources Plan of the São Francisco River Basin (2016–2025) (NEMUS, 2016), and based on the literature review stating that, in the Northeast of Brazil, land-use changed minimally during the 2000 – 2016 period with greater agricultural expansion in the southwestern zone (DIAS et al., 2016; NOOJIPADY et al., 2017), a spatial database with over 30 variables was built. Within this set of variables, we have two types of data:

- i. Variables were dependent on land use and land cover: from the classes established in the "MapBiomass Project – collection 5 of the Annual Series of Land Cover Maps of Brazil", through the link: <https://mapbiomas.org/produtos>, where data from LULC were organized into six (6) classes of interest: agriculture, planted forest, natural vegetation, mosaic, pasture, and the unobserved area and others were reclassified to the class "other". The data periods of land use and occupation changes analyzed were from 2010 to 2050, being used 2010-2015 (for calibration), 2015-2019 (for validation), and 2020-2050 (for land use scenarios).
- ii. Independent variables related to socioeconomic, environmental, and political factors that influence the land-use change, are described in Table 2.

Both variables were integrated into a spatial resolution cellular space of 100km<sup>2</sup> (10 km x 10 km), created in the TerraView GIS environment using the Fill Cell Plugin (BEZERRA et al., 2022). The use of cellular space made it possible to homogenize the factors described above, regardless of their source format (vector data, matrix data, etc.), aggregating them in the same space-time basis, through operators (e.g., percentage of each class, minimum distance, etc.) used according to the geometric representation and semantics of the attributes of the input data.

### **2.2.2.2 Model description**

An open-source modeling framework, LuccME (<http://luccme.ccst.inpe.br/luccme/>), originally developed on the TerraME computational environment at the Earth System Science Center of the National Institute for Space Research (CCST/INPE) and partners (BEZERRA et al., 2022; CARNEIRO et al., 2013), was adopted in this work to build a new spatially explicit LUCC model to project future scenarios of land use/cover changes for the São Francisco River Basin.

Through LuccME framework modeling, the modelers can combine (existing and/or creating new) different components, such as demand (quantifying the changes), potential (calculation of the suitability of change for each cell), and allocation (spatial distribution of changes based on land demand and each cell's potential to change), to create different land use and land cover change (LUCC) models at different space-time scales (AGUIAR et al., 2012).

The adapted generic structure of the main spatially explicit land use/cover change models (TEJADA et al., 2016), shows that this open-source modeling framework, LuccME, follows several well-known LUCC models' structures that use a range of different approaches and techniques for their three components.

However, the LuccME modeling framework (CARNEIRO et al., 2013), allows the building of new models, combining the elements of demand, potential components, and allocation, which are designed according to the concepts of the main LUCC models found in the literature, CLUE (TIESKENS et al., 2017; VERBURG et al., 1999, 2019), Dynamic EGO (SOARES-FILHO; COUTINHO CERQUEIRA; LOPES PENNACHIN, 2002), GEOMOD (PONTIUS; CORNELL; HALL, 2001), which are classified according to the purpose, scale, approach or underlying theory.

The demand component is responsible for determining the amount/intensity of the changes of each use change that is intended to be allocated for each time step (AGUIAR et al., 2012). In this case, the *LuccME Precomputed Values component was adopted* to calculate the annual demand considering the amount of land use and occupation change for each transition period (BEZERRA, 2016), how much will be able to change annually from each class in the period from 2010 to 2050, according to equation 12.

$$C_{ca} = \frac{L_{ctf} - L_{cti}}{n_t} \quad \text{Eq. 12}$$

where  $C_{ca}$  corresponds to the annual change in the area of the land use class  $L_c$  between the initial  $t_i$  and  $t_f$  end year of the chosen period, and  $n_t$  refers to the number of years of the period.

Among the various ways of calculating the annual demand  $D_{cat_k}$ , in the present study, the demand was calculated for the period 2010 and 2050 (presented in Table 7), considering the difference in the area (km<sup>2</sup>) of each of the classes of land use and cover and redistributed equally for each year, in the period considered, according to equation 13.

$$D_{cat_k} = L_{ct_{k-1}} + C_{ca}, \quad \text{Eq. 13}$$

where  $D_{cat_k}$  corresponds to the annual demand of a given land use class in a year  $t_k$ , calculated from the sum of the class area in the previous year  $t_{k-1}$ , and the annual change  $C_{ca}$

Table 7: Land demand parameters

Precomputed values		SSP1 RCP 1.9		SSP2 RCP 4.5		SSP3 RCP 7.0	
Agriculture	from	47,046	km <sup>2</sup> (2000)	47,046	km <sup>2</sup> (2000)	47,046	km <sup>2</sup> (2000)
	to	24,725	km <sup>2</sup> (2050)	64,441	km <sup>2</sup> (2050)	214,305	km <sup>2</sup> (2050)
Natural Forest	from	283,932	km <sup>2</sup> (2000)	283,932	km <sup>2</sup> (2000)	283,932	km <sup>2</sup> (2000)
	to	318,615	km <sup>2</sup> (2050)	223,982	km <sup>2</sup> (2050)	176,665	km <sup>2</sup> (2050)
Pasture	from	30,302	km <sup>2</sup> (2000)	30,302	km <sup>2</sup> (2000)	30,302	km <sup>2</sup> (2000)
	to	33,573	km <sup>2</sup> (2050)	50,502	km <sup>2</sup> (2050)	53,815	km <sup>2</sup> (2050)
Mosaic of Agr. /Pasture	from	105,791	km <sup>2</sup> (2000)	105,791	km <sup>2</sup> (2000)	105,791	km <sup>2</sup> (2000)
	to	137,164	km <sup>2</sup> (2050)	209,918	km <sup>2</sup> (2000)	178,687	km <sup>2</sup> (2050)
Forest plantation	from	4,214	km <sup>2</sup> (2000)	4,214	km <sup>2</sup> (2050)	4,214	km <sup>2</sup> (2000)
	to	2,024	km <sup>2</sup> (2050)	5,274	km <sup>2</sup> (2000)	1,592	km <sup>2</sup> (2050)

In the initial year, the demand value corresponds to the observed value of the land use class, calculated based on the land use and land cover data used; in this case, MapBiomias LULC data.

For the potential module, the LuccME / São Francisco model used a component alternative based on *Spatial Lag Regression*, which considers the spatial autocorrelation between the determining factors (explanatory factors) (AGUIAR et al., 2012), and dependence to estimate the potential of cellular space to change at each time step (BEZERRA, 2016), and can be translated by equations 14 and 15.

$$Potential_{x,y,t,u} = \% \text{ of estimated usage}_{x,y,t} - \% \text{ of the usage}_{x,y,t-1} \quad \text{Eq. 14}$$

$$Potential_{x,y,t,u} = \% \text{ use}_{x,y,t} \text{ estimate} \quad \text{Eq. 15}$$

where:  $u$  is related to the type of land use or cover;  $x$  and  $y$  correspond to the location of the cell in the cellular plane in time  $t$ .

Finally, the allocation component used in the LuccME/São Francisco model was based on components of the CLUE Like (VERBURG et al., 1999) implemented by the INPE (AGUIAR et al., 2012) to generate annual maps of land use and occupation changes.

This module distributes spatially and interactively the land use changes according to the previous components (demand and potential), based on the competition between the types of land uses in each cell and within a previously established maximum error, according to equation 16, proposed by (BEZERRA, 2016) that describes the allocation process for each type of land use/cover.

$$L_{c,x,y,t} = L_{c,x,y,t-1} + Pot_{c,x,y,t} * ITF_c \quad \text{Eq. 16}$$

where the amount of area allocated from a given class of land use  $L_c$  at a given  $xy$  location in the cell plane at time  $t$  is determined in an iterative process of the sum of  $L_{c, x, y}$  at time  $t - 1$  and the potential

$Pot_{c,x,y,t}$  multiplied by an adjustment factor proportional to the difference between the allocated area, the reported demand, and the direction of the change  $ITF_c$ .

### 2.2.2.3 Model parameterization/calibration

After compiling the database, a statistical analysis was performed to select the set of variables to be considered in the model. First linear regression was carried out using R software (stepwise regression<sup>8</sup> included), and then the variables considered significant in this analysis were submitted for spatial correlation analysis between them, through the GeoDa software (ANSELIN; SYABRI; KHO, 2006), which identified *Spatial Lag Regression* as the appropriate regression, based on the correlation coefficient ( $R^2$ ) and the significance of each variable presented in Table 8.

When the spatial correlation was identified, the *Potential CS Spatial Lag Regression* was used, according to equation 17, which is based on and adapted from the spatial lag model (AGUIAR; CÂMARA; ESCADA, 2007; ANSELIN; SYABRI; KHO, 2006), and based on the correlation coefficient ( $R^2$ ), whose significance of each variable was selected for the model setup.

In this component, it is considered that the influence of neighboring areas occurs, a characteristic that is intrinsic to changes in land use and land cover (BEZERRA et al., 2022). In addition, this component allows this potential to be dynamic over the modeled period, that is, every year.

$$Pot_{c,x,y,t} = \%RegL_{c,x,y,t} - \%L_{c,x,y,t-1} : \{Pot_{cxyt} \in \mathcal{R} \parallel -1 \leq Pot_{cxyt} \leq 1\} \quad \text{Eq. 17}$$

where  $Pot_{c,x,y,t}$  corresponds to the potential for the occurrence of a given land use class  $L_c$  in a given location  $xy$  in a given time step  $t$ . To determine the potential, the percentage of land use estimated by the regression  $RegL_{c,x,y,t}$  is subtracted from the percentage of existing use  $L_{c,x,y}$  at time  $t - 1$ .

Table 8 details the general parameters, spatial lag regression parameters, and final components of LuccME, such as Spatial Lag Regression, *Clue Like Allocation Saturation*, and Pre-Computed Values, in which we externally calculate demand and inform the expected area for each land use class annually from 2010 to 2050.

---

<sup>8</sup>Stepwise regression is a method of fitting regression models in which the choice of predictive variables is carried out by an automatic procedure. In each step, a variable is considered for addition to or subtraction from the set of explanatory variables based on some prespecified criterion (ANDREW et al., 2017; TRANCOSO et al., 2016).

Table 8: Description of model components, temporal, and spatial resolution, selected determinant variables, and scenario assumptions regarding land use projections

General parameters	Spatial scale	Extent		Entire São Francisco River basin	
		Resolution (Cellular Space)		10 km x 10 km (100km <sup>2</sup> )	
		Extent		2010 – 2050	
	Temporal scale	Resolution		Yearly	
		Period	Calibration	2010 – 2015	
			Validation	2015 – 2019	
			Scenarios	2020 – 2050	

SPATIAL LAG REGRESSION PARAMETERS					
POTENTIAL:					
	Drivers	Metric	Regression coefficient	std Error	Significance
<b>Agriculture</b> (R-squared: 0.795721)	Temporary protection	Area	6.45455e-008	6.8895e-009	0.00000
	Livestock	Area	-5.99827e-008	1.26092e-008	0.00000
	Permanent protection	Area	3.26743e-007	1.16139e-007	0.00490
	Population	Average (in the year 2010)	2.59976e-008	7.6434e-009	0.00067
	Railroad	Distance	1.30584e-007	1.78403e-008	0.00000
	State highways	Distance	-3.95903e-007	7.68316e-008	0.00000
	Priority areas	Area	-0.0205208	0.00213161	0.00000
	Conservation areas	Area	-0.0166808	0.00316594	0.00000
	Settlement	Area	-0.0307039	0.00902494	0.00067
	Aptitude (good)	Area	0.0345094	0.00541664	0.00000
	Regular areas	Area	0.0324042	0.00332226	0.00000
	Restricted areas	Area	0.0124764	0.00314856	0.00007
	<b>Forest Plantation</b> (R-squared: 0.557428)	Priority areas	Area	-0.00415734	0.000970073
Regular area		Area	0.00462673	0.00166935	0.00558
Restricted areas		Area	-0.00347557	0.00166454	0.03680
Sugarcane mills		Distance	-2.0069e-008	2.87803e-009	0.00000
ag_pv		Average	0.00796724	0.00175907	0.00001
Unsuitable areas		Area	-0.00933544	0.00210178	0.00001
<b>Natural Forest</b> R-squared: 0.808121	Livestock enterprises	Number	-6.76544e-006	2.32028e-006	0.00355
	Temporary protection	Area	-4.23389e-008	1.30666e-008	0.00119
	Livestock	Area	2.00632e-007	2.77826e-008	0.00000
	Gini index	Average	0.263603	0.0362989	0.00000
	Priority areas	Area	0.0461646	0.00395371	0.00000
	Conservation areas	Area	0.0388826	0.005736	0.00000
	ag_pv	Average	0.0708852	0.00752883	0.00000
	Unsuitable areas	Area	0.161762	0.00847408	0.00000
	Regular area	Area	0.0736055	0.00645427	0.00000
	Restricted areas	Area	0.0796189	0.00642088	0.00000
	Priority areas	Average	0.00129813	0.000147786	0.00000
	State highways	Distance	6.63987e-007	1.28749e-007	0.00000
<b>Mosaic of Agriculture and Pasture</b> (R-squared: 0.782430)	State highways	Distance	-9.99207e-008	3.29047e-008	0.00239
	Regular area	Area	0.00369373	0.00149181	0.01329
	Restricted areas	Area	0.0130552	0.00153997	0.00000
	avprech	Average	-8.05443e-005	1.80587e-005	0.00001
	arem	Area	0.00841796	0.00137817	0.00000
<b>Pasture</b> (R-squared: 0.837762)	Livestock	Area	-5.23291e-008	1.71047e-008	0.00222
	Gini index	Average	-0.135681	0.0253183	0.00000
	State highways	Distance	-5.95004e-007	9.75338e-008	0.00000
	Priority areas	Area	-0.0144852	0.00286281	0.00000
	Conservation areas	Area	-0.0263836	0.00435291	0.00000
	ag_pv	Average	0.0289874	0.00565199	0.00000
	Regular area	Area	0.0276702	0.00432994	0.00000
	Restricted areas	Area	0.0330068	0.00426209	0.00000
	aveap	Average	-0.000291749	6.60039e-005	0.00001
	avtmh	Average	0.00409536	0.000460744	0.00000

#### 2.2.2.4 Model validation

For the validation of the models implemented in the LuccME, two routines are available: multiresolution of the entire area (ext.) and multiresolution of the areas where there were changes (dif.). The two routines compare the difference between the actual data and the simulated data.

For the validation of the model, the adjustment validation metric was adopted by multiple resolutions (COSTANZA, 1989), to compare the results of the model and the changes in land use and occupation observed between 2015 and 2019.

Centrally, the common metric is the level of similarity between the simulated and original map at different levels of coincidence on a scale of 1 to 10 (BEZERRA, 2016; COSTANZA, 1989).

Therefore, this approach allows the evaluation, of both localization errors in the resolution of the model itself and spatial pattern errors, degrading the resolution of maps (BEZERRA et al., 2022). The similarity level can be calculated based on equation 18:

$$NSi = 1 - \left[ \frac{\sum_{j=1}^n (|\sum_{c=1}^k dif_{sim,c} - \sum_{c=1}^k dif_{real,c}|)}{2 * \sum_{j=1}^n \sum_{c=1}^k dif_{real,c}} \right] * 100 \quad \text{Eq. 18}$$

where  $NS$  corresponds to the level of similarity between the actual and simulated maps at a given resolution  $i$ ;  $j$  is the window considered;  $n$  establishes the number of windows/cells to be considered;  $tex.tif$   $c$  is the number of cells in a resolution  $k(i*i)$ ; and  $dif_{real} = \%real_{t_f} - \%real_{t_i}$  and  $dif_{sim} = \%sim_{t_{final}} - \%real_{inicial}$ , being  $t_i$ , and  $t_f$  the initial and real years, respectively, considered in the validation.

The results are shown in percentages of hit considered through resolution windows (multiresolution), according to the similarity between the maps observed and simulated in various resolutions (1x1, 2x2, 3x3, 4x4, 5x5, 6x6, 7x7, 8x8, 9x9 and 10x10) (AGUIAR et al., 2016; FONSECA et al., 2019), through the sampling windows that increase in each period, having adopted the permission of 0% error per cell. This metric is particularly useful for characterizing land use and land cover change and for validating land use and land cover change models (JOHLL; POISTER; FERGUSON, 2002).

#### 2.2.3 Scenario assumptions

The scenarios developed in the present study were based on assumptions suggested by (BEZERRA et al., 2022), i.e.:

- SSP1 RCP 1.9 (sustainable development scenario) – is a scenario that assumes that all existing environmental laws are in force and policies to reduce deforestation, encourage

environmental restoration, and preserve conservation units and indigenous lands, providing an initial framework for our analysis of sustainability pathways.

- SSP2 RCP 4.5 (intermediate scenario) – this scenario assumes maintaining some of the positive trends of the last decade).
- SSP3 RCP 7.0 (scenario of strong unevenness) – which reflects a weakening of efforts in recent years, especially in the socio-environmental dimension.

## 2.3 Results and Discussion

### 2.3.1 Model performance

The distribution of land-use classes and dissimilarities between the observed and simulated data in the validation year 2019 are presented in Figures 6 and 7. The model presented satisfactory performance (BEZERRA et al., 2022), with an average spatial adjustment index between observed and simulated data in 2019 corresponding to 89.48%, as shown in Table 9.

Table 9: Percentage of spatial adjustment and errors

Land use class.	Adjustment	Spatial adjustment		Errors	
		Patterns	Modified areas %	Omissions	Commission
Agriculture	88.75	61.53	1.60	2.27	
Natural Forest	97.13	56.47	2.35	0.53	
Pasture	94.48	49.44	2.99	2.83	
Mosaic of Agr. /Pasture	78.13	49.85	3.12	2.05	
Forest plantation	88.93	55.62	2.88	3.14	
Average	89.48	54.58	2.59	2.16	

When considering only the areas where some change occurred, the average adjustment index was 54.58%. The average percentage of adjustment errors corresponding to omissions was 2.59%, while commission errors were approximately 2.16%. The lowest omission and commission errors were observed in the Agriculture and Natural Forest classes, with 1.60% and 0.53%, respectively. Among all classes of land use, the highest general values of spatial adjustment were observed for natural forest and pasture, with 88.75% and 97.13%, respectively, if considered pattern changes.

When considering the areas where changes occurred, the average of the adjustment index of all classes was 54.58%; and among the classes that presented the highest values of spatial adjustment, agriculture, natural forest, and forest plantation stand out, with 61.53%, 56.47%, and 55.62%, respectively.

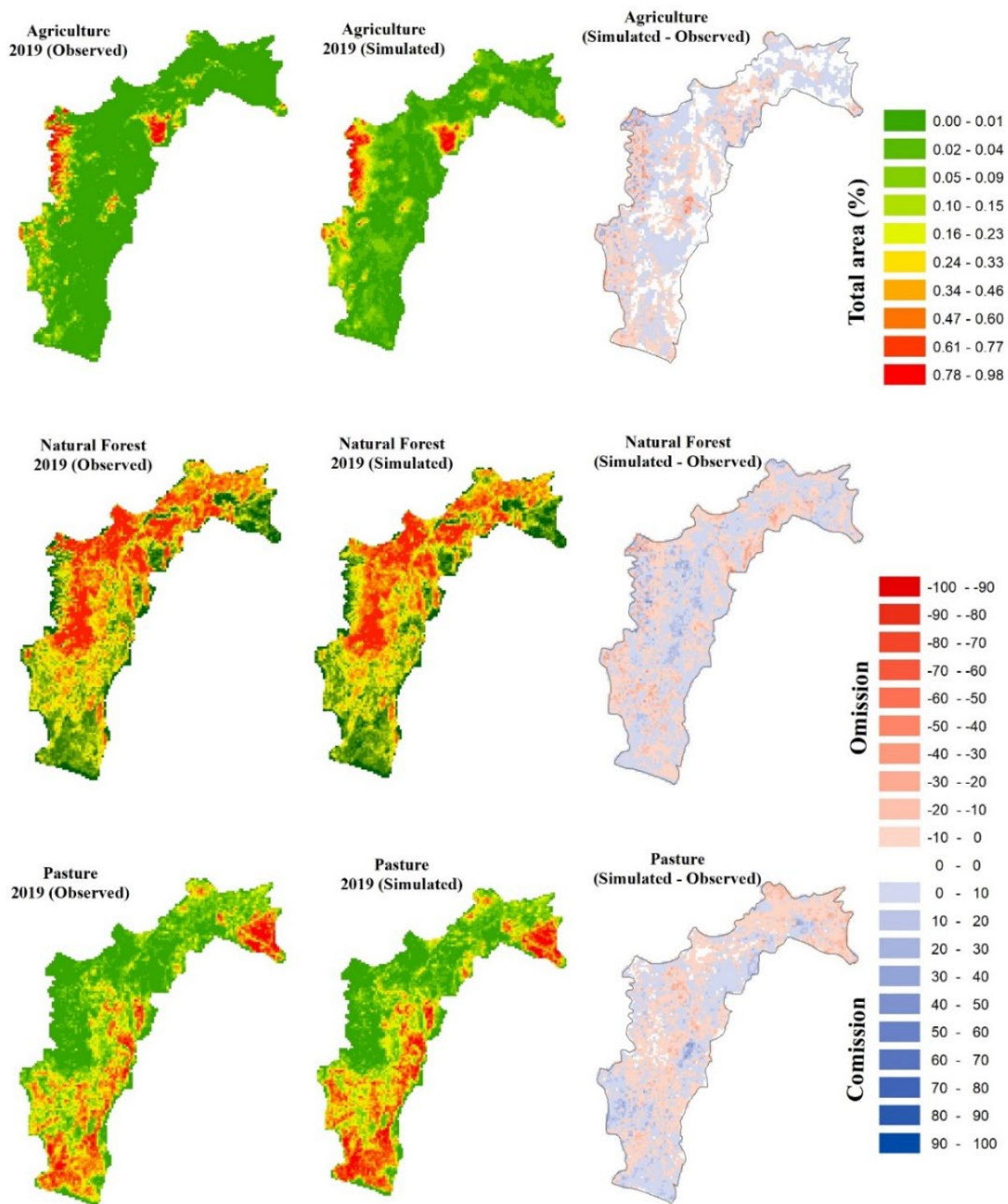


Figure 6: Percentage of agriculture, natural forest, and pasture observed versus simulated in 10 x 10 km<sup>2</sup> cells in 2019, and the spatial distribution of omission and commission errors

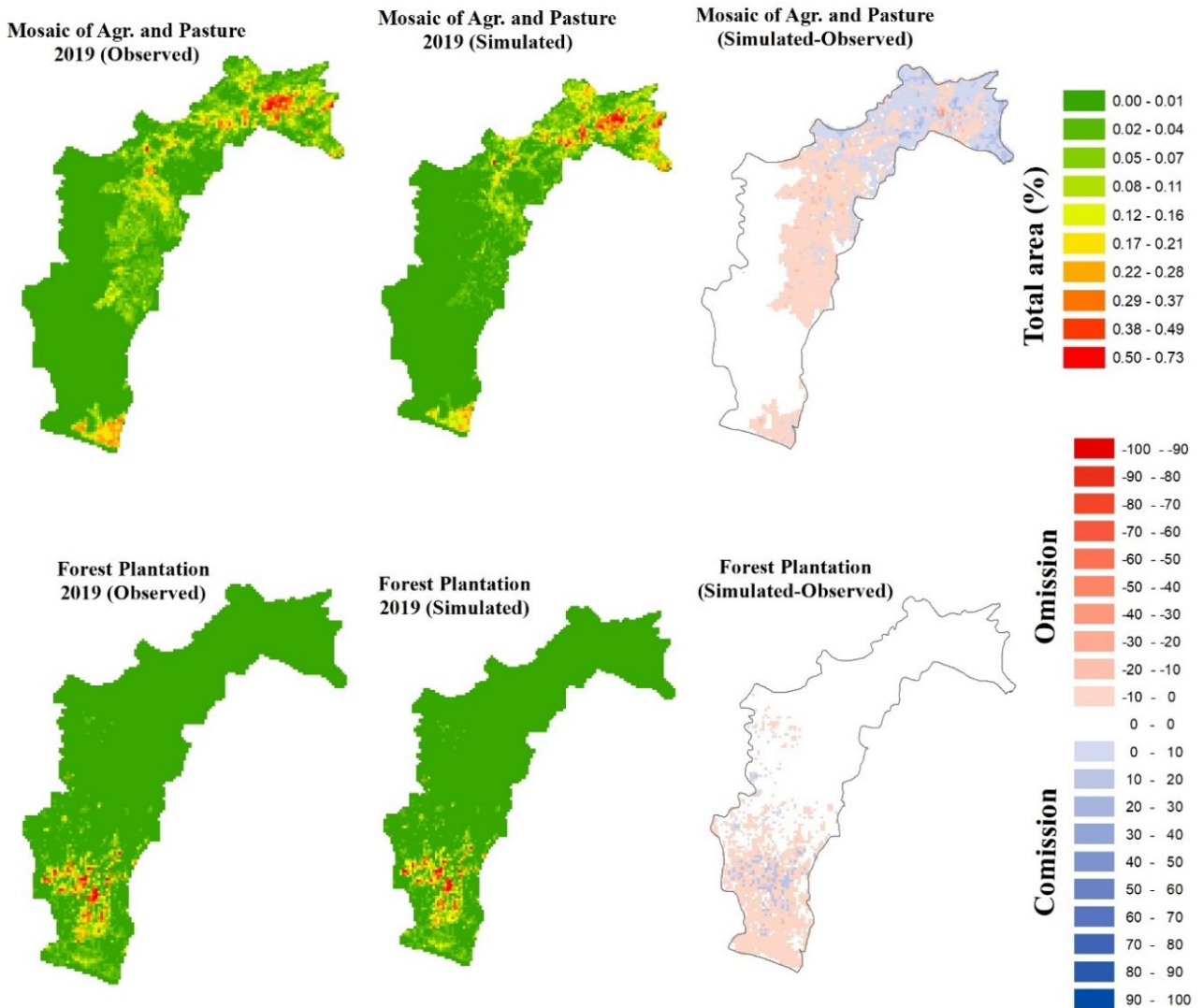


Figure 7: Percentage of the mosaic of agriculture and pasture, forest plantation observed versus simulated in 10 x 10 km<sup>2</sup> cells in 2019, and the spatial distribution of errors of omission and commission

Fig 8 shows the spatially explicit distribution of the classes of land use in the initial year of the simulation (2010) and the three scenarios considered in this work (for the year 2050). It can be seen that the scenarios of the middle of the road and strong inequality, present similar patterns in all classes of use, with emphasis on the significant increase in the classes of pasture, and mosaic of agriculture and pasture, with intensification in the regions of middle and Sub-middle, and lower São Francisco, where equally were observed the regeneration of forest vegetation in both scenarios.

### 2.3.2 Scenarios of land-use Change

Figure 8 presents the spatial distribution of areas and land use according to the scenarios from 2010 to 2050.

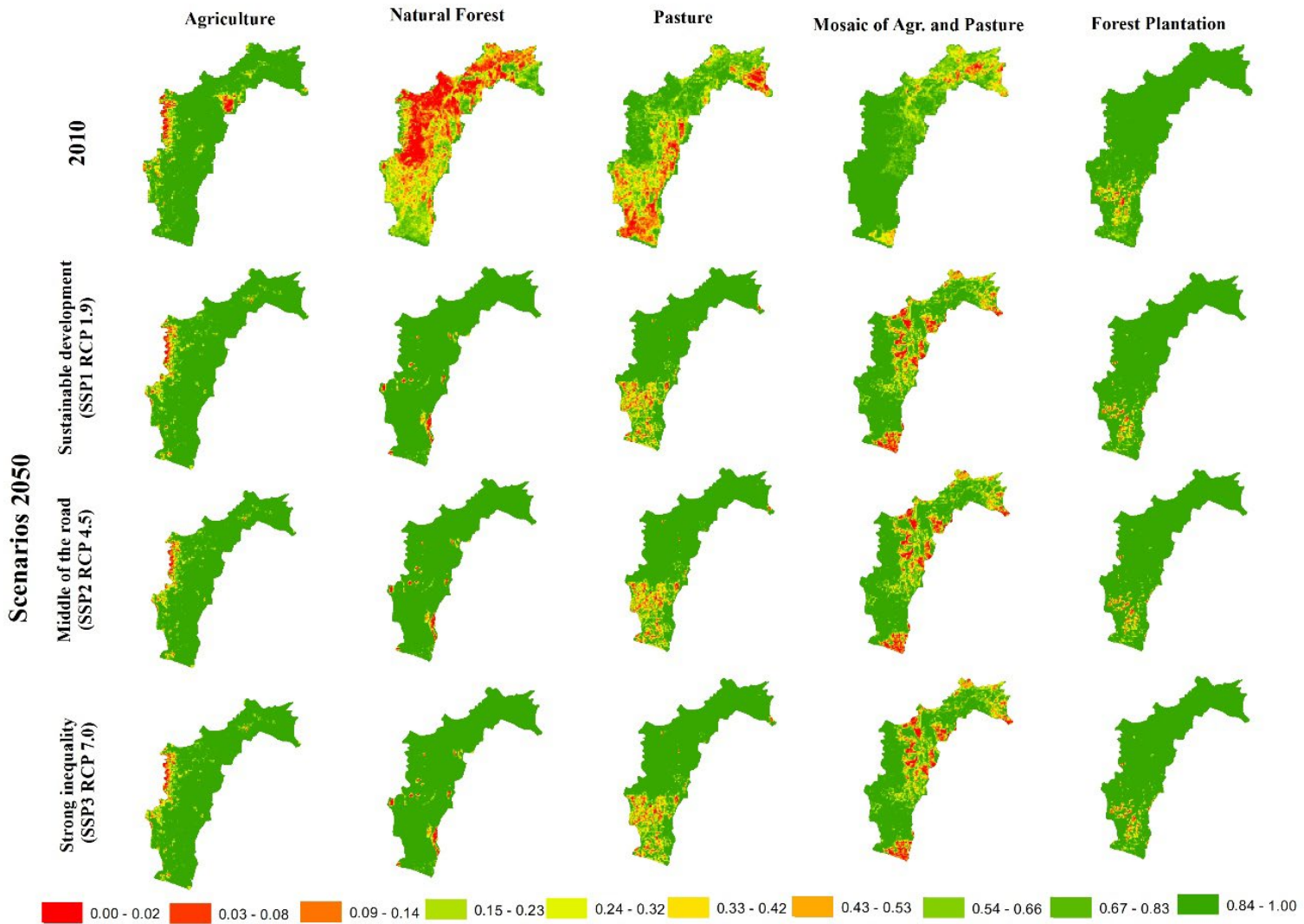


Figure 8: Spatial distribution (%) of areas and land use according to the scenarios from 2010 to 2050

Table 10 shows the direction of change in land use and coverage, according to classes and scenarios between 2010 (observed year) and 2050 (final year).

Table 10: The direction of change in land use change, according to classes and scenarios between 2010 and 2050

Legend: ↗ = Increase and ↘ = Reduction.

	Agriculture	Natural Forest	Pasture	Forest Plantation	Mosaic of Agr. /Pasture
SSP1 RCP 1.9	↗	↗	↗	↘	↗
SSP1 RCP 4.5	↗	↘	↗	↗	↗
SSP1 RCP 7.0	↗	↘	↗	↗	↗

Analyzing the dynamics of land use change (Table 10), according to the scenarios considered, has been observed that agriculture, pasture, and mosaic of agriculture and pasture, will continue in the same direction, regardless of the scenario considered.

Regarding the class of agriculture, this will triple from one scenario to another by 2050. These results corroborate with estimated increase of irrigated areas by 130,323 ha between 2018 and 2025 (BETTENCOURT et al., 2022), more than double the expansion of agriculture by the year 2035 (MORAES et al., 2013). Similar results of the expansion of agriculture over the next two decades were also observed (FACHINELLI FERRARINI et al., 2020; LIMA et al., 2022), with the clearest expansion and water demand increase occurring in Upper and Middle São Francisco.

As shown in Table 10 and Figure 8, the expansion of the agriculture class will be led by the decrease of conservation areas, protection (temporary and permanent), and the regular suitability of these areas for the practice of agriculture.

Differently to the class of forest plantation, which will increase in these two scenarios (SSP1 RCP 4.5 and SSP1 RCP 7.0), the class of natural forest in the middle road and strong inequality scenarios, corroborating with an accelerated modification of the natural conditions of the basin reported by between 1985 and 2015 (LIMA et al., 2022), specifically in Upper São Francisco due to the observed urbanization process and planted forest area growth.

According to scenarios of halfway and strong inequality (SSP1 RCP 4.5 and SSP1 RCP 7.0), the natural forest will suffer a reduction of approximately 59,950 km<sup>2</sup> and 69.627 km<sup>2</sup>, respectively, until 2050, mainly in Upper and Middle San Francisco. However, in the sustainable development scenario (SSP1 RCP 1.9), the natural forest will increase by 34,683 km<sup>2</sup>. This increase occurs mainly in the Sub-middle and Lower São Francisco, as shown in Figure 4.

Total loss estimates of 7,496,128 ha in different types of native vegetation between 1997 and 2017 reported live up to what will happen with natural forests (FERNANDES et al., 2021), which will tend to reduce its length in the scenarios of the middle of the road and strong

inequalities (59,950 and 107.267 km<sup>2</sup>, respectively). Differently from the sustainable development scenario, there will be an increase of 34,683 km<sup>2</sup>.

Although the results have shown an increase in agriculture, pasture, and mosaic of agriculture and pasture, regardless of the scenario considered, the increase will occur with greater intensity in the scenarios of the middle of the road and strong inequalities for the class of mosaic and pasture, unlike the agriculture that will register the largest increase in the scenario of the middle of the road; with a difference of about 149,863 km<sup>2</sup>, when compared to the scenario of strong inequality.

The set of scenarios presented in this work provides important information, which can help establish public policies that can contribute to biodiversity conservation and reduce emissions from deforestation and degradation, especially those resulting from land use/cover changes. In addition, this set of scenarios with extension throughout the São Francisco region makes it possible to understand how decision-making and the demands of all States that compose this region can influence different processes, including hydrologic, along the São Francisco river basin.

## 2.4 Conclusion

In this work, we assess land use change in the SFRB by building a spatially explicit land use change model that considers drivers of deforestation, different land needs, land policies, and governance arrangements, and operates under three Scenarios running to 2050: optimistic), intermediate (similar to "business as usual") and fragmented (worst).

In the last two cases (road-centric and fragmented), we observed a tendency for the plantation category to increase. It was observed that the classes defined by planted forests tend to increase in his last two scenarios (road-centric and fragmented). It can be concluded that advanced agricultural development in the San Francisco River basin may be directly related to flow changes in this region.

Significant and increasing changes in land use in the SFRB were agriculture, pasture, and mosaic of agriculture and pasture, for the three scenarios, which will be led by the reduction of conservation units, protection (temporary and permanent), and regular adaptation of these areas for the practice of agriculture.

Preventing the expansion of the agricultural practices in the SFRB cannot ensure biodiversity conservation or carbon savings in the absence of complementary measures committed to land use efficiency, controlled land use expansion, and new economic alternatives. In this perspective, recognizing land-use systems as open and human-driven systems is a first and central challenge in designing more efficient land-use policies, the author recommends carrying out future studies to analyze the changes considering more classes of land-use and other land-use databases, instead of the 5 land-use classes from the MapBiomias initiative adopted in the present study.

Land-use change scenarios are useful in showing how present and future decisions could affect land change trends in the São Francisco region. A real-life scenario could be a combination of the three scenarios presented in this study. Observing the potential impacts of land use in a spatially explicit way, as a valuable discussion on the existing laws of the three scenarios considered in this work, can help to prevent (or reduce) and influence policy markers' actions to improve land-use governance.

It is expected that this work can contribute to adequate planning and better management of water resources in the SFRB since changes in LULC can directly interfere with the regime of monthly average flows of the region.

## References

- AGUIAR, A. P. D. et al. Land use change emission scenarios: Anticipating a forest transition process in the Brazilian Amazon. **Global Change Biology**, v. 22, n. 5, p. 1821–1840, 2016.
- AGUIAR, A. P. D. A. N. A. et al. Modeling the spatial and temporal heterogeneity of deforestation-driven carbon emissions : the INPE-EM framework applied to the Brazilian Amazon. p. 3346–3366, 2012.
- AGUIAR, A. P. D.; CÂMARA, G.; ESCADA, M. I. S. Spatial statistical analysis of land-use determinants in the Brazilian Amazonia: Exploring intra-regional heterogeneity. **Ecological Modelling**, v. 209, n. 2–4, p. 169–188, 2007.
- ANDREW, V. et al. An ensemble of spatially explicit land-cover model projections : prospects and challenges to retrospectively evaluate deforestation policy MODELING EARTH SYSTEMS AND ENVIRONMENT. 2017.
- ANSELIN, L.; SYABRI, I.; KHO, Y. <Anselin et al\_2005\_GeoDa\_An Introduction to Spatial Data Analysis.pdf>. v. 38, p. 5–22, 2006.
- BETTENCOURT, P. et al. Prospective Water Balance Scenarios (2015–2035) for the Management of São Francisco River Basin, Eastern Brazil. **Water (Switzerland)**, v. 14, n. 15, p. 1–24, 2022.
- BEZERRA, B. G. et al. Changes of precipitation extremes indices in São Francisco River Basin, Brazil from 1947 to 2012. **Theoretical and Applied Climatology**, v. 135, n. 1–2, p. 565–576, 2019.
- BEZERRA, F. G. S. Contribuição de fatores socioeconômicos, biofísicos e da agropecuária à degradação da cobertura vegetal como “proxy” da desertificação no semiárido do nordeste do brasil. **Instituto Nacional de Pesquisas Espaciais - Tese de Doutor**, p. 207, 2016.
- BEZERRA, F. G. S. et al. New land-use change scenarios for Brazil: Refining global SSPs with a regional spatially-explicit allocation model. **PLoS ONE**, v. 17, n. 4 April, p. 1–17, 2022.
- CARNEIRO, T. G. DE S. et al. An extensible toolbox for modeling nature-society interactions. **Environmental Modelling and Software**, v. 46, p. 104–117, 2013.
- COSTANZA, R. Model goodness of fit: A multiple resolution procedure. **Ecological Modelling**, v. 47, n. 3–4, p. 199–215, 1989.
- DIAS, L. C. P. et al. Patterns of land use, extensification, and intensification of Brazilian

- agriculture. **Global change biology**, v. 22, n. 8, p. 2887–2903, 2016.
- FACHINELLI FERRARINI, A. DOS S. et al. Water demand prospects for irrigation in the São Francisco river: Brazilian public policy. **Water Policy**, v. 22, n. 3, p. 449–467, 2020.
- FERNANDES, J. G. Estimativa de vazão e produção de sedimentos na Bacia Hidrográfica do Rio São Francisco, utilizando o modelo SWAT. **Universidade Federal de Pernambuco - Tese de doutorado**, p. 186, 2015.
- FERNANDES, M. M. et al. Land use and land cover changes and carbon stock valuation in the São Francisco river basin, Brazil. **Environmental Challenges**, v. 5, n. August, p. 100247, 2021.
- FONSECA, M. G. et al. Effects of climate and land-use change scenarios on fire probability during the 21st century in the Brazilian Amazon. **Global Change Biology**, v. 25, n. 9, p. 2931–2946, 2019.
- FRANCESCONI, W. et al. Using the Soil and Water Assessment Tool (SWAT) to model ecosystem services: A systematic review. **Journal of Hydrology**, v. 535, p. 625–636, 2016.
- JOHLL, M. E.; POISTER, D.; FERGUSON, J. Statistical Comparison of Multiple Methods for the Determination of Dissolved Oxygen Levels in Natural Waters. **The Chemical Educator**, v. 7, n. 3, p. 146–148, 2002.
- LIMA, C. E. S. et al. Anthropogenic Changes in Land Use and Land Cover and Their Impacts on the Hydrological Variables of the São Francisco River Basin, Brazil. **Sustainability (Switzerland)**, v. 14, n. 19, 2022.
- MARQUES, É. T.; GUNKEL, G.; SOBRAL, M. C. Management of tropical river basins and reservoirs under water stress: Experiences from northeast Brazil. **Environments - MDPI**, 2019.
- MORAES, A. DE et al. The impact of global changes on economic values of water for Public Irrigation Schemes at São Francisco river basin in Brazil. p. 1–24, 2013.
- NEMUS. PLANO DE RECURSOS HÍDRICOS DA BACIA A BACIA HIDROGRÁFICA DO RIO SÃO FRANCISCO. In: [s.l.: s.n.]. v. 2.
- NOOJIPADY, P. et al. Forest carbon emissions from cropland expansion in the Brazilian Cerrado biome. **Environmental Research Letters**, v. 12, n. 2, 2017.
- OLIVEIRA, P. T.; SANTOS E SILVA, C. M.; LIMA, K. C. Climatology and trend analysis of extreme precipitation in subregions of Northeast Brazil. **Theoretical and Applied**

**Climatology**, v. 130, n. 1–2, p. 77–90, 2017.

PONTIUS, R. G.; CORNELL, J. D.; HALL, C. A. S. Modeling the spatial pattern of land-use change with GEOMOD2: Application and validation for Costa Rica. **Agriculture, Ecosystems and Environment**, v. 85, n. 1–3, p. 191–203, 2001.

PRESTELE, R. et al. Hotspots of uncertainty in land-use and land-cover change projections: a global-scale model comparison. **Global Change Biology**, v. 22, n. 12, p. 3967–3983, 2016.

SOARES-FILHO, B. S.; COUTINHO CERQUEIRA, G.; LOPES PENNACHIN, C. DINAMICA - A stochastic cellular automata model designed to simulate the landscape dynamics in an Amazonian colonization frontier. **Ecological Modelling**, v. 154, n. 3, p. 217–235, 2002.

SOUZA, C. M. et al. Reconstructing three decades of land use and land cover changes in Brazilian biomes with Landsat archive and Earth Engine. **Remote Sensing**, v. 12, n. 17, 2020.

TEIXEIRA, A. L. DE F. et al. Operationalizing water security concept in water investment planning: Case study of São Francisco river basin. **Water (Switzerland)**, v. 13, n. 24, 2021.

TEJADA, G. et al. Deforestation scenarios for the Bolivian lowlands. **Environmental Research**, v. 144, p. 49–63, 2016.

TIESKENS, K. F. et al. Cultural landscapes of the future : using agent-based modeling to discuss and develop the use and management of the cultural landscape of South West Devon. **Landscape Ecology**, v. 32, n. 11, p. 2113–2132, 2017.

TRANCOSO, R. et al. Linking the Budyko framework and the Dunne diagram. **Journal of Hydrology**, v. 535, p. 581–597, 2016.

VAN ASSELEN, S.; VERBURG, P. H. Land cover change or land-use intensification: Simulating land system change with a global-scale land change model. **Global Change Biology**, v. 19, n. 12, p. 3648–3667, 2013.

VAN BEEK, L. et al. Anticipating futures through models: the rise of Integrated Assessment Modelling in the climate science-policy interface since 1970. **Global Environmental Change**, v. 65, n. October, p. 102191, 2020.

VERBURG, P. H. et al. A spatial explicit allocation procedure for modelling the pattern of land use change based upon actual land use. **Ecological Modelling**, v. 116, n. 1, p. 45–61, 1999.

VERBURG, P. H. et al. Anthropocene Land system science and sustainable development of

the earth system : A global land project perspective. **Biochemical Pharmacology**, v. 12, p. 29–41, 2015.

VERBURG, P. H. et al. ScienceDirect Beyond land cover change : towards a new generation of land use models. n. June, 2019.

ZIMM, C.; SPERLING, F.; BUSCH, S. Identifying sustainability and knowledge gaps in socio-economic pathways vis-à-vis the sustainable development goals. **Economies**, v. 6, n. 2, 2018.

# CHAPTER III

---

## Multi-model ensemble for long-term statistical trend analysis of observed gridded precipitation and temperature data in the São Francisco River Basin, Brazil<sup>9</sup>

### **Abstract**

For effective management practices and decision-making, the uncertainties associated with regional climate models (RCMs) and their scenarios need to be assessed in the context of climate change. This study analyzes long-term trends in precipitation and temperature data sets (maximum and minimum values) from the NASA Earth Exchange Global Daily Downscaled Prediction (NEX-GDDP) under the São Francisco River Basin Representative Concentration Path (RCP) 4.5 and 8.5, using the REA (Reliable Ensemble Average) method. In each grid, the built multi-model was bias-corrected using the CMhyd model for annual, dry, wet, and pre-season periods – for historical (1961 – 2005) and future (2006 – 2100) periods. The multi-model and four different methods, namely: The Mann-Kendall, Mann-Kendall pre-brightening test, bias-corrected pre-brightening, and Spearman correlation, were used to detect trends in precipitation, and minimum and maximum temperature. The results show an increasing trend in mean annual temperature and precipitation across the basin. When analyzed by subregion, the results show an increasing trend in monthly average minimum and maximum temperatures in the lower, middle, and lower SFRB, while average monthly rainfall increases during the rainy season. and pre-season games in Upper São Francisco. These climate predictions can be provided to decision-makers such as Civil Defense who can use them to take actions/measures to relocate people/communities to less risky locations to minimize risk situations or vulnerabilities.

**Keywords:** reliable ensemble averaging, bias correction, trend analysis; nonparametric trend tests; Mann–Kendall; modified Mann–Kendall; climate uncertainties; projections, modifiedmk package.

---

<sup>9</sup>A modified version of this chapter will be shortly submitted to a peer-review international journal.

### 3.1 Introduction

The occurrence of climate change, which can change both the frequency and intensity of climate events (CARVALHO et al., 2020), has exposed a wide range of impacts on food production, water supply, and the environment (GEBRECHORKOS; HÜLSMANN; BERNHOFER, 2019), and are one of the major challenges for environmental and water resource management in the 21<sup>st</sup>-century (LIU et al., 2017).

Recent climate change has altered precipitation variability – spatial and temporal distribution, annual and seasonal patterns (BANERJEE et al., 2020), and increased temperature (in the order of 1.1°C and 6.4°C throughout the 2<sup>st</sup>-century) in different parts of the world (BERLATO; CORDEIRO, 2018), which have received much attention by researchers and water and environmental policymakers (PANDA; SAHU, 2019).

More severe extreme events will occur due to more severe climate change, causing significant consequences (HAZELEGER et al., 2012; LAKKU; BEHERA, 2022). Therefore, given the water scarcity, the prediction of climatic extremes is essential to analyze the impacts of climate change on the environment and in the numerous agricultural irrigation projects (ASSIS; SOUZA; SOBRAL, 2015).

The analysis of hydrometeorological time series trends gained importance in recent years (WANG et al., 2020), due to the impacts that are becoming very evident in the environment, in the hydrological cycle on a global, regional, and local scale, and in the social and economic well-being (FEREIDON; KOCH, 2018; KOTIR, 2011; MALLAKPOUR et al., 2022; NASCIMENTO DO VASCO; DE OLIVEIRA AGUIAR NETTO; GONZAGA DA SILVA, 2019). In addition, these analyses are relevant to assessing climate-induced changes and planning viable adaptation strategies related to these changes (PANDA; SAHU, 2019).

Precipitation and temperature are two of the most important variables in the field of climate sciences and hydrology often used to trace the extent and magnitude of climate changes and variability (CARVALHO et al., 2020), as these physical parameters determine the environmental condition of the particular region that affects agricultural productivity for food provision (KHAVSE et al., 2015; KUMAR; RAJ GAUTAM, 2014; SINGH; ARYA; CHAUDHARY, 2013).

The spatial and temporal variability of precipitation and temperature is notorious in several studies already pulsing around the world, studying patterns of trends concerning climate change, based on the observed data available for longer periods (BURI et al., 2022; HUNDECHA; BÁRDOSSY, 2005; ISOTTA; BEGERT; FREI, 2019; KANDA et al., 2020; LI et al., 2022; MALLAKPOUR et al., 2022).

In Brazil, scientific efforts to understand hydrometeorological aspects of the SFRB have been carried out, given its relevance to the Brazilian semiarid (BEZERRA et al., 2019;

MONTENEGRO; RAGAB, 2012; NETO et al., 2016), as there are still few detailed studies on the patterns of the long-term trend for precipitation and temperature (minimum and maximum) in the São Francisco River basin (ASSIS; SOUZA; SOBRAL, 2015; BEZERRA et al., 2019; FONSECA et al., 2019; SILVEIRA et al., 2016; SOUTO; BELTRÃO; TEODORO, 2019), which has suffered from systematic drought problems in recent years, leading to serious threats to water and environmental security (TEIXEIRA et al., 2021).

In this context, the SFRB is being considered as one of the areas of study for the development of an integrated water resource management model in climate change scenarios, as part of the ongoing BRICS-STI multilateral project (BURI et al., 2022).

Therefore, given the importance of redefining water resource management policies and making the system more resilient to the challenges of climate change, the main objective of this study is to analyze the seasonality, variability, and long-term trend of precipitation and temperature data available in the SFRB, using four different trending methods.

## **3.2 Materials and Methods**

### **3.2.1 Study area brief description**

The present study was carried out in the São Francisco River basin, located entirely in Brazil, covering an area of 636,920 km<sup>2</sup> (7.5% of the Brazilian national territory). It drains areas of seven federative units, with an extension of approximately 2.700 km, discharging 94 000 000 m<sup>3</sup> annually.

The average annual season and the flow of the 95<sup>th</sup> percentile (i.e., Q95 — a low flow metric) in the SFRB are 2914 m<sup>3</sup>/s and 875 m<sup>3</sup>/s, respectively (LUCAS et al., 2021). This includes fragments of different biomes, Atlantic forest, caatinga, coastal, and Cerrado that cover practically half of the basin area, in addition to the predominance of soils with an aptitude for irrigated agriculture (MARQUES; GUNKEL; SOBRAL, 2019).

The average annual evapotranspiration is 896 mm, presenting high values between 1400 and 840 mm, due to the high temperatures (22–32°C), the intertropical geographical location and the reduced cloudiness, high incidence of solar radiation, and the relatively high annual evaporation rates of around 2300 to 3000 mm.

The area has an irregular distribution of rainfall throughout the year, from November to January, the wettest quarter, contributing 55 to 60% of annual rainfall, while the driest quarter is from June (MARQUES; GUNKEL; SOBRAL, 2019).

The basin is an area of strategic economic and development importance, with socioeconomic disparities between the sub-basins, with emphasis on predominantly urban uses and occupations in the highest part, and agricultural and mining activity spread throughout the

basin, in addition to a robust industrial park, covering the metallurgical, textile, food, and chemical companies areas (BEZERRA et al., 2019).

In addition, the Lower Middle San Francisco is vulnerable to the occurrence of severe droughts, usually associated with strong El Niño (BEZERRA et al., 2019), besides being challenged by water conflicts for multiple uses (LUCAS et al., 2021), which makes it imperative to understand precipitation and temperature trends and their extremes over the Basin of the São Francisco River for flood vulnerability mapping and risk assessment, to improve water resource management strategies.

### 3.2.2 Data description

A 44-year dataset (1961 - 2005) was obtained through two databases, (i) daily rainfall data (mm) through the APAC website (Pernambuco State Agency for Water and Climate; <https://www.apac.pe.gov.br/monitoramento>), and ANA (National Water Agency; <https://www.snirh.gov.br/hidroweb/serieshistoricas>); (ii) complete meteorological data such as precipitation (mm), solar radiation ( $MJ/m^2$ ), relative humidity or dew point temperature (%), average air temperature, maximum and minimum air temperatures ( $^{\circ}C$ ), and wind speed (m/s) through the INMET (National Institute of Meteorology) database; <http://www.inmet.gov.br/projetos/rede/pesquisa/inicio.php>).

For the preparation of grid data, daily rainfall records of rainfall stations in Brazil and APAC stations (for the State of Pernambuco) were used. The grid data set was developed after the quality control of the rainfall stations, performed as follows: (i) replace all missing values (currently coded as – 99.9) into an internal format that the software recognizes (i.e., NA, not available) and (ii) replace all unreasonable values into NA.

Further, a 149-year dataset of historical climate data in  $0.25^{\circ} \times 0.25^{\circ}$  grids for precipitation and a  $1^{\circ} \times 1^{\circ}$  grid for temperature, were shared by the Indian team, as part of the ongoing multilateral BRICS research project, titled “*Integrated Water Management Model for Brazil, India, and South Africa under climate change scenarios*” (BURI et al., 2022).

### 3.2.3 The Multi-Model Ensemble Approach

Multi-model ensembles (MEMEs) are widely employed in short-range climate forecasting to reduce the underlying uncertainties related to GEOS-5 Atmosphere-Ocean General Circulation Models (AOGCMs) simulations/projections (AHMED et al., 2020), due to the models' complexity caused by measurement error, randomness, and systematic error in multiple climate models (CLARK et al., 2016). To address the underlying uncertainties in climate modeling, several RCMs and emission scenarios are employed and termed as Multi-Model Ensemble (MME) through a Reliability Ensemble Averaging (REA) approach (BURI et

al., 2022), which measures the multi-model uncertainty in the form of model performance to increases confidence when projecting climate data into the future, while projecting variables in the future periods.

Aiming to identify the optimum number of AOGCMs required for an MME from a pool of AOGCMs ranked based on their performance in simulating past observed climates, in this work, a total of nine driving CMIP5 AOGCMs (CAnESM2, CM5A-MR, CSIRO, EC-EARTH, GFDL-ESM2M, HadGEM2-ES, MIROC5, NORESM1, and SHMI-ESM) (BURI et al., 2022), and two emission scenarios (RCP 4.5 and RCP 8.5) (SCHWALM; GLENDON; DUFFY, 2020; THOMSON et al., 2011) – representing the present-day climate factually and involving comparing GCM<sup>10</sup> simulations with observed climate by considering performance measures.

The process of integrating an ensemble of models was done by taking a simple arithmetical average or by following a weighting procedure developed on the performance indicators of the RCMs simulating historic climate data, and BIAS Correction.

1. Performance indicators: To evaluate RCMs' ability to match the actual climate, the performance indicators used in this work were, Root Mean Square Deviation (RMSD), Normalized Root Mean Square Deviation (NRMSD), Absolute Normalized Mean Bias Deviation (ANMBD), Pearson Correlation Coefficient (CC), Nash–Sutcliffe Efficiency (NSE) and Skill Score (SS), whose mathematical equations for each indicator as well as their ideal values are summarized in Table 11.

For the calculation of performance indices, average monthly precipitation, and temperature data sets of observed (IMD) and simulated (RCM) values are used for the period 1961–2005. The observed and simulated values of the respective datasets are  $x_i$  and  $y_i$ . The mean of observed and simulated values is denoted by  $\bar{x}$  and  $\bar{y}$ . The number of datasets is denoted by  $T$ . The standard deviations of observed and simulated values are denoted by  $\sigma_{obs}$  and  $\sigma_{sim}$ , respectively.

Table 11: The mathematical equations and ideal values of performance metrics  
Source: adapted from (BURI et al., 2022)

S. No.	Performance Metric	Equation	Ideal Value
1	Root Mean Square Deviation (RMSD)	$\sqrt{\frac{1}{T} \sum_{i=1}^T (X_i - Y_i)^2}$	0
2	Normalized Root Mean Square Deviation (NRMSD)	$\frac{\sqrt{\frac{1}{T} \sum_{i=1}^T (X_i - Y_i)^2}}{\bar{X}}$	0

<sup>10</sup> RCM data can be accessed at: <https://esg-dn1.nsc.liu.se/search/esgf-liu/>.

3	Absolute Normalized Mean Bias Deviation (ANMBD)	$\left  \frac{\frac{1}{T} \sum_{i=1}^T (Y_i - X_i)}{\bar{X}} \right $	0
4	Pearson Correlation Coefficient (CC)	$\frac{\sqrt{\frac{1}{T} \sum_{i=1}^T (z_i - \bar{z})(y_i - \bar{y})}}{(T-1)\sigma_{obs}^{sim}}$	1
5	Nash–Sutcliffe Efficiency (NSE)	$1 - \frac{\sqrt{\frac{1}{T} \sum_{i=1}^T (x_i - y_i)^2}}{\sum_{i=1}^T (x_i - \bar{x})^2}$	1

## 2. Normalization Technique

The mathematical representation for normalization is shown in Equation 19 (PATAKAMURI; MUTHIAH; SRIDHAR, 2020), which helps the conversion of different proportionate indicators into the same space.

$$k_{aj} = \frac{k_j(a)}{\sum_{a=1}^N k_j(a)} \quad \text{Eq. 19}$$

where  $k_j(a)$  is the value of indicator  $j$  for RCM  $a$ ;  $N$  represents the total number of RCMs.

## 3. Entropy technique

The mathematical representation of the entropy technique is shown in Table 12 ((BURI et al., 2022).

Table 12: Methodology of entropy technique

Step	Description	Mathematical expression
1	Normalize the payoff matrix if required	$k_{aj}$
2	Entropy for each indicator	$En_j = -\frac{1}{\ln(T)} \sum_{a=1}^T k_{aj} \ln(k_{aj}), \text{ for } j = 1, \dots, J$ $a$ is index for GCMs; ( $j = 1, 2, \dots, j$ ) where $J$ is number of indicators; $T$ represents total number of GCMs.
3	Degree of diversification	$Dd_j = 1 - En_j$
4	Normalize the weight of indicators	$r_j = \frac{Dd_j}{\sum_{j=1}^J Dd_j}$

## 4. Methodology of weighted average technique

In this step normalize the payoff matrix if required, where the utility of RCM ( $V_a$ ) is calculated by Equation 20.

$$V_a = [\sum_{j=1}^J r_j k_j] \quad \text{Eq. 20}$$

here,  $k_j$  represents the value of indicator  $j$  for RCM, and  $r_j$  denotes the weight assigned to indicator  $j$ . A higher  $V_a$  indicates a suitable RCM.

For each RCM, the strengths, weaknesses, and net strengths were calculated based on individual ranking techniques and were integrated to form a single ranking pattern based on an individual ranking analysis (MORAIS; DE ALMEIDA, 2012). Weights were assigned to all RCMs using a weighted average method considering the net strengths. All nine ranked RCMs for the precipitation and temperature datasets at each grid point were ensembled by assigning weights to reduce uncertainty.

### 3.2.4 Non-parametric trend tests

This section lends itself to describe the non-parametric tests adopted in the present study, such as the Mann-Kendall Test (MK), Spearman correlation (Spearman), Mann-Kendall Test of Pre-Whitened (PWMK), and Bias Corrected Pre-whitening (BCPW) Tests, which are widely used to detect tessellations<sup>11</sup> in the trend of undistributed environmental and hydro-meteorological data (BAYAZIT; ÖNÖZ, 2007; BURI et al., 2022; WANG et al., 2020). The determination of values of the adopted tests was determined using R Software (modifiedmk package; <https://cran.r-project.org/web/packages/modifiedmk/index.html>).

#### 3.2.4.1 Teste de Mann-Kendall (MK)

The Mann-Kendall (MK) (MANN, 1945; WANG et al., 2020), suggested by the World Meteorological Organization (WMO), was adopted to detect significant trends in agrometeorological, hydrological (BLAIN, 2015), and other related environmental variables, such as water quality, flow, air temperature, precipitation and drought in different regions of the world (MODARRES, 2007).

The premise for such a test is that the data are independent, because if the observations present a positive serial correlation, the test may present a significant response even without a tendency (COX; STUART, 1955).

This method is considered advantageous because it does not assume that the data is normally distributed and is flexible for discrepant values in the data provided (PATAKAMURI, 2017; PATAKAMURI; MUTHIAH; SRIDHAR, 2020).

In this test, a series of  $n$  dimensions consisted of the annual values  $x_j$  and  $x_i$ , and in years  $i$  and  $j$ , respectively, with  $j > i$ . The MK test statistics are obtained by equations 21 and 22:

$$S = \sum_{i=1}^{n-1} \sum_{j=i+1}^n \text{sgn}(x_j - x_i), \quad \text{Eq. 21}$$

with

---

<sup>11</sup>Coating of a two-dimensional surface (a plane), having, as basic units, congruent polygons or not, without spaces between them and so that the total surface is equal to the partitioned space.

$$\text{sgn}(x_j - x_i) = \begin{cases} 1, & \text{if } (x_j - x_i) > 0 \\ 0, & \text{if } (x_j - x_i) = 0 \\ -1, & \text{if } (x_j - x_i) < 0 \end{cases} \quad \text{Eq. 22}$$

$S$ , follows a normal distribution with a mean of zero if the values are independent, random, and ordered to  $n > 0$ , with  $SS \geq 8$ , the distribution of  $s$  approaches the Gaussian form with mean  $E(S) = 0$ , such that the  $V(S)$  statistic and variance are given by equation 23:

$$\text{Var}(S) = \frac{[n(n-1)(2n+5) - \sum_{i=1}^m t_i i(i-1)(2i+5)]}{18} \quad \text{Eq. 23}$$

Where  $n$  is the number of tied groups in the entire dataset,  $t_i$  is the total number of data points in group  $i$  tied. The standardized test statistic is calculated by the following equation 24:

$$Z_{MK} = \begin{cases} \frac{s-1}{\sqrt{\text{Var}(S)}} & \text{for } S > 0 \\ 0 & \text{for } S = 0 \\ \frac{s+1}{\sqrt{\text{Var}(S)}} & \text{for } S < 0 \end{cases} \quad \text{Eq. 24}$$

The null hypothesis of the Mann-Kendall test assumes that the data are independent and identically distributed. For a specific significance level  $\alpha$  (90%, 95%), the null hypothesis is rejected  $Z_{MK}$  if it is greater than  $Z_{1-\alpha/2}$  (for a two-tailed test) or  $Z_{1-\alpha}$  (for a one-tailed test), where  $\alpha$  is the level of statistical significance.

The non-acceptance of the null hypothesis implies that the data do not follow these characteristics and thus cannot be taken as independent and identically distributed random variables (BLAIN, 2013).

However, this rejection is often taken as evidence of a trend in a given time series, even when it possibly presents positive autocorrelation, as occurs in most environmental and hydrological data, specifically in water resources data sets (HELSEL et al., 2020).

The trend will be considered ascending or decreasing based on the signal, where  $\beta > 0$  and  $\beta < 0$  indicate a growing and decreasing trend, respectively. The magnitude of the trend is determined by the Theil-Sem (PATAKAMURI; MUTHIAH; SRIDHAR, 2020), as illustrated in equation 25:

$$\beta = \text{median} \left[ \frac{x_j - x_i}{j - i} \right], \text{ for } j > i \quad \text{Eq. 25}$$

where:  $1 < i < j < n$ , and  $n$  is the duration of the data.

#### 3.2.4.2 Mann–Kendall test of pre-whitened time series data having a serial correlation.

The detection of trends in hydrometeorological data through the Mann-Kendall test commonly applied is challenged by the presence of the autocorrelation component in the series, given the fact that the positive autocorrelation inflates the probability of detecting trends when, in fact, there is no trend between them (BLAIN, 2013; DOS SANTOS et al., 2020).

Trendless pre-bleaching is a useful technique that has been used to eliminate the influence of serial correlation in the Mann-Kendall (MK) test in hydrological time series trend detection studies (YUE; WANG, 2002).

To this end, a process of autoregressive lag-1 (AR(1)) of time series was proposed before the application of the MK test to evaluate the importance (STORCH, 2001), to which the method is known as pre-bleaching, to remove the serial correlation of the time series as follows:

$$X'_t = X_t - r_1 X_{t-1}, \quad \text{Eq. 26}$$

where  $r_1$  is the serial lag-1 correlation coefficient of the sample data, and is formulated as follows:

$$r_1 = \frac{\frac{1}{n-1} \sum_{i=1}^{n-1} (x_i - \bar{x})(x_{i+1} - \bar{x})}{\frac{1}{n} \sum_{i=1}^n (x_i - \bar{x})^2} \quad \text{Eq. 27}$$

when satisfying the following condition  $\frac{-1-1.645\sqrt{n-2}}{n-2} \leq r_1 \leq \frac{1+1.645\sqrt{n-2}}{n-2}$ , then the time series is considered independent at the significance level of 10%, with no need for pre-bleaching. To remove the trend in time series data, the following equation is used.

$$X'_t = X_t - (\beta \times i), \quad \text{Eq. 28}$$

The removal of the lag-1 AR component in decompensated series is calculated by the following equation:  $Y'_t = X'_t - (r_1 \times X'_{t-1})$ , Eq. 29

The value added to the rest of the series.  $(\beta \times i)$  is  $y_i = y'_i + (\beta \times i)$ , Eq. 30

To find out the significance of the trend in the remaining series, the MK test is applied.

### 3.2.4.3 Bias corrected pre-whitening MK test.

In this test, the time series assumes that it follows a first-ordered serial correlation process, including a linear trend that can be modeled as:  $x_t = x_1, x_2, \dots, x_n$

$$x_t = \rho x_{t-1} + \alpha + \beta t + \varepsilon_t \quad \text{Eq. 31}$$

Where  $x_t$  and  $x_{t-1}$ , are observations in  $t$  and  $t - 1$  periods, respectively;  $\rho$  the serial correlation coefficient;  $\alpha$  is the constant intercept term. The estimated values of  $\rho$ ,  $\alpha$ , and  $\beta$  are given by calculating the following matrix:  $[\rho \ \alpha \ \beta]^T = (Z^T Z)^{-1} Z^T y$  Eq. 32

where  $Z$  is the matrix size  $(n - 1) \times 3$  whose second column contains  $(n - 1)$  values equal to 1, and the third column contains the numbers 2 to  $n$ , and  $y$  is a vector of size  $(n - 1)$  containing the observations  $x_2$  to  $x_n$ . The bias-corrected serial correlation  $\rho^*$  (HAMED, 2009; VAN GIERSBERGEN, 2005) used in corrected pre-bleaching studies and trend detention, is calculated using the following equation 33:

$$\rho^* = \frac{n\rho + 2}{n - 4} \quad \text{Eq. 33}$$

#### 3.2.4.4 Spearman's rank correlation (SRC) test

Spearman's Rho (BINET, 1904), is another widely used nonparametric test. This method tests the strength and direction (positive or negative) of the correlation (relationship or connection) between two variables (SEDGWICK, 2014). The power of this test is comparable to the Mann-Kendall test (YUE; WANG, 2002). For a given  $x_i = x_1, x_2, \dots, x_n$  time series, the statistic is based on the  $r_{SRC}$  (spearman rank correlation coefficient) given as follows:

$$r_{SRC} = 1 - \frac{\left\{6 \sum_{i=1}^n d_i^2\right\}}{n(n^2-1)} \quad \text{Eq. 34}$$

where  $i$  represents chronologic order,  $n$  is the number of data points in the time series;  $d_i = RX_i - RY_i$ ,  $RX_i$  is the ranking of the variable, which  $x_i$  is the chronological order of the observations. The  $y_i$  observation series is transformed into its equivalent  $RX_i$  by assigning the chronological order in the ranked series, where the average classification is considered for the draws. The test statistic is given by the following equation:

$$t_{SRC} = r_{SRC} \sqrt{\frac{(n-2)}{(1-r_{SRC}^2)}} \quad \text{Eq. 35}$$

The null hypothesis does not imply that the tendency is  $t_{v,\alpha/2} < t_{SRC} < t_{tv,1-\alpha/2}$ , accepted where the t-student distribution test with  $v = n - 2$  degrees of freedom, and  $\alpha$  level of significance.

#### 3.2.5 Future climate change scenarios

To project the possible future impacts on hydrological processes due to climate change in the São Francisco River basin, simulated climate data of NASA Earth Exchange Global Daily Downscaled Projections (NEX-GDDP), under two Representative Concentrative Pathways (RCP)<sup>12</sup>: RCP 4.5 and RCP 8.5, were used in this study.

This data was made available by the Indian team, as part of the ongoing multilateral BRICS research project, titled “*Integrated Water Management Model for Brazil, India, and South Africa under climate change scenarios*” (BURI et al., 2022; PATAKAMURI; MUTHIAH; SRIDHAR, 2020).

#### 3.2.6 Statistical Bias Correction Method

In this work, the Linear Scaling (LS) method was applied to bias-correct downscaled precipitation and temperature data of an ensembled model from nine climate models. This technique was chosen after a literature review (TEUTSCHBEIN; SEIBERT, 2012), which evaluated five bias correction methods for precipitation and four bias correction techniques for

---

<sup>12</sup>These RCPs are based on assumed natural and anthropogenic radiative forcing through the end of the 21<sup>st</sup> - century.

temperature, and according to other studies (ANDRADE et al., 2021), linear scaling is suitable both for precipitation and temperature.

The trendline correction procedures are used to minimize the discrepancy between observed and simulated climatic variables in a daily time step so that the hydrological simulations conducted by corrected simulated climatic data correspond to the simulations using observed climatic data reasonably well (RATHJENS et al., 2016).

To this end, the *Climate Model Data for Hydrologic Modeling* (CMhyd) (RATHJENS et al., 2016), can be applied to extract and correct (correct) data obtained from global and regional climate models with the observed data, given the difficulty in using simulated climatic data as direct input data for hydrological models.

For bias removal for the projected climatic data, the CMhyd model needs observed data, historical data, and Climate Change Projections for South America, adopting the *Linear Scaling* (LS) technique, which uses monthly correction values established in the differences between observed and historical simulated data (ANDRADE et al., 2021; TEUTSCHBEIN; SEIBERT, 2012, 2013), according to below-given equations 36 to 39.

$$P^*_{\text{contr}}(d) = P_{\text{contr}}(d) \cdot \left[ \frac{\mu_m(P_{\text{obs}}(d))}{\mu_m(P_{\text{contr}}(d))} \right] \quad \text{Eq. 36}$$

$$P^*_{\text{scen}}(d) = P_{\text{scen}}(d) \cdot \left[ \frac{\mu_m(P_{\text{obs}}(d))}{\mu_m(P_{\text{contr}}(d))} \right] \quad \text{Eq. 37}$$

$$T^*_{\text{contr}}(d) = T_{\text{contr}}(d) + \mu_m(T_{\text{obs}}(d)) - \mu_m(T_{\text{contr}}(d)) \quad \text{Eq. 38}$$

$$T^*_{\text{scen}}(d) = T_{\text{scen}}(d) + \mu_m(T_{\text{obs}}(d)) - \mu_m(T_{\text{contr}}(d)) \quad \text{Eq. 39}$$

where: P(d) and T(d) are daily precipitation and temperatures, respectively;  $\mu_m$  is the monthly mean value of the variable m; and "contr", "scen" and "obs", refer to the control (baseline period), scenarios and observed data, respectively.

In the LS approach, bias-corrected simulation data should agree, in their monthly average values, with the observed data and a factor based on the ratio of long-term monthly average observed and control run data is used for adjustment of precipitation and temperature variable (ANDRADE et al., 2021), being expected that these factors will continue unvaried under future conditions of the study area basin (TEUTSCHBEIN; SEIBERT, 2013).

The observed precipitation and temperature data comprised ten representative stations, distributed throughout the SFRB (referred to in chapter 3 of this thesis), both chosen based on the Principal Component Analysis (PCA) (EDWARDS; CAVALLI SFORZA, 1965).

This PCA approach is determined as a linear combination of the original variables, to help reduce the dimensionality of the data set and determine the variables that better explain the variability of the data with a lesser number of variables (TEIXEIRA et al., 2021).

The simulated historical data corresponding to the same period came from the historical series of the ensemble climate data.

### 3.2.7. Bilinear interpolation and IDW

To bring the same resolution for both precipitation and temperature datasets, a bilinear-interpolation technique was applied. For generating spatial plots, inverse distance weighting (IDW) geostatistical interpolation explicitly technique (BARTIER; KELLER, 1996), which assumes that things that are close to one another are more alike than those that are farther apart, was used by considering the Z-value of respective trend tests.

To predict a value for any unmeasured location, IDW uses the measured values surrounding the prediction location (BISWAS et al., 2020). The measured values closest to the prediction location have more influence on the predicted value than those farther away.

The IDW technique assumes that each measured point has a local influence that diminishes with distance (BARTIER; KELLER, 1996). It gives greater weights to points closest to the prediction location, and the weights diminish as a function of distance, hence the name inverse distance weighted.

The annual analysis was carried out for the entire study area. However, given the great heterogeneous along the basin with four climatic types (FILHO et al., 2018; MARQUES; GUNKEL; SOBRAL, 2019), trend analysis in the dry, rainy, and pre-season periods was performed, in a sub-region subdivided by Lower (S1 and 2), Middle and Sub-Middle (S2 – S6), and Upper São Francisco (S7 – S10), as shown in table 13, and spatially scattered in Figure 9.

Table 13: Sub-regions and stations for trend analysis in the dry, rainy, and pre-season periods

Region (stations)	Season	Period	Chosen month
Lower (S1 and S2)	Dry	May – October	July
	Rainy	November – April	January
		Pre-season	October
Middle and Sub-Middle (S3 – S6)	Dry	June – November	September
	Rainy	December – May	February
		Pre-season	November
Upper (S7 – S10)	Dry	September – February	November
	Rainy	March-August	May
		Pre-season	February

Source: adapted from (ASSIS et al., 2022; FREITAS et al., 2022; GALVÍNCIO, 2000; MUTTI, 2020; SIQUEIRA; SIQUEIRA; FILHO, 2022).

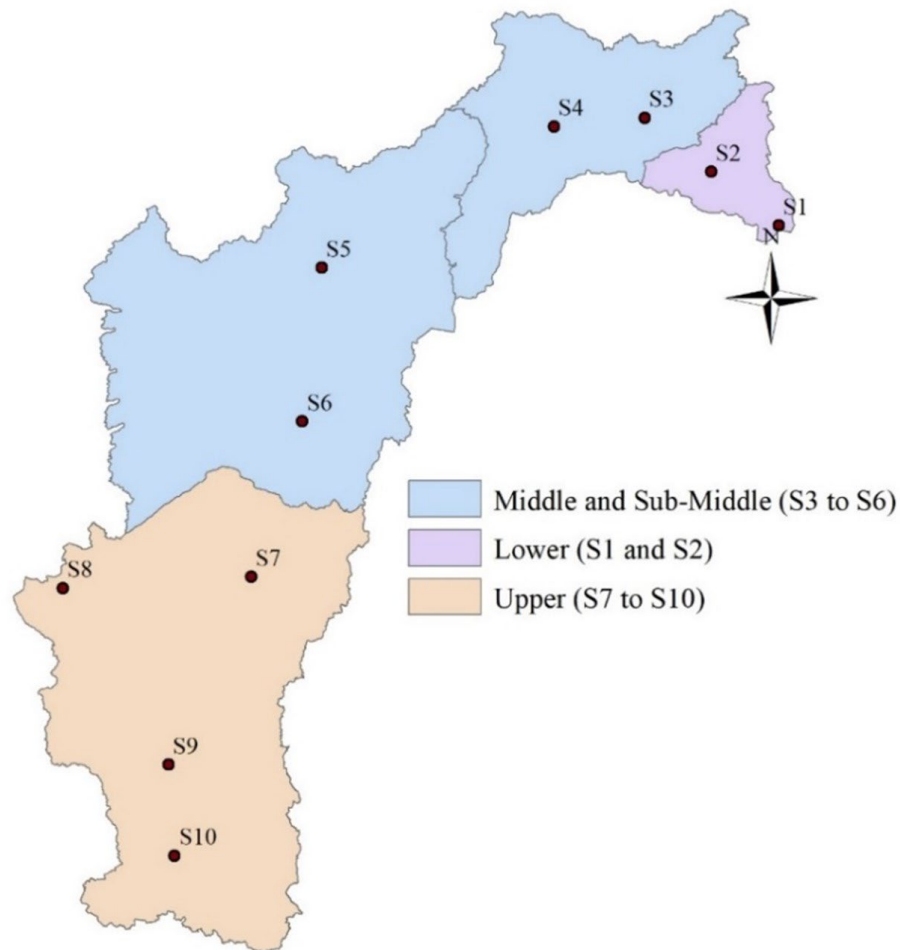


Figure 9: Spatial distribution of selected stations along the São Francisco River basin

The methodology followed in this study, as shown in Figure 9, was demonstrated at a climate model grid point, and the same procedure was followed for the remaining grid points of the study area.

### 3.3 Results and Discussion

At each grid point, the net strength of each RCM was evaluated using suitable performance indicators for precipitation and temperature data, as presented in Figure 10 and Appendix A. These weighting schemes were applied to find the best historical fit of three climate variables (precipitation, and minimum and maximum temperature).

As a results, each point on the scatter plot is each nine model's weight ( $V_a$ ) of nine models based on their performance in creating the multi-model, for precipitation (a), minimum (b) and maximum (c) temperature, presented in Figure 11. The x-axis is the accuracy when the weights of each of the nine climatic models are averaged (i.e., its weight in the creation of the multi-model) while the y-axis, represents each of the 10 points selected for the present study.

The various model weights from each scheme were calculated, and the derived sets of weights were then applied to create ensemble means for three variables.

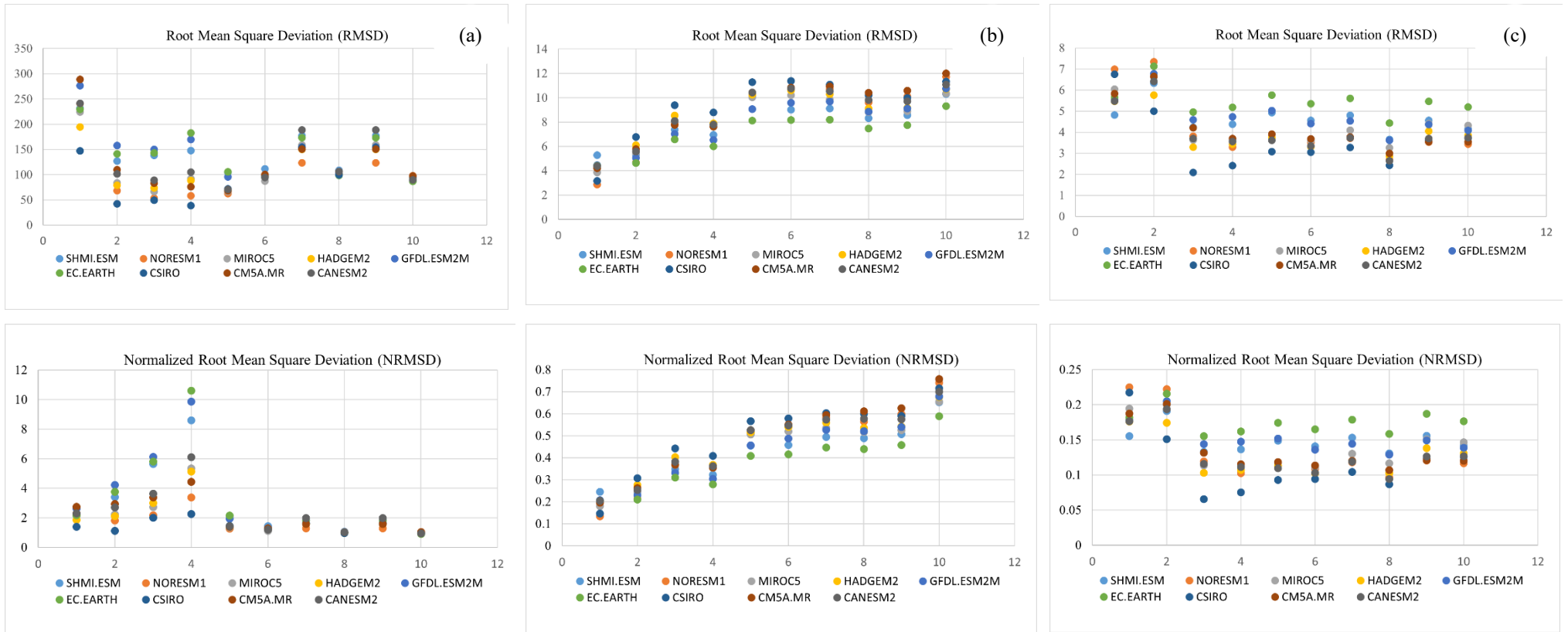


Figure 10: Performance analysis of RMSD and NRMSD metrics of precipitation (a), and minimum (b) and maximum temperature (c) for 9 RCMs in 10 points

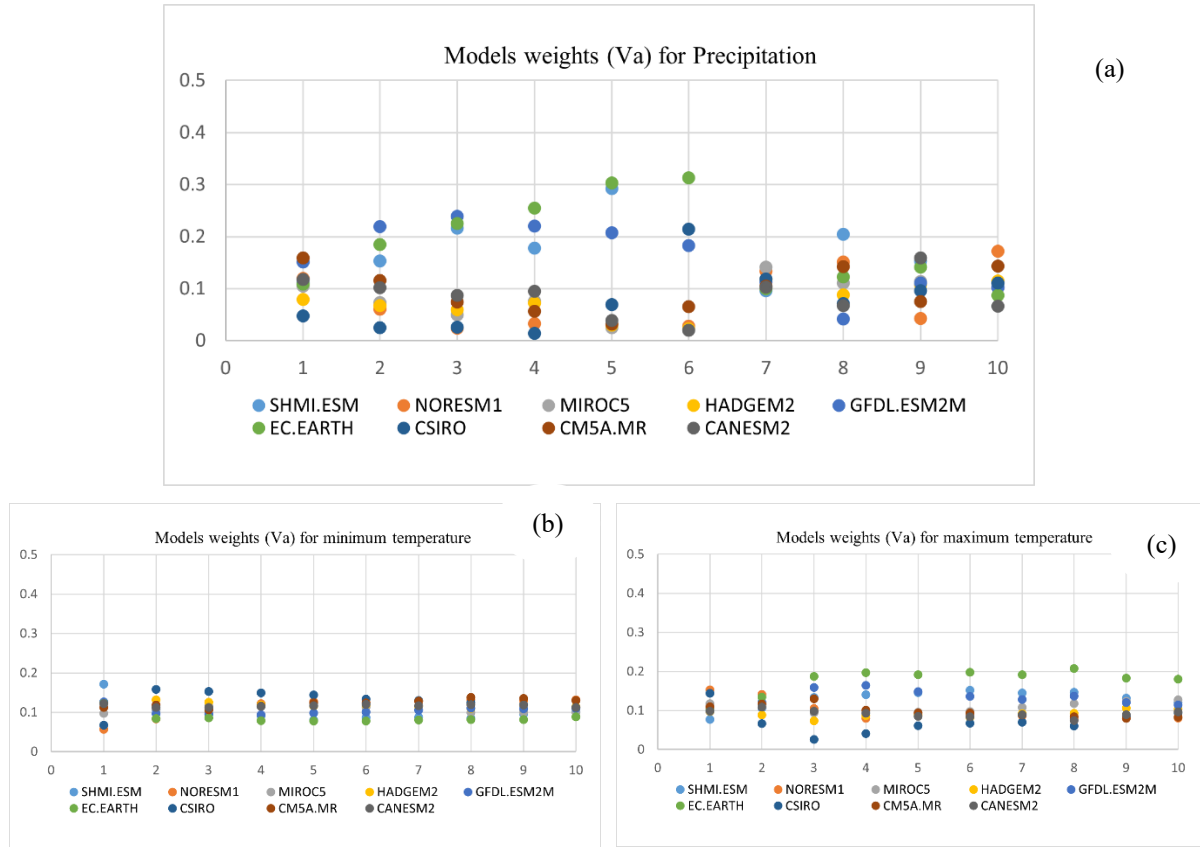


Figure 11: Models weights ( $V_a$ ) for precipitation (a), and minimum (b) and maximum temperature (c) based on their individual performance to create the multi-model

While the ensembles often perform slightly more than individual models, among nine models considered in this study, when evaluated by RMSD, NRMSD metrics (Figure 10), and ANMBD, CC, and NSE metrics (Appendix A), the EC.EARTH model had greater weight for precipitation (a) and maximum temperature (c), differently for the SHMI.ESM model which had greater weight for the minimum temperature (b) to create the multi-model.

### 3.3.1 Analysis of observed trends in precipitation

Appendix B represents the variations of annual average p precipitation (a), minimum (b), and maximum temperature (c) for different periods under the RCP 4.5 and RCP 8.5 scenarios, for the three sub-regions aforementioned in Table 13 and Figure 9.

The Inverse Distance Weightage (IDW) interpolation technique was used to generate spatial plots in the spatial variation of Z-value and show grid points in four trend tests for the entire river basin (Figures 13, 18 and 19), and for three sub-regions (Lower, Middle, and Sub-middle, and Upper), shown in Appendix C (Figures 1 – 8).

Figure 12 demonstrates mean annual precipitation over the São Francisco River basin (in 10 selected stations), clearly indicating the variation in future periods under RCP 4.5 and RCP 8.5, compared to the observed period.

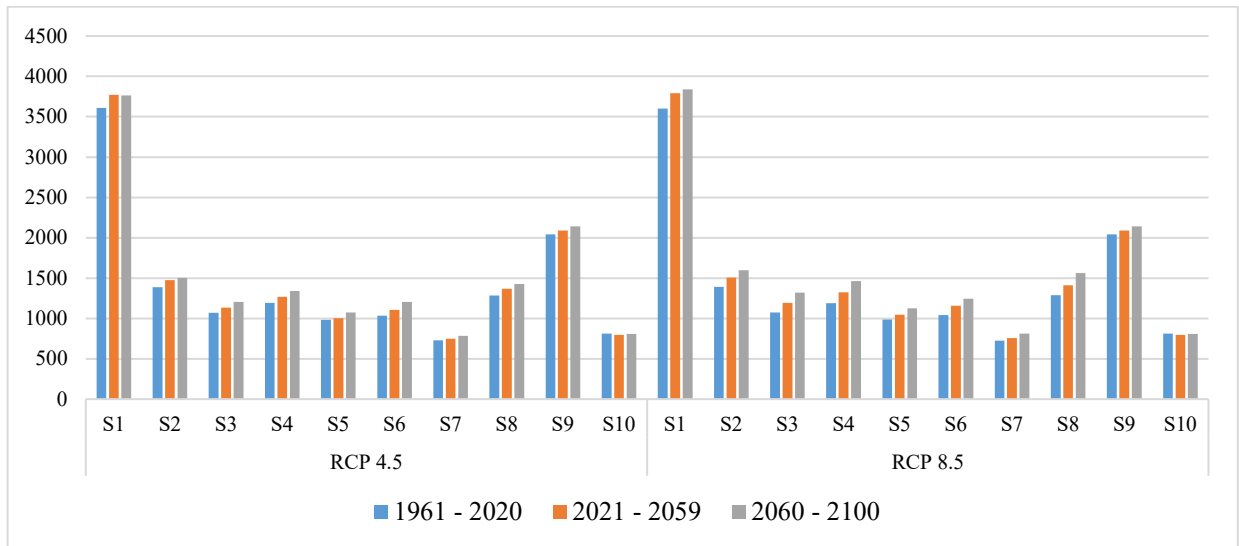


Figure 12: Mean annual precipitation (mm) for the entire São Francisco River basin

Due to the action of different large, meso, and local scale meteorological systems (OLIVEIRA; SANTOS E SILVA; LIMA, 2017), the rainfall regime in the basin presented high spatiotemporal variability (geographically and seasonally), indicating a well-defined annual cycle with wet and dry periods (FREITAS et al., 2022). The SFRB will certainly experience more rainfall and greater temperatures in the future for both emission scenarios, based on the results obtained in this study, which report a trend of increasing average annual precipitation in the two future periods under the RCP 4.5 and RCP 8.5 scenarios compared to the historical period (Figure 12).

Similar agreement of a possible scenario increasing in magnitude and frequency of extreme precipitation (BEZERRA et al., 2019), was found with rainfall changes in various parts of South America by 2070–2100 (MANATSA; CHINGOMBE; MATARIRA, 2008; MARENGO et al., 2010), using different regional models, as well as the projected changes of rainfall from the IPCC AR4 multi-model ensemble for the same scenarios, and the rainfall projections derived from Eta-CPTEC by the end of the 21<sup>st</sup>-century, showing increases in rainfall in southeastern South America (MARENGO et al., 2012).

This increasing trend is influenced by different atmospheric systems (POLZIN; HASTENRATH, 2014), such as the Intertropical Convergence Zone (ITCZ) (PAREDES-TAVARES et al., 2018), Easterly Wave Disturbances (EWD) (GOMES et al., 2015) Frontal Systems (FS) in the São Francisco river basin, and South Atlantic Convergence Zone (SACZ) (MARENGO; TORRES; ALVES, 2017; SIQUEIRA; SIQUEIRA; FILHO, 2022; VALVERDE; MARENGO, 2014), the influences of tropical climatic phenomena (FERREIRA et al., 2021), and the El Niño phenomenon, which interferes in the rainy season between the years (ANDREOLI; KAYANO, 2005).

This increasing trend of precipitation when evaluated through four (4) non-parametric trend tests adopted in this study (Figure 13), the Mann-Kendall Test (MK) showed an increasing trend in the Upper, Medium, and Sub-medium São Francisco, and a high correlation was evidenced by the Spearman correlation test, even after eliminating possible adverse effects of autocorrelation in the MK test and Spearman's rho trend tests, through the Mann-Kendall Test of Pre-Whitened (PWMK) test.

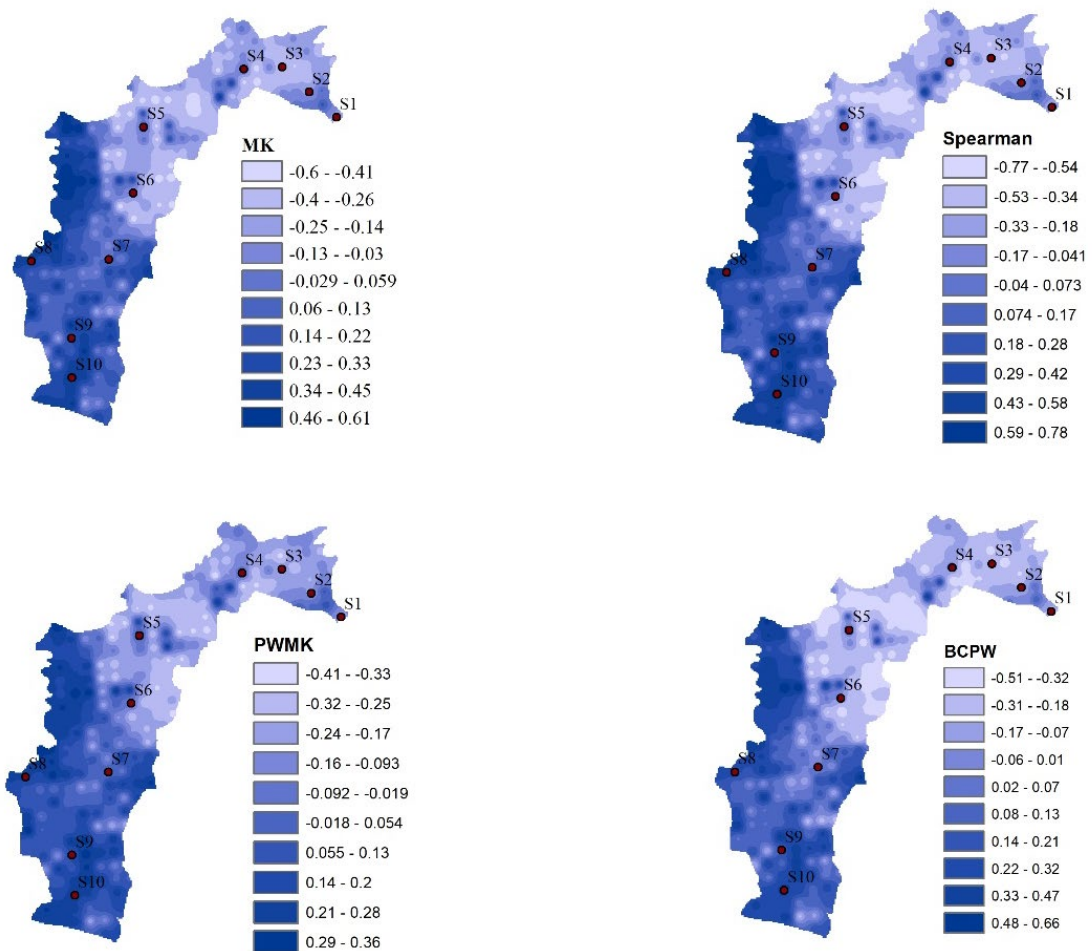


Figure 13: Spatial variation of Z-value and trend showing grid points in four trend tests of precipitation data annual period over the São Francisco River Basin

Figures 14 – 16, show the stations-wise mean monthly precipitation (mm) in the dry (a), rainy (b), and pre-season (c) periods, over the São Francisco River basin (Lower, Middle, and Sub-Middle, and Upstream sub-regions).

In the lower São Francisco region affected by easterly wave disturbances and sea and land breezes (REBOITA et al., 2010), the lowest precipitation values were observed in the pre-season period, which jointly with the dry period, recorded lower precipitation values when compared to the observed period, differently from the rainy period, which observed an increase in means monthly precipitation for both RCPs.

These results are consistent with the historical phenomenon of rainfall deficit registered during the dry summer of 2001, which reached up to 40% in most of central (FREITAS et al.,

2022), northeastern, and southeastern Brazil, resulting in a significant reduction in river streamflow throughout this regions, thereby reducing the capacity to produce hydroelectric power in these areas, and compromising the amount of water available along the basin (FREITAS et al., 2022).

The alignment of these results can also be verified in the consequence of the multiyear drought, for the period 2014–2019 observed rainfall in the São Francisco basin reported in the past (DE JONG et al., 2021), was 37% below if compared to its 1961–1990 baseline average and consequently observed streamflow declined by approximately 60%.

Further, the São Francisco River basins’ streamflow and hydroelectric production could potentially cease in the second half of the 21<sup>st</sup> century (DE JONG et al., 2021). Therefore, to face the upcoming scenarios of climate change, impositions of energy conservation measures from the government side will be required to avoid total loss of power (blackouts), as well as the reconfiguration in the NE electrical matrix shortly, considering economic, technical and social environmental constraints (BARBOSA et al., 2021).

Alternatively, the design of PV-hydro hybrid systems (based on complementary resources) for providing energy (VASCO et al., 2019), can be explored as an effective strategy to cope with future climate change scenarios, and supply water for irrigation (among other uses) as the major component of water demand accounted for 67% of the total demand (TEIXEIRA et al., 2021).

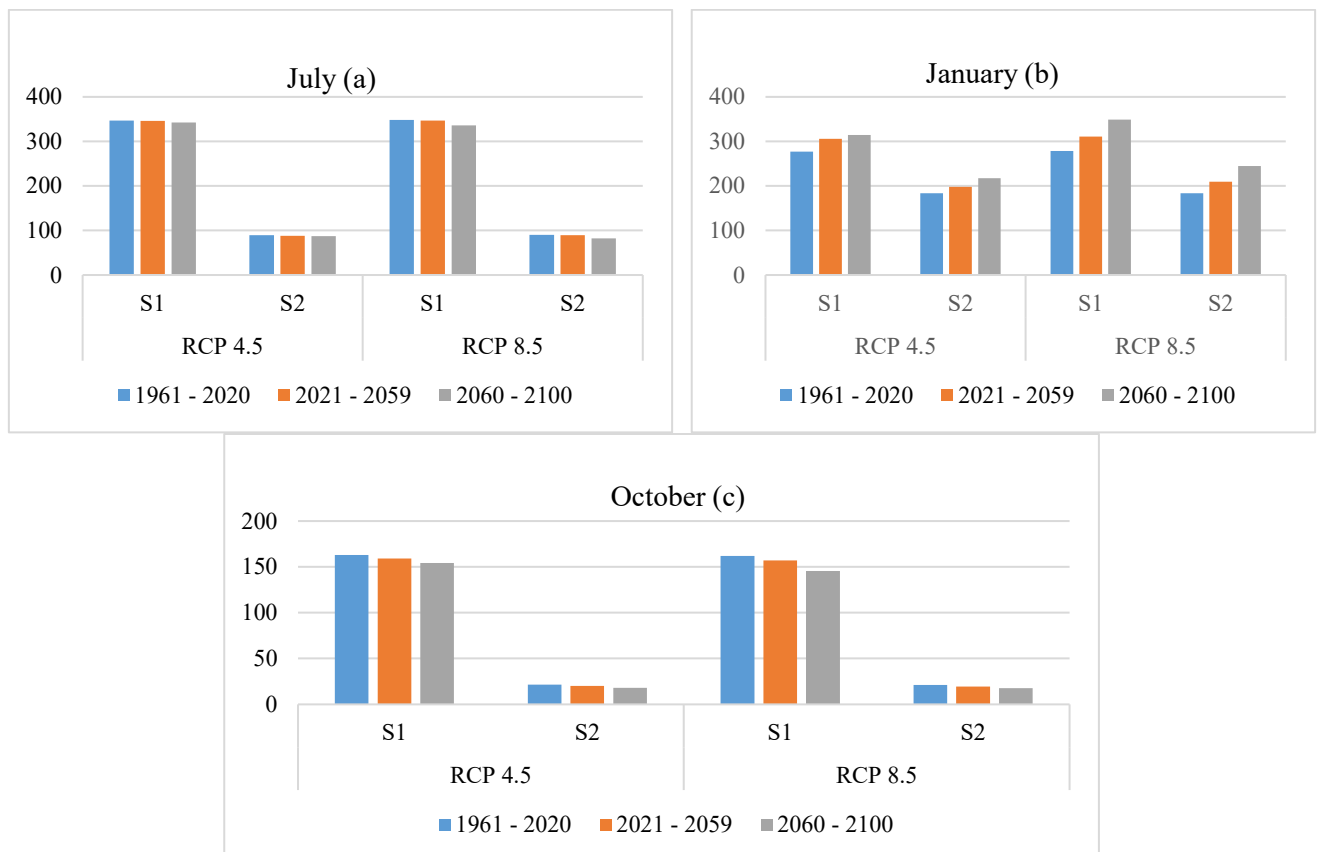


Figure 14: Station-wise means monthly precipitation (mm) in the dry (a), rainy (b), and pre-season (c) periods over Lower São Francisco

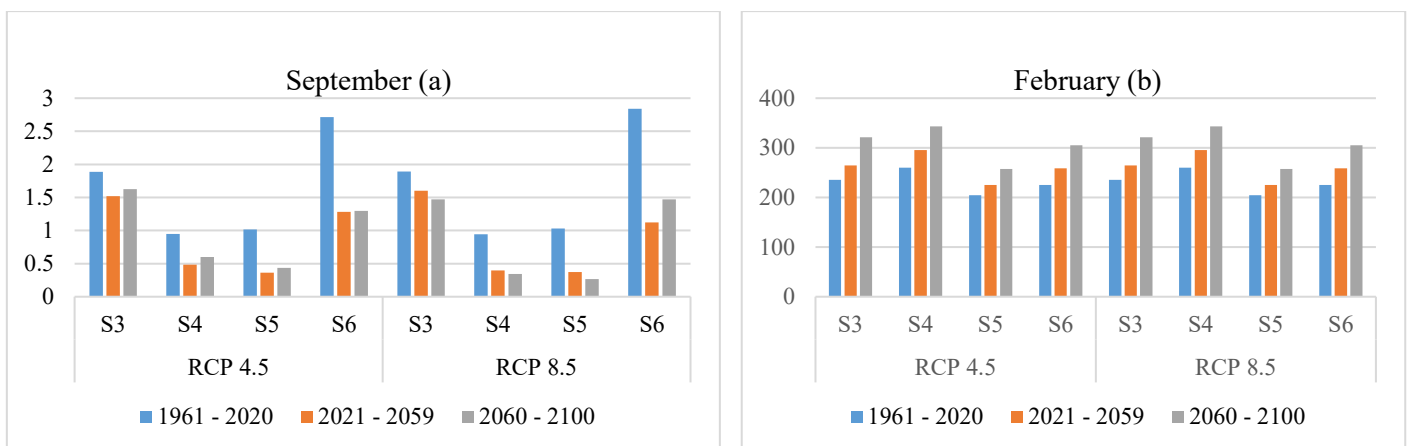
A station-wise mean monthly precipitation (mm) analysis over Middle and Sub-Middle São Francisco presented in Figure 5, shows a decreasing trend in rainfall in the dry and pre-season periods, the precipitation values in two future periods will decrease if compared to those historically observed in both RCPs. Similar negative trend or decreasing trends in annual precipitation were detected by (FABIANA MEIJON FADUL, 2019) and (ANA LÚCIA BEZERRA CANDEIAS, 2021) while analyzing the two river basins in the Sertão region of the State of Pernambuco in the years between 1964 – 2004, and in the State of Ceará, using 23 rainfall stations between 1974 and 2003, respectively.

The greatest variations occurred in the rainy season, with emphasis on the predominance of positive anomalies were also reported (SALES et al., 2015), in their study on precipitation and temperature projections for the Brazilian Northeast, considering the CMIP5 models and the RCP8.5 scenario.

These results' alignment, also can be seen with the report of the Brazilian Panel on Climate Change (PBMC, 2013), stating that the Northeastern semiarid region of Brazil is likely to have its precipitation reduced by 20% in 2040, and highlighting that the more intense in the Northern part of the region, mainly located in the State of Pernambuco (ASSIS et al., 2022).

Differently in the rainy period, observed precipitation values for future periods were high in both RCPs. All of this variation in precipitation in the region is due to large-scale circulation, whereas the rainfall intensity may be influenced by climate variability (ASSIS et al., 2022).

Based on the exposed above, it is noted that the reported reduction in rainfall in the Middle and Sub-Middle São Francisco regions corroborates with the past aforementioned studies, a persisting problem in the semiarid region of the Brazilian Northeast, which is currently facing its worst drought in decades (ASSIS et al., 2022).



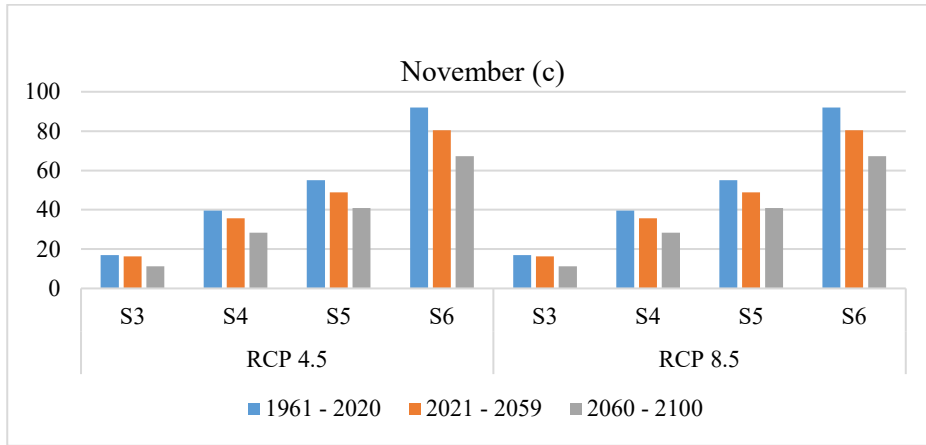
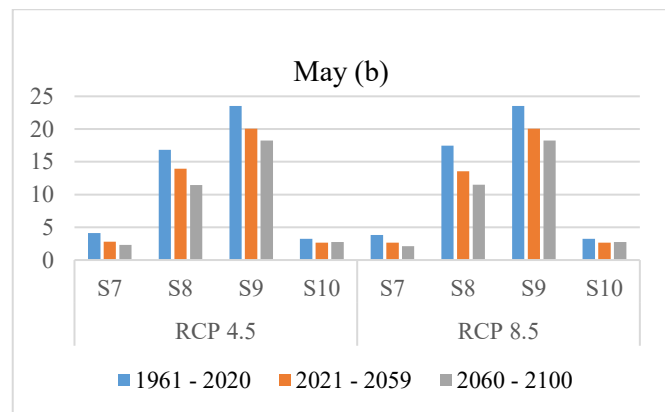
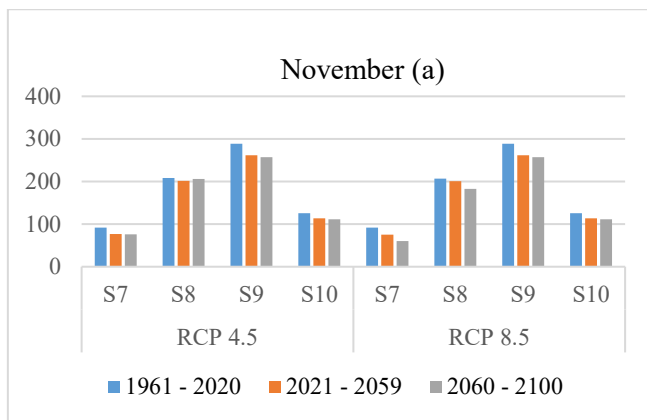


Figure 15: Station-wise mean monthly precipitation (mm) in the dry (a), rainy (b), and pre-season (c) periods over Middle and Sub-Middle São Francisco

In the Upstream São Francisco in Minas Gerais State, where the weather systems are associated with the South Atlantic Convergence Zone (SAZC), FS, LI, CCM, and isolated convection (SIQUEIRA; SIQUEIRA; FILHO, 2022), the precipitation monthly averages presented in Figure 6, showed lowest precipitation values for two future periods will be observed in the pre-season period, which also showed an increasing trend in the precipitation values in both future periods and RCPs. While for the dry and rainy periods, there will be decreasing trends, in two considered scenarios.

To face these upcoming water demand increases in the Upper and Middle (and water scarcity in the sub-Middle and Lower) due to the irrigated areas to be expanded in the next decades, there is needed a public policy of incentives on improving the mobility of cropland to increase water conservation for irrigation (FACHINELLI FERRARINI et al., 2020); and policies for preventing water losses as well as expanding new irrigation techniques; developing alternate sources, such as rainfall harvest by small reservoirs and reuse of return flow in farming.



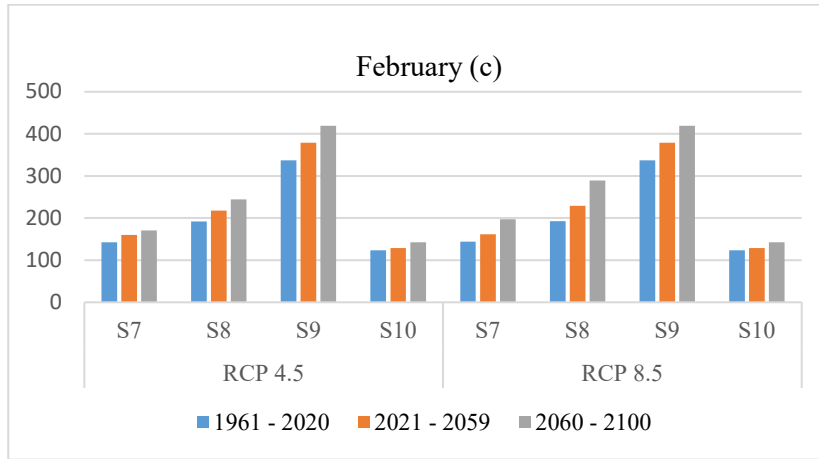


Figure 16: Station-wise mean monthly precipitation (mm) in the dry (a), rainy (b), and pre-season (c) periods over Upper São Francisco

### 3.3.2. Analysis of observed trends in temperature

Figure 17 demonstrates a mean annual minimum and maximum temperature (°C) over the São Francisco River basin (in 10 selected stations), clearly indicating the variation in future periods under RCP 4.5 and RCP 8.5, compared to the observed period.

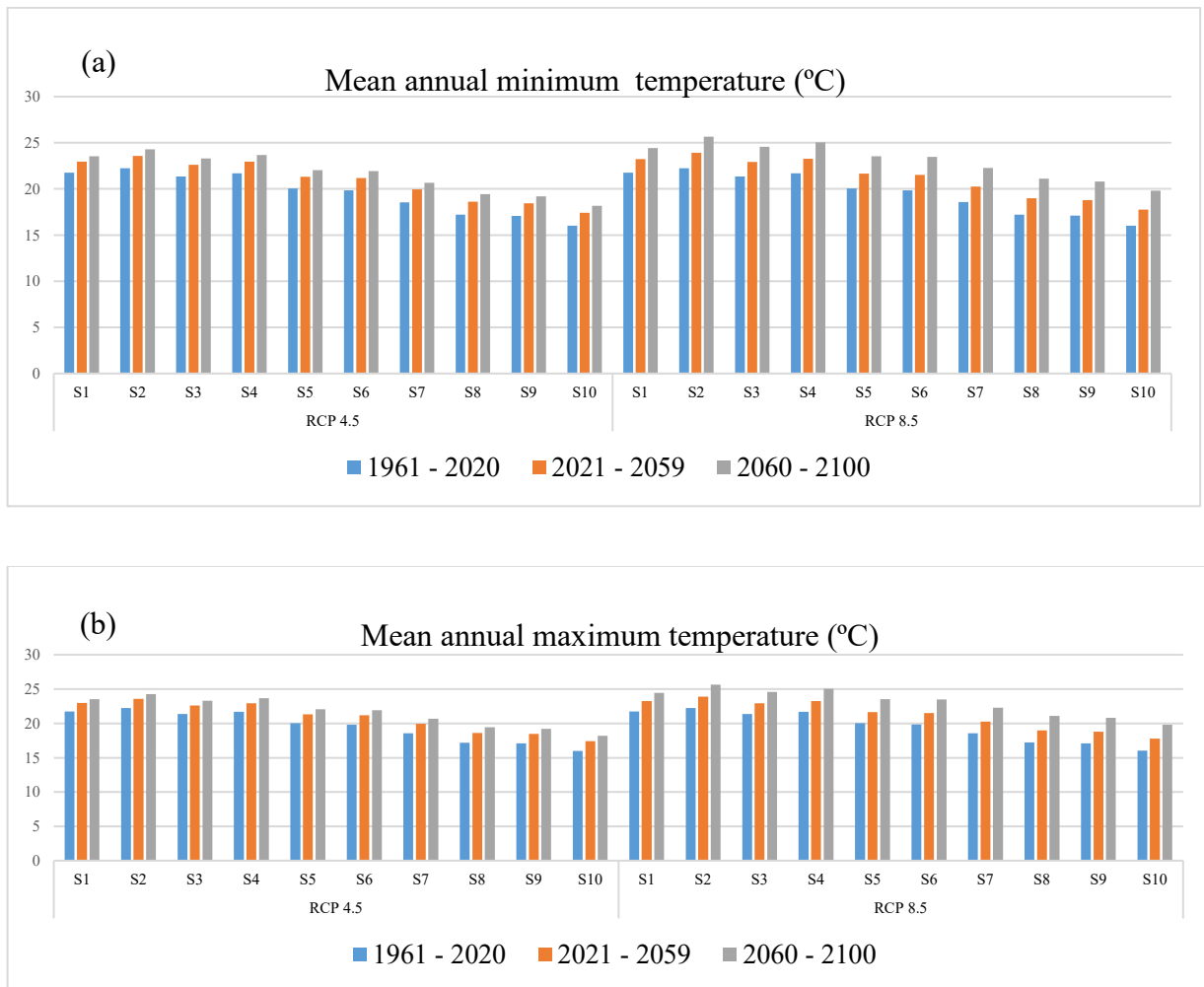


Figure 17: Mean annual minimum (a) and maximum (b) temperature (°C) for the entire São Francisco River basin

Compared to the historical period, the results showed increasing minimum and maximum temperature values in the two future scenarios, and both RCPs. Higher annual averages, both for the minimum temperature and the maximum temperature, were observed in the Lower, Medium, and Sub-Medium São Francisco.

These results corroborate those obtained comparing 27 CMIP5 models for the São Francisco River Basin (SILVEIRA et al., 2016), all of which showed a positive trend (increase) in temperature in the period from 2011 to 2100, but more significant between 2041 and 2100. In all of them, the 8.5 scenarios showed a higher positive trend than the 4.5 RCP scenario.

When compared through four (4) no-parametric trend tests used in this work, the increasing trend minimum temperature was evidenced by the Mann-Kendall Test (MK), and the Spearman correlation test shows a strong trend correlation except for station S7 which showed a decreasing trend.

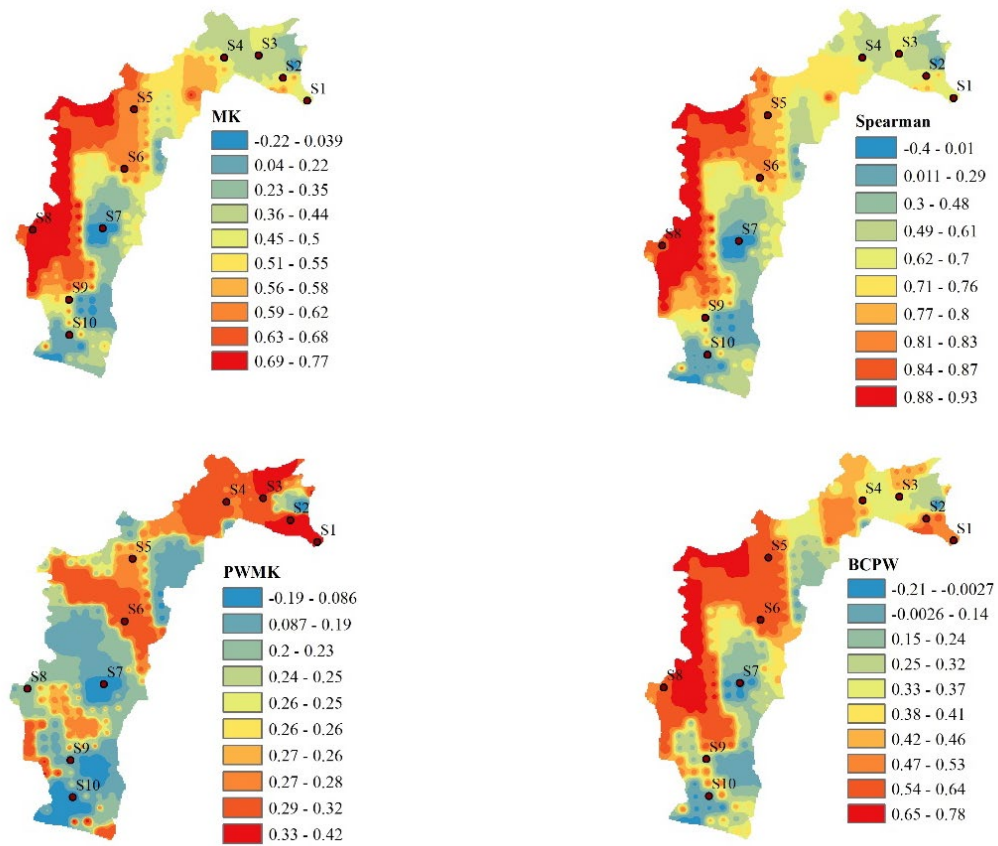


Figure 18: Spatial variation of Z-value and trend showing grid points in four trend tests of minimum temperature data annual period over the São Francisco River Basin

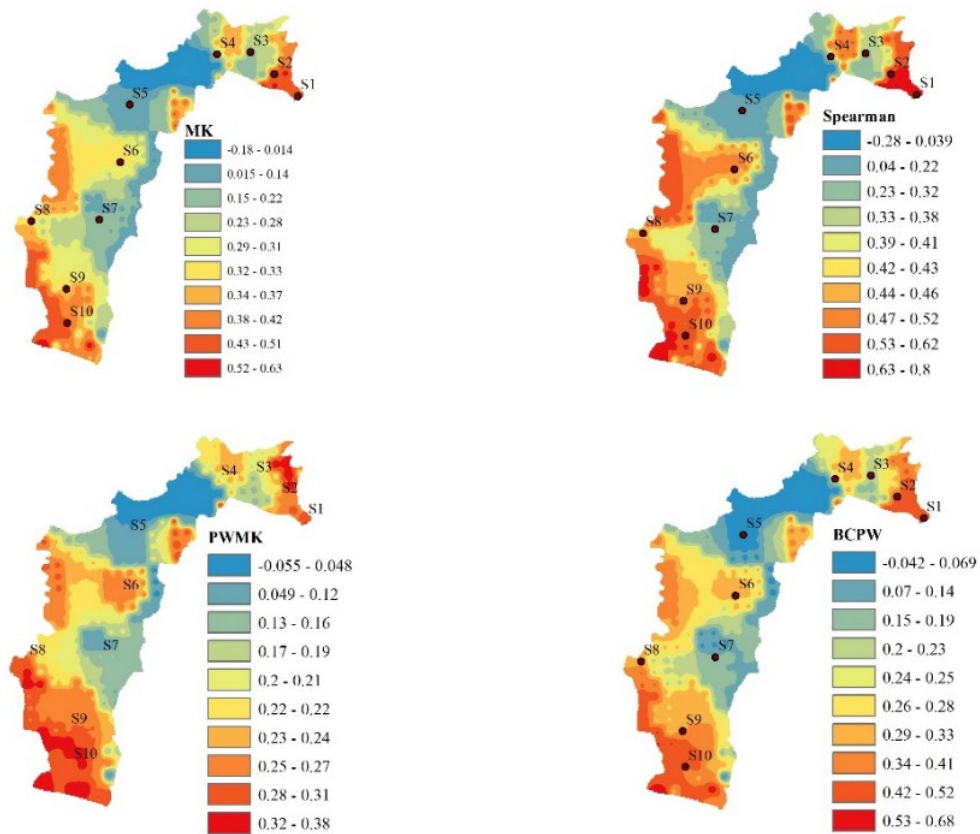
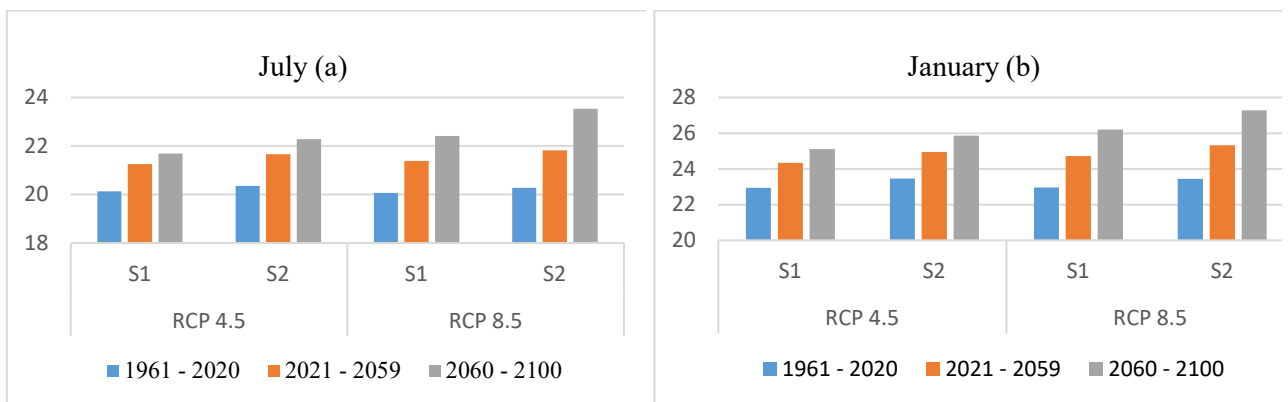


Figure 19: Spatial variation of Z-value and trend showing grid points in four trend tests of maximum temperature data annual period over the São Francisco River Basin

### 3.3.3 Analysis observed trends in minimum temperature

Figures 20 – 22, show the stations-wise mean monthly minimum temperature in the dry (a), rainy (b), and pre-season (c) periods, over the São Francisco River basin (Lower, Middle, and Sub-Middle, and Upstream sub-regions).

For the Lower São Francisco, the station-wise mean monthly minimum temperature will increase over the two future periods, when compared to the historical observed period, in both future RCPs.



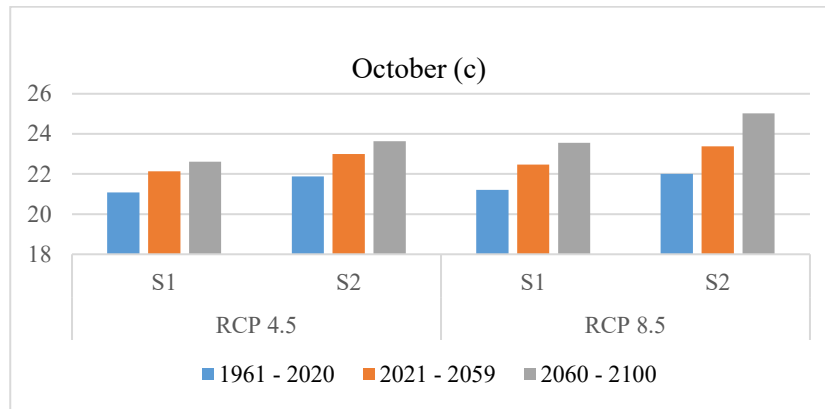


Figure 20: Station-wise mean monthly minimum temperature (°C) in the dry (a), rainy (b), and pre-season (c) periods over Lower São Francisco

For the Middle and Sub-Middle São Francisco, the obtained results compared to the observed period, the monthly average of the minimum temperature will increase over the two future periods, regardless of the RCP to be considered.

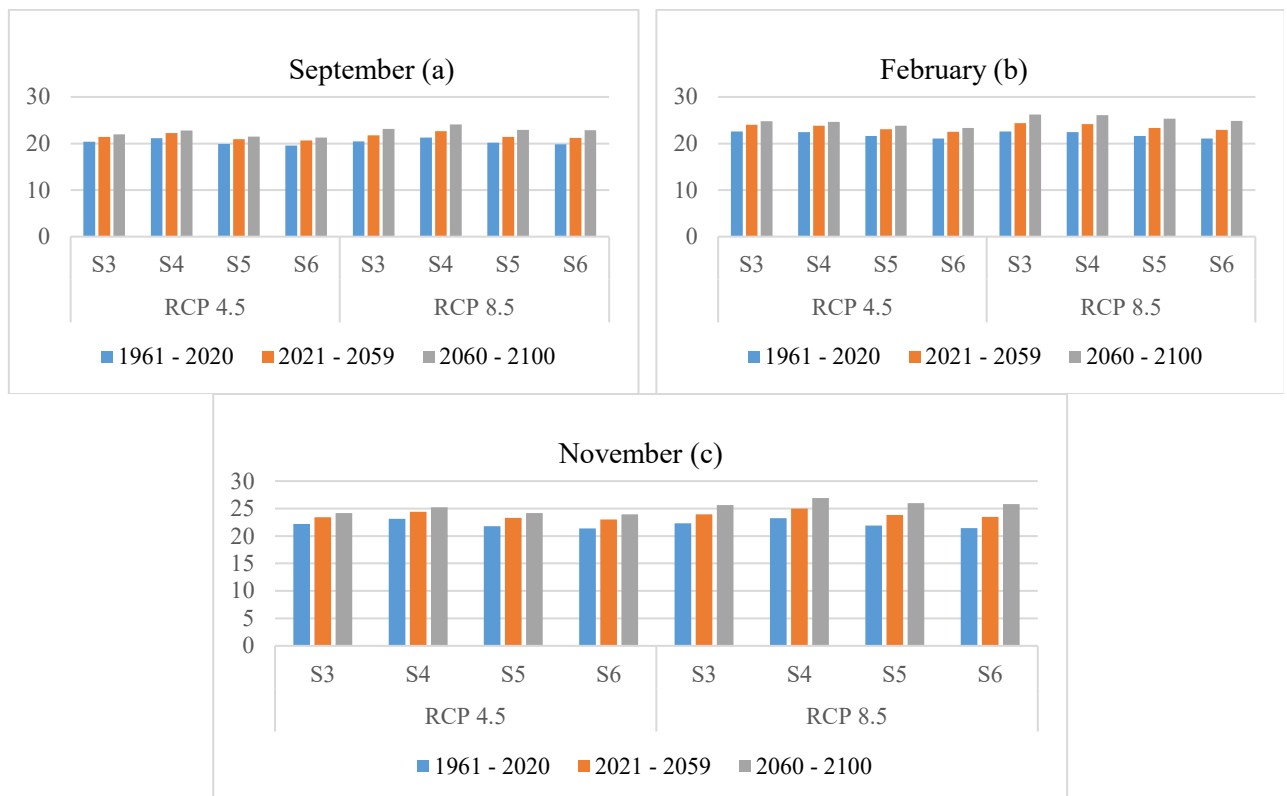


Figure 21: Station-wise mean monthly minimum temperature (°C) in the dry (a), rainy (b), and pre-season (c) periods over Middle and Sub-Middle São Francisco

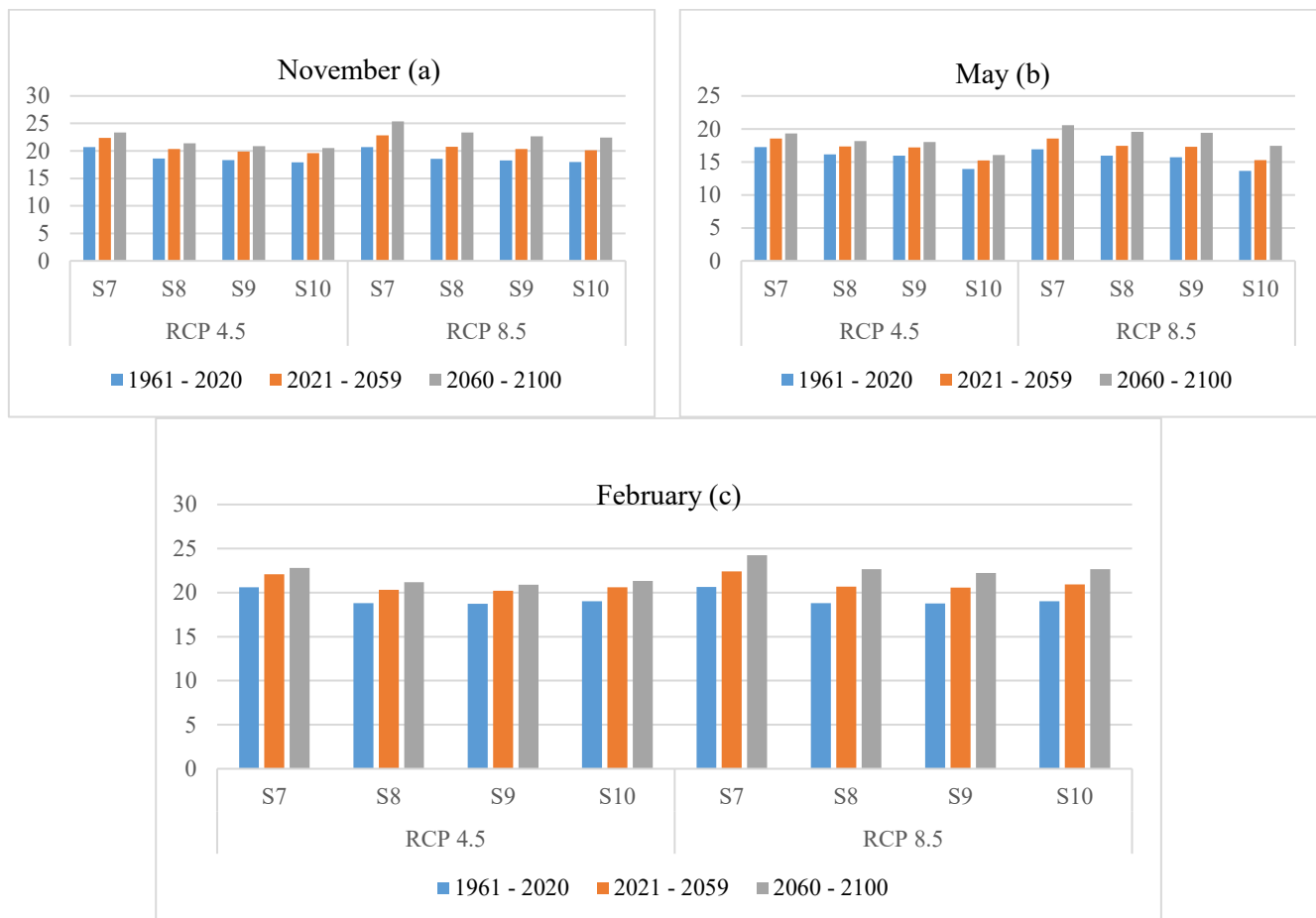
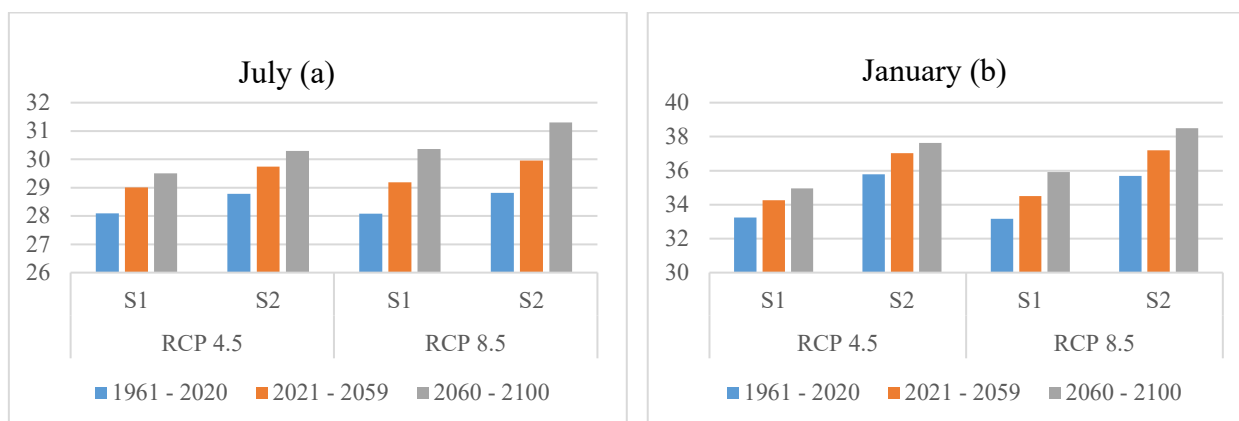


Figure 22: Station-wise mean monthly minimum temperature (°C) in the dry (a), rainy (b), and pre-season (c) periods over Upper São Francisco

### 3.3.4 Observed trends in maximum temperature

Figure 24, presents a station-wise mean maximum temperature (°C) analysis over Middle and Sub-Middle São Francisco, showing an increasing average annual maximum temperature in the two future periods under the RCP 4.5 and RCP 8.5 scenarios if compared to the historical observed period.



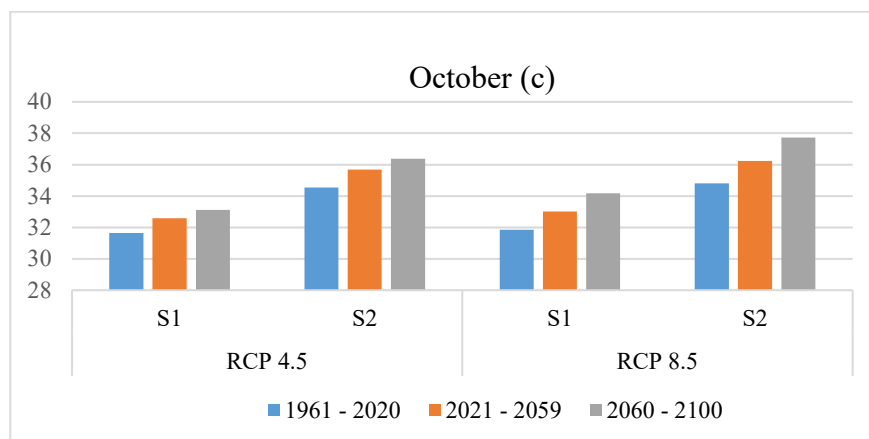


Figure 23: Station-wise mean monthly maximum temperature (°C) in the dry (a), rainy (b), and pre-season (c) periods over Lower São Francisco

These results corroborate with the ones found evaluating climate change detection indices for the Bahia State between 1970 and 2006 (SILVA; AZEVEDO, 2012); and diagnosed that the number of days with daily maximum temperature increased, while the daily rainfall and total annual precipitation reduced. Also, a faster increase of daily maximum temperature due to the climate change scenarios for 2010 – 2050, over Northeastern compared to that simulated for the recent past was reported (BURI et al., 2022), indicating aridification processes.

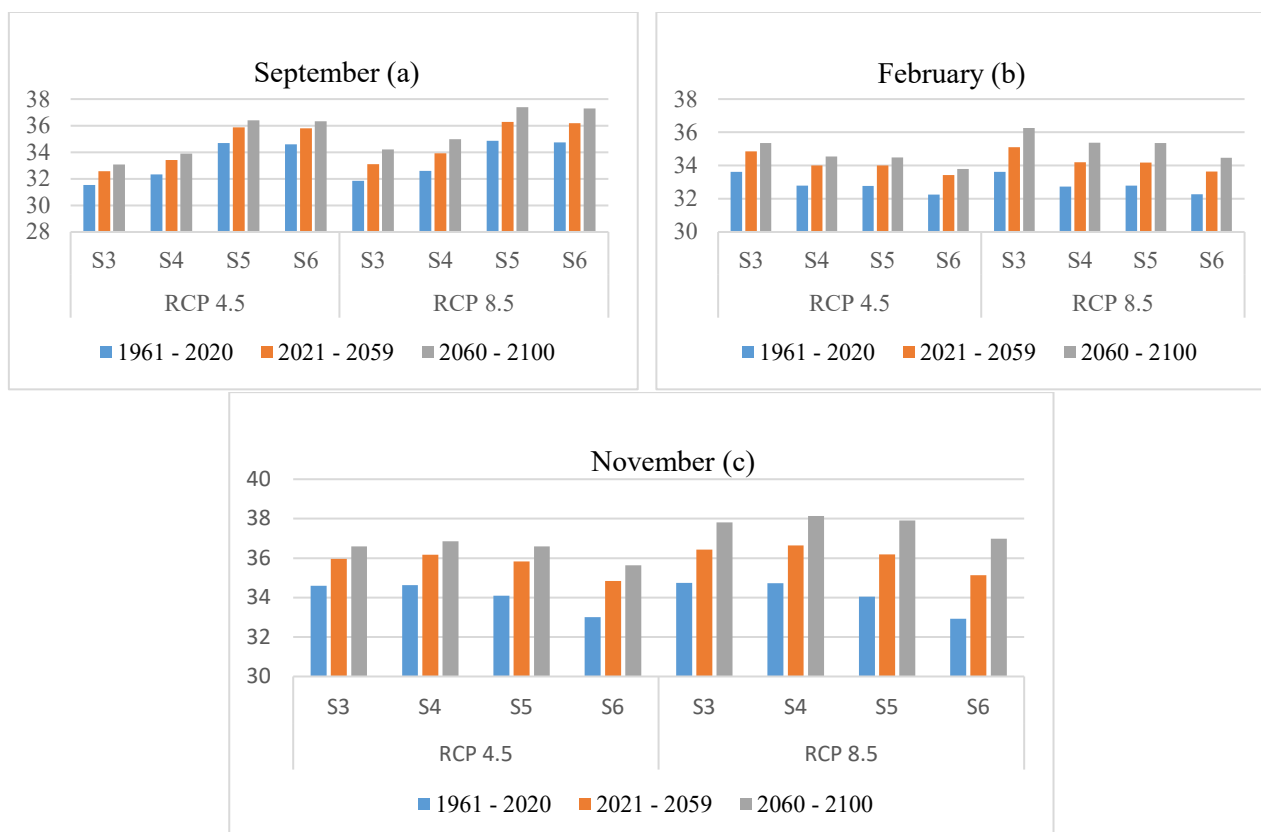


Figure 24: Station-wise mean monthly maximum temperature (°C) in the dry (a), rainy (b), and pre-season (c) periods over Middle and Sub-Middle São Francisco

Comparing four (4) no-parametric trend tests to detect reported increasing trend minimum temperature (Appendix B), the Mann-Kendall Test (MK) clearly showed this trend,

and the Spearman correlation tests showed a strong trend correlation except for station S7 which showed a decreasing trend.

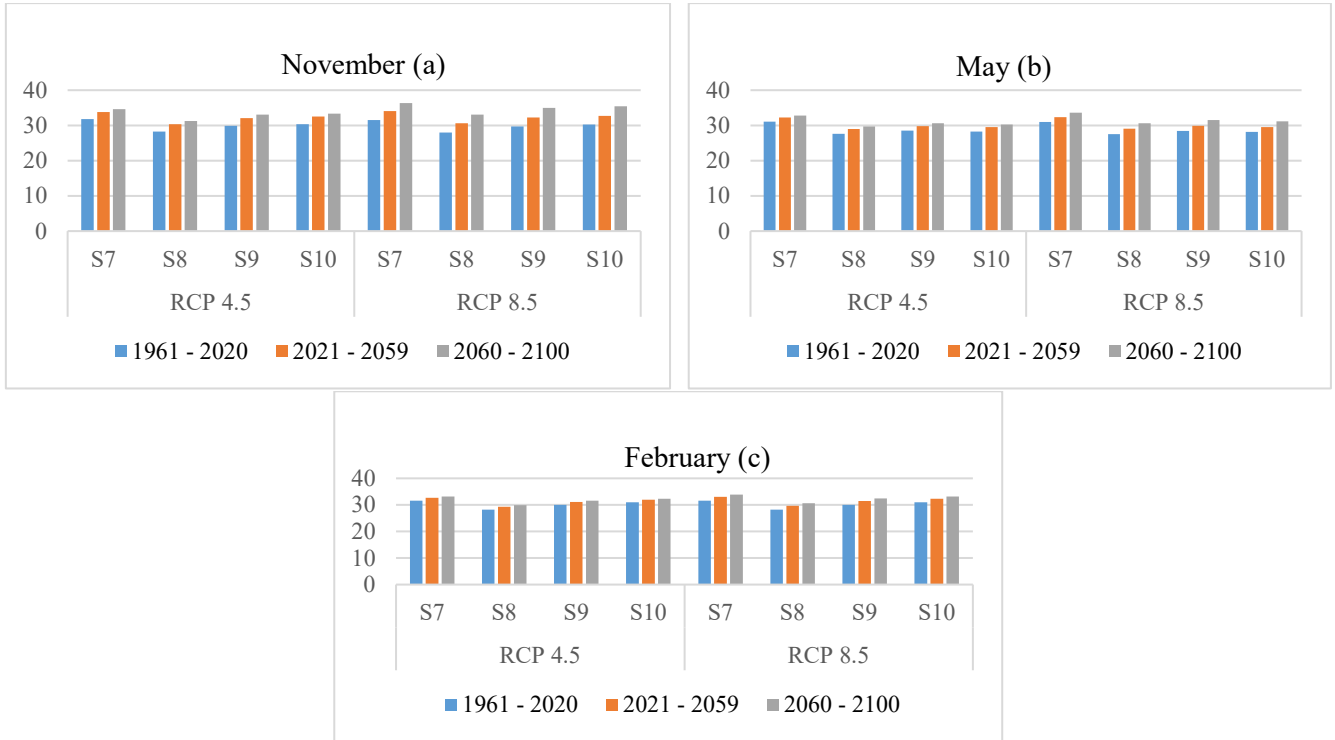


Figure 25: Station-wise mean monthly maximum temperature (°C) in the dry (a), rainy (b), and pre-season (c) periods over Upper São Francisco

### 3.4 Conclusions

This study analyzes long-term trends in precipitation and temperature data sets (maximum and minimum values) projected by NEX-GDDP in the São Francisco River Basin under RCP 4.5 and RCP 8.5 scenarios.

The 9 RCMs available were compiled using the REA method and biased at each grid point for the historical (1961 - 2005) and future (2006 - 2100) periods for the annual, drought, wet, and pre-season periods using the CMhyd model. Four different methods, namely the Mann-Kendall test, Mann-Kendall pre-brightening test, bias-corrected pre-brightening process, and Spearman correlation, were used to detect precipitation trends as well as maximum and minimum temperature data sets.

Performance analysis of various metrics was evaluated, and model weights were assigned. The spatial and temporal variations of the mean annual fluctuations in different periods was studied.

Throughout the SFRB, precipitation and maximum and minimum temperatures increase compared to the observation period (1961 – 2005). When analyzed by subregion, results show an increasing trend in monthly average minimum and maximum temperatures in the northern region of the SFRB, while average monthly precipitation increases during the rainy season. Pre-season preparations in Upper San Francisco. The high correlation of these trends was also demonstrated by comparing the four nonparametric trend tests used in this study.

In the context of climate change, the uncertainties associated with RCMs and scenarios need to be assessed in order to implement effective management practices and make informed decisions. The results are used as input to hydrological and water resource management models under climate change scenarios.

## References

- AHMED, K. et al. Multi-model ensemble predictions of precipitation and temperature using machine learning algorithms. **Atmospheric Research**, v. 236, n. November 2019, p. 104806, 2020.
- ANA LÚCIA BEZERRA CANDEIAS, D. D. M. G. A. F. DA S. Revista Brasileira de Geografia Física. **Revista Brasileira de Geografia**, v. 02, p. 758–769, 2021.
- ANDRADE, C. W. L. et al. Climate change impact assessment on water resources under RCP scenarios: A case study in Mundaú River Basin, Northeastern Brazil. **International Journal of Climatology**, v. 41, n. S1, p. E1045–E1061, 2021.
- ANDREOLI, R. V.; KAYANO, M. T. ENSO-related rainfall anomalies in South America and associated circulation features during warm and cold Pacific decadal oscillation regimes. **International Journal of Climatology**, v. 25, n. 15, p. 2017–2030, 2005.
- ASSIS, J. M. O. DE et al. Analysis of climate indices and impacts on the rainfall regime in the Submedium region of the São Francisco river basin – Brazil. **Revista Principia - Divulgação Científica e Tecnológica do IFPB**, v. 59, p. 1475–1486, 2022.
- ASSIS, J. M. O. DE; SOUZA, W. M. DE; SOBRAL, M. DO C. Análise climática da precipitação no submédio da bacia do Rio São Francisco com base no índice de anomalia de chuva. **Revista Brasileira de Ciências Ambientais (Online)**, n. 36, p. 115–127, 2015.
- BANERJEE, A. et al. An analysis of long-term rainfall trends and variability in the uttarakhand himalaya using google earth engine. **Remote Sensing**, v. 12, n. 4, 2020.
- BARBOSA, C. et al. An exploratory scenario analysis of strategic pathways towards a sustainable electricity system of the drought-stricken São Francisco River Basin. **Energy Systems**, v. 12, n. 3, p. 563–602, 2021.
- BARTIER, P. M.; KELLER, C. P. Multivariate interpolation to incorporate thematic surface data using inverse distance weighting (IDW). **Computers and Geosciences**, v. 22, n. 7, p. 795–799, 1996.
- BAYAZIT, M.; ÖNÖZ, B. To prewhiten or not to prewhiten in trend analysis? **Hydrological Sciences Journal**, v. 52, n. 4, p. 611–624, 2007.
- BERLATO, M. A.; CORDEIRO, A. P. A. Sinais de mudanças climáticas globais e regionais, projeções para o século XXI e as tendências observadas no Rio Grande do Sul: uma revisão. **Agrometeoros**, v. 25, n. 2, p. 273–302, 2018.
- BEZERRA, B. G. et al. Changes of precipitation extremes indices in São Francisco River Basin, Brazil from 1947 to 2012. **Theoretical and Applied Climatology**, v. 135, n. 1–2, p. 565–576, 2019.
- BINET, A. Spearman “The proof and measurement of association between two things General intelligence objectively determined and measured”. **L’Année psychologique**, v. 11,

n. 1, p. 623–624, 1904.

BISWAS, R. N. et al. Modeling on the spatial vulnerability of lightning disaster in Bangladesh using GIS and IDW techniques. **Spatial Information Research**, v. 28, n. 5, p. 507–521, 2020.

BLAIN, G. C. Teste de Mann-Kendall: A necessidade de considerar a interação entre correlação serial e tendência. **Acta Scientiarum - Agronomy**, v. 35, n. 4, p. 393–402, 2013.

BLAIN, G. C. Influência de tendências não lineares sobre o rigor da abordagem ‘trend-free prewhitening’. **Acta Scientiarum - Agronomy**, v. 37, n. 1, p. 21–28, 2015.

BURI, E. S. et al. Spatio-Temporal Analysis of Climatic Variables in the Munneru River Basin, India, Using NEX-GDDP Data and the REA Approach. **Sustainability (Switzerland)**, v. 14, n. 3, 2022.

CARVALHO, A. A. DE et al. Trends of rainfall and temperature in Northeast Brazil Tendências da precipitação pluvial e da temperatura no Nordeste brasileiro. **Revista Brasileira de Engenharia Agrícola e Ambiental**, v. 24, p. 15–23, 2020.

CLARK, M. P. et al. Characterizing Uncertainty of the Hydrologic Impacts of Climate Change. **Current Climate Change Reports**, v. 2, n. 2, p. 55–64, 2016.

COX, D. R.; STUART, A. Some Quick Sign Tests for Trend in Location and Dispersion. **Biometrika**, v. 42, n. 1/2, p. 80, 1955.

DE JONG, P. et al. The Impact of Regional Climate Change on Hydroelectric Resources in South America. **Renewable Energy**, v. 173, p. 76–91, 2021.

DOS SANTOS, T. V. et al. Teste de Mann-Kendall aplicado à dados hidrológicos – Desempenho dos filtros TFPW e CV2 na análise de tendências. **Ciência e Natura**, v. 42, p. e87, 2020.

EDWARDS, A. W. F.; CAVALLI SFORZA, L. L. A Method for Cluster Analysis and L . L . Cavalli-Sforza Published by : International Biometric Society Stable URL : <http://www.jstor.org/stable/2528096> . **Biometrics**, v. 21, n. 2, p. 362–375, 1965.

FABIANA MEIJON FADUL. THE RAINFALL TREND OVER CEARA AND ITS IMPLICATIONS. p. 315–323, 2019.

FACHINELLI FERRARINI, A. DOS S. et al. Water demand prospects for irrigation in the são francisco river: Brazilian public policy. **Water Policy**, v. 22, n. 3, p. 449–467, 2020.

FEREIDOON, M.; KOCH, M. SWAT-MODSIM-PSO optimization of multi-crop planning in the Karkheh River Basin, Iran, under the impacts of climate change. **Science of the Total Environment**, v. 630, p. 502–516, 2018.

FERREIRA, D. B. et al. Pluviometric patterns in the são francisco river basin in minas gerais, Brazil. **Revista Brasileira de Recursos Hídricos**, v. 26, 2021.

FILHO, A. J. P. et al. A step towards integrating CMORPH precipitation estimation with rain

gauge measurements. **Advances in Meteorology**, v. 2018, 2018.

FONSECA, M. G. et al. Effects of climate and land-use change scenarios on fire probability during the 21st century in the Brazilian Amazon. **Global Change Biology**, v. 25, n. 9, p. 2931–2946, 2019.

FREITAS, A. A. et al. Drought Assessment in São Francisco River Basin, Brazil: Characterization through SPI and Associated Anomalous Climate Patterns. **Atmosphere**, v. 13, n. 1, 2022.

GALVÍNCIO, J. D. Impactos dos eventos el nino na precipitação da bacia do rio São Francisco. **Universidade Federal da Paraíba (Pós-graduação em Meteorologia)**, 2000.

GEBRECHORKOS, S. H.; HÜLSMANN, S.; BERNHOFER, C. **Changes in temperature and precipitation extremes in Ethiopia, Kenya, and Tanzania** *International Journal of Climatology*, 2019.

GOMES, H. B. et al. Easterly wave disturbances over Northeast Brazil: An observational analysis. **Advances in Meteorology**, v. 2015, 2015.

HAMED, K. H. Enhancing the effectiveness of prewhitening in trend analysis of hydrologic data. **Journal of Hydrology**, v. 368, n. 1–4, p. 143–155, 2009.

HAZELEGER, W. et al. EC-Earth V2.2: Description and validation of a new seamless earth system prediction model. **Climate Dynamics**, v. 39, n. 11, p. 2611–2629, 2012.

HELSEL, D. R. et al. Statistical methods in water resources. **U.S. Geological Survey Techniques and Methods**, v. 2020, n. 4-A3, p. 1–484, 2020.

HUNDECHA, Y.; BÁRDOSSY, A. Trends in daily precipitation and temperature extremes across western Germany in the second half of the 20th century. **International Journal of Climatology**, v. 25, n. 9, p. 1189–1202, 2005.

ISOTTA, F. A.; BEGERT, M.; FREI, C. Long-Term Consistent Monthly Temperature and Precipitation Grid Data Sets for Switzerland Over the Past 150 Years. **Journal of Geophysical Research: Atmospheres**, v. 124, n. 7, p. 3783–3799, 2019.

KANDA, N. et al. Performance of various gridded temperature and precipitation datasets over northwest himalayan region. **Environmental Research Communications**, v. 2, n. 8, p. 2000–2008, 2020.

KHAVSE, R. et al. Statistical Analysis of Temperature and Rainfall Trend in Raipur District of Chhattisgarh. **Current World Environment**, v. 10, n. 1, p. 305–312, 2015.

KOTIR, J. H. Climate change and variability in Sub-Saharan Africa: A review of current and future trends and impacts on agriculture and food security. **Environment, Development and Sustainability**, v. 13, n. 3, p. 587–605, 2011.

KUMAR, R.; RAJ GAUTAM, H. Climate Change and its Impact on Agricultural Productivity in India. **Journal of Climatology & Weather Forecasting**, v. 2, n. 1, p. 1–4, 2014.

- LAKKU, N. K. G.; BEHERA, M. R. Skill and Inter-Model Comparison of Regional and Global Climate Models in Simulating Wind Speed over South Asian Domain. **Climate**, v. 10, n. 6, 2022.
- LI, Y. et al. Evaluation of Long-Term and High-Resolution Gridded Precipitation and Temperature Products in the Qilian Mountains, Qinghai–Tibet Plateau. **Frontiers in Environmental Science**, v. 10, n. May, p. 1–16, 2022.
- LIU, J. et al. Earth ' s Future Water scarcity assessments in the past , present , and future Earth ' s Future. **Earth{textquotesingle}s Future**, v. 5, n. 6, p. 545–559, 2017.
- LUCAS, M. C. et al. Significant baseflow reduction in the sao francisco river basin. **Water (Switzerland)**, v. 13, n. 1, p. 1–17, 2021.
- MALLAKPOUR, I. et al. Discrepancies in changes in precipitation characteristics over the contiguous United States based on six daily gridded precipitation datasets. **Weather and Climate Extremes**, v. 36, n. March, p. 100433, 2022.
- MANATSA, D.; CHINGOMBE, W.; MATARIRA, C. H. The impact of the positive Indian Ocean dipole on Zimbabwe droughts Tropical climate is understood to be dominated by. **International Journal of Climatology**, v. 2029, n. March 2008, p. 2011–2029, 2008.
- MANN, H. B. Non-Parametric Test Against Trend. **Econometrica**, v. 13, n. 3, p. 245–259, 1945.
- MARENGO, J. A. et al. Future change of climate in South America in the late twenty-first century: Intercomparison of scenarios from three regional climate models. **Climate Dynamics**, v. 35, n. 6, p. 1089–1113, 2010.
- MARENGO, J. A. et al. Development of regional future climate change scenarios in South America using the Eta CPTEC/HadCM3 climate change projections: Climatology and regional analyses for the Amazon, São Francisco and the Paraná River basins. **Climate Dynamics**, v. 38, n. 9–10, p. 1829–1848, 2012.
- MARENGO, J. A.; TORRES, R. R.; ALVES, L. M. Drought in Northeast Brazil—past, present, and future. **Theoretical and Applied Climatology**, v. 129, n. 3–4, p. 1189–1200, 2017.
- MARQUES, É. T.; GUNKEL, G.; SOBRAL, M. C. Management of tropical river basins and reservoirs under water stress: Experiences from northeast Brazil. **Environments - MDPI**, 2019.
- MODARRES, S. Rainfall trends in arid and semi-arid regions of Iran. **Journal of Arid Environments**, v. 70, n. 2, p. 344–355, 2007.
- MONTENEGRO, S.; RAGAB, R. Impact of possible climate and land use changes in the semi arid regions : A case study from North Eastern Brazil. **Journal of Hydrology**, v. 434–435, p. 55–68, 2012.

MORAIS, D. C.; DE ALMEIDA, A. T. Group decision making on water resources based on analysis of individual rankings. **Omega**, v. 40, n. 1, p. 42–52, 2012.

MUTTI, P. R. Drought characterization in the Northeast Brazil: a multiscale watershed analysis and remote sensing monitoring. n. December, p. 161, 2020.

NASCIMENTO DO VASCO, A.; DE OLIVEIRA AGUIAR NETTO, A.; GONZAGA DA SILVA, M. The influence of dams on ecohydrological conditions in the São Francisco River Basin, Brazil. **Ecohydrology and Hydrobiology**, v. 19, n. 4, p. 556–565, 2019.

NETO, A. R. et al. Hydrological Processes and Climate Change in Hydrographic Regions of Brazil. p. 1103–1127, 2016.

OLIVEIRA, P. T.; SANTOS E SILVA, C. M.; LIMA, K. C. Climatology and trend analysis of extreme precipitation in subregions of Northeast Brazil. **Theoretical and Applied Climatology**, v. 130, n. 1–2, p. 77–90, 2017.

PANDA, A.; SAHU, N. Trend analysis of seasonal rainfall and temperature pattern in Kalahandi, Bolangir and Koraput districts of Odisha, India. **Atmospheric Science Letters**, v. 20, n. 10, p. 1–10, 2019.

PAREDES-TAVARES, J. et al. Impacts of climate change on the irrigation districts of the Rio Bravo Basin. **Water (Switzerland)**, v. 10, n. 3, p. 1–20, 2018.

PATAKAMURI, S. K. **Trend Free Pre-Whitening - Mann-Kendall test**, 2017.

PATAKAMURI, S. K.; MUTHIAH, K.; SRIDHAR, V. Long-Term homogeneity, trend, and change-point analysis of rainfall in the arid district of ananthapuramu, Andhra Pradesh State, India. **Water (Switzerland)**, v. 12, n. 1, 2020.

PBMC. Contribuição do Grupo de Trabalho 1 ao Primeiro Relatório de Avaliação Nacional do Painel Brasileiro de Mudanças Climáticas. Sumário Executivo GT1. **Base Científica das Mudanças Climáticas**, p. 23, 2013.

POLZIN, D.; HASTENRATH, S. CLIMATE OF BRAZIL ' S NORDESTE AND TROPICAL ATLANTIC SECTOR : PREFERRED TIME SCALES OF VARIABILITY  
 DIERK POLZIN , STEFAN HASTENRATH University of Wisconsin-Madison ,  
 Atmospheric and Oceanic Sciences , Madison , Wisconsin , USA Received September 2013 -  
 Ac. **Revista Brasileira de Meteorologia**, v. 29, n. 2, p. 153–160, 2014.

RATHJENS, H. et al. CMhyd User Manual Documentation for preparing simulated climate change data for hydrologic impact studies. p. p.16p, 2016.

REBOITA, M. S. et al. Regimes de precipitação na América do Sul: uma revisão bibliográfica. **Revista Brasileira de Meteorologia**, v. 25, n. 2, p. 185–204, 2010.

SALES, D. C. et al. Projeções de mudanças na precipitação e temperatura no nordeste Brasileiro utilizando a técnica de downscaling dinâmico. **Revista Brasileira de Meteorologia**, v. 30, n. 4, p. 435–456, 2015.

SCHWALM, C. R.; GLENDON, S.; DUFFY, P. B. RCP8.5 tracks cumulative CO<sub>2</sub> emissions. **Proceedings of the National Academy of Sciences of the United States of America**, v. 117, n. 33, p. 19656–19657, 2020.

SEDGWICK, P. Spearman's rank correlation coefficient. **BMJ (Online)**, v. 349, n. November, p. 1–3, 2014.

SILVA, G. B.; AZEVEDO, P. V. DE. Cenários de Mudanças Climáticas no Estado da Bahia através de Estudos Numéricos e Estatísticos. **Revista de geografia Física**, v. 05, p. 1019–1034, 2012.

SILVEIRA, C. DA S. et al. Mudanças climáticas na bacia do rio São Francisco: Uma análise para precipitação e temperatura. **Revista Brasileira de Recursos Hídricos**, v. 21, n. 2, p. 416–428, 2016.

SINGH, O.; ARYA, P.; CHAUDHARY, B. S. On rising temperature trends at Dehradun in Doon valley of Uttarakhand, India. **Journal of Earth System Science**, v. 122, n. 3, p. 613–622, 2013.

SIQUEIRA, N. A. DOS S.; SIQUEIRA, A. H. B.; FILHO, A. J. P. Statistical Analysis of Precipitation Extremes in São Francisco River Basin, Brazil. **Atmospheric and Climate Sciences**, v. 12, n. 02, p. 383–408, 2022.

SOUTO, J.; BELTRÃO, N.; TEODORO, A. Performance of remotely sensed soil moisture for temporal and spatial analysis of rainfall over São Francisco River basin, Brazil. **Geosciences (Switzerland)**, v. 9, n. 3, p. 1–15, 2019.

STORCH, H. VON. Statistical Analysis in Climate Research. **Computers & Geosciences**, v. 27, n. 3, p. 371–373, 2001.

TEIXEIRA, A. L. DE F. et al. Operationalizing water security concept in water investment planning: Case study of São Francisco river basin. **Water (Switzerland)**, v. 13, n. 24, 2021.

TEUTSCHBEIN, C.; SEIBERT, J. Bias correction of regional climate model simulations for hydrological climate-change impact studies: Review and evaluation of different methods. **Journal of Hydrology**, v. 456–457, p. 12–29, 2012.

TEUTSCHBEIN, C.; SEIBERT, J. Is bias correction of regional climate model (RCM) simulations possible for non-stationary conditions. **Hydrology and Earth System Sciences**, v. 17, n. 12, p. 5061–5077, 2013.

THOMSON, A. M. et al. RCP4.5: A pathway for stabilization of radiative forcing by 2100. **Climatic Change**, 2011.

VALVERDE, M. C.; MARENGO, J. A. Extreme Rainfall Indices in the Hydrographic Basins of Brazil. **Open Journal of Modern Hydrology**, v. 04, n. 01, p. 10–26, 2014.

VAN GIERSBERGEN, N. P. A. On the effect of deterministic terms on the bias in stable AR models. **Economics Letters**, v. 89, n. 1, p. 75–82, 2005.

VASCO, G. et al. A Hydro PV Hybrid System for the Laranjeiras Dam (in Southern Brazil) Operating with Storage Capacity in the Water Reservoir. **Smart Grid and Renewable Energy**, v. 10, n. 04, p. 83–97, 2019.

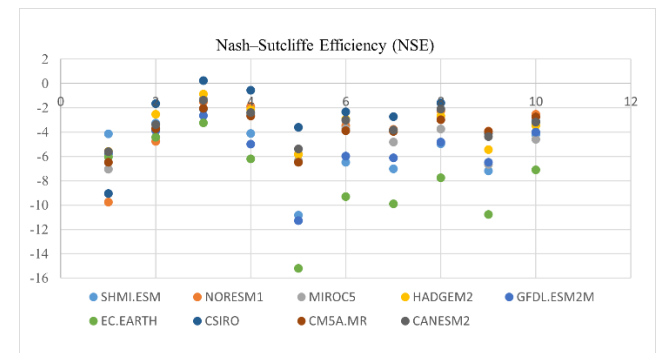
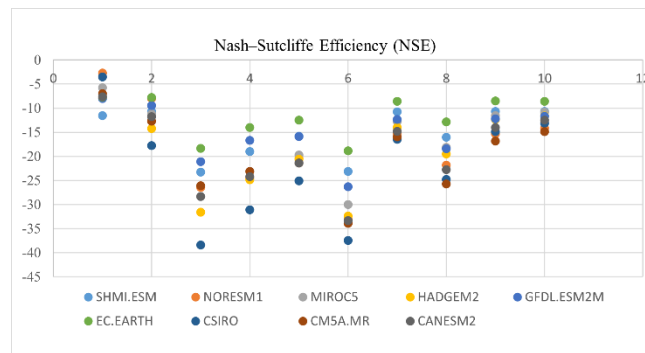
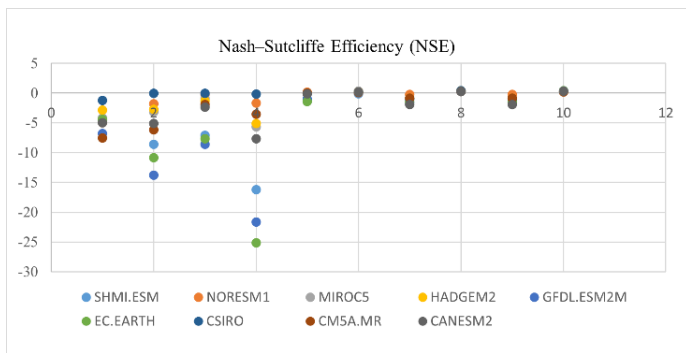
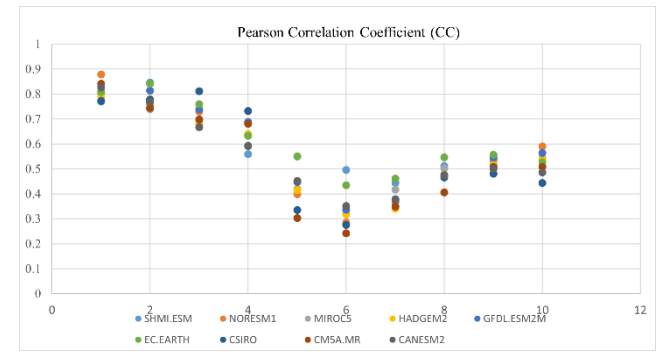
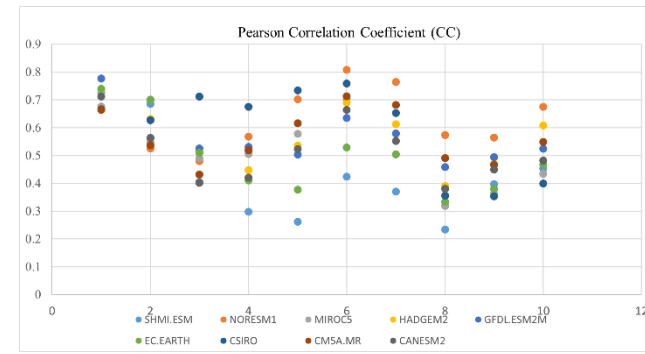
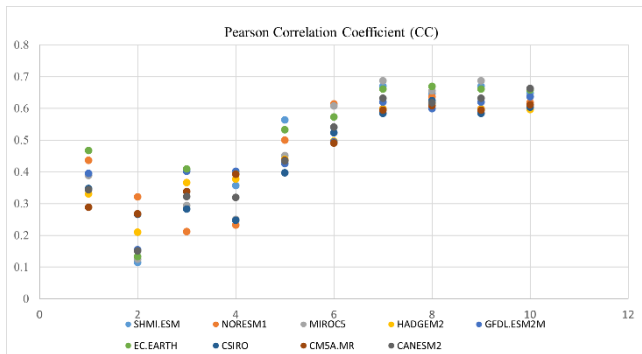
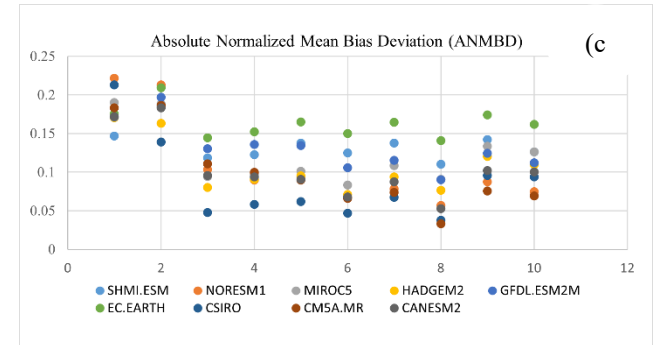
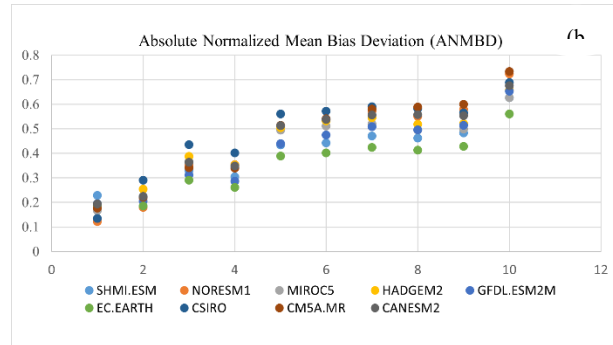
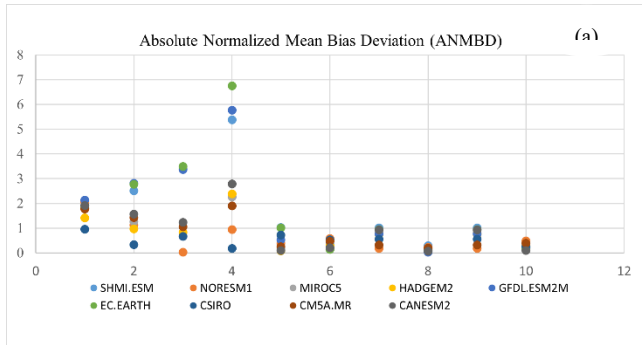
WANG, F. et al. Re-evaluation of the Power of the Mann-Kendall Test for Detecting Monotonic Trends in Hydrometeorological Time Series. **Frontiers in Earth Science**, v. 8, n. February, p. 1–12, 2020.

WATANABE, M. et al. Improved climate simulation by MIROC5: Mean states, variability, and climate sensitivity. **Journal of Climate**, v. 23, n. 23, p. 6312–6335, 2010.

WATANABE, S. et al. MIROC-ESM 2010: Model description and basic results of CMIP5-20c3m experiments. **Geoscientific Model Development**, v. 4, n. 4, p. 845–872, 2011.

YUE, S.; WANG, C. Y. Applicability of prewhitening to eliminate the influence of serial correlation on the Mann-Kendall test. **Water Resources Research**, v. 38, n. 6, p. 4-1-4–7, 2002.

Appendix A: Performance analysis of ANMBD, CC, and NSE metrics of precipitation (a), minimum (b), and maximum temperature (c) for 9 RCMs in 10 points.



Appendix B: Variation of annual average precipitation (a) minimum (b), and maximum temperature (c) for different periods under the RCP 4.5 and RCP 8.5 scenarios.

<b>(a)</b>								
<b>Scenario</b>	Station	Region	1961 - 2020	2021 - 2059	2060 - 2100	V1	V2	V3
			(T1) mm	(T2) mm	(T3) mm	(T2-T1) mm	(T3-T2) mm	(T3-T1) mm
<b>RCP 4.5</b>	S1	Upper	3609.53	3770.70	3763.13	161.17	-7.57	153.59
	S2		1388.90	1475.72	1500.92	86.81	25.21	112.02
	S3		1071.25	1134.01	1203.85	62.76	69.84	132.60
	S4	MSM	1194.32	1267.09	1338.51	72.77	71.42	144.19
	S5		983.62	1003.51	1072.00	19.89	68.50	88.39
	S6		1034.00	1104.90	1204.34	70.90	99.44	170.34
	S7		728.87	748.31	784.22	19.45	35.91	55.35
	S8	Lower	1283.80	1368.45	1427.85	84.65	59.40	144.06
	S9		2041.58	2088.41	2139.46	46.83	51.06	97.88
	S10		813.25	794.30	808.53	-18.94	14.22	-4.72
<b>RCP8.5</b>	S1	Upper	3599.59	3791.37	3840.49	191.78	49.12	240.90
	S2		1389.79	1506.43	1596.01	116.64	89.58	206.22
	S3		1072.85	1193.43	1319.57	120.58	126.14	246.72
	S4	MSM	1189.64	1324.11	1461.23	134.47	137.12	271.59
	S5		986.07	1047.81	1124.21	61.74	76.41	138.14
	S6		1040.53	1158.44	1244.76	117.91	86.32	204.23
	S7		726.44	757.75	810.21	31.31	52.46	83.77
	S8	Lower	1286.62	1412.40	1560.88	125.78	148.48	274.26
	S9		2041.58	2088.41	2139.46	46.83	51.06	97.88
	S10		813.25	794.30	808.53	-18.94	14.22	-4.72

<b>(b)</b>									
<b>Scenario</b>	Station	Region	1961 - 2020	2021 - 2059	2060 - 2100	V1	V2	V3	
			(T1) °C	(T2) °C	(T3) °C	(T2-T1) °C	(T3-T2) °C	(T3-T1) °C	
<b>RCP 4.5</b>	S1	Upper	21.74	22.97	23.53	1.23	0.57	1.79	
	S2		22.24	23.59	24.29	1.34	0.70	2.05	
	S3		21.36	22.62	23.29	1.26	0.66	1.93	
	S4	MSM	21.69	22.95	23.66	1.26	0.71	1.97	
	S5		20.04	21.31	22.05	1.27	0.74	2.01	
	S6		19.83	21.17	21.93	1.34	0.76	2.10	
	S7		18.56	19.93	20.68	1.37	0.75	2.13	
	S8		17.20	18.61	19.42	1.41	0.81	2.22	
	S9		Lower	17.09	18.45	19.21	1.37	0.75	2.12
	S10			16.01	17.42	18.18	1.41	0.76	2.17
<b>RCP 8.5</b>	S1	Upper	21.74	23.24	24.44	1.50	1.20	2.69	
	S2		22.24	23.90	25.64	1.66	1.74	3.40	
	S3		21.36	22.93	24.57	1.57	1.64	3.21	
	S4	MSM	21.69	23.28	25.03	1.58	1.75	3.33	
	S5		20.05	21.65	23.52	1.60	1.87	3.47	
	S6		19.84	21.52	23.48	1.68	1.96	3.64	
	S7		18.57	20.26	22.28	1.70	2.02	3.72	
	S8		17.21	18.98	21.10	1.77	2.12	3.89	
	S9		Lower	17.10	18.80	20.81	1.71	2.01	3.72
	S10			16.02	17.77	19.81	1.75	2.04	3.79

<b>(c)</b>								
<b>Scenario</b>	<b>Station</b>	<b>Region</b>	<b>1961 - 2020</b>	<b>2021 - 2059</b>	<b>2060 - 2100</b>	<b>V1</b>	<b>V2</b>	<b>V3</b>
			(T1) °C	(T2) °C	(T3) °C	(T2-T1) °C	(T3-T2) °C	(T3-T1) °C
<b>RCP 4.5</b>	S1	Upper	31.20	32.20	32.77	1.00	0.57	1.57
	S2		33.21	34.33	34.93	1.20	0.61	1.72
	S3		32.10	33.23	33.78	1.12	0.56	1.68
	S4	MSM	32.19	33.40	33.99	1.21	0.59	1.80
	S5		33.27	34.56	35.12	1.29	0.57	1.85
	S6		32.61	33.89	34.42	1.27	0.53	1.80
	S7		31.56	32.89	33.46	1.33	0.57	1.90
	S8	Lower	28.18	29.60	30.26	1.42	0.65	2.07
	S9		29.46	30.86	31.51	1.40	0.65	2.04
	S10		29.67	31.03	31.65	1.36	0.62	1.97
<b>RCP 8.5</b>	S1	Upper	31.20	32.43	33.74	1.23	1.31	2.54
	S2		33.22	34.60	36.01	1.38	1.40	2.79
	S3		32.12	33.50	34.74	1.38	1.24	2.62
	S4	MSM	32.20	33.69	34.94	1.49	1.24	2.73
	S5		33.29	34.83	36.09	1.54	1.26	2.80
	S6		32.64	34.13	35.32	1.49	1.19	2.68
	S7		31.59	33.15	34.50	1.56	1.36	2.92
	S8	Lower	28.21	29.90	31.42	1.70	1.52	3.22
	S9		29.48	31.14	32.73	1.66	1.59	3.25
	S10		29.69	31.29	32.90	1.59	1.61	3.20

Appendix C: Spatial variation of Z-value and trend showing grid points in four trend tests for three sub-regions for the entire São Francisco River basin

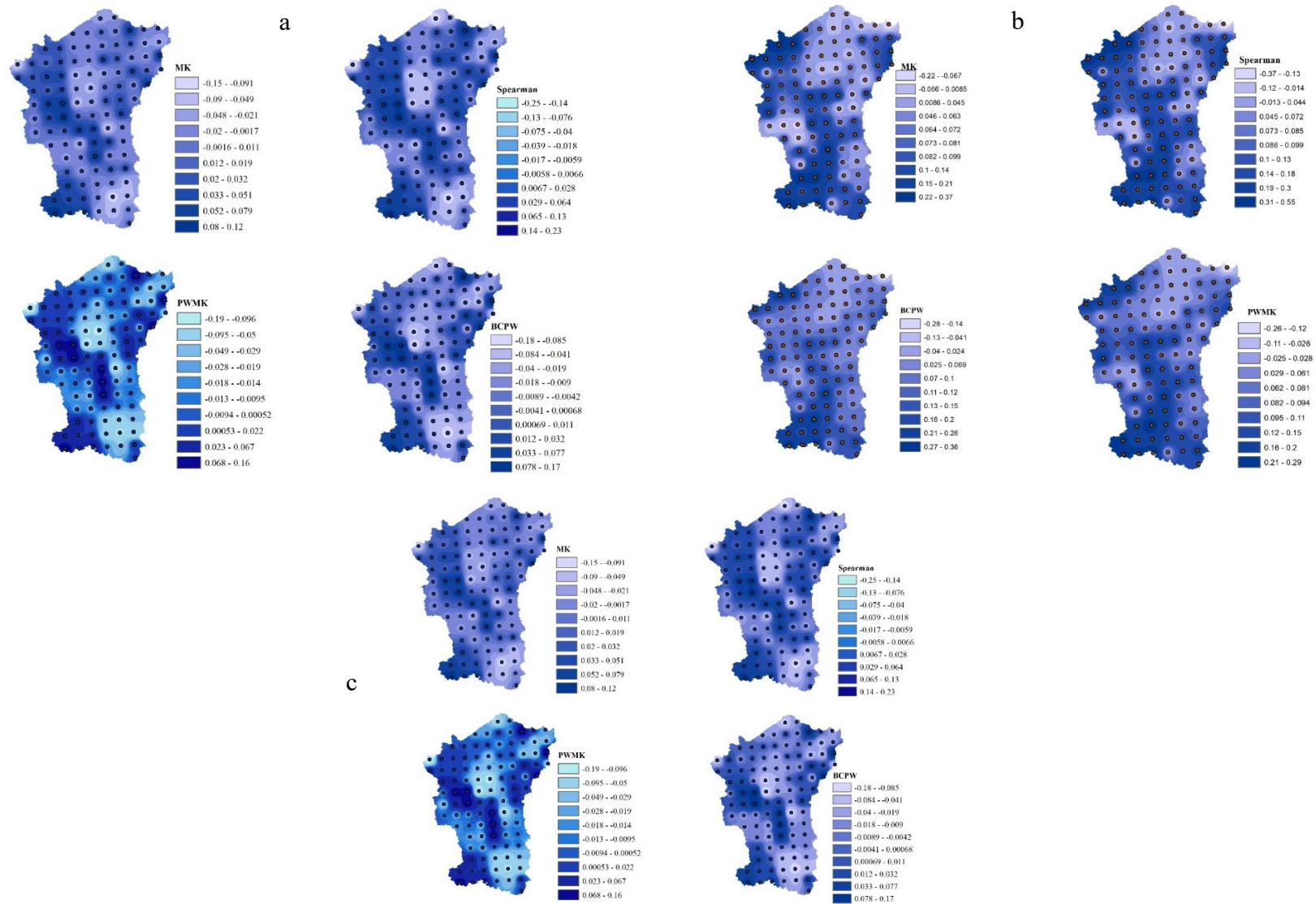


Figure 1: Spatial variation of Z-value and trend showing grid points in four trend tests of precipitation data in the dry (a), rainy (b), and pre-season (c) periods over Upper São Francisco

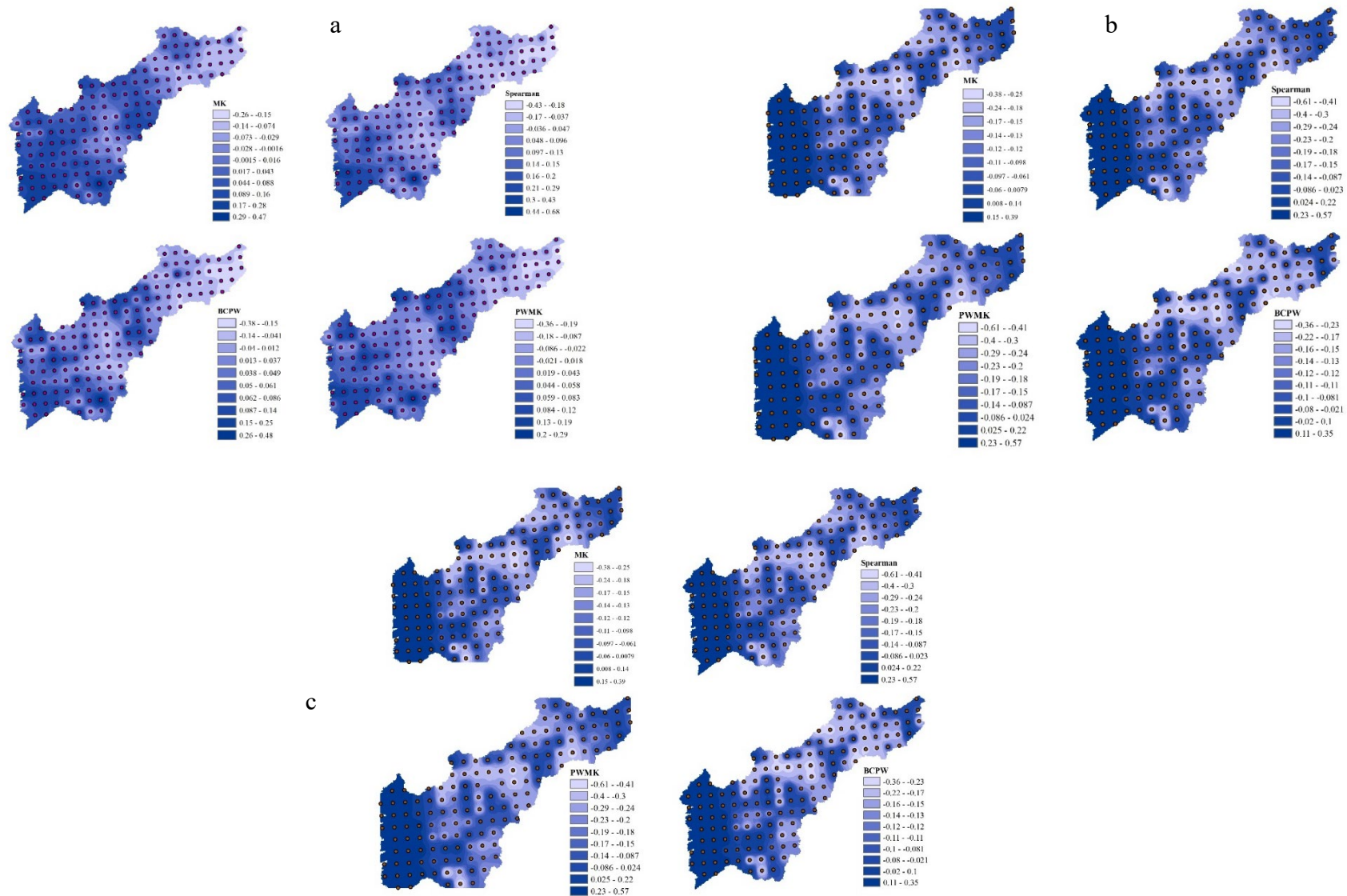


Figure 2: Spatial variation of Z-value and trend showing grid points in four trend tests of precipitation data in the dry (a), rainy (b), and pre-season (c) periods over Middle and Sub-Middle São Francisco

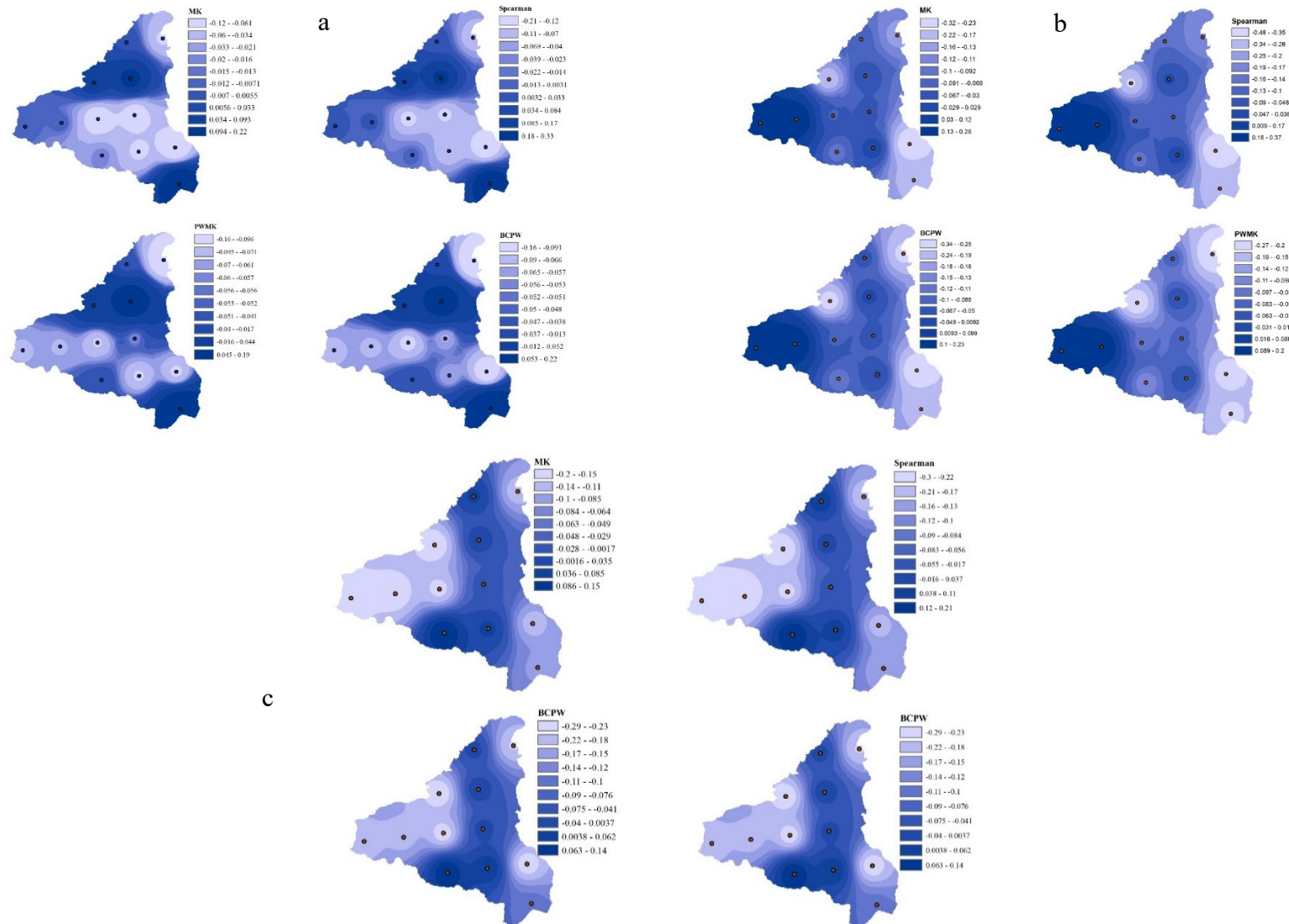


Figure 3: Spatial variation of Z-value and trend showing grid points in four trend tests of precipitation data in the dry (a), rainy (b), and pre-season (c) periods over Lower São Francisco.

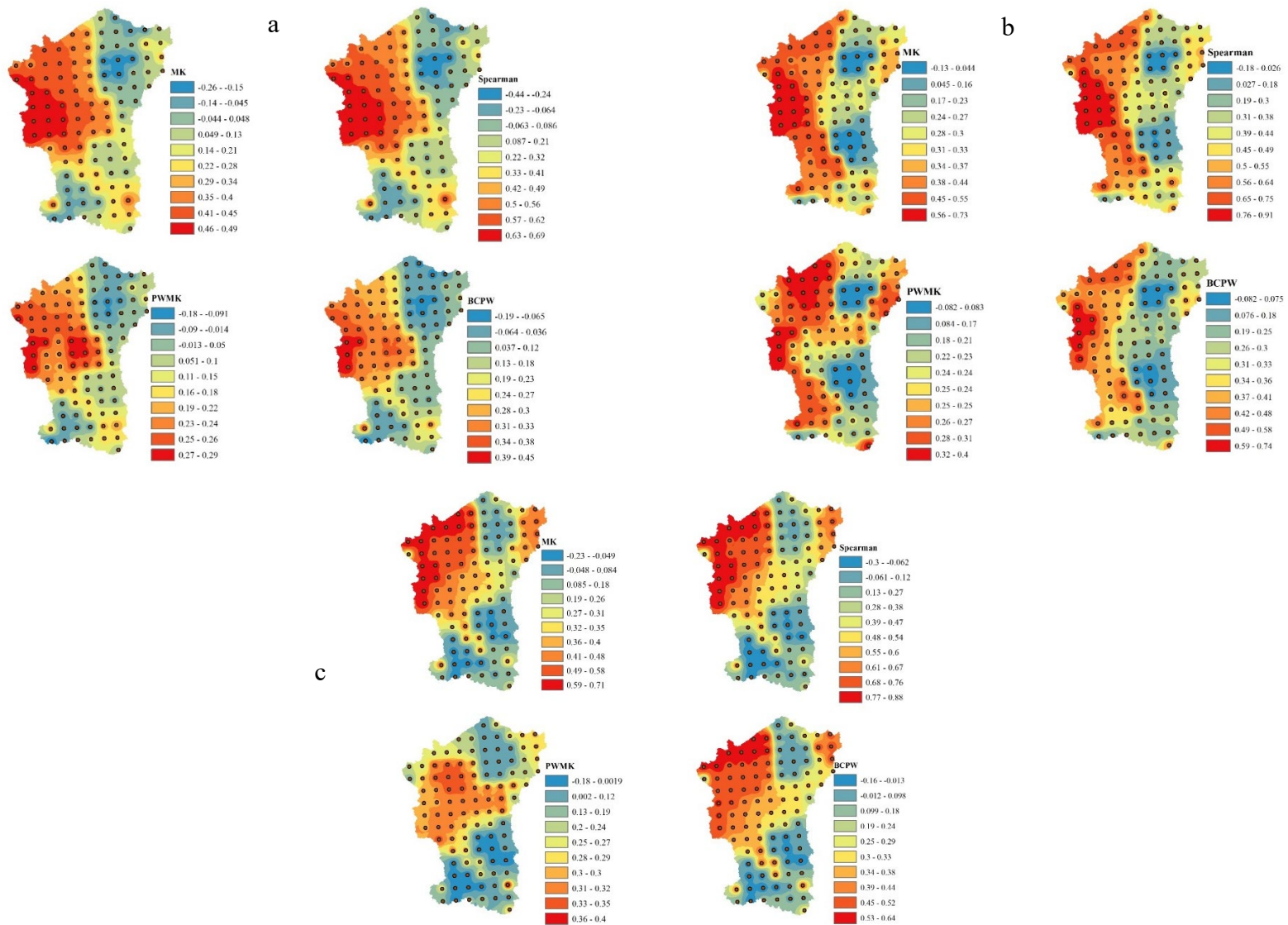


Figure 4: Spatial variation of Z-value and trend showing grid points in four trend tests of minimum temperature data in the dry (left) and rainy (right) periods over Upper São Francisco.

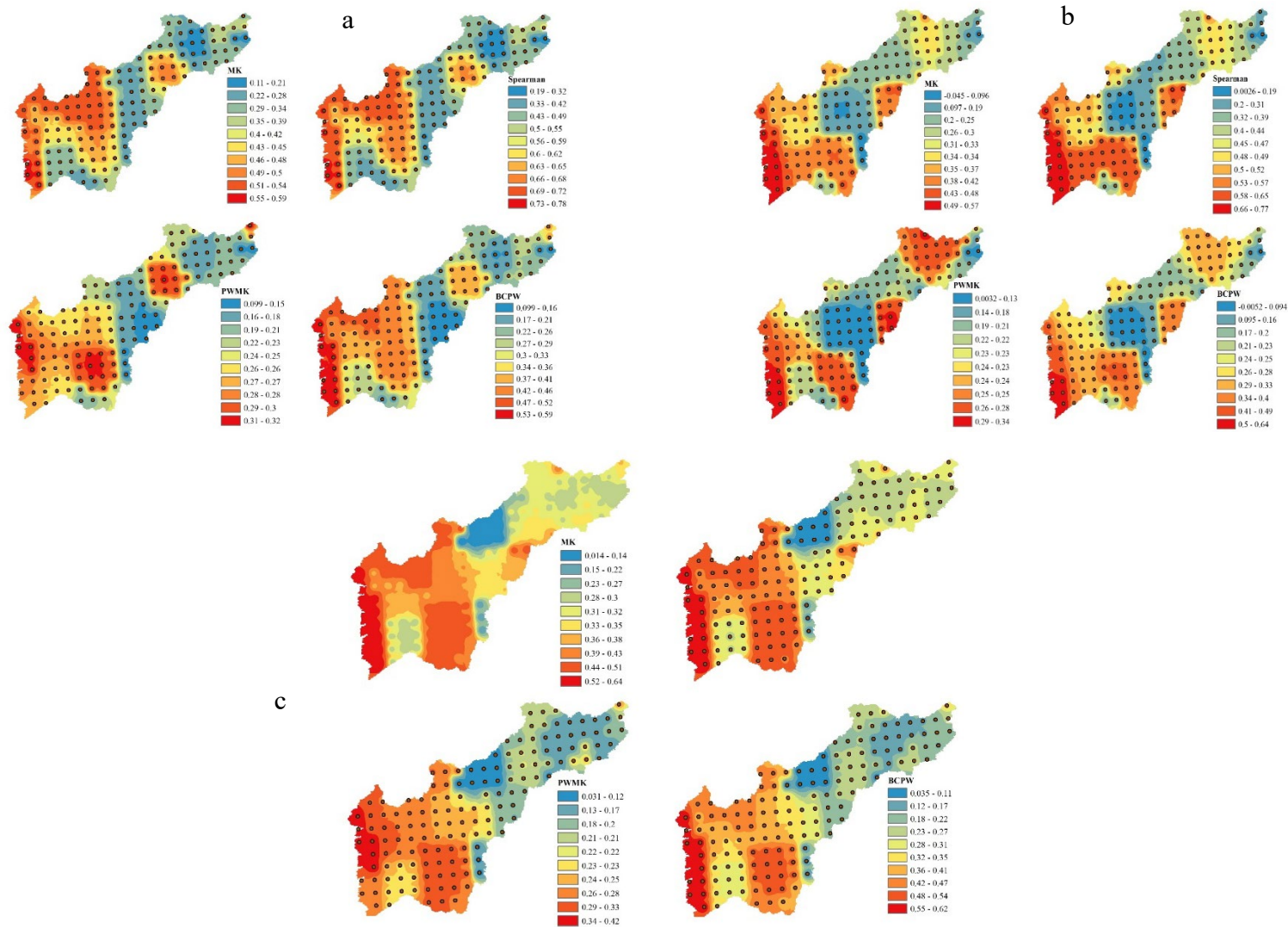


Figure 5: Spatial variation of Z-value and trend showing grid points in four trend tests of minimum temperature data in the dry (a), rainy (b), and pre-season (c) periods over Middle and Sub-Middle São Francisco.

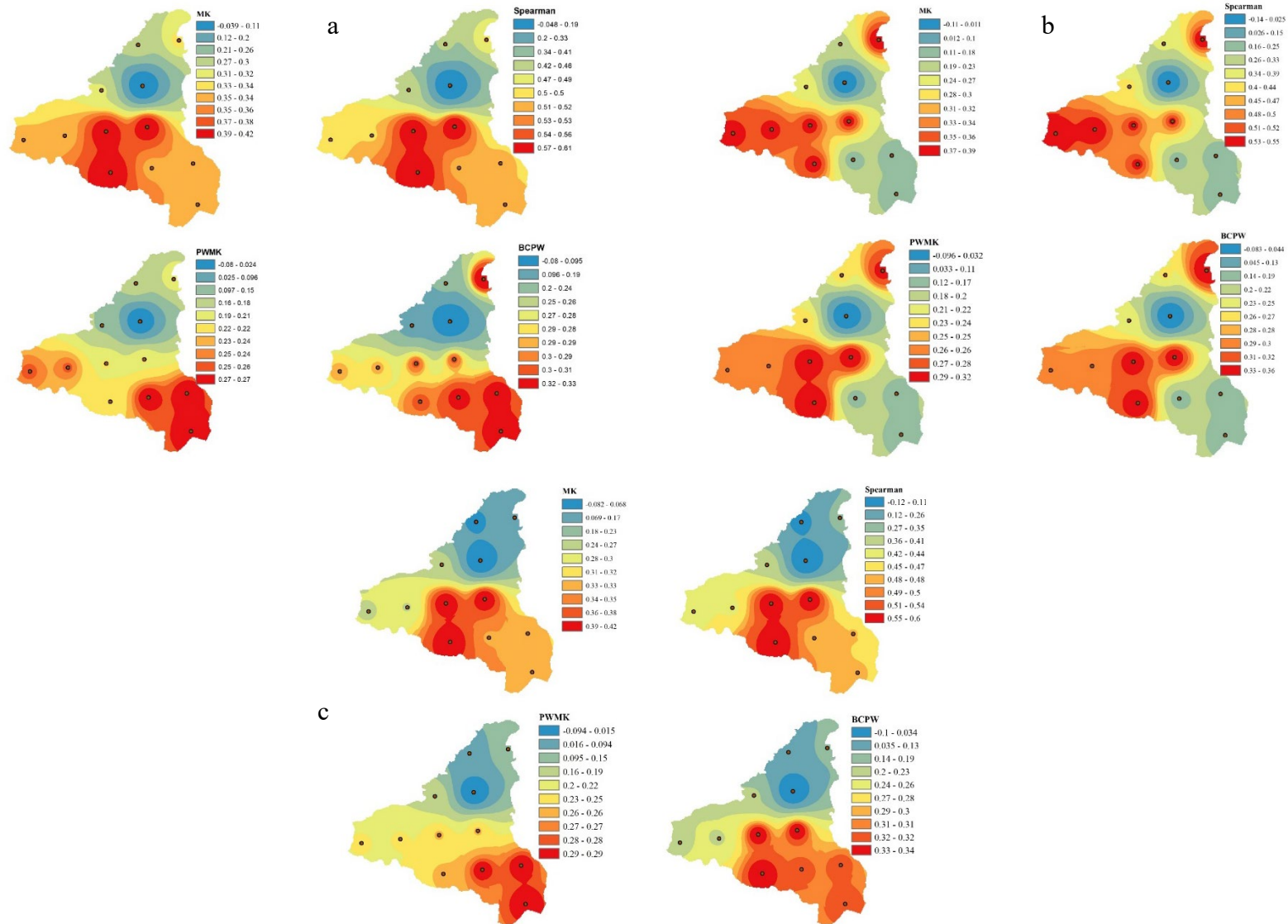


Figure 6: Spatial variation of Z-value and trend showing grid points in four trend tests of minimum temperature data in the dry (a), rainy (b), and pre-season (c) periods over Lower São Francisco.

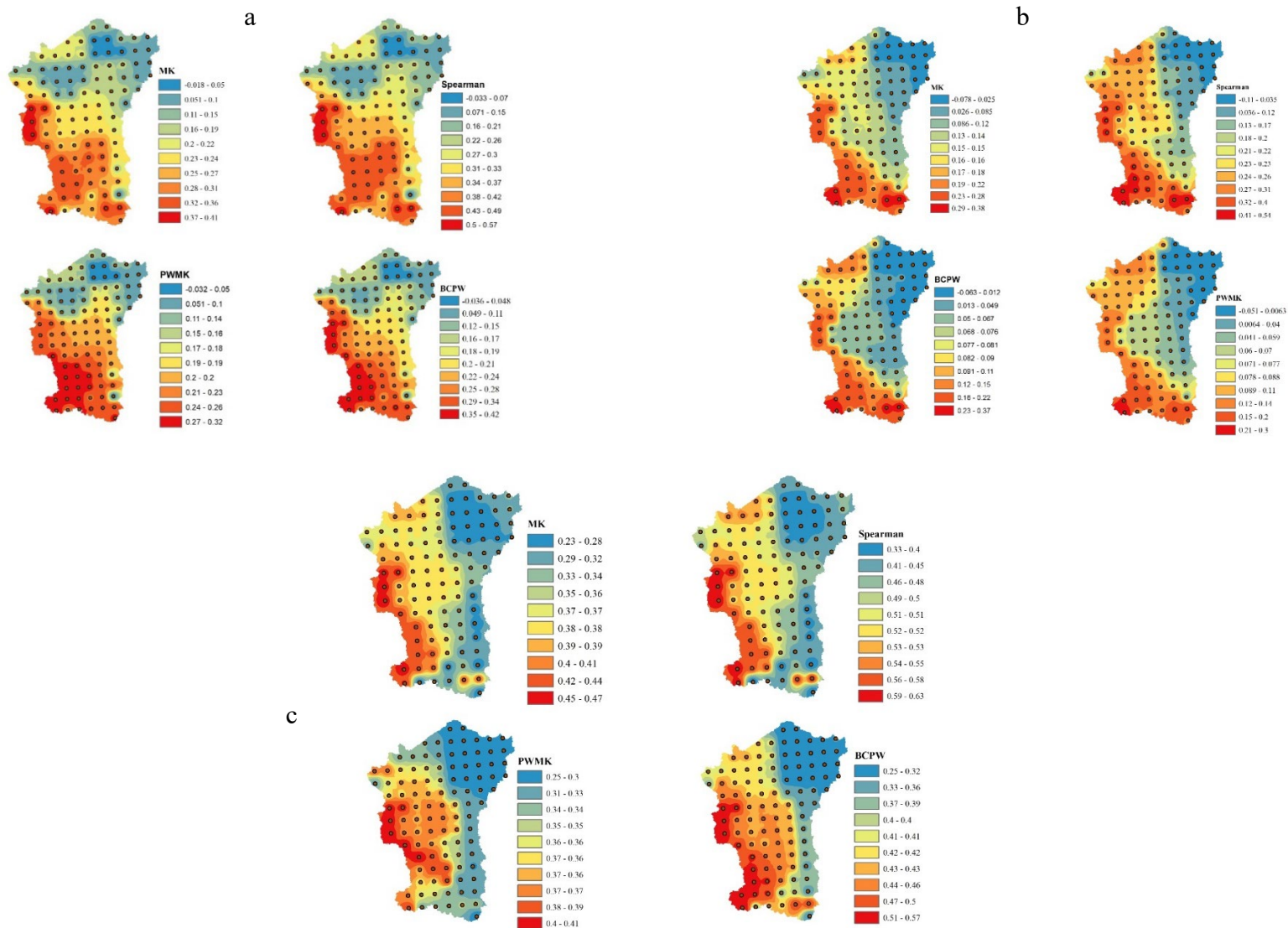


Figure 7: Spatial variation of Z-value and trend showing grid points in four trend tests of maximum temperature data in the dry (a), rainy (b), and pre-season (c) periods over Upper São Francisco.

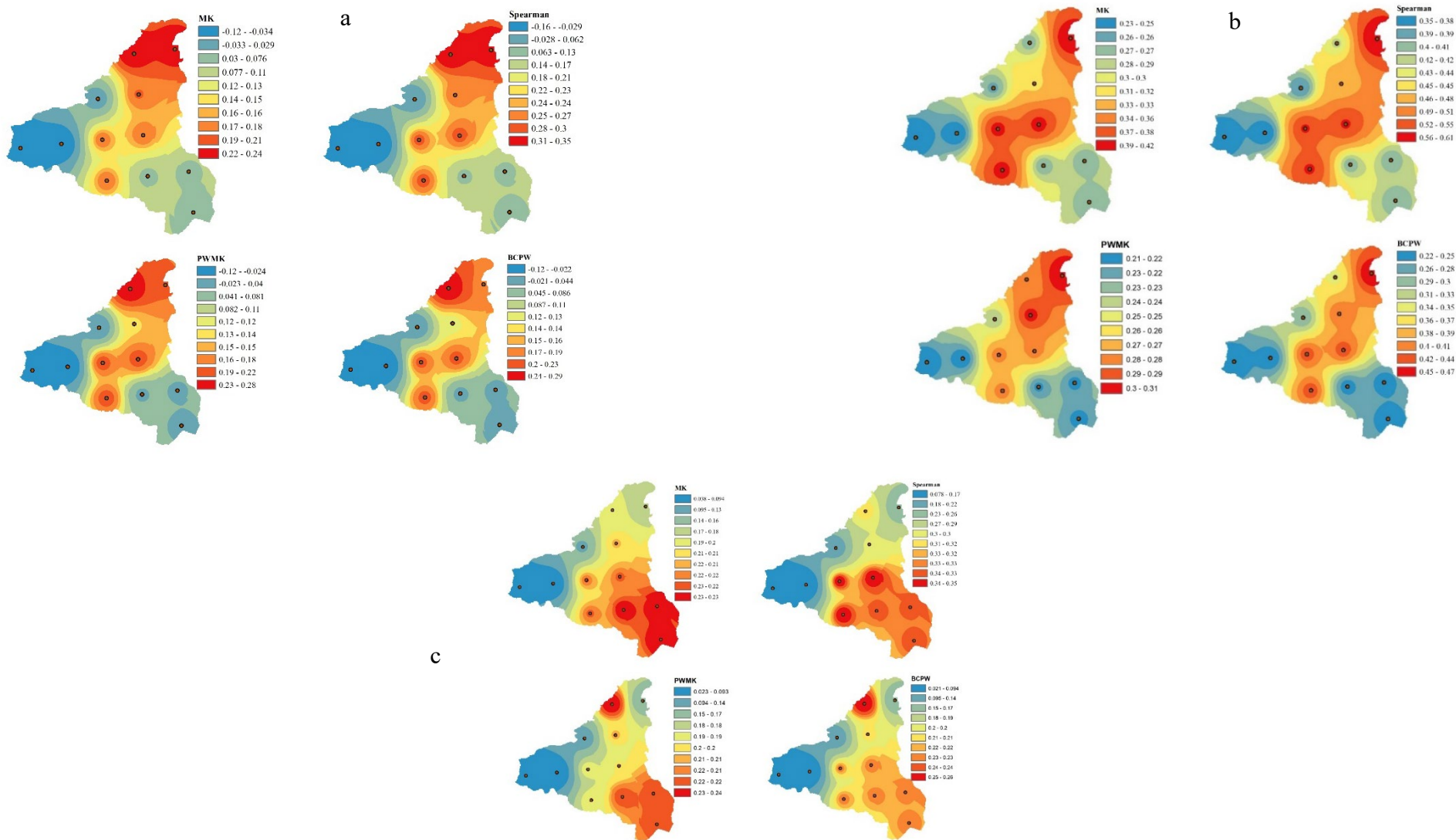


Figure 8: Spatial variation of Z-value and trend showing grid points in four trend tests of maximum temperature data in the dry (a), rainy (b), and pre-season (c) periods over Lower São Francisco.

## CHAPTER IV

---

# Climate change impact assessment on water resources in the São Francisco River Basin<sup>13</sup>

### Abstract

Climate change is one of the most important factors that directly impact water resources, affecting both water quantity and water quality. The objective of this study was to use the SWAT model and a multi-model ensemble to investigate the effects of projected climate scenarios on the São Francisco River Basin (SFRB) water balance. The hydrological SWAT model used in this chapter was calibrated as part of his ongoing BRICS multilateral research project entitled “*Integrated water management model for Brazil, India, and South Africa under climate change scenarios*”. Climate change scenarios were analyzed using climate-related data for three time periods and a delta-based statistical downscaling approach for two representative concentration pathways (RCPs), RCP 4.5 and RCP 8.5. The results show that water balance patterns in the SFRB can be strongly influenced by future climate change scenarios. Processes that are expected to increase over time are evapotranspiration, infiltration, base flow, and water yield; in contrast, potential evapotranspiration is expected to decrease. The results also predict that the average monthly water flow will decrease over time until the end of the 21<sup>st</sup>-century. The results of this study will help water resource managers reduce future risks associated with climate change in the study area and will also help public authorities address agroecological risks in this and other areas. It can also be used by environmental and water decision-makers designing policies. Similar waters around the world.

**Keywords:** climate change, water resources, water balance, water yield, evapotranspiration, evapotranspiration, percolation, groundwater contribution, streamflow dynamic.

---

<sup>13</sup>A modified version of this chapter will be shortly submitted to a peer-review international journal.

## 4.1 Introduction

Climate change has been recognized as one of the main 21<sup>st</sup>-century environmental problems throughout the world (ASHRAF VAGHEFI et al., 2017; LIU et al., 2017), being identified as a major socioeconomic challenge both globally and regionally (PAREDES-TAVARES et al., 2018).

However, river basins across the globe are experiencing varying degrees of impact from global climate change events (PANDEY et al., 2019), which have increased in frequency and intensity in recent years (CUNHA et al., 2019). The São Francisco River is one of the main surface water resources in Brazil and is facing environmental challenges that threaten its sustainability (BETTENCOURT et al., 2022).

The Intergovernmental Panel on Climate Change-IPCC Fourth (AR4) and Fifth (AR5) Assessment Reports highlight the regions on Earth that are more vulnerable to climate change (NETO et al., 2016). Due to demographic changes (CARLUCCI et al., 2020), some climate change scenarios were projected, such as rainfall (e.g. increase or decrease of the total annual precipitation), dryness, or wetness that in the long term affect the basin-scale water budget (NETO et al., 2016).

These are expected not only to affect the intensity and frequency of extreme events in the next decades but also to amplify existing socioenvironmental risks in urban areas (ALVES et al., 2020; PAULO et al., 2016), uncertainties and tension between water availability and water demand–energy–food (WEF) production, as well as, for ecosystems services, on regional and local scales (GESUALDO et al., 2019; WOZNICKI; NEJADHASHEMI; PARSINEJAD, 2015).

With the increasing scarcity of water resources, especially in arid and semi-arid areas, the hydrological impacts of climate uncertainties, particularly on surface runoff are drawing increasing attention from hydrological researchers, and policymakers (PANDEY et al., 2016; WANG et al., 2013; YIN et al., 2016). Modeling studies were undertaken in many different environments (ARNELL; GOSLING, 2013; BASIN et al., 2016; GUDMUNDSSON et al., 2012; RANGE et al., 2011), showing that climate change has the potential to modify substantially river flow regimes (JÚNIOR; TOMASELLA; RODRIGUEZ, 2015), altering hydrological processes.

The key climate variables influencing streamflow, are precipitation and temperature (DELMONTE OLIVEIRA; TOMASELLA; DEL'ARCO SANCHES, 2019), with the effect of the latter, manifested largely through altered evapotranspiration and snowmelt (PATTERSON; LUTZ; DOYLE, 2013), interception, and infiltration (FLEISCHMANN et al., 2019), resulting in spatial-temporal alterations of the water cycle (MARHAENTO; BOOIJ; HOEKSTRA,

2018). The increase in temperature, variations in precipitation, and changes in the frequency of extreme events increase the probability of flood occurrences and change the total and seasonal water supply (KHALILIAN; SHAHVARI, 2018). The nature of the evaporating material and the spatiotemporal variations in the area affect the evapotranspiration rate due to complications in physical characteristics and climatic settings (NESRU; NAGARAJ; SHETTY, 2020).

The spatial variability of precipitation influences meltwater regimes, and surface water and groundwater recharge may be directly affected by changes in rainfall and increases in air temperature that cause higher evapotranspiration rates (NETO et al., 2014). The occurrence of these processes may turn affect the availability of water for the rivers downstream (SU et al., 2015), and its management, with more frequent and extended droughts, more severe floods, and lower water quality (ORTIZ-PARTIDA et al., 2020).

On the other hand, the spatial-temporal patterns that characterize the hydrological response of a watershed to climate change will be highly different due to the combined effects of natural processes and human influences (WANG; SUN; ZHAO, 2019). These may include, climatic conditions and meteorological forcing (WANG et al., 2018), physiological characteristics related to soil (WANG et al., 2011), vegetation, geological and topographical elements (HU; SI, 2014), relief, and drainage network of the basins (NETO et al., 2016), and human activities (GAO; GUO, 2014; ZUCCO et al., 2014).

Human activities can modify streamflow directly by affecting hydrological pathways or indirectly by disturbing soil-atmosphere fluxes (DELMONTE OLIVEIRA; TOMASELLA; DEL'ARCO SANCHES, 2019). The direct human impacts on streamflow include land use changes, reservoir construction and operation, surface water and groundwater extraction, and return flow (WANG; HEJAZI, 2011).

Given different climate changes around the world, Brazil cannot be excluded from these large-scale changes, the consequences of which are observed in many Brazilian basins (MONTENEGRO; RAGAB, 2012; NETO et al., 2016). Hence, climate change impacts on water resources are still needed due to the socio-global changes. As seen, very few studies have evaluated the effects of climate change on renewable water resources. Thus, in this work, the SWAT model (ARNOLD et al., 1998), was used to fill this gap in the literature, by investigating the hydrological responses of climate change scenarios in the São Francisco River Basin, Brazil.

This will allow to development of water resources sustainable management plans (GESUALDO et al., 2019), aiming to assist policymakers in implementing appropriate prevention, adaptation, and mitigation strategies (FAKHRUDDIN et al., 2020; GAO et al., 2016; GEBREMICAEL et al., 2013; SU et al., 2015).

## **4.2 Materials and Methods**

### **4.2.1 Study area description**

This work was developed at the São Francisco River basin, the largest river that runs entirely in Brazilian territory, and is the fourth longest in South America and in Brazil (after the Amazon, the Paraná, and the Madeira) (LUCAS et al., 2021a; NASCIMENTO DO VASCO; DE OLIVEIRA AGUIAR NETTO; GONZAGA DA SILVA, 2019; SIQUEIRA; SIQUEIRA; FILHO, 2022). It is an important river for Brazil, called "the river of national integration" not only because of the volume of transported water, linking southeast and northeast Brazil (LUCAS et al., 2021a) but also because it unites diverse climates and regions of the country, in particular, the Southeast with the Northeast (BEZERRA et al., 2019).

The São Francisco River basin presents different types of climates according to Köppen's classification (LUCAS et al., 2021a), ranging from Aw type – hot and humid with summer rains (in higher SFRB), Aw – also presenting another climatic variation BShw (in middle SFRB), BShw (semiarid) – with seven to eight dry months and an autumn rainfall regime with an annual total of about 550 mm, mainly concentrated between November and March (in sub-middle SFRB), and As – hot and humid with winter rains, and BSh (semiarid with a short-wet season) ( in lower SFRB) (LUCAS et al., 2021a; MARQUES; GUNKEL; SOBRAL, 2019).

Soils with an aptitude for irrigated agriculture predominate in the São Francisco River Basin (MARQUES; GUNKEL; SOBRAL, 2019), with annual precipitations normally below 800 mm irregularly distributed over the year (CARVALHO et al., 2020); as about 58% of the basin's territory cross some of the driest parts of the Brazilian semiarid region, mostly in northeastern Brazil (DE CARVALHO BARRETO et al., 2020).

### **4.2.2 Brief description of the used SWAT hydrological model**

#### **4.2.2.1. Input data and SWAT model setup**

In this work, we applied a SWAT hydrological model, a physically based, semi-distributed, continuous-time, long-term, and basin-scale hydrological model (ARNOLD et al., 1998), a widely used tool for studying simulated hydrological and water quality responses to climate change around the world (BONUMA; REICHERT; RODRIGUES, 2015; BRESSIANI et al., 2015; BRIGHENTI et al., 2019; DE AMORIM; CHAFFE, 2019; FRANCESCONI et al., 2016; PRASKIEVICZ; CHANG, 2009; SHIFERAW et al., 2018; TAN et al., 2019; TUPPAD et al., 2011; VENETSANOUE et al., 2020).

A methodological flowchart for the SWAT model set up and calibration to simulate the climate change scenarios is presented in Figure 26.

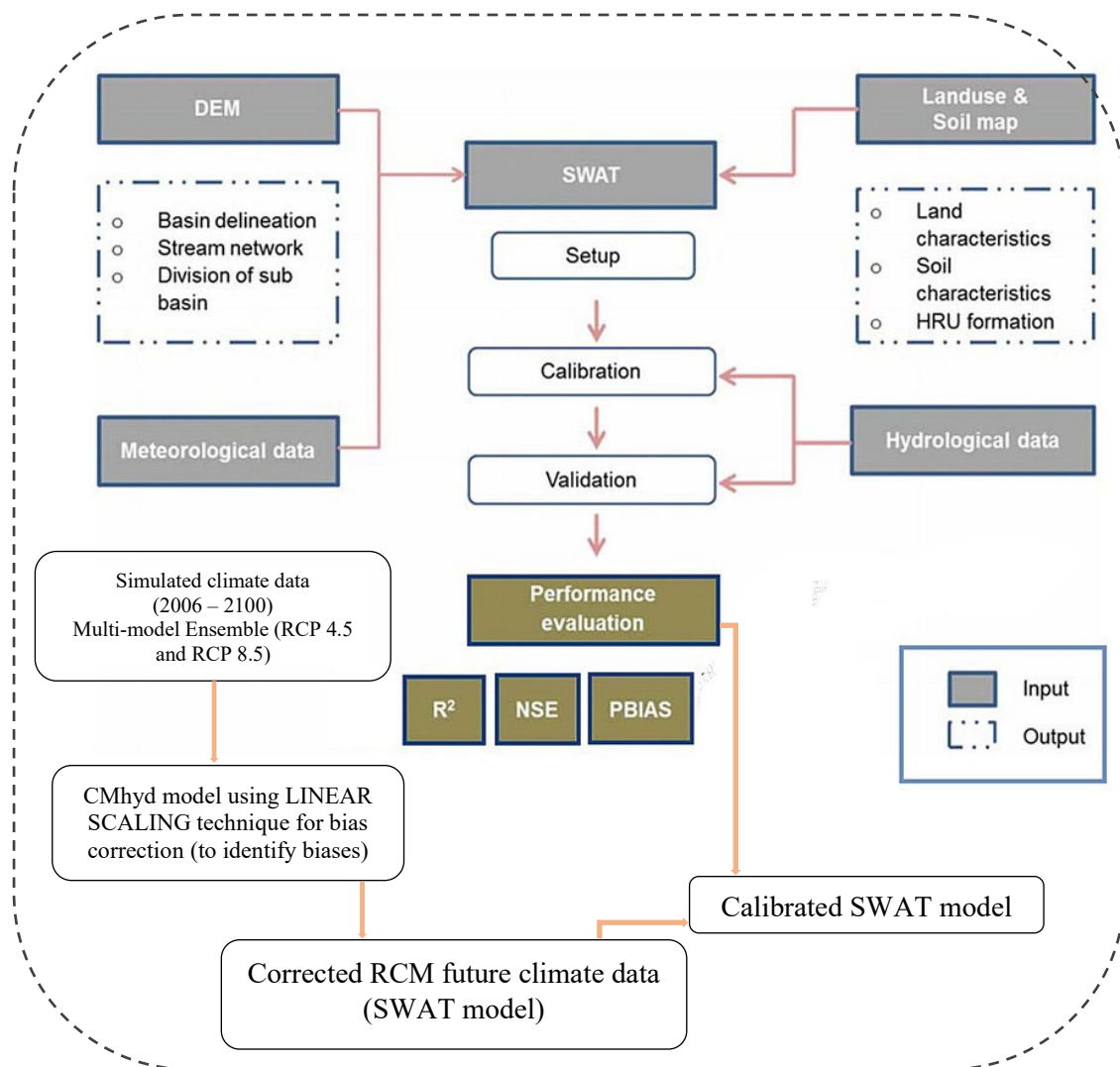


Figure 26: Flow chart of data processing, SWAT model setup, and bias correction methodology

To set up the SWAT hydrological model, four main types of data are required, including three maps, which are land use and soil type maps, a Digital Elevation Model (DEM), and a series of meteorological data such as precipitation (mm), minimum and maximum air temperatures ( $^{\circ}\text{C}$ ), relative humidity (%), wind speed ( $\text{m}\cdot\text{s}^{-1}$ ) and solar radiation.

Hence, firstly, careful work was done on database building, containing geospatial files and tabular data on the climatic conditions of the study for a period of 55 years (1961–2016), as summarized in Table 14, to represent greater spatiotemporal variability of hydrological processes (NEACHELL, 2014).

The climatic data from 1961 to 2016 were obtained through two databases, (i) daily rainfall data (i.e. precipitation) through the APAC (<https://www.apac.pe.gov.br/>), and (ii) complete meteorological data (precipitation, global radiation, relative air humidity or dew point temperature, average air temperature, maximum and minimum air temperatures, and wind speed) through the INMET (<http://www.inmet.gov.br/projetos/rede/pesquisa/inicio.php>).

The soil-types map was based on soil mapping carried out by EMBRAPA-Soils, from the information provided by the Agroecological Zoning of Pernambuco (ZAPE) project, with a resolution of 1: 5 000 000, identifying nineteen predominant soil types presented in Figure 27, which shows slope (a), land-use (b), and soil type (c) maps of the SFRB.

The DEM was obtained from the STRM, a partnership between NASA and NIMA, Germany (DLR), and Italy (ASI), available at the Embrapa website, where there are archives of the altimetry of Brazil. The images are in Geo Tiff format (16 bits) with a spatial resolution of the 90-m grid and SIRGAS2000 Geographic Coordinate System.

The lan- use map of the SFRB was obtained from Landsat 8 satellite images, a TM instrument with a spatial resolution of 30 m, obtained together with the MapBiomass project, referring to the year 2019. The mapping was performed using the supervised classification method through ArcGIS 10.3 software, adopting a maximum likelihood classifier. Land-use was divided into eleven classes of interest, and for the characterization of the land use in SFRB, the information contained in the SWAT database, which has multiple types of land use and vegetation cover, was associated with the classes listed by the Brazilian Company of Agricultural Research (EMBRAPA).

Table 14: SWAT input data used for the São Francisco River basin model setup

<b>Data</b>	<b>Description / Properties</b>	<b>Scale</b>	<b>Source</b>
DEM (Digital Elevation Model)		90-m grid	EMBRAPA/NASA (SRTM)
Lan-use map	Developed from Landsat Thematic Mapper (TM) image (year 2019)	30 x 30 m	MapBiomass
Soil-types map	Soil map of the seven states	1: 5000.000	IBGE
Soil parameters	Soil depths, texture, and organic matter Hydrological groups	Typical soil profile per soil type from the study area	EMBRAPA
Climate data	Other soil parameters were estimated based on Pedo-transfer functions Precipitation, minimum and maximum temperatures (°C), wind speed (m.s <sup>-1</sup> ), relative humidity (%), and insolation (converted to solar radiation (MJ m <sup>-2</sup> . d <sup>-1</sup> ))	Daily Mean (averages and total),	INMET, ANA, and APAC (for Pernambuco state)
Flow	Discharge river data (for calibration purposes)	Monthly averages (m <sup>3</sup> /s)	ANA and APAC

Source: adapted by the author (2023) from several private and public agencies (BRESSIANI et al., 2015)\*

\*The agencies include the Shuttle Radar Topography Mission (SRTM) of the National Aeronautics and Space Administration (NASA), the Ministry of the Environment (MMA), the National Supply Company (CONAB), the Brazilian Institute of Geography and Statistics (IBGE), Brazilian Agricultural Research Corporation (EMBRAPA), MAPBIOMAS initiative, National Water Agency (ANA), Pernambuco State Agency for Water and Climate (APAC), National Institute of Meteorology (INMET).

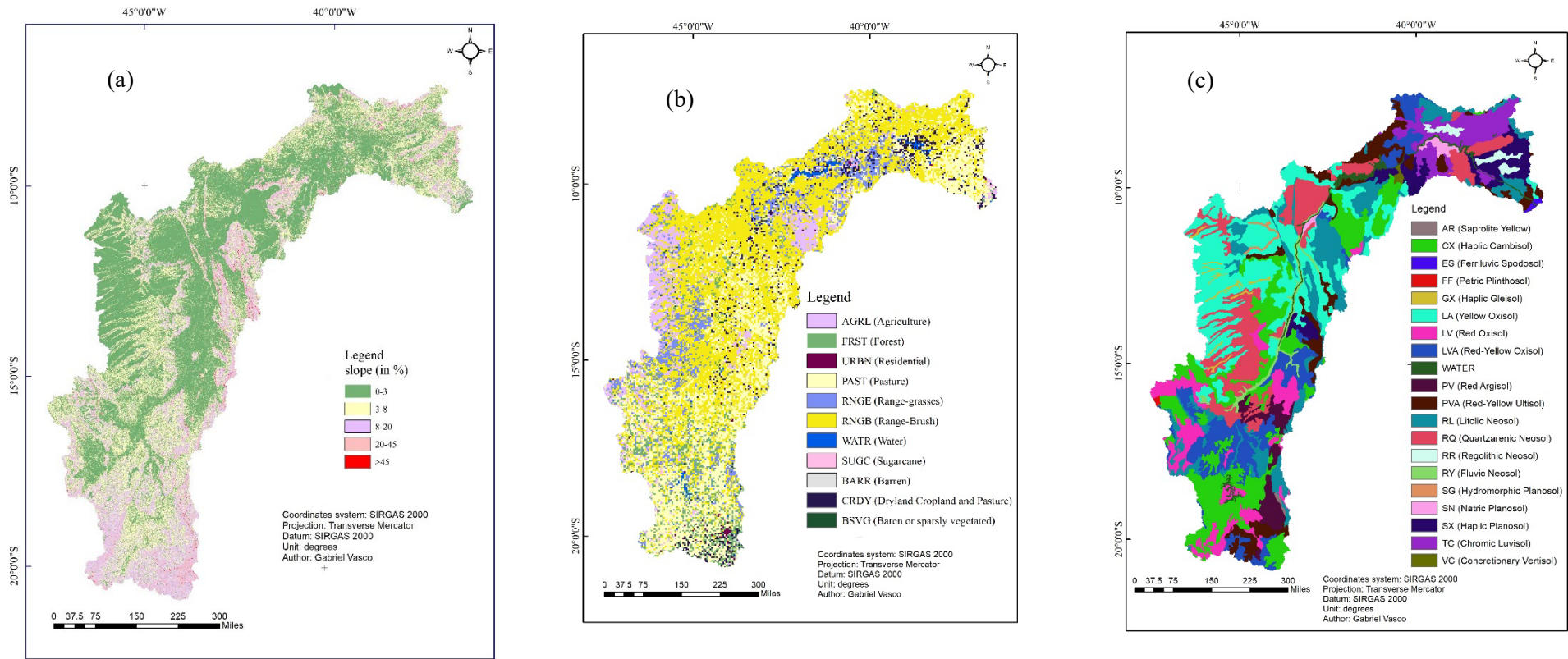


Figure 27: Slope (a), land-use (b), and soil type (c) maps of the São Francisco River Basin

Table 15 presents the main characteristics of the main reservoirs considered in this study, namely: Luiz Gonzaga/Itaparica (3,549 hm<sup>3</sup>) and Sobradinho (28,669 hm<sup>3</sup>) located in the Sub-Middle São Francisco, Paulo Afonso I–IV (26,0 hm<sup>3</sup>) located in Upper São Francisco, Xingó (0,4028 hm<sup>3</sup>), and Três Marias (15,278 hm<sup>3</sup>), located in the Upper São Francisco; where Sobradinho, Três Marias and Luiz Gonzaga account to 58,20%, 31,02%, and 6,62%, respectively, of the water used for power generation in the northeast (SUN et al., 2016).

Table 15: The main characteristics of the main reservoirs considered in this study

Reservoir	IYRES	RES_ESA	RES_EVOL	RES_PSA	RES_PVOL
Luiz Gonzaga	1988	85846.00146	1223945.59	79126.7917	1108691.86
Sobradinho	1979	438423.0522	3897109.83	398496.517	3479056.686
Paulo Afonso I–IV	1979	438.0617869	2253.47312	411.042626	2039.847769
Xingó	1954	6223.309189	379313.54	6205.2632	373095.435
Três Marias	1994	105460	1885526	88987.9	1497413

More details of the reservoirs considered in this study are represented in Annex A, which contains the height x area x volume curves, as recommended in paragraph 1, item II, of Article 8 of the ANA and Ministry of Environment joint resolution (MINISTÉRIO DO MEIO DO MEIO AMBIENTE / ANA - AGÊNCIA NACIONAL DE ÁGUAS, 2013).

The hydrological group was adopted following the Brazilian soils classification (SARTORI ET AL, 2005), and Pedo-transfer Functions (PTF) listed in Table 16 were used to estimate the other soil parameters/ physical-chemical characteristics needed for SWAT (e.g., soil depths, texture, and organic matter) of each type of soil, from the soil data made available by Embrapa soils.

Table 16: Most used Pedo-transfer Functions (PTF)

Equation/model	Eq.	Ref.
<ul style="list-style-type: none"> <li>• <math>SOL\_BD = \rho_B = \rho_N \times (1 - R_v) + (R_v \times 2.65)</math> <ul style="list-style-type: none"> <li>◦ <math>\rho_N = (1 - \theta_s) \times 2.65</math> <ul style="list-style-type: none"> <li>▪ <math>\theta_s = \theta_{33} + \theta_{(s-33)} - 0.097 \times (SOL\_SAND/100) + 0.043</math> <ul style="list-style-type: none"> <li>• <math>\theta_{33} = \theta_{33t} + [1.283 \times (\theta_{33t})^2 - 0.374 \times (\theta_{33t}) - 0.015]</math> <ul style="list-style-type: none"> <li>◦ <math>\theta_{33t} = -0.251 \times (SOL\_SAND/100) + 0.195 \times (SOL\_CLAY/100) + 0.011 \times OM + 0.006 \times [(SOL\_SAND/100) \times OM] - 0.027 \times [(SOL\_CLAY/100) \times OM] + 0.452 \times [(SOL\_SAND/100) \times (SOL\_CLAY/100)] + 0.299</math> <ul style="list-style-type: none"> <li>▪ <math>OM = (SOL\_CBN/100) \times 1.72</math> (1) (SAXTON; RAWLS, 2006)</li> <li><i>Possibly, this factor will be modified to 2 instead of 1.72 for soils in Pernambuco (PRIBYL, 2010).</i></li> </ul> </li> </ul> </li> </ul> </li> </ul> </li> </ul> </li> </ul>		

---

- $\theta_{(s-33)} = \theta_{(s-33)t} + (0.636 \times \theta_{(s-33)t} - 0.107)$ 
  - $\theta_{(s-33)t} = 0.278 \times (\text{SOL\_SAND}/100) + 0.034 \times (\text{SOL\_CLAY}/100) + 0.022 \times \text{OM} - 0.018 \times [(\text{SOL\_SAND}/100) \times \text{OM}] - 0.027 \times [(\text{SOL\_CLAY}/100) \times \text{OM}] - 0.584 \times [(\text{SOL\_SAND}/100) \times (\text{SOL\_CLAY}/100)] + 0.078$
  - $R_v = (\alpha \times R_w) / [1 - R_w \times (1 - \alpha)]$ 
    - $\alpha = \rho_N / 2.65$
    - $R_w = \text{SOL\_ROCK} / 100$

---

- $\text{SOL\_AWC} = \theta_{33} - \theta_{1500}$ 
  - $\theta_{33} = \theta_r + \frac{\theta_s - \theta_r}{[1 + (\alpha \times |\Psi|)^n]^m}$ 
    - $\theta_r = \left[ \frac{23.3867 + 0.1103 \times \text{SOL\_CLAY} - 4.7949 \times \text{SOL\_BD} + 0.0047 \times (\text{SOL\_SILT} \times \text{SOL\_CLAY}) - 0.0027 \times \text{CS}^2 - 0.0022 \times \text{FS}^2 - 0.0048 \times \text{SOL\_SILT}^2}{100} \right]$ 
      - $\text{SOL\_SAND} = \text{CS} + \text{FS}$
    - $\theta_s = \left[ \frac{91.6203 - 30.0046 \times \text{SOL\_BD} + 1.5925 \times \text{SOL\_CBN} + 0.0022 \times (\text{CS} \times \text{SOL\_SILT}) - 0.0036 \times (\text{CS} \times \text{SOL\_CLAY}) - 0.0018 \times \text{CS}^2 - 0.001 \times \text{FS}^2}{100} \right]$  (2) (TOMASELLA; HODNETT; ROSSATO, 2000)
    - $\alpha = e^{\left\{ \frac{205.6546 - 2.556 \times \text{SOL\_SILT} - 0.1329 \times \text{SOL\_CLAY} - 247.4904 \times \text{SOL\_BD}}{0.0189 \times (\text{CS} \times \text{FS}) + 0.1177 \times (\text{CS} \times \text{SOL\_SILT}) + 0.0517 \times (\text{FS} \times \text{SOL\_CLAY}) + 0.0617 \times \text{CS}^2} \right\}}$
    - $n = \left( \frac{168.8617 - 0.0258 \times (\text{CS} \times \text{SOL\_SILT}) - 0.0261 \times ((\text{FS} \times \text{SOL\_CLAY}) + 0.0093 \times \text{FS}^2) - 0.0077 \times \text{SOL\_SILT}^2}{100} \right)$
    - $\Psi = 33$
  - $\theta_{1500} = \theta_r + \frac{\theta_s - \theta_r}{[1 + (\alpha \times |\Psi|)^n]^m}$

$\Psi = 1500$

---

  - $\text{SOL\_K} = 1930 \times (\theta_s - \theta_{33})^{(3-\lambda)}$  (3)
    - $\lambda = 1/B$ 
      - $B = [\ln(1500) - \ln(33)] / [\ln(\theta_{33}) - \ln(\theta_{1500})]$  (SAXTON; RAWLS, 2006)

---

  - $\text{SOL\_ALB} = 0.6 / e^{(0.4 \times \text{OM})}$  (4)

---

  - $\text{USLE\_K} = \left\{ 0.2 + 0.3 \times e^{-0.0256 \times \text{SOL\_SAND} \times \left( 1 - \frac{\text{SOL\_SILT}}{100} \right)} \right\} \times \left( \frac{\text{SOL\_SILT}}{\text{SOL\_CLAY} \times \text{SOL\_SILT}} \right)^{0.3} \times \left[ 1 - \left( \frac{0.25 \times \text{SOL\_CBN}}{\text{SOL\_CBN} \times e^{(3.72 - 2.95 \times \text{SOL\_CBN})}} \right) \times \left[ 1 - \left( \frac{0.7 \times \text{SN1}}{\text{SN1} \times e^{(-5.51 + 22.9 \times \text{SN1})}} \right) \right] \right]$  (5) (SHARPLEY; WIL LIAMS, 1993)
    - $\text{SN1} = 1 - (\text{SOL\_SAND}/100)$

---

The physical properties obtained by the above pedotransfer functions are maximum soil depth (SOL\_ZMX; mm), clay (<0.002 mm; SOL\_CLAY; %), silt (> 0.002 and <0.05 mm; SOL\_SILT; %), sand (> 0.05 and <2 mm; SOL\_SAND; %), stone (> 2 mm; SOL\_ROCK; %), and organic carbon (SOL\_CBN; %).

#### 4.2.2.2 SWAT model calibration procedures

The SWAT model used in the present work was calibrated as part of the BRICS project (ANDRADE et al., 2023). The calibration procedure was performed in the SWAT-CUP, using the SUFI-2 algorithm (ABBASPOUR et al., 2007).

The calibration took place considering one of the outputs of the model: flow data (1961 – 2016), obtained through the ANA website (<http://hidroweb.ana.gov.br/>), with the warm period of the first five years. Such calibration was also performed by the simultaneous multi-site method, which consisted of using flow data from all fluvimetric stations to calibrate the model by changing and optimizing the parameters of all sub-basins at the same time (NKIAKA; NAWAZ; LOVETT, 2018).

The performance of the SWAT model used in this thesis was assessed using three (3) performance rating indices, namely: The coefficient of determination ( $r^2$ ), Nash- Sutcliffe Simulation Efficiency Coefficient<sup>14</sup> (NSE), and the Percent bias (PBIAS), within the range of variation (MORIASI et al., 2007), which considers the evaluation of the modeling at a time-step.

#### 4.2.2.3 Model parameterization and simulations in SWAT-CUP

In order to improve the performance of the SWAT model, before initiating the calibration process some parameters were modified in relation to the default values of the model; such modifications are presented in Table 17. These are parameters used in the monthly calibration of the São Francisco River basin (sub-medium region), describing the standard intervals of the model, the minimum and maximum values adopted, as well as the adjusted values obtained in the best SWAT model simulations.

Table 17: Used parameters in the calibration of the São Francisco River basin (sub-medium region)

Parameter	Adjusted value	Minimum value	Maximum value
1: A GWQMN.gw	4000,00	4000,00	4000,00
2: V GW_DELAY.gw	338,81	307,64	390,74
3: R_CN2.mgt	-0,18	-0,19	-0,18
4: R_SOL_AWC(..).sol	0,35	0,35	0,35
5: R_SOL_Z(..).sol	0,19	0,19	0,20
6: R_SOL_K(..).sol	0,21	0,21	0,27
7: A_CH_K2.rte	25,17	24,98	25,43
8: V_SURLAG.bsn	17,22	17,15	17,25
9: V_LAT_TTIME.hru	21,22	19,51	27,10
10: R_SLSUBBSN.hru	-0,08	-0,08	-0,08
11: R_HRU_SLP.hru	-0,20	-0,21	-0,20
12: V_RCHRG_DP.gw	0,26	0,23	0,31
13: R_ALPHA_BF.gw	-0,05	-0,06	-0,05
14: R_SOL_BD(..).sol	0,04	0,04	0,05
15: V_ALPHA_BNK.rte	-0,29	-0,29	-0,27

<sup>14</sup>Additionally, the Nash- Sutcliffe Simulation Efficiency Coefficient (NSE) was used as the objective function.

16: V	GW REVAP.gw	0,20	0,20	0,20
17: V	REVAPMN.gw	34,68	30,00	35,67

Source: (ANDRADE et al., 2023)

The letter at the beginning of the parameters indicates the type of operator adopted by the SWAT-CUP during the calibration process, as follows: R (relative) V (replace), or even A (absolute). Thus, if the operator is of type "V" (replace), the program replaces the value of the parameter resulting from the best simulation of the previous iteration by a new value (within the range of minimum and maximum variation adopted by the user).

While, if the parameter is used with the "R" (relative) operator, the SWAT-CUP multiplies the parameter value resulting from the best simulation of the previous iteration by a new value (also within the minimum and maximum variation range adopted by the user). For method "A" (absolute), a value (within the variation range) is added to the value of the parameter resulting from the best simulation of the previous iteration.

In this work, 20 simulations and a single iterative process were carried out, since the large area of the basin brings limitations in terms of processing time. However, acceptable values were found in these simulations, with the best simulation being number 19.

In general, parameters related to groundwater and soil characteristics were the most adopted, representing 9 parameters among the 17. Nevertheless, it should be noted that for calibration of SWAT model simulations with streamflow data, one of the most used parameters in the literature is the Curve Number for the AMCII moisture condition (CN2.mgt), since small modifications in its minimum and maximum interval values can produce significant changes in the resulting hydrograph.

#### 4.2.3 Linear scaling technique for bias correction

As clearly described in Chapter 3, the climate future projection data (2006–2100) used in this study were submitted for bias correction using the CMhyd model (RATHJENS et al., 2016), adopted the Linear Scaling method (TEUTSCHBEIN; SEIBERT, 2012, 2013).

In the LS approach, bias-corrected simulation data should agree, in their monthly average values, with the observed data and a factor based on the ratio of the long-term monthly average observed (ANDRADE et al., 2021).

#### **4.2.4 Assessment of climate change impacts on water resources**

The SWAT model used in this work was calibrated for the baseline conditions (1961 to 2005) and then, applied to assess climate change impacts on water resources in the São Francisco River Basin.

After performing the bias correction of the climate future projections data (2006–2100) using the Linear Scaling method (TEUTSCHBEIN; SEIBERT, 2012, 2013), the water balance components (surface runoff, evapotranspiration, and groundwater recharge) were simulated by the SWAT model and compared in three future periods.

The referred periods are – short-term (2011 to 2040), medium-term (2041 to 2070), and long-term (2071 to 2100) – and compared with the baseline period (1961 to 2005), under two RCPs (RCP 4.5 and RCP 8.5).

### **4.3 Results and Discussions**

#### **4.3.1. Performance analysis of the simulated hydrographs by the SWAT model with the observed data**

As a results, figure 28 shows the monthly hydrographs with data observed and simulated by the SWAT model in the calibration period (1966-2016), considering three stations: 127 (Figure 28a), 187 (Figure 28b), and 268 (Figure 28c), respectively.

For the São Francisco River basin, it appears that among the three fluviometric stations evaluated, all presented acceptable NS indices, with NS classified as satisfactory or good, varying between 0.55 and 0.69, according to the adopted classification (MORIASI et al., 2007).

Regarding the  $r^2$  values, the stations presented values of 0.6 and 0.7, indicating that, in general, there is good agreement between the data observed and simulated by the model. Such agreement is quite visible in the hydrographs, where the observed data are well accompanied by simulated data. However, it is verified that in the seasons, some observed peaks are not well represented by the model, with, in general, underestimation of the peaks from the beginning of the period until mid-1994, when from that year, the peaks begin to be overestimated by the SWAT model.

In this study, considering the entire São Francisco River basin, the flow simulated by SWAT was slightly lower than the observed flow, with a relative difference of approximately 2% for both periods (January to April) in the years 1993 and 1994.

Very good NS values (0.58 and 0.49) were obtained when calibrating the Salt Lake Sub-Basin, in Iran (KHALILIAN; SHAHVARI, 2018). Good model performance was achieved after calibration and validation with daily discharge ( $NSE > 0.7$  for both model setups) in a tropical inland valley catchment of central Uganda, East Africa (GABIRI et al., 2019).

Similar results were obtained calibrating the SWAT model using evapotranspiration (ET) and leaf area index (LAI), whereas remotely sensed precipitation and other climatic parameters were used as forcing data for the 6300 km<sup>2</sup> Day Basin, a tributary of the Red River in Vietnam (HA et al., 2018). The monthly flow at two flow measurement stations was adequately estimated ( $NSE = 0.71$  and  $0.63$ , for Phu Ly and Ninh Binh, respectively). According to the authors, this outcome demonstrates the capability of the SWAT model to obtain a spatial and accurate simulation of eco-hydrological processes, also when rivers are ungauged, and the water withdrawal system is very complex.

Regarding the base flow, in general, it appears that there are overestimations by the model, especially in the final years of seasons 127 and 187.

Similar agreements were obtained when calibrating the Tons River Basin, India, using the SUFI-2 algorithm, where the authors obtained the coefficient of determination ( $R^2$ ) values of 0.74 and 0.75 during the calibration and validation periods, respectively (KUMAR et al., 2017). Analogous findings were reported modeling hydrological response under climate change scenarios using the SWAT model, in the Ilala watershed, Northern Ethiopia (SHIFERAW et al., 2018), the simulated and observed hydrographs of the total river yield showed a good agreement during calibration ( $NSE = 0.51$ ,  $R^2 = 0.54$ ) and validation ( $NSE = 0.54$ ,  $R^2 = 0.63$ ).

Similar results were obtained evaluating the potential impacts of climate change on water resources of the Kelantan River Basin in north-eastern Peninsular Malaysia using the SWAT model (TAN et al., 2017), the results showed good performance in monthly streamflow simulation, with the NSE values of 0.75 and 0.63 for calibration and validation, respectively.

Regarding the PBIAS values, it appears that all stations presented values classified as satisfactory (station 187), good (station 127), and very good (station 268), according to the classification proposed by the literature (VAN LIEW et al., 2007), indicating good accuracy in the simulation of the model. PBIAS values of -3,55 were obtained while calibrating and uncertainty analyzing for streamflow prediction of the Tons River Basin, India, using the SUFI-2 algorithm (KUMAR et al., 2017), being classified as very good.

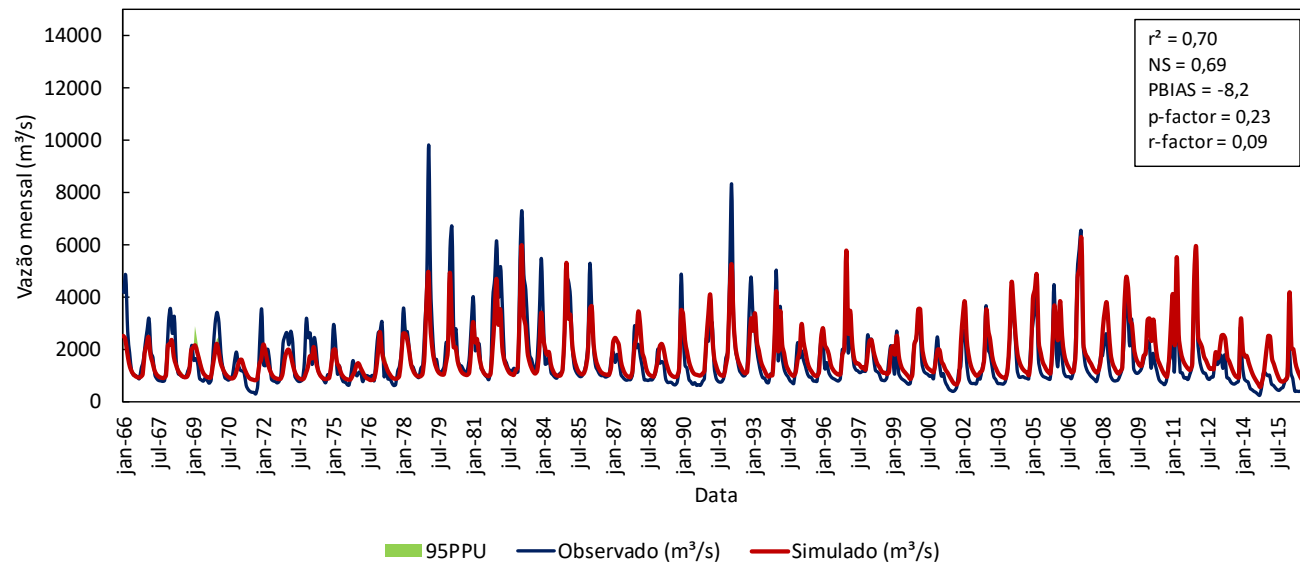
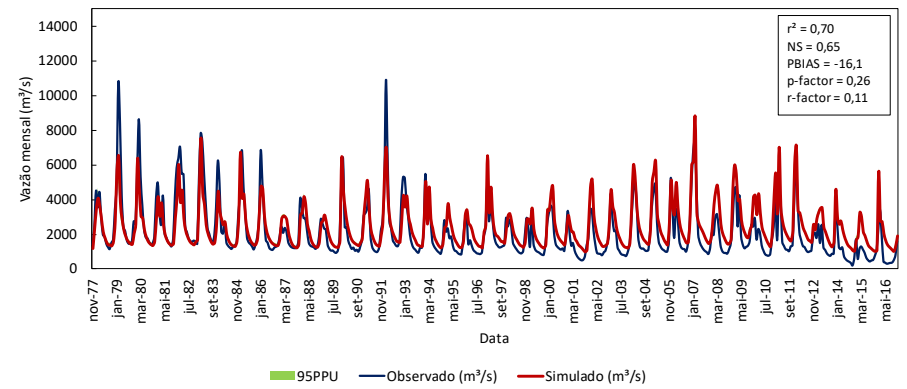
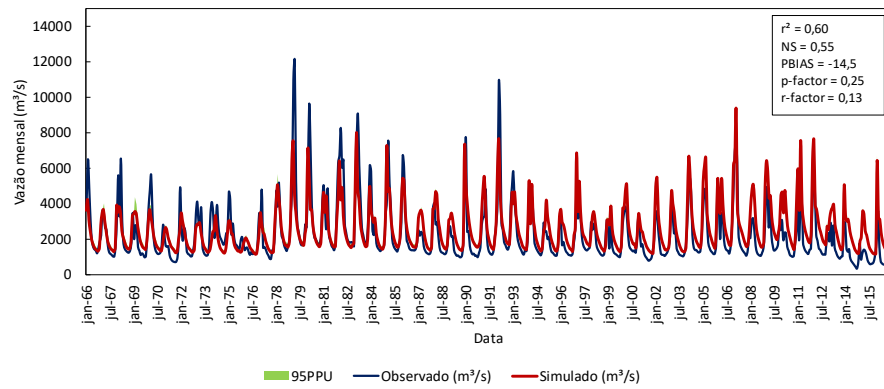


Figure 28: Monthly hydrogram with data observed and simulated by the SWAT model in the calibration period (1966 – 2016) in the São Francisco Basin, considering stations 127 (A), 187 (B), and 268 (C)  
 Source: (ANDRADE et al., 2023)

### 4.3.2 Hydrological Processes under future climate change scenarios

The Multi-model used in this chapter was built through a modified Reliability Ensemble Averaging (REA) approach (BURI et al., 2022) – as described in Chapter 3. This measures the multi-model uncertainty in the form of model performance to increase confidence when projecting climate data into the future while projecting variables in the future periods.

The Linear Scaling method adopted in this study was suitable to correct the raw historical ensembled climate data (1961-2005). This approach has been demonstrated to be effective for the study of precipitation and temperature data in previous works (ANDRADE et al., 2021; TEUTSCHBEIN; SEIBERT, 2012, 2013).

The results of the changes in average annual hydrological processes for the SFRB simulated by the SWAT model under climate scenarios and also for the baseline period are presented in Table 18. Simulated precipitation for the medium-term period (2041 – 2070) was 842.13 mm and 903.67 mm under RCPs 4.5 and 8.5, respectively, showing an increase in both scenarios compared to the baseline period.

Simulated evapotranspiration (ET) under RCP 8.5 also increases over time, since this process is closely related to precipitation, which also increased. In the baseline period, simulated ET was 287.6 mm, while for the ensembled climate data predictions the values increased to a minimum of 1349.57 mm under the short-term RCP 4.5.

The percolation in the SFRB is projected to increase over time. Simulated values for near-, mid-, and far-futures was 336.41 mm, 345.50 mm, and 363.84 mm, respectively under RCP 4.5, showing an increase compared to the baseline period.

On the other hand, simulated values were 330.96 mm, 383.09 mm, and 404.31 mm (for near-, mid-, and far-futures, respectively) under the RCP 8.5, also showing an increase compared to the baseline period. Similar agreements were found applying the SWAT model for the analysis of hydrological processes in the experimental basin of the Jatobá Stream, in the semiarid region of the State of Pernambuco, Brazil, considering the calibration and validation of the model from streamflow and soil moisture data (MARONEZE et al., 2014), where the regeneration of the vegetative cover over 21% of the hilltop areas of arborescent Caatinga led to a significant increase in percolation (42%).

Overall, the groundwater contribution to streamflow is projected to decrease under the short-term RCP 4.5. and RCP 8.5 periods (compared to the baseline period), with simulated values of 297.18 mm and 290.60 mm, respectively. Similar results were obtained investigating how significant baseflow reductions are related to the observed SFRB trends (LUCAS et al., 2021b). And in the other two periods (mid-, and far-futures), the simulated values showed an increase in the groundwater contribution to streamflow for both scenarios.

Table 18: Average annual hydrological processes for the SFRB simulated by the SWAT model

PROCESS	BASELINE (1961 – 2005)	Short-term (2011 – 2040)		Medium-term (2041 – 2070)		Long-term (2071 – 2100)	
		RCP 4.5	RCP 8.5	RCP 4.5	RCP 8.5	RCP 4.5	RCP 8.5
Precipitation (mm)	790.7	847.67	845.25	842.13	903.67	866.80	919.90
ET (mm)	287.6	1349.57	1360.24	1358.71	1409.63	1402.82	1542.03
ET <sub>0</sub> (mm)	586.9	476.78	472.69	458.14	467.12	461.40	452.63
PERC (mm)	314.66	336.41	330.96	345.50	383.09	363.84	404.31
GW_Q (mm)	311.03	297.18	290.60	303.90	337.75	321.03	358.80
WYLD (mm)	340.07	357.10	349.81	368.05	411.47	389.49	443.78

ET – evapotranspiration; ET<sub>0</sub> – potential evapotranspiration; PERC – percolation; GW\_Q – groundwater contribution to streamflow; WYLD – water yield.

The ET<sub>0</sub> in SFRB is projected to decrease over time. In the baseline period the potential evapotranspiration was 586.9 mm and in the short-, medium- and long-term scenarios this value, decreased by 110.12, 128.76, and 125.5 mm under RCP 4.5, and in the more pessimistic scenario (RCP 8.5) these values decreased by 114.21 mm, 119.78 mm, and 134.27 mm, reaching 452.63 mm by the end of the 21<sup>st</sup>-century.

The results projected a minimum of 113.6 mm (decrease of 27.4%) for the period 2071 – 2100 under RCP 8.5. This results aligns with those found in an assessment of the future climate change impacts on water resources of the Upper Sind River Basin, India, highlighting a baseflow decrease of 8.9% when comparing the baseline period (1961 – 1990) with the midcentury (2021 – 2050) (NARSIMLU; GOSAIN; CHAHAR, 2013).

The water yield is a hydrological process that can be representative of the water availability within a watershed (SUN et al., 2006). The results obtained in this study suggest that water yield within the SFRB will increase in the future, reaching 443.78 mm in RCP 8.5 in the long-term. Even though the water yield will be increasing in the upcoming climate change scenarios, effective, and suitable water management planning should be conducted to safeguard water security to reduce the risk of conflict – for different stakeholders and water resource management policymakers.

#### 4.3.3 Variations in streamflow under climate change

Projected annual streamflow changes for the 2017–2040, 2041–2070, and 2071–2100 periods under the two RCP scenarios are shown in Figure 29. Although there were some differences between the scenarios and among the future periods, in general streamflow was predicted to decrease over time, which could be attributed to rainfall decreases and temperature increases over the SFRB.

These findings corroborate those found using three different downscaled global climate models to analyze the impact of climate change on the hydroelectric potential of various basins

across South America (DE JONG et al., 2021), having determined that as a consequence of climate change, streamflow in the São Francisco River is projected to decline 46% in the coming 3 decades compared to data from 1961 to 1990, and this could become greater challenging to the increasing consumptive demands for water from the basin by the 2030s (DA SILVA et al., 2021), especially for irrigation, and reduced power generation.

The streamflow changes are generally associated with changes in rainfall projected to be marked by the high levels of mean annual precipitations (COUTINHO; CATALDI, 2021), interspersed by long droughts between 2010 to 2100 for both scenarios. Increases and decreases were also reported in projected annual streamflow under three RCPs, namely: RCP 2.6, RCP 4.5, and RCP 8.5 (OUYANG et al., 2015).

Monthly simulated streamflow for the future periods under RCPs scenarios are presented in Figure 29. In general, the streamflow patterns of the RCP 4.5 and 8.5 scenarios are very similar, but the magnitudes are different. Compared with the baseline streamflows, monthly streamflows tend to decrease over time. Mean monthly low flows are projected to decrease throughout the São Francisco River Basin, and the reductions were more pronounced for RCP 8.5 compared to RCP 4.5, reaching a minimum flow of  $4.18 \text{ m}^3\text{s}^{-1}$  in September of the period 2071-2100. High flows are also projected to decrease over the São Francisco river basin, with a maximum flow of  $2060.78 \text{ m}^3 \text{ s}^{-1}$  in January of the period 2070 – 2100 under the scenario RCP 4.5.

Predicted streamflow decreases in all months in the future were also stated in the past (LUCAS et al., 2021b), and were attributed to a significant decreasing baseflow trend along the São Francisco river basin with the spatial agreement between decreased baseflow, increased ET, and irrigated agricultural land.

Similar decreasing trends in average monthly and annual discharges by the end of the century under different scenarios were also reported in previous studies (OLIVEIRA; SANTOS E SILVA; LIMA, 2017; OUYANG et al., 2015), due to the extreme and prolonged droughts, which may negatively impact water availability and other ecosystem services.

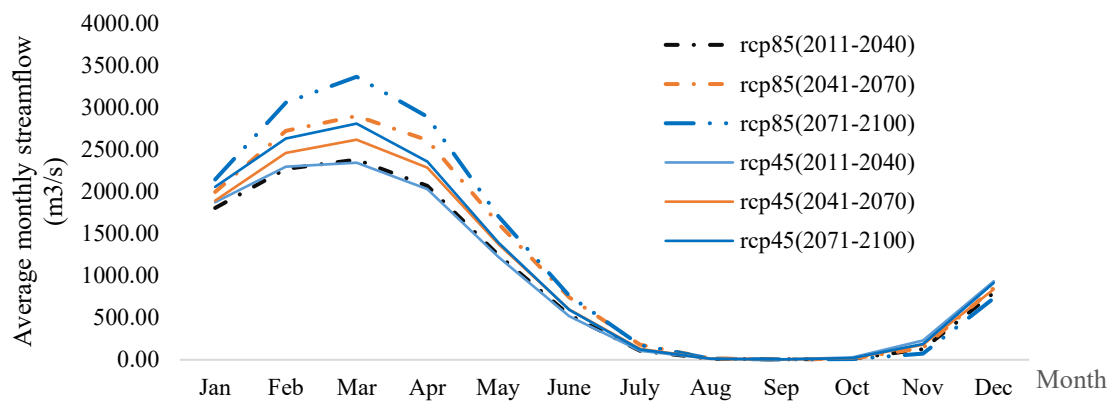


Figure 29: Mean monthly simulated streamflows for the future periods under RCPs scenarios

The results presented in this work reinforce the uncertainties associated with climate projections highly challenging, which can be attributed to the uncertainty linked to the selection of appropriate Global Climate Models (GCM).

These are highly complex because of measurement error, randomness, and systematic error in multiple climate models (1) (BURI et al., 2022), the uncertainty associated with each representative concentration pathway (RCPs) (2) (ANDRADE et al., 2021), uncertainty to downscaling and bias correction methods and uncertainty of multiple hydro-climatic models (3) (ANDRADE et al., 2021; OUYANG et al., 2015), which can be reduced/improved by combining independent models in an ensemble, proposed as the best solution to increases confidence when projecting climate data into the future (BURI et al., 2022).

Hence, all these both independent or combined uncertainties in future precipitation and temperature data can be propagated into streamflow simulation, and influence future water balance components projections (TAN et al., 2017). Therefore, studies such as these are needed to better understand such projections and to make more realistic and reliable inferences about the future of the climate in the regions (ANDRADE et al., 2021).

#### 4.4. Conclusions

In this study, the SFRB was calibrated using flow data in monthly time-step between 1961 and 2016. Considering the representativeness of the basin hydrographic for hydrological modeling, the results were very satisfactory. One good agreement between time series of simulated and observed monthly flow was demonstrated using hydrographs, and also by statistical indices, with a performance from "satisfactory" to "very good".

The calibrated SWAT model was used to assess the combined impacts of projected future climate changes on the water balance components in the SFRB. The results showed that more pronounced changes will occur if the drivers are combined, in particular for the mean annual streamflow and surface runoff. When combining the RCP 4.5 climate scenario, the mean annual streamflow and surface runoff are expected to change.

The findings show that land-use planning can be one of the promising measures to reduce future water-related risks in the SFRB. However, it remains a challenge to accurately predict the future hydrological changes due to land use and climate change, since there are various uncertainties, in particular, associated with possible climate uncertainties and systematic errors due to the bias correction methods, RCPs, and the choice of the appropriate hydrological model, and the number of ensembled GCMs.

Nevertheless, studies like this (bias corrected ensemble climate data) are extremely important since they seek to reduce these uncertainties and provide important information for the development of more effective climatic adaptation strategies to ensure coordinated management between different aspects of water issues.

Based on historical observations and regional climate modeling, there is a strong indication that climate change considering a high emissions scenario will cause significant changes in the São Francisco River basin by the end of this century or the three time periods analyzed under the two RCP scenarios. In the future, increases in temperatures are expected in the SFRB for the three time periods analyzed under the two RCP scenarios.

This study predicts large effects of climate change on the water balance of the study area. The processes expected to increase over time were evapotranspiration, percolation, baseflow, and water yield. On the other hand, the potential of evapotranspiration and mean monthly streamflows are expected to decrease over time. These forecasts point to serious water availability problems and increased vulnerability of the region to water shortages in the future.

## References

- ABBASPOUR, K. C. et al. Modelling hydrology and water quality in the pre-alpine/alpine Thur watershed using SWAT. **Journal of Hydrology**, v. 333, n. 2–4, p. 413–430, 2007.
- ALVES, L. M. et al. Trends in extreme rainfall and hydrogeometeorological disasters in the Metropolitan Area of São Paulo : a review. p. 1–16, 2020.
- ANDRADE, C. W. L. et al. Climate change impact assessment on water resources under RCP scenarios: A case study in Mundaú River Basin, Northeastern Brazil. **International Journal of Climatology**, v. 41, n. S1, p. E1045–E1061, 2021.
- ANDRADE, C. W. L. et al. Técnica de calibração para modelagem da bacia hidrográfica do Rio São Francisco, Brasil, utilizando o SWAT. **Revista Brasileira de Geografia Física**, v. 16, n. 03, p. 1621–1628, 2023.
- ARNELL, N. W.; GOSLING, S. N. The impacts of climate change on river flow regimes at the global scale. **Journal of Hydrology**, v. 486, p. 351–364, 2013.
- ARNOLD, J. G. et al. LARGE AREA HYDROLOGIC MODELING AND ASSESSMENT PART I: MODEL DEVELOPMENT ' basin scale model called SWAT ( Soil and Water speed and storage , advanced software debugging policy to meet the needs , and the management to the tank model ( Sugawara et al ., 1. v. 34, n. 1, p. 73–89, 1998.
- ASHRAF VAGHEFI, S. et al. A toolkit for climate change analysis and pattern recognition for extreme weather conditions – Case study: California-Baja California Peninsula. **Environmental Modelling and Software**, v. 96, p. 181–198, 2017.
- BASIN, R. et al. Potential Impacts of Climate Change on Water. p. 1–24, 2016.
- BETTENCOURT, P. et al. Prospective Water Balance Scenarios (2015–2035) for the Management of São Francisco River Basin, Eastern Brazil. **Water (Switzerland)**, v. 14, n. 15, p. 1–24, 2022.
- BEZERRA, B. G. et al. Changes of precipitation extremes indices in São Francisco River Basin, Brazil from 1947 to 2012. **Theoretical and Applied Climatology**, v. 135, n. 1–2, p. 565–576, 2019.
- BONUMA, N.; REICHERT, J. M.; RODRIGUES, M. F. Modeling Surface Hydrology , Soil Erosion , Nutrient Transport , and Future Scenarios With the ... n. July, p. 241–290, 2015.
- BRESSIANI, D. DE A. et al. A review of soil and water assessment tool (SWAT) applications in Brazil: Challenges and prospects. **International Journal of Agricultural and Biological Engineering**, 2015.
- BRIGHENTI, T. M. et al. Simulating sub-daily hydrological process with SWAT: a review. **Hydrological Sciences Journal**, v. 64, n. 12, p. 1415–1423, 2019.
- BURI, E. S. et al. Spatio-Temporal Analysis of Climatic Variables in the Munneru River Basin,

India, Using NEX-GDDP Data and the REA Approach. **Sustainability (Switzerland)**, v. 14, n. 3, 2022.

CARLUCCI, M. et al. The long breadth of cities: revisiting worldwide urbanization patterns, 1950–2030. **Applied Economics**, v. 00, n. 00, p. 1–13, 2020.

CARVALHO, A. A. DE et al. Trends of rainfall and temperature in Northeast Brazil Tendências da precipitação pluvial e da temperatura no Nordeste brasileiro. **Revista Brasileira de Engenharia Agrícola e Ambiental**, v. 24, p. 15–23, 2020.

COUTINHO, P. E.; CATALDI, M. Assessment of water availability in the period of 100 years at the head of the São Francisco river basin, based on climate change scenarios. **Revista Engenharia na Agricultura - Reveng**, v. 29, p. 107–121, 2021.

CUNHA, A. P. M. A. et al. Extreme Drought Events over Brazil from 2011 to 2019. 2019.

DA SILVA, M. V. M. et al. Projection of climate change and consumptive demands projections impacts on hydropower generation in the Sao Francisco river basin, Brazil. **Water (Switzerland)**, v. 13, n. 3, 2021.

DE AMORIM, P. B.; CHAFFE, P. L. B. Integrating climate models into hydrological modelling: What’s going on in Brazil? **Revista Brasileira de Recursos Hidricos**, v. 24, p. 1–17, 2019.

DE CARVALHO BARRETO, I. D. et al. Complexity Analyses of Sao Francisco River Streamflow: Influence of Dams and Reservoirs. **Journal of Hydrologic Engineering**, v. 25, n. 10, p. 1–8, 2020.

DE JONG, P. et al. The Impact of Regional Climate Change on Hydroelectric Resources in South America. **Renewable Energy**, v. 173, p. 76–91, 2021.

DELMONTE OLIVEIRA, K.; TOMASELLA, J.; DEL’ARCO SANCHES, L. Spatial-temporal analysis of the climatic and anthropogenic influences on runoff in the Jucu River Basin, Southeastern Brazil. **Land Degradation and Development**, v. 30, n. 17, p. 2073–2087, 2019.

FAKHRUDDIN, B. (SHM) et al. **Assessing vulnerability and risk of climate change**. [s.l.] Elsevier Inc., 2020.

FLEISCHMANN, A. et al. Precipitation as a proxy for climate variables : application for hydrological modelling. **Hydrological Sciences Journal**, v. 64, n. 3, p. 361–379, 2019.

FRANCESCONI, W. et al. Using the Soil and Water Assessment Tool (SWAT) to model ecosystem services: A systematic review. **Journal of Hydrology**, v. 535, p. 625–636, 2016.

GABIRI, G. et al. Modelling the impact of land use management on water resources in a tropical inland valley catchment of central Uganda, East Africa. **Science of the Total Environment**, v. 653, p. 1052–1066, 2019.

GAO, G. et al. Determining the hydrological responses to climate variability and land use/cover change in the Loess Plateau with the Budyko framework. **Science of the Total Environment**, v.

557–558, p. 331–342, 2016.

GAO, W.; GUO, H. C. Nitrogen research at watershed scale: A bibliometric analysis during 1959-2011. **Scientometrics**, v. 99, n. 3, p. 737–753, 2014.

GEBREMICHAEL, T. G. et al. Trend analysis of runoff and sediment fluxes in the Upper Blue Nile basin: A combined analysis of statistical tests, physically-based models and landuse maps. **Journal of Hydrology**, v. 482, p. 57–68, 2013.

GESUALDO, G. C. et al. Assessing water security in the São Paulo metropolitan region under projected climate change. **Hydrology and Earth System Sciences**, v. 23, n. 12, p. 4955–4968, 2019.

GUDMUNDSSON, L. et al. Evaluation of nine large-scale hydrological models with respect to the seasonal runoff climatology in Europe. v. 48, n. September, p. 1–20, 2012.

HA, L. T. et al. Calibration of spatially distributed hydrological processes and model parameters in SWAT using remote sensing data and an auto-calibration procedure: A case study in a Vietnamese river basin. **Water (Switzerland)**, v. 10, n. 2, 2018.

HU, W.; SI, B. C. Revealing the relative influence of soil and topographic properties on soil water content distribution at the watershed scale in two sites. **Journal of Hydrology**, v. 516, p. 107–118, 2014.

JÚNIOR, J. L. S.; TOMASELLA, J.; RODRIGUEZ, D. A. Impacts of future climatic and land cover changes on the hydrological regime of the Madeira River basin. p. 117–129, 2015.

KHALILIAN, S.; SHAHVARI, N. A SWAT Evaluation of the Effects of Climate Change on Renewable Water Resources in Salt Lake Sub-Basin, Iran. **AgriEngineering**, v. 1, n. 1, p. 44–57, 2018.

KUMAR, N. et al. SWAT Model calibration and uncertainty analysis for streamflow prediction of the Tons River Basin, India, using Sequential Uncertainty Fitting (SUFI-2) algorithm. **Modeling Earth Systems and Environment**, v. 3, n. 1, p. 1–13, 2017.

LIU, J. et al. Effects of Climate and Land Use Changes on Water Resources in the Taoer River. **Advances in Meteorology**, v. 2017, 2017.

LUCAS, M. C. et al. Significant baseflow reduction in the sao francisco river basin. **Water (Switzerland)**, v. 13, n. 1, p. 1–17, 2021a.

LUCAS, M. C. et al. Significant baseflow reduction in the sao francisco river basin. **Water (Switzerland)**, v. 13, n. 1, p. 1–16, 2021b.

MARHAENTO, H.; BOOIJ, M. J.; HOEKSTRA, A. Y. Hydrological response to future land-use change and climate change in a tropical catchment. **Hydrological Sciences Journal**, v. 63, n. 9, p. 1368–1385, 2018.

MARONEZE, M. M. et al. A tecnologia de remoção de fósforo: Gerenciamento do elemento em

resíduos industriais. **Revista Ambiente e Agua**, v. 9, n. 3, p. 445–458, 2014.

MARQUES, É. T.; GUNKEL, G.; SOBRAL, M. C. Management of tropical river basins and reservoirs under water stress: Experiences from northeast Brazil. **Environments - MDPI**, 2019.

MINISTÉRIO DO MEIO DO MEIO AMBIENTE / ANA - AGÊNCIA NACIONAL DE ÁGUAS. Orientações para atualização das curvas cota x área x volume. v. D, p. 36, 2013.

MONTENEGRO, S.; RAGAB, R. Impact of possible climate and land use changes in the semi arid regions : A case study from North Eastern Brazil. **Journal of Hydrology**, v. 434–435, p. 55–68, 2012.

MORIASI, D. N. et al. Model Evaluation Guidelines for Systematic Quantification of Accuracy in Watershed Simulations. **Transactions of the ASABE**, v. 50, n. 3, p. 885–900, 2007.

NARSIMLU, B.; GOSAIN, A. K.; CHAHAR, B. R. Assessment of Future Climate Change Impacts on Water Resources of Upper Sind River Basin, India Using SWAT Model. **Water Resources Management**, v. 27, n. 10, p. 3647–3662, 2013.

NASCIMENTO DO VASCO, A.; DE OLIVEIRA AGUIAR NETTO, A.; GONZAGA DA SILVA, M. The influence of dams on ecohydrological conditions in the São Francisco River Basin, Brazil. **Ecohydrology and Hydrobiology**, v. 19, n. 4, p. 556–565, 2019.

NEACHELL, E. Book Review - Environmental flows: Saving rivers in the thrid millennium. **River Research and Applications**, v. 30, n. January, p. 132–133, 2014.

NESRU, M.; NAGARAJ, M. K.; SHETTY, A. Assessment of consumption and availability of water in the upper Omo-Gibe basin, Ethiopia. **Arabian Journal of Geosciences**, v. 13, n. 1, 2020.

NETO, A. R. et al. Infrastructure sufficiency in meeting water demand under climate-induced socio-hydrological transition in the urbanizing Capibaribe River basin – Brazil. p. 3449–3459, 2014.

NETO, A. R. et al. Hydrological Processes and Climate Change in Hydrographic Regions of Brazil. p. 1103–1127, 2016.

NKIAKA, E.; NAWAZ, N. R.; LOVETT, J. C. Effect of single and multi-site calibration techniques on hydrological model performance, parameter estimation and predictive uncertainty: a case study in the Logone catchment, Lake Chad basin. **Stochastic Environmental Research and Risk Assessment**, v. 32, n. 6, p. 1665–1682, 2018.

OLIVEIRA, P. T.; SANTOS E SILVA, C. M.; LIMA, K. C. Climatology and trend analysis of extreme precipitation in subregions of Northeast Brazil. **Theoretical and Applied Climatology**, v. 130, n. 1–2, p. 77–90, 2017.

ORTIZ-PARTIDA, J. P. et al. Managing Water Differently : Integrated Water Resources Management as a Framework for Adaptation to Climate Change in Mexico. In: [s.l: s.n.]. p. 59–

72.

OUYANG, F. et al. Impacts of climate change under CMIP5 RCP scenarios on streamflow in the Huangnizhuang catchment. **Stochastic Environmental Research and Risk Assessment**, v. 29, n. 7, p. 1781–1795, 2015.

PANDEY, A. et al. Physically based soil erosion and sediment yield models revisited. **Catena**, v. 147, p. 595–620, 2016.

PANDEY, V. P. et al. Hydrological response of Chamelia watershed in Mahakali Basin to climate change. **Science of the Total Environment**, v. 650, p. 365–383, 2019.

PAREDES-TAVARES, J. et al. Impacts of climate change on the irrigation districts of the Rio Bravo Basin. **Water (Switzerland)**, v. 10, n. 3, p. 1–20, 2018.

PATTERSON, L. A.; LUTZ, B.; DOYLE, M. W. Climate and direct human contributions to changes in mean annual streamflow in the South Atlantic, USA. **Water Resources Research**, v. 49, n. 11, p. 7278–7291, 2013.

PAULO, V. DE et al. Water Footprint and Virtual Water Trade of Brazil. p. 1–12, 2016.

PRASKIEVICZ, S.; CHANG, H. A review of hydrological modelling of basin-scale climate change and urban development impacts. **Progress in Physical Geography**, v. 33, n. 5, p. 650–671, 2009.

PRIBYL, D. W. A critical review of the conventional SOC to SOM conversion factor. **Geoderma**, v. 156, n. 3–4, p. 75–83, maio 2010.

RANGE, K. et al. Modeling snowmelt-runoff under climate scenarios in the Hunza River basin ,. **Journal of Hydrology**, v. 409, n. 1–2, p. 104–117, 2011.

RATHJENS, H. et al. CMhyd User Manual Documentation for preparing simulated climate change data for hydrologic impact studies. p. p.16p, 2016.

SARTORI ET AL. Classificação Hidrológica de Solos Brasileiros para a Estimativa da Chuva Excedente com o Método do Serviço de Conservação do Solo dos Estados Unidos Parte 1: Classificação. **Revista Brasileira de Recursos Hídricos**, v. 10, n. 4, p. 5–18, 2005.

SAXTON, K. E.; RAWLS, W. J. Soil Water Characteristic Estimates by Texture and Organic Matter for Hydrologic Solutions. **Soil Science Society of America Journal**, v. 70, n. 5, p. 1569–1578, 2006.

SHIFERAW, H. et al. Modelling hydrological response under climate change scenarios using SWAT model: the case of Ilala watershed, Northern Ethiopia. **Modeling Earth Systems and Environment**, v. 4, n. 1, p. 437–449, 2018.

SIQUEIRA, N. A. DOS S.; SIQUEIRA, A. H. B.; FILHO, A. J. P. Statistical Analysis of Precipitation Extremes in S&#227;o Francisco River Basin, Brazil. **Atmospheric and Climate Sciences**, v. 12, n. 02, p. 383–408, 2022.

SU, F. et al. Hydrological response to future climate changes for the major upstream river basins in the Tibetan Plateau. 2015.

SUN, G. et al. Potential water yield reduction due to forestation across China. **Journal of Hydrology**, v. 328, n. 3–4, p. 548–558, 2006.

SUN, T. et al. Water availability of São Francisco river basin based on a space-borne geodetic sensor. **Water (Switzerland)**, v. 8, n. 5, 2016.

TAN, M. L. et al. Climate change impacts under CMIP5 RCP scenarios on water resources of the Kelantan River Basin, Malaysia. **Atmospheric Research**, v. 189, p. 1–10, 2017.

TAN, M. L. et al. A review of SWAT studies in Southeast Asia: Applications, challenges and future directions. **Water (Switzerland)**, v. 11, n. 5, p. 1–25, 2019.

TEUTSCHBEIN, C.; SEIBERT, J. Bias correction of regional climate model simulations for hydrological climate-change impact studies: Review and evaluation of different methods. **Journal of Hydrology**, v. 456–457, p. 12–29, 2012.

TEUTSCHBEIN, C.; SEIBERT, J. Is bias correction of regional climate model (RCM) simulations possible for non-stationary conditions. **Hydrology and Earth System Sciences**, v. 17, n. 12, p. 5061–5077, 2013.

TOMASELLA, J.; HODNETT, M. G.; ROSSATO, L. Pedotransfer Functions for the Estimation of Soil Water Retention in Brazilian Soils. **Soil Science Society of America Journal**, v. 64, n. 1, p. 327–338, 2000.

TUPPAD, P. et al. (swat) h. v. 54, n. 2007, p. 1677–1684, 2011.

VAN LIEW, M. W. et al. Suitability of SWAT for the Conservation Effects Assessment Project: Comparison on USDA Agricultural Research Service Watersheds. **Journal of Hydrologic Engineering**, v. 12, n. 2, p. 173–189, 2007.

VENETSANO, P. et al. Hydrological impacts of climate change on a data-scarce Greek catchment. **Theoretical and Applied Climatology**, 2020.

WANG, D.; HEJAZI, M. Quantifying the relative contribution of the climate and direct human impacts on mean annual streamflow in the contiguous United States. **Water Resources Research**, v. 47, n. 9, 2011.

WANG, Q. et al. Effects of dynamic land use inputs on improvement of SWAT model performance and uncertainty analysis of outputs. **Journal of Hydrology**, v. 563, n. June, p. 874–886, 2018.

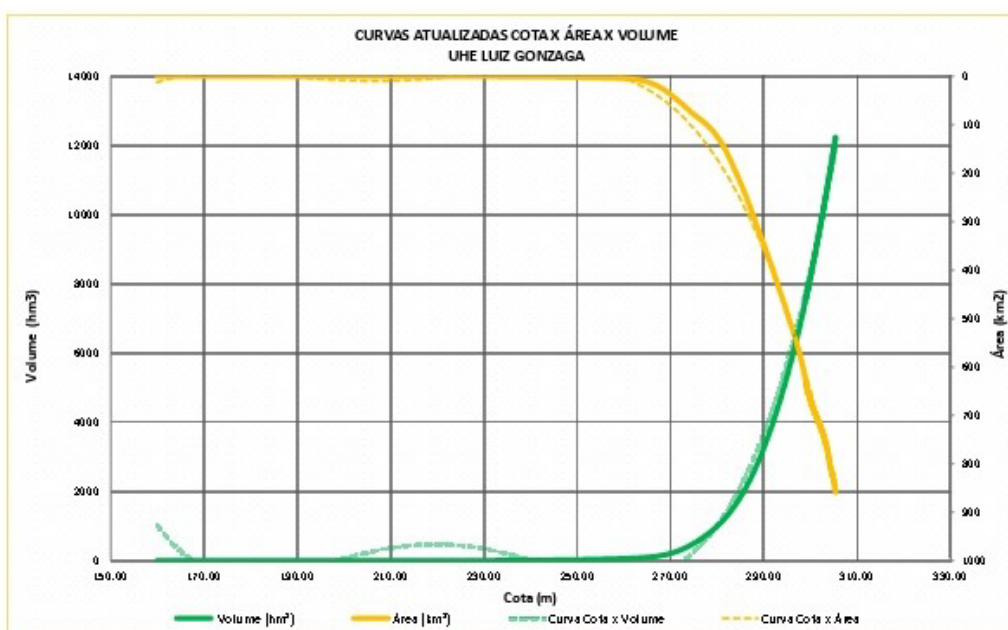
WANG, S. et al. Isolating the impacts of climate change and land use change on decadal streamflow variation: Assessing three complementary approaches. **Journal of Hydrology**, v. 507, p. 63–74, 2013.

WANG, Y. et al. Impacts of land use and plant characteristics on dried soil layers in different

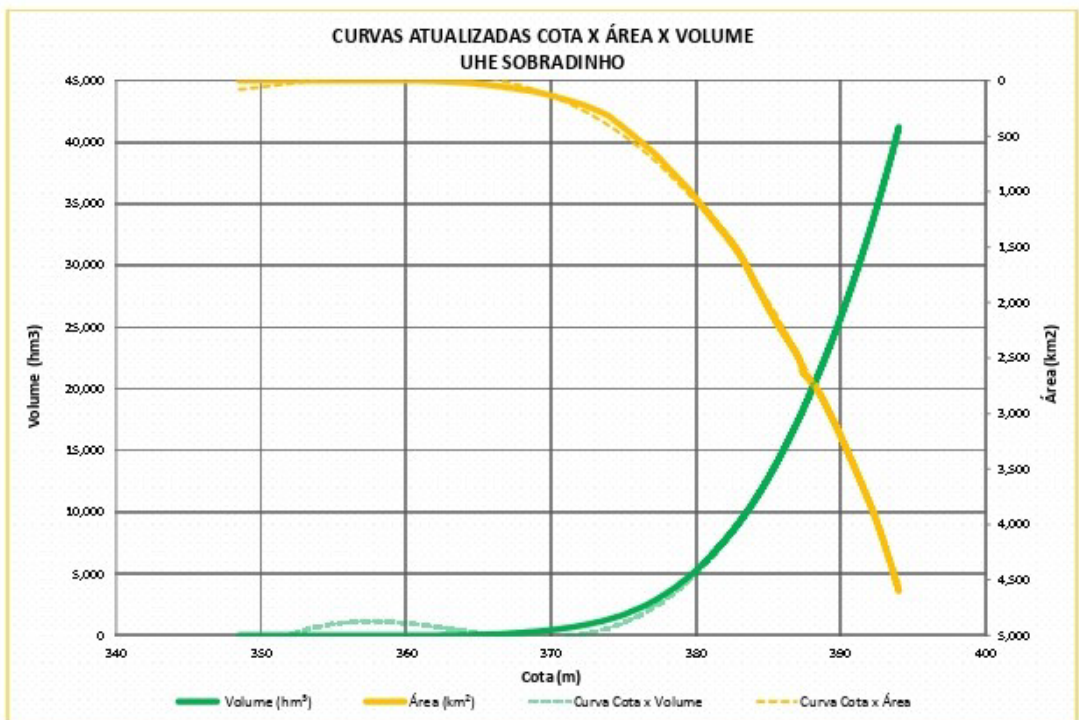
- climatic regions on the Loess Plateau of China. **Agricultural and Forest Meteorology**, v. 151, n. 4, p. 437–448, 2011.
- WANG, Y.; SUN, H.; ZHAO, Y. Characterizing spatial-temporal patterns and abrupt changes in deep soil moisture across an intensively managed watershed. **Geoderma**, v. 341, n. October 2018, p. 181–194, 2019.
- WOZNICKI, S. A.; NEJADHASHEMI, A. P.; PARSINEJAD, M. Climate change and irrigation demand: Uncertainty and adaptation. **Journal of Hydrology: Regional Studies**, v. 3, p. 247–264, 2015.
- YIN, J. et al. Effect of land use/land cover and climate changes on surface runoff in a semi-humid and semi-arid transition zone in Northwest China. **Hydrology and Earth System Sciences Discussions**, n. June, p. 1–23, 2016.
- ZUCCO, G. et al. Influence of land use on soil moisture spatial-temporal variability and monitoring. **Journal of Hydrology**, v. 516, p. 193–199, 2014.

Annex A: Detailed characteristics of the main reservoirs used in this study

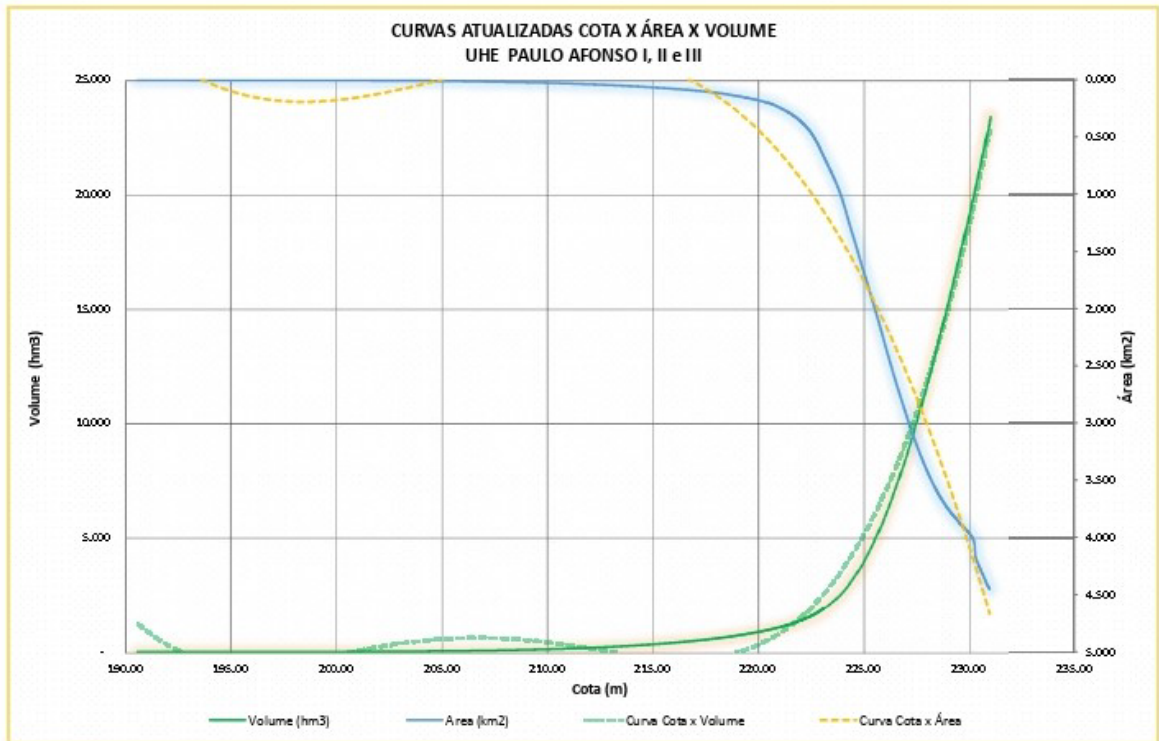
UHE LUIZ GONZAGA	
Empresa	Companhia Hidro Elétrica do São Francisco
Estado UHE (UF)	Pernambuco (PE)
Municípios Margem Direita	Glória (BA)
Municípios Margem Esquerda	Petrolândia (PE)
Bacia Hidrográfica	Bacia do Rio São Francisco
Sub-Bacia Hidrográfica	Bacia do Rio São Francisco - Trecho médio
Rio	Rio São Francisco
Potência Instalada (MW)	1479.6
Vazão Média de Longo Termo (m³/s)	1770
Latitude / Longitude do Barramento (Coordenada Geográfica)	09° 06' 00" S / 38° 19' 00" W
Área de Drenagem Total da UHE (km²)	591.465
Área Incremental da UHE (km²)	93.040
Área Inundada Original N.A Máximo Normal (km²)	828.00
Área Inundada Atualizada N.A Máximo Normal (km²)	791.27
Volume Útil Original (hm³)	3549.00
Volume Útil Atualizado (hm³)	3542.84
Volume Máximo Normal Original (Hm³)	10782.00
Volume Máximo Normal Atualizado (Hm³)	11086.92
Volume Máximo Máximo Original (Hm³)	12060.00
Volume Máximo Máximo Atualizado (Hm³)	12239.46
N.A Montante (Sistema Local) (m)	305,40 (Max. Máximo)
	304,00 (Max. Normal)
	299,00 (Min. Normal)
N.A Jusante (Sistema Local) (m)	252,00 (Máximo Normal)
Potencial de Produção de Sedimentos (Baixo, Médio ou Alto) (Pss) (ton/km²/ano)	Médio (2.5 a 100 ton/km²/ano)
Posição Relativa da Cascata (Prc) : Baixa Suscetibilidade ao Assoreamento (Pequena área de bacia incremental < 5.000 km²), Média (área de bacia incremental > 5.000 km²) ou Alta ( Reservatório de cabeceira)	Média (área de bacia incremental > 5.000 km²)
Índice de Regularização, Regime de Operação do Reservatório (Ror) IR = Volume útil (hm³) / Vazão Turbinada Média (hm³/dia) (Baixa: IR<30dias, Média: IR entre 30 e 150dias, Alta Suscetibilidade: IR>150 dias)	Baixa Suscetibilidade: IR<30dias
Magnitude e Importância dos efeitos do assoreamento (MI) (Baixa, Média ou Alta Suscetibilidade)	Média Suscetibilidade
Nível de Criticidade NC = (Pss+Prc+4Ror+MI)/21	Nível de Criticidade Baixo (Nc<0,50)
Data de atualização da CAV	09/23/2019



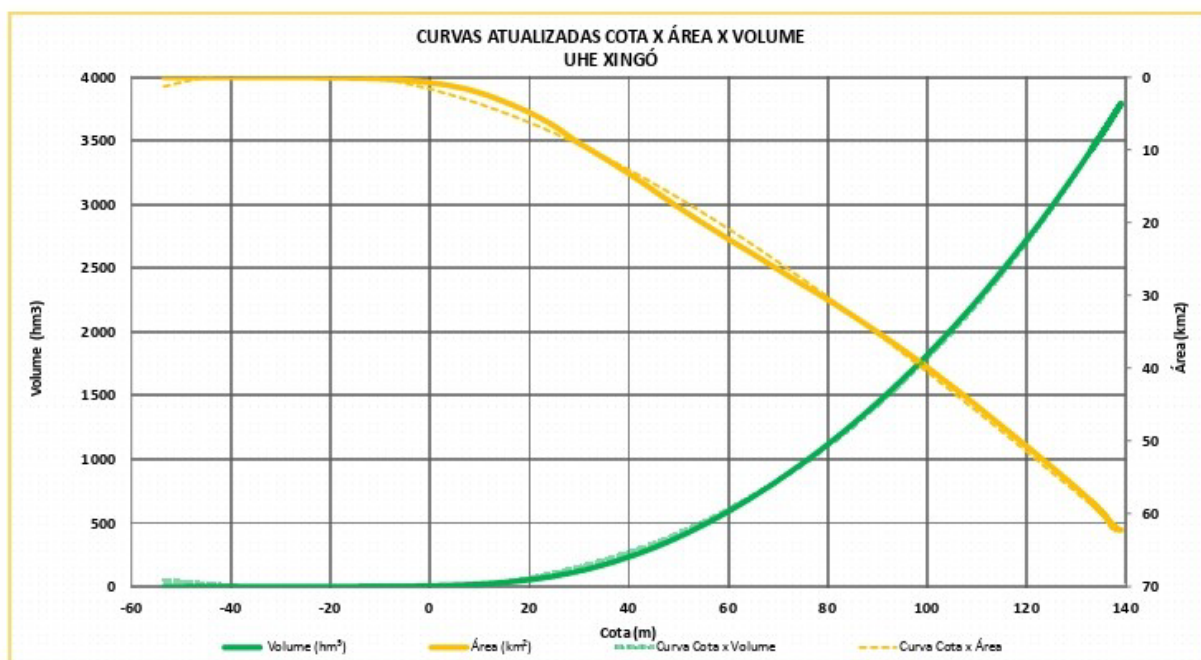
UHE SOBRADINHO	
Empresa	Companhia Hidro Elétrica do São Francisco
Estado UHE (UF)	Bahia (BA)
Municípios Margem Direita	Sobradinho (BA)
Municípios Margem Esquerda	Casa Nova (BA)
Bacia Hidrográfica	Bacia do Rio São Francisco
Sub-Bacia Hidrográfica	Bacia do Rio São Francisco - Sub-médio
Rio	Rio São Francisco
Potência Instalada (MW)	1050.3
Vazão Média de Longo Termo (m³/S)	1872
Latitude / Longitude do Barramento (Coordenada Geográfica)	09° 35' 00" S / 40° 50' 00" W
Área de Drenagem Total da UHE (km²)	498.425
Área Incremental da UHE (km²)	448
Área Inundada Original (km²)	4.214.000
Área Inundada Atualizada (km²)	3.984.965
Volume Útil Original (hm³)	28669.000
Volume Útil Atualizado (hm³)	28978.404
Volume Máximo Normal Original (Hm³)	34117.000
Volume Máximo Normal Atualizado (Hm³)	34790.567
Volume Máximo Maximorum Original (Hm³)	38539.000
Volume Máximo Maximorum Atualizado (Hm³)	38971.098
N.A Montante (Sistema Local) (m)	393,50 (Max. Maximorum)
	392,50 (Max. Normal)
	380,50 (Min. Normal)
N.A. Jusante (Sistema Local) (m)	371.90 (Máximo Normal)
Potencial de Produção de Sedimentos (Baixo, Médio ou Alto) (Pss) (ton/km²/ano)	Médio (25 a 100 ton/km²/ano)
Posição Relativa da Cascata (Pre): Baixa Suscetibilidade ao Assoreamento (Pequena área de bacia incremental < 5.000 km²), Média (área de bacia incremental > 5.000 km²) ou Alta (Reservatório de cabeceira)	Média (área de bacia incremental > 5.000 km²)
Índice de Regularização, Regime de Operação do Reservatório (Ror) IR = Volume útil (hm³) / Vazão Turbinada Média (hm³/dia) (Baixa: IR<30dias, Média: IR entre 30 e 150dias, Alta Suscetibilidade: IR>150 dias)	Alta Suscetibilidade: IR>150 dias
Magnitude e Importância dos efeitos do assoreamento (MI) (Baixa, Média ou Alta Suscetibilidade)	Alta Suscetibilidade
Nível de Criticidade NC = (Pss+Pre+4Ror+MI)/21	Nível de Criticidade Alto (Nc>0,75)
Data de atualização da CAV	05/13/2021



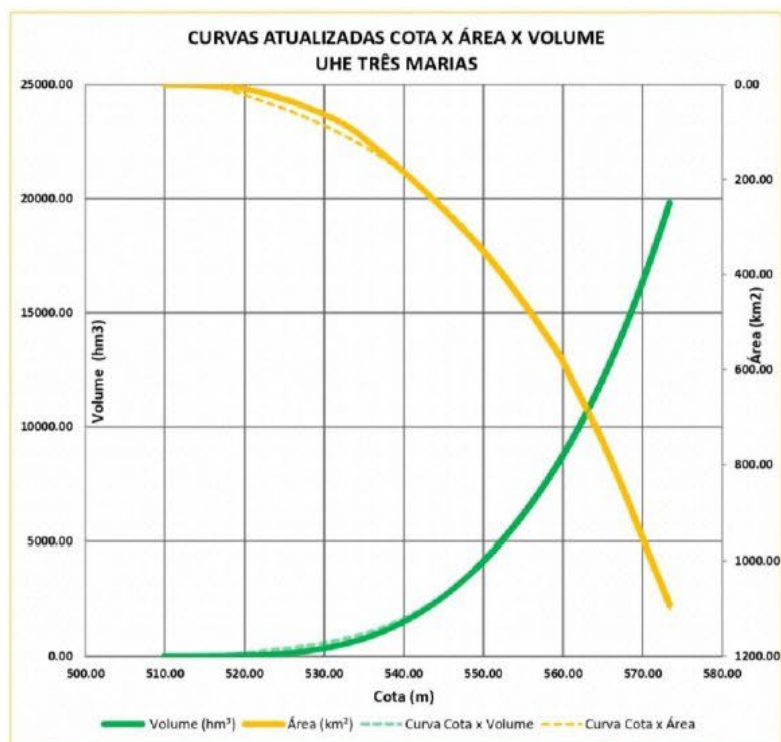
UHE PAULO AFONSO I, II e III	
Empresa	Companhia Hidro Elétrica do São Francisco
Estado UHE (UF)	Bahia (BA)
Municípios Margem Direita	Paulo Afonso (BA)
Municípios Margem Esquerda	Delmiro Gouveia (AL)
Bacia Hidrográfica	Bacia do Rio São Francisco
Sub-Bacia Hidrográfica	Bacia do Rio São Francisco Trecho médio
Rio	Rio São Francisco
Potência Instalada (MW)	180, 443 e 794,20
Vazão Média de Longo Termo (m <sup>3</sup> /S)	1,120
Latitude / Longitude do Barramento (Coordenada Geográfica)	09° 22' 00" S / 38° 16' 00" W
Área de Drenagem Total da UHE (km <sup>2</sup> )	603,683
Área Incremental da UHE (km <sup>2</sup> )	Zero
Área Inundada Original N.A. Máximo Normal (km <sup>2</sup> )	indisponível
Área Inundada Atualizada N.A. Máximo Normal (km <sup>2</sup> )	4.11
Volume Útil Original (hm <sup>3</sup> ) (soma dos dois reservatórios)	9.80
Volume Útil Atualizado (hm <sup>3</sup> ) (soma dos dois reservatórios)	7.61
Volume Máximo Normal Original (Hm <sup>3</sup> )	26.00
Volume Máximo Normal Atualizado (Hm <sup>3</sup> )	20.40
Volume Máximo Maximorum Original (Hm <sup>3</sup> )	28.90
Volume Máximo Maximorum Atualizado (Hm <sup>3</sup> )	22.53
N.A. Montante (Sistema Local) (m)	230.8 (Max. Maximorum) 230.3 (Max. Normal) 228.3 (Mín. Normal)
N.A. Jusante (Sistema Local) (m)	151.0 (Max. Normal)
Potencial de Produção de Sedimentos (Baixo, Médio ou Alto) (P <sub>SS</sub> ) (ton/km <sup>2</sup> /ano)	Baixo (menor que 5 ton/km <sup>2</sup> /ano)
Posição Relativa da Cascata (Prc) : Baixa Suscetibilidade ao Assoreamento (Pequena área de bacia incremental < 5.000 km <sup>2</sup> ), Média (área de bacia incremental > 5.000 km <sup>2</sup> ) ou Alta (Reservatório de cabeceira)	Baixa Suscetibilidade
Índice de Regularização, Regime de Operação do Reservatório (Ror) IR = Volume útil (hm <sup>3</sup> ) / Vazão Turbinada Média (hm <sup>3</sup> /dia) (Baixa: IR<30 dias, Média: IR entre 30 e 150 dias, Alta Suscetibilidade: IR>150 dias)	Baixa Suscetibilidade
Magnitude e Importância dos efeitos do assoreamento (MI) (Baixa, Média ou Alta Suscetibilidade)	Baixa Suscetibilidade
Nível de Criticidade NC = (P <sub>SS</sub> +Prc+4Ror+MI)/21	Nível de Criticidade Baixo (Nc<0,50)
Data de atualização da CAV	08/02/2019



UHE XINGÓ	
Empresa	CHESF
Estado UHE (UF)	SERGIPE
Municípios Margem Direita	PAULO AFONSO/BA e CANINDÉ DO SÃO FRANCISCO/SE
Municípios Margem Esquerda	DELMIRO GOUVEIA/AL, OLHO D'AGUA DO CASADO/AL E PIRANHAS/AL
Bacia Hidrográfica	BACIA DO RIO SÃO FRANCISCO
Sub-Bacia Hidrográfica	BACIA DO RIO SÃO FRANCISCO - TRECHO BAIXO
Rio	SÃO FRANCISCO
Potência Instalada (MW)	3.162 MW
Vazão Média de Longo Termo (m <sup>3</sup> /s)	1594
Latitude / Longitude do Barramento (Coordenada Geográfica)	S 9° 37' / W 37° 47'
Área de Drenagem Total da UHE (km <sup>2</sup> )	608,722
Área Incremental da UHE (km <sup>2</sup> )	5039
Área Inundada Original N A Máximo Normal (km <sup>2</sup> )	60.000
Área Inundada Atualizada N A Máximo Normal (km <sup>2</sup> )	62.056
Volume Útil Original (hm <sup>3</sup> )	41.000
Volume Útil Atualizado (hm <sup>3</sup> )	49.579
Volume Máximo Normal Original (Hm <sup>3</sup> )	3800.000
Volume Máximo Normal Atualizado (Hm <sup>3</sup> )	3730.954
Volume Máximo Maximorum Original (Hm <sup>3</sup> )	3838.000
Volume Máximo Maximorum Atualizado (Hm <sup>3</sup> )	3793.135
N.A. Montante (Sistema Local) (m)	139 (Max. Maximorum)
	138 (Max. Normal)
	137,20 (Mín. Normal)
N.A. Jusante (Sistema Local) (m)	19,50 (Máximo Normal)
Potencial de Produção de Sedimentos (Baixo, Médio ou Alto) (P <sub>SS</sub> ) (ton/km <sup>2</sup> /ano)	Médio (Classe 2) - 30 ton/km <sup>2</sup> /ano (Estação sedimentométrica de Ibó)
Posição Relativa da Cascata (Prc): Baixa Suscetibilidade ao Assoreamento (Pequena área de bacia incremental < 5.000 km <sup>2</sup> , Média (área de bacia incremental > 5.000 km <sup>2</sup> ) ou Alta ( Reservatório de cabeceira)	Baixa Suscetibilidade (Classe 1)
Índice de Regularização, Regime de Operação do Reservatório (Ror) IR = Volume útil (hm <sup>3</sup> ) / Vazão Turbinada Média (hm <sup>3</sup> /dia) (Baixa: IR<30dias, Média: IR entre 30 e 150dias, Alta Suscetibilidade: IR>150 dias)	Baixa Suscetibilidade (Classe 1)
Magnitude e Importância dos efeitos do assoreamento (MI) (Baixa, Média ou Alta Suscetibilidade)	Baixa Externaldade (Classe 1)
Nível de Criticidade NC = (P <sub>SS</sub> +Prc+4Ror+MI)/21	0,43 (Nível de Criticidade Baixo)
Data de atualização da CAV	04/22/2019



UHE TRÊS MARIAS	
Empresa	Cemig Geração Três Marias S.A.
Estado UHE (UF)	Minas Gerais
Municípios Margem Direita	Três Marias - MG
Municípios Margem Esquerda	São Gonçalo do Abaeté - MG
Bacia Hidrográfica	Rio São Francisco
Sub-Bacia Hidrográfica	São Francisco
Rio	São Francisco
Potência Instalada (MW)	387.60
Vazão Média de Longo Termo (m³/S)	673.00
Latitude / Longitude do Barramento (Coordenada Geográfica)	18°12'54"S / 45°15'33"W
Área de Drenagem Total da UHE (km²)	50,600.00
Área Incremental da UHE (km²)	36,983.00
Área Inundada Original N.A. Máximo Normal (km²)	50,600.00
Área Inundada Atualizada N.A. Máximo Normal (km²)	36,983.00
Volume Útil Original (hm³)	1,057.98
Volume Útil Atualizado (hm³)	1,054.60
Volume Máximo Normal Original (Hm³)	15,278.00
Volume Máximo Normal Atualizado (Hm³)	14,974.13
Volume Máximo Máximo Original (Hm³)	19,534.00
Volume Máximo Máximo Atualizado (Hm³)	18,855.26
N.A. Montante (Sistema Local) (m)	20,420.39
	19,821.67
	549,20 (Min. Normal)
N.A. Jusante (Sistema Local) (m)	522,00 (Máximo Normal)
Potencial de Produção de Sedimentos (Baixo, Médio ou Alto) (Pss) (ton/km²/ano)	Alto potencial
Posição Relativa da Cascata (Pre): Baixa Suscetibilidade ao Assoreamento (Pequena área de bacia incremental < 5.000 km², Média (área de bacia incremental > 5.000 km²) ou Alta ( Reservatório de cabeceira)	Alta suscetibilidade
Índice de Regularização, Regime de Operação do Reservatório (Ror) IR = Volume útil (hm³) / Vazão Turbinada Média (hm³/dia) (Baixa: IR<30dias, Média: IR entre 30 e 150dias, Alta Suscetibilidade: IR>150 dias)	Alta suscetibilidade
Magnitude e Importância dos efeitos do assoreamento (MI) (Baixa, Média ou Alta Suscetibilidade)	Alta externalidade
Nível de Criticidade NC = (Pss+Pre+4Ror+MI)/21	Alto (1,00)
Data de atualização da CAV	jul-16



## APPENDIX D

---

### Technical Note on SWAT+ hydrological model: A brief description and limitations

#### **1. General overview of SWAT+ model features**

The Soil & Water Assessment Tool (SWAT) is a public domain, physical-based, semi-conceptual, distributed, continuous-time model that operates on a daily time step at basin scale (freely available at: <https://swat.tamu.edu/>), originally developed by the USDA-ARS and Texas A&M AgriLife Research (ARNOLD et al., 1998), to quantify the impact of land management practices in large, complex watersheds. The SWAT model integrates water quality and quantity modules and uses a two-level disaggregation scheme; a preliminary subbasin identification is carried out based on topographic criteria, followed by further discretization using land use and soil type considerations.

Areas with the same topographic characteristics, soil type, land use, and management form a hydrologic response unit (HRU), a basic computational unit assumed to be homogeneous in hydrologic response to land-use change.

This aims to predict the long-term impacts of management and the timing of agricultural practices within a year (i.e., crop rotations, planting and harvest dates, irrigation, fertilizer, and pesticide application rates and timing) and can simulate at the basin scale water and nutrients cycle in landscapes whose dominant land use in agriculture, besides being an effective tool to assess the environmental efficiency of best management practices and alternative management policies.

#### **1.2 Model discretization and hydrological response units**

The early version of the SWAT model was based on a basic computational unit assumed to be homogenous in hydrologic response to topographic characteristics, soil type, land use, and management (ARNOLD et al., 1998). Aiming to face the recent and future challenges regarding water resources management, was introduced a SWAT + model (BIEGER et al., 2017), a completely revised version of SWAT, for improved simulation of landscape position, overland routing, and floodplain processes within the watershed. GIS-based algorithms are used to extract river and floodplain geometry parameters mainly from Digital Elevation Models (DEM).

Although it uses the SWAT model similar equations in estimating runoff and/or infiltration, evapotranspiration, plant growth, and routing, SWAT+ is considerably more flexible concerning the discretization and spatial configuration/representation of interactions and processes in the watershed (BIEGER et al., 2017), with the most important model modifications and their advantages.

A schematic representation of landscape units recently introduced in the SWAT+ model is shown in Fig. 1.

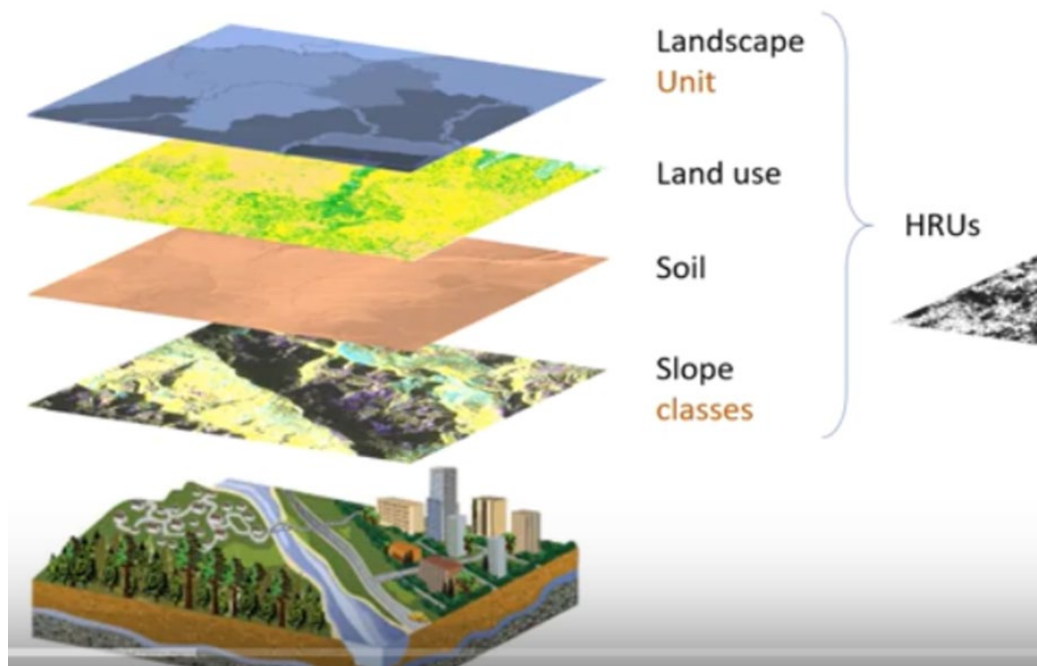


Fig. 1: Scheme of the conceptual model of water balance in the revised SWAT+ hydrological model. Source: modified from Dile *et al.* (2019)

## 2. Faced limitations of using the SWAT+ model

As stated in the general introduction section (chapter 1), this thesis is a part of the ongoing multilateral BRICS research project, titled “Integrated Water Management Model for Brazil, India, and South Africa under climate change scenarios” (BURI *et al.*, 2022), where it was originally intended to use the SWAT+ model (BIEGER *et al.*, 2017), a completely revised version of the SWAT model (ARNOLD *et al.*, 1998). During the project assembling to date of the submission of this thesis, in Brazil, studies using the SWAT+ version as a tool had not yet been published, thus we faced serious problems since we dreamed enough more than our computational power, coupled with our large-scale watershed (~639 219 sq km), and it took about 10 days (per simulation) to create landscape units using the simplest method (as described below), besides the SWAT+ and SWATplusCUP models’ algorithms which were under development or newly developed and not having been tested in large-scale basins, we changed for SWAT 2012 versions.

Firstly, for a more realistic representation of reservoir position and interactions with the landscape, among the three methods presented to create landscape units (SENENT-APARICIO; GEORGE; SRINIVASAN, 2021), the model did not allow the selection of the needed method, as aforementioned above, the **buffer stream** was the only ones fit (automatically) better for the São Francisco River basin.

This method is disadvantageous because is most likely to be used when the terrain is mostly flat (which was not the case in our study area, given the scale) and when other methods can give poor results (which were not possible to be optionally selected). So, testing (which was not possible) of the three methods would be necessary and important, to compare with the shapefile of floodable areas made available by the ANA.

Secondly, amid widely developed calibration/validation programs that have been developed to calibrate hydrological models, the SWATplusCUP is one of the indicated to assess the sensitivity of hundreds of input variables in the SWAT+ model (VENETSANOOU et al., 2020). The software allows for the fastest calibration process, and it is very optimized, but for this thesis' study area, it was producing very unrealistic values as simulated values<sup>15</sup>.

Guessing that SWATplusCUP was not handling the simulated high values well, and it was returning some extremely high values ( $>4 \cdot 10^6 \text{ m}^3/\text{s}$ ), I didn't realize it could be a SWATplusCUP limitation before, that's why I checked every detail of my model's inputs. As I did not find any problems, SWAT+ Toolbox software (CHAWANDA et al., 2020) was applied for calibration/validation purposes, and it worked perfectly.

Due to the limited number of SWAT+ and SWATplusCUP users, technical support from the developers (represented by Dr. Karim Abbaspour and his team at the Swiss Federal Institute of Aquatic Science and Technology – Switzerland), was requested. Among various recommendations, it was necessary to ensure that the provided *SWATP.exe* with the program was the same version as the one I used to run SWAT Tools.

### **3. Final remarks and recommendations for future research**

This technical note provided the information to help researchers narrow down choices on the appropriate version of the model to use for large-scale watersheds and make a final decision as to which model (either SWAT or a completely revised SWAT+ version) is best for better understanding the hydrological behavior and the strategies for coping with different climatic conditions for specific São Francisco River basin projects, being necessary for the model user to review the details placed in this technical note and make a final decision.

However, based on the undertaken effort during more than one year period in this project with the SWA+ model, we strongly do not recommend the use of developing or newly developed models for developing dissertations, theses, and related end-course works, due to the inconsistency of required testing and course completion deadlines.

---

<sup>15</sup>Typically, watersheds ranging from 10 to 20 000 sq km are considered large, thus the considered watershed in this study (~639 219 sq km) is too large in Brazil, with high flow values range that can be very high ( $>10^4 \text{ m}^3/\text{s}$ ).

Furthermore, as time passes, more new versions of SWAT+ models will be developed and many of the current model versions will be updated by developers. It should be noted that this review will require updates as new SWAT+ model versions. To model developers, providing model source codes (even under development) is encouraged whenever possible to support model (and outcome) transparency, and critically, research replicability.

## References

- ARNOLD, J. G. et al. LARGE AREA HYDROLOGIC MODELING AND ASSESSMENT PART I: MODEL DEVELOPMENT ' basin scale model called SWAT ( Soil and Water speed and storage , advanced software debugging policy to meet the needs , and the management to the tank model ( Sugawara et al ., 1. v. 34, n. 1, p. 73–89, 1998.
- BIEGER, K. et al. Introduction to SWAT+, A Completely Restructured Version of the Soil and Water Assessment Tool. **Journal of the American Water Resources Association**, 2017.
- BURI, E. S. et al. Spatio-Temporal Analysis of Climatic Variables in the Munneru River Basin, India, Using NEX-GDDP Data and the REA Approach. **Sustainability (Switzerland)**, v. 14, n. 3, 2022.
- CHAWANDA, C. J. et al. User-friendly workflows for catchment modelling: Towards reproducible SWAT+ model studies. **Environmental Modelling and Software**, v. 134, p. 104812, 2020.
- SENET-APARICIO, J.; GEORGE, C.; SRINIVASAN, R. Introducing a new post-processing tool for the SWAT+ model to evaluate environmental flows. **Environmental Modelling and Software**, v. 136, n. December 2020, p. 104944, 2021.
- VENETSANO, P. et al. Hydrological impacts of climate change on a data-scarce Greek catchment. **Theoretical and Applied Climatology**, 2020.

# CHAPTER V

---

## Key findings and concluding remarks

The research steps developed in this doctoral thesis include the projection of spatially explicit land-use scenarios and hydrological, and climatic assessments for the São Francisco river basin through coupling different modeling approaches.

In the **second chapter**, the developed model presented satisfactory performance, with an average spatial adjustment index between observed and simulated data in the 2019 validation year, of approximately 90%, with an average of commission and omission errors of approximately 2%. Among the five land use classes considered in this study, natural forest and pasture presented an average spatial adjustment means of around 88.75% and 97.13% (pattern changes); and when considering the areas where changes occurred, the classes that presented the highest values of spatial adjustment, agriculture, natural forest, and forest plantation stand out, with 61.53%, 56.47%, and 55.62%, respectively. The developed spatially explicit model successfully projected the future land-use change scenarios up to 2050, within the sustainable development, middle-of-the-road, and strong inequality scenarios, both considering the balance between global, national, regional, and local factors aligned with the global structure of SSPs and RCPs. Thus, water resources management must consider attending to the water demand for irrigation projected to increase in the upcoming decades, in addition to the conflicts/pressure for the different uses of water due to the increasing population and economic development.

The **third chapter**, in turn, concludes that the developed MME presented a good performance on statistical long-term trends analysis of observed gridded precipitation and temperature data. Relative to the observation period, the entire SFRB is expected to experience increases in temperature and precipitation by the end of the 21st century. Except for upper São Francisco, where precipitation increases early in the season, lower, central, and lower São Francisco areas experience increased precipitation during the rainy season. These increasing trends in precipitation and temperature were revealed by the Mann-Kendall (MK) test. The Mann-Kendall (MK) test showed an increasing trend upstream, midstream, and downstream of the SFRB, and the Spearman correlation test demonstrated a high correlation even after excluding the possibility of negative effects. The autocorrelation in the MK test and the Spearman rho trend test is due to his Mann-Kendall test with whitening (PWMK).

**Fourth chapter** provides an uncertainty analysis based on a multi-model approach that can provide practical support to end-users facing climate uncertainty in water resource management. The results obtained in this chapter show that, considering high-emission

scenarios, and climate change in his three time periods, analyzed based on his two RCP scenarios for the SFRB by the end of the 20th century. We showed strong evidence that it will produce significant changes in the study area.